

Probabilistische Erdbeben-Gefährdungs-Analyse für KKW-StandOrte in
der Schweiz (PEGASOS)

Probabilistic Seismic Hazard Analysis for Swiss Nuclear Power Plant Sites (PEGASOS Project)

Final Report Volume 6 Elicitation Summaries Site Response Characterisation (SP3)

prepared for the
Unterausschuss Kernenergie (UAK) der Ueberlandwerke (UeW)

by the
Nationale Genossenschaft für die Lagerung radioaktiver Abfälle (Nagra)

Wettingen, 31 July 2004



TABLE OF CONTENTS

- Part I:** Site Response Characterisation, Elicitation Summary
Dr. Pierre-Yves Bard
Laboratoire de Géophysique Interne et Tectonophysique (LGIT)
Université Joseph Fournier
Grenoble – France
- Part II:** Site Response Characterisation, Elicitation Summary
Dr. Donat Fäh
Schweizerischer Erdbebendienst (SED)
Institut für Geophysik ETH Zürich
Zürich – Switzerland
- Part III:** Site Response Characterisation, Elicitation Summary
Prof. Dr. Alain Pecker
Géodynamique et Structure,
Bagnoux – France
- Part IV:** Site Response Characterisation, Elicitation Summary
Dr. Jost A. Studer
Studer Engineering,
Zürich – Switzerland

Part I:

Site Response Characterisation, Elicitation Summary

Dr. Pierre-Yves Bard

Laboratoire de Géophysique Interne et Tectonophysique
(LGIT)
Université Joseph Fournier
Grenoble – France

Probabilistische Erdbeben-Gefährdungs-Analyse für die KKW-Stand Orte
in der Schweiz (PEGASOS)

SP3 Site Response Characterisation

Elicitation Summary

Pierre-Yves Bard

Laboratoire de Géophysique Interne et Tectonophysique (LGIT)
Université Joseph Fournier
Grenoble – France



TABLE OF CONTENTS

TABLE OF CONTENTS	1
LIST OF TABLES	5
LIST OF FIGURES	6
1 INTRODUCTION	7
2 MEDIAN AMPLIFICATION OF HORIZONTAL GROUND MOTION	9
2.1 Approach	9
2.2 Logic Tree Structure	9
2.3 Model Evaluations Common to All Sites	10
2.3.1 Material properties	10
2.3.2 Background for weighting the different approaches	11
2.3.3 SHAKE vs RVT	12
2.3.4 Non-linear computations	13
2.3.5 Magnitude / pga dependence of site amplification: Interpolation of available computations	14
2.3.5.1 RVT case	14
2.3.5.2 SHAKE case	15
2.3.5.3 Non-Linear case	17
2.3.6 Extrapolation for large pga and/or magnitude values	18
2.3.6.1 Large input acceleration levels: beyond 1.5 g – And $m \leq 7$	18
2.3.6.2 Large magnitudes (> 7) – and $pga \leq 1.5$ g	19
2.3.6.3 Large magnitudes (> 7) – and $pga > 1.5$ g	19
2.3.7 Effect of incident wavefield (wave type and incidence angle)	19
2.3.8 2-D / 3-D effects	20
2.3.9 Estimation of 'outcropping motion' NL amplification factors at depth	22
2.3.9.1 General scheme	22
2.3.9.2 Additional details	23
2.4 Beznau	23
2.4.1 Site-Specific Model Evaluations	23
2.4.1.1 Alternative velocity profiles	23
2.4.1.2 Alternative 2D parameters	24
2.4.2 Summary of weights and parameters fro Beznau	25
2.5 Gösigen	26
2.5.1 Site-Specific Model Evaluations	26
2.5.1.1 Alternative NL material properties	26
2.5.1.2 Alternative 2D parameters	26
2.5.2 Summary of weights and parameters	27
2.6 Leibstadt	28
2.6.1 Site-Specific Model Evaluations	28
2.6.1.1 Alternative velocity and NL material properties	28
2.6.1.2 Alternative 2D parameters	28
2.6.2 Summary of weights and parameters	29
2.7 Mühleberg	30
2.7.1 Site-Specific Model Evaluations	30
2.7.1.1 Alternative NL material properties	30
2.7.1.2 Estimating NL amplification factors	30
2.7.1.2 Alternative 2D parameters	30

2.7.2	Summary of weights and parameters	31
3	MEDIAN AMPLIFICATION OF VERTICAL GROUND MOTION	33
3.1	Approach	33
3.2	Logic Tree Structure	34
3.3	Model Evaluations Common to All Sites	35
3.3.1	Relative weighting between the three approaches	35
3.3.1.1	Weight of the 'no change' branch	35
3.3.1.2	Relative weighting between V/H and SHAKE approaches	35
3.3.2	V/H approach	35
3.3.2.1	Estimation formula (after Borzorgnia & Campbell, EXT-RF-0246)	35
3.3.2.2	Interpolation / extrapolation rules	36
3.3.2.3	Parameters for the V/H approach	36
3.3.3	SHAKE approach	37
3.3.3.1	Methods for determining non-linearity properties of P wave velocity and damping	37
3.3.3.2	Interpolation for arbitrary values of pga and m	38
3.3.3.3	Extrapolation for large values of pga (beyond 0.75 g)	38
3.3.3.4	Missing SHAKE computations	39
3.3.3.5	Effect of incident wavefield (wave type / incidence angle)	40
3.3.3.6	2D / 3D effects	40
3.3.4	At-Depth Amplification Factors	41
3.3.4.1	No-Change Branch	41
3.3.4.2	Changes in the "V/H" Branch	42
3.3.4.3	'SHAKE' branch	43
3.3.4.4	Incident wavefield effects at depth	43
3.3.4.5	2D/3D effects at depth	44
3.4	Beznau	44
3.4.1	Site-Specific Model Evaluations	44
3.4.1.1	Alternative velocity profiles	44
3.4.1.2	Alternative 2D parameters	44
3.4.2	Summary of weights and parameters for Beznau	45
3.5	Gösgen	46
3.5.1	Site-Specific Model Evaluations	46
3.5.1.1	Alternative material properties	46
3.5.1.2	Alternative 2D parameters	46
3.5.2	Summary of weights and parameters for Gösgen	47
3.6	Leibstadt	48
3.6.1	Site-Specific Model Evaluations	48
3.6.1.1	Alternative velocity and NL material properties	48
3.6.1.2	Alternative 2D parameters	48
3.6.2	Summary of weights and parameters	49
3.7	Mühleberg	50
3.7.1	Site-Specific Model Evaluations	50
3.7.1.1	Alternative NL material properties	50
3.7.1.2	Alternative 2D parameters	50
3.7.2	Summary of weights and parameters	51
4	ALEATORY VARIABILITY OF HORIZONTAL GROUND MOTION	53
4.1	Approach	53

4.1.1	General comments	53
4.1.1.1	Variability in the input signal waveform (SH case): σ_{ISW}	53
4.1.1.2	Variability due to aleatory variations in soil profiles	53
4.1.1.3	Variability in incident waves (oblique incidence angle, SH, SV or P wave types)	54
4.1.1.4	Variability of 2D/3D effects depending on incident wave azimuth / angle	54
4.1.2	Formulas for aleatory variability on horizontal ground motion	54
4.1.2.1	SHAKE and Non-Linear Cases	54
4.1.2.2	RVT – Base Case	54
4.1.2.3	RVT – Other cases	54
4.1.2.4	'Linear' Case	54
4.1.3	Comments	54
4.2	Logic Tree Structure	55
4.3	Evaluations Common to All Sites	55
4.3.1	Special indications for interpolating the standard deviations	55
4.3.1.1	Interpolation of SHAKE standard deviations for arbitrary (pga, m) values	55
4.3.1.2	Interpolation of RVT standard deviation values for arbitrary (pga, m) values	56
4.3.2	Variability associated with the incident wavefield	57
4.4	Beznau	57
4.5	Gösgen	57
4.6	Leibstadt	57
4.7	Mühleberg	57
5	ALEATORY VARIABILITY OF VERTICAL GROUND MOTION	59
5.1	Approach	59
5.1.1	'No change' Approach: no additional aleatory variability	59
5.1.2	SHAKE Approach	59
5.1.2.1	Variability in the input signal waveform (SH case): σ_{ISW}	59
5.1.2.2	Variability in incident waves (oblique incidence angle, SH, SV or P-wave types)	59
5.1.2.3	Variability of 2D/3D effects depending on incident wave azimuth / angle	59
5.1.3	V/H Approach	59
5.2	Logic tree structure	60
5.3	Evaluations common to all sites	61
5.3.1.1	Interpolation of SHAKE standard deviations for arbitrary (pga, m) values	61
5.3.2	Variability associated with the incident wavefield	61
5.4	Beznau	61
5.5	Gosgen	61
5.6	Leibstadt	62
5.7	Mühleberg	62
6	MAXIMUM GROUND MOTIONS	63
6.1	Horizontal Component	63
6.1.1	Evaluation of Proponent Models	63
6.1.1.1	Estimation of maximum pga's	63

6.1.1.2	Maximum recorded horizontal motion (TP3-TN-0359)	64
6.1.2.	Logic Tree Structure	65
6.1.2.1	Pecker's approach branch	65
6.1.2.2	Fäh's approach branch	65
6.1.3	Weights for Maximum Ground Motions	66
6.1.3.1	Pecker / Fäh weights	66
6.1.3.2	Pecker's branch: uncertainty in pga values.	66
6.1.3.3	Pecker's branch: associated spectra.	66
6.1.3.4	Fäh's branch: uncertainty in spectral values.	66
6.2	Maximum horizontal ground motions at depth	66
6.2.1	Discussion of models used for surface ground motion	66
6.2.1.1	Estimation of maximum pga's based on soil strength	67
6.2.1.2	Maximum recorded horizontal motion (TP3-TN-0359)	67
6.2.2	Logic Tree Structure and weights	68
6.2.2.1	Pecker's approach branch	68
6.2.2.2	Fäh's empirical approach branch	69
6.3	Vertical Component	70
6.3.1	Evaluation of Proponent Models	70
6.3.2	Logic Tree Structure	70
6.3.3	Weights for Maximum Ground Motions	70
6.4	Maximum vertical ground motions at depth	70
6.4.1	Change in the models	70
6.4.2	Logic Tree Structure and weights	71
7	REFERENCES	73
APPENDIX 1 EG3-HID-0050 SITE AMPLIFICATION AT THE SURFACE AND EMBEDDED LAYER DEPTHS FINAL MODEL P.-Y. BARD		75
A1.1	Introduction	75
A1.2	Site amplification and its aleatory variability	76
A1.2.1	Amplification of horizontal ground motion	76
A1.2.2	Aleatory variability of amplification of horizontal ground motion	77
A1.2.3	Amplification of vertical ground motion	80
A1.2.4	Aleatory variability of amplification of vertical ground motion	80
A1.2.5	Parameter ranges	81
A1.3	Maximum ground motion at the surface	81
A1.3.1	Horizontal ground motion	81
A1.3.2	Vertical ground motion	81
A1.4	Soil hazard input files (SIFs)	81
A1.4.1	Associating site amplification factors with input spectral accelerations	81
A1.4.2	Summarizing epistemic uncertainty	82
A1.4.3	Plots of the soil hazard input files	82
A1.5	Logic tree	83
A1.6	Appendix	84

LIST OF TABLES

Tab. 1-1:	Average S-wave velocities over the top 30 meters for the 4 sites	7
Tab. 1-2:	Requested depths for each NPP site	8
Tab. 2-1:	Parameters for relative weights between SHAKE, RVTBC, and RVTOM for each NPP site	13
Tab. 2-2:	Summary of weights and computational parameters for the horizontal ground motion at Beznau site	25
Tab. 2-3:	Summary of weights and computational parameters for the horizontal ground motion at Gösgen site	27
Tab. 2-4:	Summary of weights and computational parameters for the horizontal ground motion at Leibstadt site	29
Tab. 2-5:	Summary of weights and computational parameters for the horizontal ground motion at Mühleberg site	31
Tab. 3-1:	Site categories and faulting parameters for applying the V/H approach	36
Tab. 3-2:	Coefficients and statistical parameters from the regression analysis of PGA and PSA response spectra	37
Tab. 3-3:	Summary of weights and computational parameters for the vertical ground motion at Beznau site	45
Tab. 3-4:	Summary of weights and computational parameters for the vertical ground motion at Gösgen site	47
Tab. 3-5:	Summary of weights and computational parameters for the vertical ground motion at Leibstadt site	49
Tab. 3-6:	Summary of weights and computational parameters for the horizontal ground motion at Mühleberg site	51
Tab. 5-1:	Statistical bias in predicted value of vertical-to-horizontal (V/H) ratio	60
Tab. 6-1:	Weights for maximum horizontal ground motion at depth	69
Tab. 6-2:	Weights for maximum vertical ground motion at depth (<i>Fäh's empirical approach</i>)	71
Tab. A-1:	Mean and maximum building depth for the four Swiss NPP sites	75

LIST OF FIGURES

Fig. 2-1:	Generic logic tree-structure for horizontal ground motion	10
Fig. 2-2:	NS cross-section through the Leibstadt NPP site (north is to the left)	28
Fig. 3-1:	Generic logic tree-structure for vertical ground motion	34
Fig. A-1:	Site amplifications factors for horizontal ground motion at the mean building depth of NPP Beznau for the case of a magnitude 6 earthquake with PGA on rock of 1.5 g	78
Fig. A-2:	Weighted geometric mean amplification factors (AF as function of PGA on rock and frequency) for horizontal ground motion of a magnitude 6 scenario at mean building depth of NPP Beznau	79
Fig. A-3:	Aleatory variability of amplifications factors for horizontal ground motion at the mean building depth of NPP Beznau for the case of a magnitude 6 earthquake with PGA on rock of 1.5 g	79
Fig. A-4:	Assessment of alternative maximum horizontal ground motion spectra and corresponding weights for the mean building depth of NPP Beznau	82
Fig. A-5:	Summarized model of site amplification factors for ground motion of 4 Hz at mean building depth at NPP Beznau and earthquake magnitudes 5, 6 and 7	83
Fig. A-6:	Bard's general logic tree for horiz. ground motion at the surface	84

1 INTRODUCTION

The following models and weights are certainly deeply related with my personal experience and seismological background. They correspond to a physical view of the amplification effects, with an a priori larger confidence in experimental data and observations, than on computer models, however sophisticated they may be.

During the WS3 and WS4 workshops, my – still preliminary – models were shown to lead to systematically higher amplification factors and hazard levels than those of the other experts. I did revise my models and weights a little bit to account for some errors and/or misunderstandings, but I nevertheless decided to keep most of the factors that lead to higher amplification factors (2D effects, some suspicion with respect to non-linear computations).

This choice is deliberate, and comes from the observed general overestimation of NL effects in the geotechnical engineering community, and also from a personal feeling of some reluctancy in the engineering community as a whole to consider too large site effects that lead to seemingly too large ground motion levels. While I do admit that present structural design rules and habits are in some way not compatible with too large ground motion, I think, as a seismologist, that we do not have to downgrade our view of the physical reality to take into account some 'hidden overstrength' in civil engineering structures: I prefer to estimate as well as possible the site correction factor – whatever the engineering consequences may be with present design rules-, and to let the structural engineers look more carefully into the reasons of such 'hidden overstrength', or possibly look for other design methods and other ground motion parameters than the acceleration response spectrum, which has only a limited meaning.

In these introductory words, I also want to emphasize the need for sensitive accelerometers (or seismometers) on each NPP site: if such instruments had been installed for several years at each of the four sites, they would have recorded many events, and have thus brought a lot of constraints on our models – at least for the low strain case – and I am sure this would have, in the end, decreased the uncertainties.

Finally, it is also worth to remember the category of the sites according to the classical classification based on the average S-wave velocity value over the first 30 m

Tab. 1-1: Average S-wave velocities over the top 30 meters for the 4 sites

Site	V_{s30}
Beznau P1	
Beznau P2	400 m/s
Beznau P3	
Gösgen	416 m/s
Leibstadt P1	353 m/s
Leibstadt P2	353 m/s
Mühleberg	662 m/s

These sites are therefore certainly not soft sites: a large part of the computed amplifications is due to the large velocity of the reference bedrock (2000 m/s) and should be significantly reduced when 'scaled' to a 'usual' bedrock with V_s around 800 m/s. Simultaneously, because of this stiffness, I do not anticipate very significant non-linear reduction effects for "moderate" input ground motion (around 0.3 – 0.4 g).

The amplification factors are required at the surface and at two additional depths (listed in the next table) for each NPP site.

Tab. 1-2: Requested depths for each NPP site

depth \ Site	Surface		Depth 1		Depth 2	
	depth	Geol. unit	Depth	Geol. unit	depth	Geol. unit
Beznau	BZ0 : 0 m	Gravel	BZ1 : 6 m	Gravel	BZ2 : 15 m	Opalinusclay
Gösgen	GZ0 : 0 m	Gravel/sand	GZ1 : 5 m	Gravel/sand	GZ2 : 9 m	Gravel/sand
Leibstadt	LZ0 : 0 m	Gravel/sand	LZ1 : 6 m	Gravel/sand	LZ2 : 10 m	Gravel/sand
Mühleberg	MZ0 : 0 m	Gravel/sand	MZ1 : 7 m	Gravel/sand	MZ2 : 14 m	Rock

The models and weights for the at-depth amplification factors are closely linked with the weights and models proposed for the surface motion, as my choice was to have a model for depth motion as consistent as possible to the surface model. The logic trees are basically similar, as well as the weights: there are, however, some changes since the amount of available computations is reduced, and there exist specific wave propagation effects at depth.

Some general comments about the at-depth motions should be emphasized, however, in this introductory part:

- As listed in Table 1.2, the deepest sites at Beznau and Mühleberg (BZ2 and MZ2) are located within rock units with large S-wave velocities: they will thus be treated in a different way from the other sites which are located within alluvial, softer (though rather stiff) layers. This is of special concern not only for maximum ground motion, but also for surface and subsurface topography effects.
- In practice, these 'deep sites' are located at the base of civil engineering structures, and not within the soil. These structures do modify the state of stress in the soil, which in turn may modify the mechanical characteristics and the dynamical behaviour of the soil, especially at high strains (non-linear behaviour, maximum ground motion). These sometimes massive structures also interact with the soil and certainly modify the ground motion at depth. After some discussions within the elicitation meetings and workshops, it was decided not to take these effects into account. Therefore, the models for the motions at depth are derived assuming that the 'deep sites' are quasi 'free-field' sites, although personally, I feel rather uncomfortable with such an imposed assumption

2 MEDIAN AMPLIFICATION OF HORIZONTAL GROUND MOTION

2.1 Approach

The following logic tree was derived by taking into account all the pieces of information (quantitative and qualitative) that were available from the numerous site response computations performed throughout the project.

It is also based mainly on a 'physical' interpretation of site effects, which are viewed as wave propagation effects influenced by the soil geometry (not only 1D, but also 2D and 3D), the wave type (SH, SV or P waves – the incident wavefield in the very near field of strong events might be also very different from plane waves), and the soil mechanical characteristics which, under strong shaking, are modified by non-linear behaviour.

It takes into account a significant amount of epistemic uncertainty, especially at large strains.

2.2 Logic Tree Structure

The basic logic tree is described in Figure 2-1. It includes the following branches

- Velocity profile
- Non-linear properties
- Computation approach (Linear = RVT base case for $p_{ga} = 0.05g$, SHAKE, RVT, Non-linear), including two distinct subbranching:
 - the RVT approach includes a subbranching to account for two different subsets : base case (actual velocity profile and material properties), and all other cases, taking into account the spatial heterogeneities in soil profile and material properties
 - the NL approach is thought to be more and more uncertain as the p_{ga} is increasing, so that a subbranching is introduced to modify the NL results to reflect the increasing epistemic uncertainty
- 2D/3D effects : the two branches are intended to account for epistemic uncertainties of the size of those effects.

There is no sub-branching for the wave type and incidence characteristics, since it is considered here to influence only the aleatory variability. (See below).

For the ground motions at depth, the same logic trees as for the surface motion were selected, both for the median amplification factor and for the aleatory variability. Special issues that had to be addressed for the two additional depth levels included the following:

- Estimation of the proper NL (non-linear) amplification factors (i.e., for 'outcropping' motion) which were not readily available.
- Estimation of 2D/3D effects at depth
- Assumptions on the incident wavefield effects at depth (median amplification factors, aleatory variability)

Apart from these computational modifications, the weights of the different branches remain generally unchanged – unless specified.

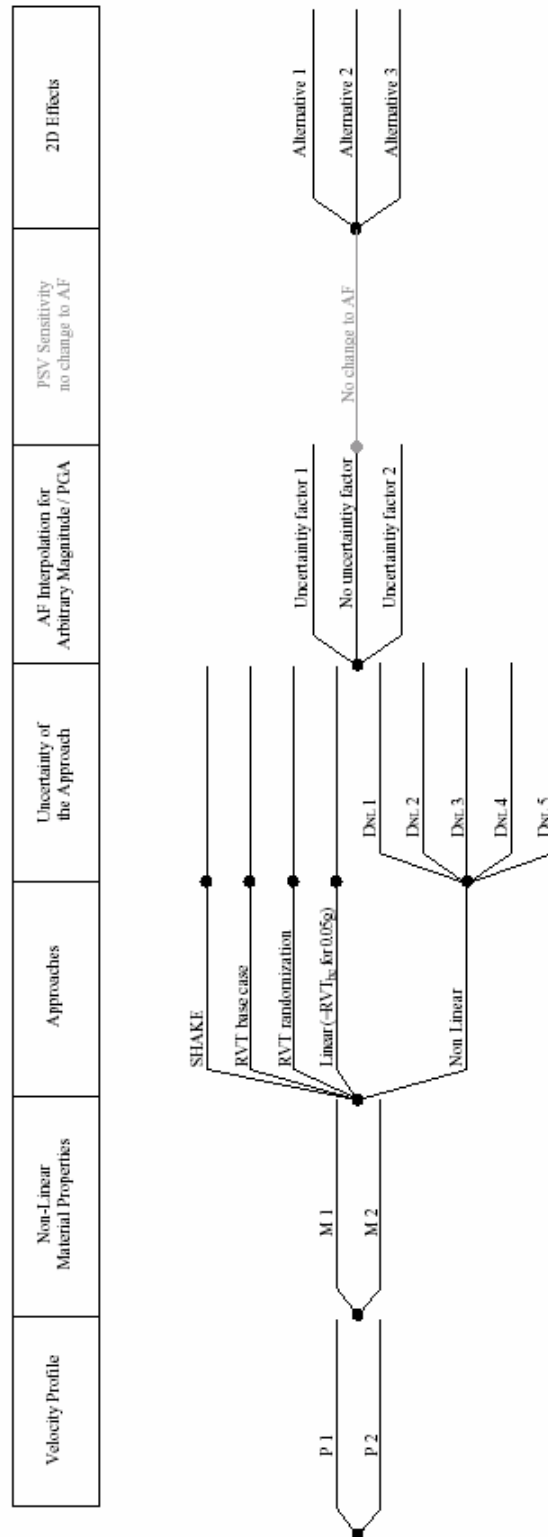


Fig. 2-1: Generic logic tree-structure for horiz. ground motion

2.3 Model Evaluations Common to All Sites

2.3.1 Material properties

Until the mid-eighties, it was widely accepted in the geotechnical earthquake engineering community that the onset of non-linear behavior was occurring at very low strains, and that NL

effects were leading to reductions of high-frequency ground motion for pga exceeding 0.15g; this result was primarily based on SHAKE computations using the "classical" Seed & Idriss curves from the early seventies.

Observations during both Mexico City and Loma Prieta events lead to a considerable re-consideration about those curves, especially for clays.

As a consequence, and considering the lack of clear experimental evidence of NL behavior for stiff gravel-like soil, I am personally somewhat reluctant to put high weight on Seed & Idriss material properties. That is why, I systematically assigned a 65% weight for Ishibashi & Zhang curves, and a 35% weight for Hardin & Drnevich curves.

2.3.2 Background for weighting the different approaches

I kept 4 different computational approaches: the purely linear case (represented by the RVT base case computations for small pga: 0.05g), the SHAKE and RVT linear-equivalent approaches, and the NL computations.

Their relative weighting depends on the strain level: at very low strains, the NL approach is not necessary; linear equivalent approaches are valid as long as strain γ is not too far beyond the 'reference strain' γ_r for which the shear modulus is reduced to half its initial value, while at very large strains ($\gamma \gg \gamma_r$), only the NL approach is – in principle – relevant. But its parameters are highly uncertain !

Therefore, the relative weighting L / LE / NL is based on the strain levels. These strains are computed with the RVT Base case approach, because it is the approach for which most results have been obtained, and interpolation errors are thus limited.

The procedure is detailed below:

- At each depth, compute γ/γ_r from RVT base case computations.
- Evaluate the maximum ratio $(\gamma/\gamma_r)_{\max}$ over the whole soil thickness
- When $(\gamma/\gamma_r)_{\max} < 1$, consider only Linear, SHAKE and RVT results. Linear approach is assigned a weight of 20%, and linear-equivalent approaches a total weight of 80%. The relative weight between SHAKE [$w_0(\text{SHAKE})$] and RVT cases [$w_0(\text{RVT})$] is detailed below in section 2.3.3

Linear approach (RVT base case 0.05 g):	20%
SHAKE approach :	$0.80 \cdot w_0(\text{SHAKE})$
RVT approach:	$0.80 \cdot w_0(\text{RVT})$
NL approach:	$w(\text{NL}) = 0.$
- When $1 < (\gamma/\gamma_r)_{\max} < 31.62$, consider simulatenously the four approaches: Linear, SHAKE, RVT, Non-linear.

Linear approach (RVT base case 0.05 g):	10%
SHAKE approach :	$0.90 \cdot w_0(\text{SHAKE}) \cdot \text{Red_LE} [(\gamma/\gamma_r)_{\max}]$
RVT approach:	$0.90 \cdot w_0(\text{RVT}) \cdot \text{Red_LE} [(\gamma/\gamma_r)_{\max}]$
NL approach:	$w(\text{NL}) = 0.90 - 0.90 \cdot [w_0(\text{SHAKE}) + w_0(\text{RVT})] \cdot \text{Red_LE} [(\gamma/\gamma_r)_{\max}]$
- When $(\gamma/\gamma_r)_{\max} > 31.62$, drop the linear approach, and keep only the SHAKE, RVT, and Non-linear ones.

Linear approach (RVT base case 0.05 g):	0%
SHAKE approach :	$w_0(\text{SHAKE}) \cdot 0.25$
RVT approach:	$w_0(\text{RVT}) \cdot 0.25$
NL approach:	$w(\text{NL}) = 1 - 0.25 [w_0(\text{SHAKE}) + w_0(\text{RVT})] = 0.75$

with the function $\text{Red_LE}(x)$ defined as follows:

$$\begin{aligned} \text{Red_LE}(x) &= 1 \text{ when } x < 1 \\ \text{Red_LE}(x) &= 1 - 0.5 \log(x) \text{ when } 1 < x < 31.62 \text{ (exact limit : } 31.62) \\ \text{Red_LE}(x) &= 0.25 \text{ when } x > 31.62 \end{aligned}$$

The minimum weight of 25% for the linear equivalent approach even at high strains is introduced as one of the means to indicate the large epistemic uncertainty for such large ground motion.

Important Notes:

- The Non-Linear results are available only for one single velocity profile (except for Leibstadt), and for one single material set which is generally different from the material sets used for the LE computations (SHAKE + RVT). The idea of the relative weighting NL / LE is that, for each subbranch corresponding to a given velocity profile and material set, the NL results will be used with the relative weighting indicated above, and with the specific interpolation formula detailed below in section 2.3.5. As a consequence, for any of the four sites, the NL results will be used several times, but with different weights (related with LE strains obtained for each soil velocity profile – material set) and slightly different interpolated values.
- There is no absolute minimum weight for SHAKE or RVT results: the minimum is set on the function Red_LE (25 %), which results in minimum weights for SHAKE and RVT at high frequencies (i.e., beyond the frequency f_2) of 12.5% and 12.5%, respectively for Leibstadt, and 15% and 10%, respectively, for the 3 other sites. BUT at low frequencies (i.e., below f_1), the RVT weights are always 0 %, while then the relative SHAKE weight is, at minimum, 25 % (very high strains).

2.3.3 SHAKE vs RVT

SHAKE and RVT approaches are based on similar concepts as to soil behavior (linear equivalent), but implement it in different ways, which have advantages and disadvantages.

Soil profile variability

The RVT approach considers variability in the soil layering and in the non-linear characteristics, while SHAKE does not. This is useful because such a variability is always present; it is, however, at least partially taken into account in the SHAKE approach with the different soil profiles and/or material properties for each site. In addition, soil heterogeneities in the RVT approach induce two artefacts which may be troublesome:

- high frequency waves may be artificially damped away in relation with "kinematic" diffraction on such heterogeneities.
- they may result in unrealistic strain concentration in thin low velocity layers, which in turn result in artificial damping and decoupling.

Therefore, my basic weights for a 'standard site' are 70% for the SHAKE approach ($RW_{\text{SHA}, f}$), and 30% for the RVT approach ($RW_{\text{RVT}, f}$, see below the definition of these terms $RW_{\text{SHA}, f}$ and $RW_{\text{RVT}, f}$). These numbers are modified for each site to take into account either the fact that geotechnical information does indicate the presence of such small scale heterogeneities (Leibstadt: alternance of cemented and non-cemented layers), or when only one velocity profile is considered in the SHAKE approach (Mühleberg, Gösigen), or when only one set of material properties (NL characteristics) is considered in the SHAKE approach (Beznau).

Input motion variability: base case subset

The RVT approach is also interesting without any soil randomization because it implicitly accounts for variability in input motion: the RVT subset corresponding to the base velocity profile / NL characteristics (= 'base case') is therefore of special interest, and I assign it a uniform weight $RW_{RVT,BC}$ of 15% (half the 'basic' weight of 30%) for high frequencies (greater than f_2 , see below); the other subset (variable velocity profile, variable material properties), is assigned the remaining weight $RW_{RVT,OM} = RW_{RVTf} - RW_{RVT,BC}$.

When such a distinction is represented by a 2 branch subtree, the corresponding relative weights are therefore $RW_{RVT,BC} / RW_{RVTf}$ (the corresponding values are either 0.375 or 0.30) and $RW_{RVT,OM} / RW_{RVTf}$ (the corresponding values are either 0.625 or 0.70)

RVT frequency-dependent reliability

The computation of response spectra through the RVT approach is reliable at intermediate and high frequencies (large number of cycles), but it is NOT reliable at low frequencies (as shown in document TP3-TN-0340). Therefore, I assign a frequency dependent weight, defined as follows:

- For $0 < f < f_1$: $w_0(\text{RVT}) = 0$ and $w_0(\text{SHA}) = 1$
- For $f_1 < f < f_2$: $w_0(\text{RVT}) = (\log(f/f_1)/(\log(f_2/f_1))) RW_{RVT,f}$ and $w_0(\text{SHA}) = 1 - w_0(\text{RVT})$
- For $f > f_2$: $w_0(\text{RVT}) = RW_{RVT,f}$ and $w_0(\text{SHA}) = 1 - RW_{RVT,f} = RW_{\text{SHA},f}$

The RVT formulas apply both to the base case subset (with $RW_{RVT,BC} = 0.15$), and the 'other model' subset (with $RW_{RVT,OM} = RW_{RVTf} - 0.15$).

As this effect is basically related to the number of cycles, the frequencies f_1 and f_2 are the same for every site.

The specific values for $RW_{RVT,f}$, $RW_{RVT,BC}$, and $RW_{RVT,OM}$ depend on the site under investigation

Tab. 2-1: Parameters for relative weights between SHAKE, RVTBC, and RVTOM for each NPP site

Site	f_1	f_2	$RW_{RVT,f}$	$RW_{RVT,BC}$	$RW_{RVT,OM}$
Beznau	0.5	1	0.4	0.15	0.25
Gösgen			0.4	0.15	0.25
Leibstadt			0.5	0.15	0.35
Muhleberg			0.4	0.15	0.25

2.3.4 Non-linear computations

Discussions during WS3/SP3 made it clear that NL results are strongly dependent on several parameters that are very poorly constrained. The higher the input p_{ga} , the larger the epistemic uncertainty in the NL behavior: the measurements of NL characteristics are very few, and when they exist, they are performed on remodeled samples, which may not be large enough given the material (mainly 'gravel'). Even if some agreement could be reached afterwards between Pelli's and Pecker's approaches, I prefer to specifically include the epistemic uncertainties in the NL approach by introducing 5 sub-branches, compatible with what is proposed for very large p_{ga} (see below section 2.3.6 about extrapolation for large M and p_{ga} values).

For the 5 branches on the NL subtree, the amplification factors computed with the NL approach are modified by multiplying them by an 'NL uncertainty' factor U_{NL} defined as follows

$$U_{NL}(f, f_0, p_{ga}, D_{NL}) = 1. + D_{NL} E(k f/f_0),$$

Where

f_0 is the low strain fundamental frequency of the site (given for each of the 4 sites).

k is a multiplying factor introduced to account for the decrease of fundamental frequency at large strains: $k = 1. + 2*U_a$, with $U_a = [\log(pga/0.4) / \log(1.5/0.4)]$, and k bounded by 1 ('low' pga) and 3 (pga > 1.5g).

E is a generic function defined as

$$\begin{aligned} E(x) &= 0. && \text{for } x < 0.5 \\ E(x) &= \log(2x) / \log(2) && \text{for } 0.5 < x < 1.0 \\ E(x) &= 1 && \text{for } 1.0 < x \end{aligned}$$

D_{NL} is a factor that is highly uncertain and for which several values are proposed, with corresponding weights

$$\begin{aligned} D_{NL} &= 2 U_a : \text{weight} : 15\% \\ D_{NL} &= U_a : \text{weight} : 25\% \\ D_{NL} &= 0 : \text{weight} : 30\% \\ D_{NL} &= -0.5 U_a : \text{weight} : 20\% \\ D_{NL} &= -0.67 U_a : \text{weight} : 10\% \end{aligned}$$

with $U_a = [\log(pga/0.4) / \log(1.5/0.4)]$, limited within 0. (pga < 0.4g) and 1. (pga > 1.5 g)

The slight assymetry in the weights is intended to introduce a slight bias towards higher amplification values: it is related with the Mexico City / Loma prieta experiences, as well as with the recent work by Bonilla et al., who did show on the basis of the Japanese K-NET / KIK-NET data set, that usual LE or NL models overestimate non-linearities, and underestimate actual ground motion amplification factors.

2.3.5 Magnitude / pga dependence of site amplification: Interpolation of available computations

Direct results from RVT, SHAKE and NL computations are available only for discrete values of magnitudes and pga. In addition, some of them (NL computations) have been computed only for a specific soil profile.

Some interpolation scheme therefore needs to be described in order to estimate the corresponding amplification factors for any value of the (M, pga) couple.

As the wider set of available results corresponds to RVT computations, the interpolation scheme is based on the RVT base case, which consists a kind of skeleton for the sets of results. Despite the apparent complexity of formulas, the interpolation is very simple, based on a linear interpolation on a log scale for pga, and linear scale for magnitude.

2.3.5.1 RVT case

Amplification factor

The objective is to estimate the amplification factor $AF_{RVT}(pga, m)$ corresponding to RVT approach for arbitrary values of pga and m.

Let $M_1 < m < M_2$ be the two nearest magnitudes for which the RVT amplification factor is known, and let $A_1 < pga < A_2$ be the two nearest peak accelerations for which the RVT amplification factor is known, then the interpolation formula is:

$$AF_{RVT}(pga, m) = C_{11} * AF_{RVT}(A_1, M_1) + C_{21} * AF_{RVT}(A_2, M_1) + C_{12} * AF_{RVT}(A_1, M_2) + C_{22} * AF_{RVT}(A_2, M_2)$$

With

$$\begin{aligned} C_{11} &= (M_2 - m) \cdot (LA_2 - L_{pga}) / [(M_2 - M_1) \cdot (LA_2 - LA_1)] \\ C_{12} &= (m - M_1) \cdot (LA_2 - L_{pga}) / [(M_2 - M_1) \cdot (LA_2 - LA_1)] \\ C_{21} &= (M_2 - m) \cdot (L_{pga} - LA_1) / [(M_2 - M_1) \cdot (LA_2 - LA_1)] \\ C_{22} &= (m - M_1) \cdot (L_{pga} - LA_1) / [(M_2 - M_1) \cdot (LA_2 - LA_1)] \end{aligned}$$

Where

$$L_{pga} = \log(pga) ; LA_1 = \log(A_1); LA_2 = \log(A_2)$$

Strains $(\gamma/\gamma_r)_{max}$

The weights between the various approaches are based on the estimation of the ratio $(\gamma/\gamma_r)_{max}$ for the RVT base case (see section 2.3.2).

This ratio has thus to be estimated for any arbitrary value of (pga, m) .

The proposed scheme is similar to the one proposed above for the amplification factor: Once having computed the coefficients C_{11} , C_{12} , C_{21} and C_{22} as indicated above, the coefficients should be used to interpolate $(\gamma/\gamma_r)_{max}$ values, with the following formula:

$$\begin{aligned} (\gamma/\gamma_r)_{max}(pga, m) &= C_{11} * (\gamma/\gamma_r)_{max}(A_1, M_1) + C_{21} * (\gamma/\gamma_r)_{max}(A_2, M_1) + C_{12} * (\gamma/\gamma_r)_{max}(A_1, M_2) \\ &\quad + C_{22} * (\gamma/\gamma_r)_{max}(A_2, M_2) \end{aligned}$$

2.3.5.2 SHAKE case

For $M=6$, the SHAKE amplification factors AF_{SHA} are available only for 3 acceleration levels (0.1, 0.4, 0.75 g) and for each velocity profile / material properties. For other magnitudes (5, 7), AF_{SHA} is generally available only for a limited number of profiles (B1_M1 for Beznau, G1_M1 for Gösigen, L2_M1 for Leibstadt, M1_M1 for Mühleberg). A more complex interpolation scheme, referring to the RVT base case, had therefore to be defined.

The objective is thus to estimate $AF_{SHA}(pga, m)$ for arbitrary values of pga and m . The basis of the interpolation is the proximity between RVT base case ("RVTBC") and SHAKE computations.

Let $A_1 < pga < A_2$ be the two nearest peak accelerations for which the amplification factor is known with SHAKE computations and let $M_1 < m < M_2$ be the two nearest magnitudes for which the amplification factors are known, then the estimation formula for any soil column is:

$$AF_{SHA}(pga, m) = AF_{RVTBC}(pga, m) * R_{SHA-RVTBC} * COR_m$$

where :

- $AF_{RVTBC}(pga, m)$ is derived as described in section 2.3.5.1
- $R_{SHA-RVTBC}$ is the SHAKE to RVTBC ratio computed on the exact soil profile and for magnitude 6
- COR_m is a correction factor to account for the effects of magnitude (which might have different effects on RVT computations and SHAKE computations).

Estimating the 'SHAKE to RVTBC' ratio $R_{SHA-RVTBC}$

$R_{SHA-RVTBC}$ is computed *using the actual soil profile under consideration and for magnitude 6*

$$R_{SHA-RVTBC} = B_1 * AF_{SHA}(A_1, 6) / AF_{RVTBC}(A_1, 6) + B_2 * AF_{SHA}(A_2, 6) / AF_{RVTBC}(A_2, 6)$$

with

$$\begin{aligned} B_1 &= (LA_2 - L_{pga}) / (LA_2 - LA_1) \\ B_2 &= (L_{pga} - LA_1) / (LA_2 - LA_1) \end{aligned}$$

where

$$Lpga = \log(pga); LA_1 = \log(A_1); LA_2 = \log(A_2)$$

Estimating the 'magnitude correction factor' COR_m

The magnitude correction factor, COR_m, is computed using the "reference site profile", defined as the site profile for which both RVT and SHAKE computations are available *for all magnitude levels*

$$COR_m = \sum_{i=1,2; j=1,2} C_{ij} * COR_{ij}$$

Where COR_{ij} is the specific magnitude correction factor for A_i and M_j, defined as the ratio between the M correction factor for SHAKE and the M correction factor for RVT:

$$COR_{ij} = [AF_{SHA,ref}(A_i, M_j) / AF_{SHA,ref}(A_i, 6)] / [AF_{RVTBC,ref}(A_i, M_j) / AF_{RVTBC,ref}(A_i, 6)]$$

and C_{ij} are interpolation weighting factors based on the distance of pga and m to A_i and M_j values [elementary 2-dimensional weighting]

$$\begin{aligned} C_{11} &= (M_2 - m) \cdot (LA_2 - Lpga) / [(M_2 - M_1) \cdot (LA_2 - LA_1)] \\ C_{12} &= (m - M_1) \cdot (LA_2 - Lpga) / [(M_2 - M_1) \cdot (LA_2 - LA_1)] \\ C_{21} &= (M_2 - m) \cdot (Lpga - LA_1) / [(M_2 - M_1) \cdot (LA_2 - LA_1)] \\ C_{22} &= (m - M_1) \cdot (Lpga - LA_1) / [(M_2 - M_1) \cdot (LA_2 - LA_1)] \end{aligned}$$

where

$$Lpga = \log(pga); LA_1 = \log(A_1); LA_2 = \log(A_2)$$

In other words :

$$\begin{aligned} COR_m &= C_{11} * [AF_{SHA,ref}(A_1, M_1) / AF_{SHA,ref}(A_1, 6)] / [AF_{RVTBC,ref}(A_1, M_1) / AF_{RVTBC,ref}(A_1, 6)] \\ &+ C_{22} * [AF_{SHA,ref}(A_2, M_2) / AF_{SHA,ref}(A_2, 6)] / [AF_{RVTBC,ref}(A_2, M_2) / AF_{RVTBC,ref}(A_2, 6)] \\ &+ C_{12} * [AF_{SHA,ref}(A_1, M_2) / AF_{SHA,ref}(A_1, 6)] / [AF_{RVTBC,ref}(A_1, M_2) / AF_{RVTBC,ref}(A_1, 6)] \\ &+ C_{21} * [AF_{SHA,ref}(A_2, M_1) / AF_{SHA,ref}(A_2, 6)] / [AF_{RVTBC,ref}(A_2, M_1) / AF_{RVTBC,ref}(A_2, 6)] \end{aligned}$$

Special cases:

If, for one particular value, A₀, of pga, SHAKE and RVTBC results are both available for the two magnitudes M1 and M2, then the formula above should be replaced by the following, simpler one:

$$COR_m = C_1 * [AF_{SHA,ref}(A_0, M_1) / AF_{SHA,ref}(A_0, 6)] / [AF_{RVTBC,ref}(A_0, M_1) / AF_{RVTBC,ref}(A_0, 6)] + C_2 * [AF_{SHA,ref}(A_0, M_2) / AF_{SHA,ref}(A_0, 6)] / [AF_{RVTBC,ref}(A_0, M_2) / AF_{RVTBC,ref}(A_0, 6)]$$

with

$$C_1 = (M_2 - m) / (M_2 - M_1); C_2 = (m - M_1) / (M_2 - M_1)$$

pga < 0.1g : apply the 0.1g correction factors:

$$COR_m = C_1 * [AF_{SHA,ref}(0.1g, M_1) / AF_{SHA,ref}(0.1g, 6)] / [AF_{RVTBC,ref}(0.1g, M_1) / AF_{RVTBC,ref}(0.1g, 6)] + C_2 * [AF_{SHA,ref}(0.1g, M_2) / AF_{SHA,ref}(0.1g, 6)] / [AF_{RVTBC,ref}(0.1g, M_2) / AF_{RVTBC,ref}(0.1g, 6)]$$

with

$$C_1 = (M_2 - m) / (M_2 - M_1); C_2 = (m - M_1) / (M_2 - M_1)$$

and

$$R_{SHA-RVTBC} = AF_{SHA}(0.1g, 6) / AF_{RVTBC}(0.1g, 6)$$

pga > 0.75 : apply the 0.75 g correction factors:

$$\text{COR}_m = C_1 * [\text{AF}_{\text{SHA,ref}}(0.75\text{g}, M_1) / \text{AF}_{\text{SHA,ref}}(0.75\text{g}, 6)] / [\text{AF}_{\text{RVTBC,ref}}(0.75\text{g}, M_1) / \text{AF}_{\text{RVTBC,ref}}(0.75\text{g}, 6)] \\ + C_2 * [\text{AF}_{\text{SHA,ref}}(0.75\text{g}, M_2) / \text{AF}_{\text{SHA,ref}}(0.75\text{g}, 6)] / [\text{AF}_{\text{RVTBC,ref}}(0.75\text{g}, M_2) / \text{AF}_{\text{RVTBC,ref}}(0.75\text{g}, 6)]$$

with

$$C_1 = (M_2 - m) / (M_2 - M_1); \quad C_2 = (m - M_1) / (M_2 - M_1)$$

and

$$R_{\text{SHA-RVT}} = \text{AF}_{\text{SHA}}(0.75\text{g}, 6) / \text{AF}_{\text{RVTBC}}(0.75\text{g}, 6)$$

2.3.5.3 Non-Linear case

The non-linear amplification factors, $\text{AF}_{\text{NL}}(\text{pga}, m)$, are available only for one magnitude ($M=6$), three acceleration levels (0.4, 0.75, 1.5 g) and for one single set of velocity profile and material properties per site; in addition, the latter are not directly related to the material properties accounted for in the linear equivalent approaches. There is an exception, however, for Leibstadt, where two velocity profiles, L_i ($i=1,2$), have been considered: $\text{AF}_{\text{NL}}(\text{pga}, 6, L_i)$.

The objective is thus to estimate the NL amplification factor AF_{NL} for arbitrary values of pga and m. The interpolation scheme is again based on the RVT base case, with similar formulas, but over a modified acceleration range: 0.4 – 1.5g

General case ($0.4 \text{ g} \leq \text{pga} \leq 1.5 \text{ g}$, $5 \leq m \leq 7$)

Let $A_1 < \text{pga} < A_2$ be the two nearest peak accelerations for which the amplification factor is known with NL computations (here, implicitly, $\text{pga} \geq 0.4 \text{ g}$).

Let $M_1 < m < M_2$ be the two nearest magnitudes for which the amplification factors are known for RVT base case.

Then the estimation formula for any soil column $S_i_M_j$ (vel. profile i for site S, material set j) is:

$$\text{AF}_{\text{NL}}(\text{pga}, m) = \text{AF}_{\text{RVTBC}}(\text{pga}, m, S_i_M_j) * R_{\text{NL-RVTBC}}(\text{pga}, S_i_M_j)$$

where:

$\text{AF}_{\text{RVTBC}}(\text{pga}, m, S_i_M_j)$ is the RVT base case amplification factor computed for the actual soil column under consideration, $S_i_M_j$, and for the (pga,m) values, as detailed above in section 2.3.5.1

$R_{\text{NL-RVTBC}}$ is the estimated ratio between NL response and RVT response, computed only at magnitude 6

Estimating the 'NL to RVTBC' ratio $R_{\text{NL-RVTBC}}$: general case:

$R_{\text{NL-RVTBC}}$ is computed on the exact soil profile and for magnitude 6

$$R_{\text{NL-RVTBC}}(\text{pga}, S_i_M_j) = B_1 * \text{AF}_{\text{NL}}(A_1, 6) / \text{AF}_{\text{RVTBC}}(A_1, 6, S_i_M_j) \\ + B_2 * \text{AF}_{\text{NL}}(A_2, 6) / \text{AF}_{\text{RVTBC}}(A_2, 6, S_i_M_j)$$

with

$$B_1 = (LA_2 - L\text{pga}) / (LA_2 - LA_1)$$

$$B_2 = (L\text{pga} - LA_1) / (LA_2 - LA_1)$$

where

$$L\text{pga} = \log(\text{pga}); \quad LA_1 = \log(A_1); \quad LA_2 = \log(A_2)$$

Estimating the "NL to RVTBC" ratio $R_{\text{NL-RVTBC}}$: Leibstadt case

As NL amplification factors are available for the two velocity profiles (with or without cementation in the deep layers), the same interpolation formula is proposed, but considering the relevant velocity profile

$$R_{NL-RVTBC}(pga, L_i, M_j) = B_1 * AF_{NL}(A_1, 6, L_i) / AF_{RVTBC}(A_1, 6, L_i, M_j) + B_2 * AF_{NL}(A_2, 6, L_i) / AF_{RVTBC}(A_2, 6, L_i, M_j)$$

Particular case ($pga < 0.4 \text{ g}$)

It may occur that one also needs NL amplification factors below 0.4 g (Leibstadt for instance, for which the strain ratio $(\gamma/\gamma_r)_{max}$ exceeds one at very low acceleration levels). Then the estimation procedure has to be slightly modified, as described below:

$$AF_{NL}(pga, m) = AF_{RVTBC}(pga, m) * R_{NL-RVTBC}$$

with

$$R_{NL-RVTBC} = D_1 * AF_{NL}(0.4g, 6) / AF_{RVTBC}(0.4g, 6) + D_2$$

where

$$D_1 + D_2 = 1$$

$$D_2 = 1, D_1 = 0 \text{ if } (\gamma/\gamma_r)_{max} < 1$$

$$D_2 = \log [(\gamma/\gamma_r)_{max}] / [\log (\gamma/\gamma_r)_{max, 0.4g}] \text{ if } (\gamma/\gamma_r)_{max} > 1$$

Here $(\gamma/\gamma_r)_{max, 0.4g}$ is the value of $(\gamma/\gamma_r)_{max}$ obtained for the RVT base case at 0.4g pga level and magnitude 6.

2.3.6 Extrapolation for large pga and/or magnitude values

The input acceleration levels and/or corresponding magnitudes may exceed the maximum values considered for the computations, i.e., 1.5 g and 7, respectively. It is therefore necessary to define an extrapolation scheme.

The procedures detailed below apply to amplification factors obtained with the Linear Equivalent (SHAKE, RVT) and Non Linear approaches. They do not apply to the "linear approach" (RVT base case 0.05g) – in case it would be required with a non-zero weight at high acceleration levels.

2.3.6.1 Large input acceleration levels: beyond 1.5 g – And $m \leq 7$

As the experience is very limited at such high acceleration levels, the epistemic uncertainty is considered to be very large: that is why a subbranching, with three branches, is introduced. This subbranching applies to all estimates, whatever the approach used.

The main idea is to base the estimates on the results computed for $pga = 1.5 \text{ g}$., by multiplying them by an 'uncertainty' function E_H which is assigned different values along each subbranch

$$AF(pga, m) = AF(1.5g, m) \cdot E_H(f, f_0, C_H)$$

with

$$E_H(f, f_0, C_H) = \exp[C_H(pga) \cdot E(kf/f_0)]$$

E is a function introduced to describe the frequency dependence of uncertainty, which is thought to be limited at low frequency, and larger at high frequency:

$$\begin{aligned} E(x) &= 0. & \text{for } x \leq 0.5 \\ E(x) &= \log(2x) / \log(2) & \text{for } 0.5 \leq x \leq 1.0 \\ E(x) &= 1. & \text{for } x > 1.0 \end{aligned}$$

f_0 is the low strain fundamental frequency of the site (the value is given for each site). The multiplying factor 3 is introduced to account for the decrease of fundamental frequency at very large strains.

k is a frequency scaling factor introduced to take into account the low frequency shift at high strains:

$$k = 3 \{ 1 + \log(\text{pga}/1.5) / \log(2.5/1.5) \}$$

C_H is a 'correcting factor' which is uncertain, and takes different values for each subbranch. It is dependent on pga , as the epistemic uncertainty is increasing with increasing pga . The values and weights are given below:

$C_H = \text{Min} \{ \log(\text{pga}/1.5) / \log(2.5/1.5) , 1.5 \}$	weight : 25%
$C_H = 0$	weight : 50%
$C_H = \text{Max} \{ - \log(\text{pga}/1.5) / \log(2.5/1.5) , -1.5 \}$	weight : 25%

where pga is expressed in g units

This functional form ensures that the median estimate is unchanged: only the epistemic uncertainty is increased at large pga / strains. The C_H values are bounded in order to avoid unrealistic highs or lows in the amplification factor (although I really do not know what may happen for input pga as large as 3 g !).

2.3.6.2 Large magnitudes (> 7) – and $\text{pga} \leq 1.5$ g

For magnitudes > 7, simply use the results or estimates corresponding to magnitude 7.

2.3.6.3 Large magnitudes (> 7) – and $\text{pga} > 1.5$ g

In that case, the 3 branches already introduced for $\text{pga} > 1.5$ g should be used, with similar weights, as detailed below:

$$\text{AF}(\text{pga}, m) = \text{AF}(1.5\text{g}, 7) \cdot E_H(f, f_0, C_H)$$

with

$$E_H(f, f_0, C_H) = \exp[\exp[C_H(\text{pga}) \cdot E(kf/f_0)]]$$

$k = 3 \{ 1 + \log(\text{pga}/1.5) / \log(2.5/1.5) \}$	
$C_H = \text{Min} \{ \log(\text{pga}/1.5) / \log(2.5/1.5) , 1.5 \}$	weight : 25%
$C_H = 0$	weight : 50%
$C_H = \text{Max} \{ - \log(\text{pga}/1.5) / \log(2.5/1.5) , -1.5 \}$	weight : 25%

2.3.7 Effect of incident wavefield (wave type and incidence angle)

There is neither branching, nor any systematic modification of amplification factor derived for vertically incident SH waves. Wave type (SV, P, SH, ...) and incidence / azimuth angles are thought to affect only the aleatory variability and not the average value. This assessment on the effects the incident wave field characteristics holds for the surface motion as well as the motions at depth.

The question that has to be answered is how to modify the surface aleatory variability value σ_{PSV} at the different sites for the two additional depth levels:

- Sites BZ1, GZ1, GZ2, LZ1, LZ2, MZ1 are very close to the surface and in the same geological unit as the surface site: given the wavelengths at frequencies below 10 Hz, I propose to keep the same σ_{PSV} values as for the surface sites.
- Site MZ2 is located within the underlying, much stiffer bedrock. Considering also the proximity to the sediment-basement interface, I consider the additional aleatory variability should be reduced, but cannot vanish. I therefore propose to apply values reduced by half : $0.5 \sigma_{PSV}$ (σ_{PSV} = value for the site surface).
- Site BZ2 is also located within a much stiffer sub layer (Opalinuston); however, it is involved in the fundamental resonance of the site. I therefore propose to apply here an intermediate value: $0.75 \sigma_{PSV}$ (σ_{PSV} = value for the site surface).

2.3.8 2-D / 3-D effects

The subsoil / surface topography structure always exhibit some amount of lateral variations. The few 2D-computations for the Leibstadt case indicate the possibility of significant geometrical effects due to nearby lateral heterogeneities, in relation – in that particular case – to the topography of the river terrace. A survey of the cross-sections for each NPP site shows the existence of such lateral heterogeneities, at variable distances from the NPP site, and with variable geometrical characteristics.

In addition, NPP themselves, which are very stiff concrete structures, constitute heterogeneities that do radiate some energy back into the soil, which then propagate at least partly as surface waves.

The physics of the wave diffraction makes this phenomenon sensitive to many parameters: wave type (plane / surface wave, P, SV, SH – in relation to source depth and mechanism), incidence characteristics (incidence, azimuth). It seems impossible to account for all these effects in a 'pseudo-deterministic' way, especially when the consideration of the source (magnitude, distance, azimuth) and the site effects are completely decoupled.

A simplified model has therefore been built to account for these geometrical effects. Its formulation is based on the interpretation of 2D/3D effects as surface waves diffracted by the main lateral heterogeneities, and its quantitative parameters have been calibrated on the results obtained for the Leibstadt case.

This model is described below; its parameters are heavily site dependent and are therefore detailed for each site in the relevant sections. Since some uncertainties exist in the estimates of these effects, a subbranching has been introduced with different parameter values, and different weights.

General formula:

The amplification factors derived with either approach should be multiplied by a 2D factor A_{2D} defined as:

$$A_{2D}(f, \zeta) = 1 + C_{2D}(f, \zeta)$$

with

$$C_{2D}(f, \zeta) = A(f, f_0) B(f, \zeta)$$

where

f is the frequency

f_0 is the fundamental frequency at the site under consideration

ζ is an average damping value in the surficial soils where surface waves diffracted on lateral heterogeneities are propagating.

Frequency dependence: $A(f, f_0)$

The Leibstadt computations (from D. Fäh and P.-Y. Bard), as well as the abundant scientific literature, indicate that 2D and 3D effects appear only above the site fundamental frequency, f_0 . $A(f, f_0)$ is therefore defined as a ramp function on a logarithmic frequency axis:

$$A(f, f_0) = A_0(f/f_0)$$

with

$$\begin{aligned} A_0(x) &= 0 && \text{for } x \leq 0.7 \\ A_0(x) &= -(\log(x/0.7)) / \log(0.7) && \text{for } 0.7 < x \leq 1 \\ A_0(x) &= 1 && \text{for } 1 < x \end{aligned}$$

Geometrical / damping dependence : $B(f, \zeta)$

The diffracted waves are generated on the lateral heterogeneities, and then propagate to the site; their amplitude at the site will therefore depend both on the distance to the heterogeneities, and on the damping values. The proposed model therefore is:

$$B(f, \zeta) = C_{2D}^0 \cdot \exp(-2\pi\zeta_{av} f l / \beta_m)$$

where

- C_{2D}^0 represents, in some way, the amplitude of the diffracted waves (normalized to the incident wavefield) on the heterogeneity; it is also, approximately, the largest possible 2D effect at the site (corresponding to the low strain / very low damping case). *This value is uncertain, and, for each site, different values are proposed with different weights.*
- the last term $\exp(-2\pi\zeta_{av} f l / \beta_m)$ represents the amplitude decay due to the propagation from the heterogeneity to the site:

ζ_{av} is the average damping over the soil column: it is pga dependent because of NL material degradation (see below).

l is the distance of the NPP site to the closest lateral heterogeneity

β_m is the average S-wave velocity in the soil column

Estimating ζ_{av}

- Linear case : $\zeta_{av} = 0.0125$ (corresponds to a quality factor Q value of 40)
- Linear equivalent case (SHAKE and RVT):

The simplest procedure is to start from the normalized strain values $\gamma/\gamma_r(z)$ computed in the RVT base case (from which is also derived the maximum strain $(\gamma/\gamma_r)_{max}$ used for weighting the NL approach), and to derive the damping in each layer through the formula $\zeta(z) = \zeta_{max} (\gamma/\gamma_r) / [1 + (\gamma/\gamma_r)] = 0.3 (\gamma/\gamma_r) / [1 + (\gamma/\gamma_r)]$. The last step is to average $\zeta(z)$ over the whole soil column of thickness h by weighting the value in each thin individual layer i with the corresponding thickness h_i , and dividing by the total thickness h): $\zeta_{av} = \sum_i \zeta(z_i) \cdot h_i / h$

Another procedure could have been to start directly from the $\zeta(z)$ computed in the RVT base case, and to average it over the whole soil column as described in the previous paragraph: $\zeta_{av} = \sum_i \zeta(z_i) \cdot h_i / h$. However, as those values are not available from the RVT computations, the first, simpler procedure is selected.

- NonLinear case : simply apply the ζ_{av} values from the linear equivalent approach

The Tables 2-2 to 2-5 presented in the next sections provide, for each NPP site, the values of f_0 , C_{2D}^0 , l , β_m and h , as well as the corresponding weighting. Three subbranches are introduced with different weights to account for the uncertainties in the parameter estimates (mainly indeed

C_{2D}^0). One of the subbranches corresponds to $C_{2D} = 0$, as it is likely, that the input motion estimates underlying the site effect computations contain (at least partly) some unknown amount of 2D/3D effects. The other values are based on the actual geological cross-sections at each site, and some subjective 'expert judgement', calibrated on the computed effects for Leibstadt. The parameter studies performed in that case also show the large sensitivity to damping values. From the Leibstadt 2D-computations, one may conceive that NL 1D-effects may have been overemphasized in the existing literature based on observed strong motion data simply because 2D/3D effects become less and less important as damping increases.

2D/3D Effects at depth

For the motion at depth, the same surface wave interpretation will be kept: as the amplitude of ground motion is strongly depth-dependent for surface waves, the 2D/3D surface factors are modified by a depth-dependent factor $C(z)$, except for the sites which are located beneath the sediment-basement interface responsible for the trapping of surface waves.

The 1D-amplification factors derived with either approach should thus be multiplied by a 2D factor A_{2D} defined as:

$$A_{2D}(f, \zeta, z) = 1 + A(f, f_0) B(f, \zeta) \cdot C(z)$$

The $C(z)$ factor is estimated with a very simple assumption, corresponding both to the depth dependence due to vertically incident S-waves, and to mode shapes around the fundamental frequencies:

$$C(z) = \text{Max} \{ |\cos(\omega z/c)|, 0.2 \} \approx \text{Max} \{ |\cos(2\pi f z/\beta_m)|, 0.2 \}$$

Where β_m is the average shear wave velocity already specified for these 2D effects.

The minimum value of 0.2 is introduced to avoid the vanishing at some frequencies, as it is considered that in real nature, the interferences at depth can never be totally destructive because of heterogeneities.

Comparing the thicknesses h of the 'trapping layers' (see relevant section for surface motion) with the actual depth of the various sites, this formulation should therefore be applied to the two deep sites at Beznau ($h = 65 \text{ m} > z_2$), Gösigen ($h = 25 \text{ m} > z_2$), Leibstadt ($h = 25 \text{ m} > z_2$), to the intermediate site MZ1 at Mühleberg ($h = 10 \text{ m} > z_1$).

However, this 2D-overamplification term should NOT be applied to the deepest site MZ2 at Mühleberg ($h=10 \text{ m} < z_2 = 14 \text{ m}$): for this particular case, there is no subbranching for 2D effects (or, in other terms, 1 single branch with weight 100% for the value $C_{2D} = 0$).

2.3.9 Estimation of 'outcropping motion' NL amplification factors at depth

2.3.9.1 General scheme

The available NL amplification factors are the AFNL values at the surface (outcrop, noted as $AFNL_{surf}$) and at depth for within motion (noted as $AFNL_{depth, within}$).

Simultaneously, the Linear Equivalent amplification factors are available both for within and outcropping motion.

Therefore, the following ways were considered to estimate the requested values of $AFNL_{depth, outcrop}$. were considered:

- Option 1 : considering only outcropping motions

$$AFNL_{depth, outcrop} = AFNL_{surf} \cdot AFLE_{depth, outcrop} / AFLE_{surf}$$

The correcting factor is here based on the assumption that the variations with depth are similar for NL and LE approaches

- Option 2 : considering only motions at depth

$$AFNL_{\text{depth,outcrop}} = AFNL_{\text{depth,within}} \cdot AFLE_{\text{depth,outcrop}} / AFLE_{\text{depth,within}}$$

The correcting factor is here based on the assumption that the variations between outcropping and within motions are similar for NL and LE approaches

Each option has some advantages and drawbacks: Option 1 leads to more stable estimates (no destructive interferences in outcropping motion), but it does not take into account the possible localization of deformation in NL computations. And vice-versa for option 2.

As a consequence, the estimations of $AFNL_{\text{depth,outcrop}}$ are made with a subbranching considering these two options, with weights $W_1 = 40\%$ for option 1 and weight $W_2 = 60\%$ for the second one. Option 2 is slightly preferred because it takes into account only ground motion at depth, which should be better in case of strain localization at some depth)

2.3.9.2 Additional details

The Non-Linear amplification factors AFNL are available, at surface and depth, only for magnitude 6 signals, 3 acceleration levels (0.4, 0.75, 1.5 g) and for one single set of velocity profile and material properties per site; in addition, the latter are not directly related to the material properties accounted for in the linear equivalent approaches [there is an exception, however, for Leibstadt, where the 2 velocity profiles L_i ($i=1,2$) have been considered].

One must thus detail which LE model should be used for the correction factors. Since the outcrop and within motion have been simultaneously computed only for the SHAKE approach, AFLE, in the above formula, should be read as follows:

- estimate the AFNL depth,outcrop for magnitude 6 signals, the 3 acceleration levels and each velocity profile S_i / material characteristics M_j

$$\text{Option 1: } AFLE_{\text{depth,outcrop}} / AFLE_{\text{surf}} = AF_{\text{SHA,, depth,outcrop}}(\text{pga},6,S_i,M_j) / AF_{\text{SHA,, depth,outcrop}}(\text{pga},6,S_i,M_j)$$

$$\text{Option 2: } AFLE_{\text{depth,outcrop}} / AFLE_{\text{depth,within}} = AF_{\text{SHA,, depth,outcrop}}(\text{pga},6,S_i,M_j) / AF_{\text{SHA,, depth,within}}(\text{pga},6,S_i,M_j)$$

- extrapolate to other magnitude and pga values as detailed for the surface NL amplification factors, on the basis of the RVT base case for the $S_i_M_j$

2.4 Beznau

2.4.1 Site-Specific Model Evaluations

2.4.1.1 Alternative velocity profiles

Three alternative velocity models are proposed for Beznau: B1 is based on cross-hole measurements and a nearby deep borehole, B2 and B3 are based on surface microtremor measurements.

My weighting is based on the following considerations:

- assigning an equal weight on either approach (borehole / surface investigations), which results in B1 50% – B2+B3 50% –

- between B2 and B3: B2 is mainly based on fitting the H/V curve with Rayleigh wave ellipticity, with some assumptions on the energy ratio between Love and Rayleigh waves, and a quality of fit theory / observation that is not so impressive. On the contrary, B3 is derived from the inversion of phase velocities obtained with array measurements, which, up to now, I consider more reliable than inversion from H/V ellipticity. Therefore I assign a weight of 20% to B2 and 30% to B3.

2.4.1.2 Alternative 2D parameters

According to the cross-sections provided by PROSEIS, the subsoil structure is varying mainly along the EW direction for the very surface, but there also exist some variations at larger depth along the NS cross-section. From the cross-section NPP_B_CENTRE, the edge is located 250 m to the west. I anticipate an 'edge' effect in the shallow surficial layer; however, the velocity profiles show that there is not much impedance contrast at this interface, so that the profile may not be relevant. From the cross-section NPP_B_NS, the edge is located 300 m to the north. I anticipate a significant 'edge' effect in the opalinuston unit.. This should clearly produce some effects around the fundamental frequency.

In addition, from all cross-sections, the surface layer thickness irregularities just below the NPP should induce some wave trapping. Therefore, the parameters for the additional 2D/3D effects take into account the NS 2D variations in the deep structure, and are associated with the fundamental frequency $f_0 = 2.5$ Hz, and the thick layers including opalinustone, with $h=65$ m. Since this unit has a limited NL behavior, I do not expect much NL reduction effect in this 2D amplification; it is, however, 'automatically' adjusted through the damping parameter ζ_{av} .

2.4.2 Summary of weights and parameters fro Beznau

Tab. 2-2: Summary of weights and computational parameters for the horizontal ground motion at Beznau site

Weights for the median site amplification factor and corresponding aleatory variability for horizon tal ground motion: Site Beznau			
<i>Velocity profile</i>			
B1	B2	B3	
0.50	0.20	0.30	
<i>Nonlinear properties</i>			
irrelevant (One single model)			
<i>Approaches</i>			
Deformation range (γ/γ_r) _{max}	RWF(SHAKE)	RWF(RVT)	Linear (Base case RVT 0.05g) Non-linear
< 1	0.48	0.32	0.20 0
> 1 and < 31.62	0.48*Red_LE[(γ/γ_r) _{max}]	0.32*Red_LE[(γ/γ_r) _{max}]	Complement to 1, i.e., 0.9 0.8*Red_LE[(γ/γ_r) _{max}] + sub-branching
> 31.62	0.15	0.10	0.75 + sub-branching
Fixed parameters for computing the frequency dependence of the relative SHAKE and RVT weights		f1=0.5 Hz	f2=1.0 Hz
<i>RVT Subsets</i>			
Base case			
15/40=0.375			
Random model			
25/40=0.625			
<i>Magnitude / pga interpolation + extrapolations</i>			
<i>Linear</i>		<i>Non-linear</i>	
SHAKE		RVT	
See formulas			
<i>P-SV sensitivity</i>			
No change on the median			
For the aleatory variability, consider three possibilities	$\sigma_{P-SV} = 0\%$ $\sigma_{\log10P-SV} = 0.0$ Weighting = 0.3	$\sigma_{P-SV} = 20\%$ $\sigma_{\log10P-SV} = 0.079$ Weighting = 0.4	$\sigma_{P-SV} = 50\%$ $\sigma_{\log10P-SV} = 0.176$ Weighting = 0.3
<i>2D effects :</i>			
$A_{2D} = 1 + C_{2D}(f, \zeta) = 1 + C_{2D}^0 \cdot A_0(f/f_0) \cdot \exp(-2\pi\zeta_{av} \cdot f l / \beta_m) \cdot \zeta_{av} = \sum_i h_i \cdot 0.3 (\gamma/\gamma_r) / [1. + (\gamma/\gamma_r)] / h$			
Fixed parameters	f0 = 2.5 Hz	l = 300 m	$\beta_m = 500$ m/s h = 65 m
Alternative choice for parameters and corresponding weights	$C_{2D}^0 = 0.0$ weight 0.10	$C_{2D}^0 = 0.20$ weight 0.60	$C_{2D}^0 = 0.50$ weight 0.30
For the aleatory variability, consider the associated aleatory variability	$\sigma_{2D} = 0\%$ $\sigma_{\log102D} = 0.0$	$\sigma_{2D} = 20\%$ $\sigma_{\log102D} = 0.08$	$\sigma_{2D} = 50\%$ $\sigma_{\log102D} = 0.18$

2.5 Gösgen

2.5.1 Site-Specific Model Evaluations

2.5.1.1 Alternative NL material properties

As already discussed above (section 2.3.1), I assign a 65% weight to the Ishibashi & Zhang curves (M1), and a 35% weight to the Hardin & Drnevich curves (M2)

2.5.1.2 Alternative 2D parameters

According to the cross-sections provided by PROSEIS, the subsoil structure is varying mainly along the NS direction, and these variations are only very slight.

- The NS cross-section NPP_G_CENTRE exhibits a thinning of the surface layer down to about 10 m at 550 m north of the NPP site. There also exist some thickness irregularities under the NPP (but this is probably due to the larger density of borings).
- From the cross-section NPP_G_EW, I do not anticipate significant effects since the thickness is rather regular, and the distance to the thinning section on the West is about 900 m: diffracted waves have time and distance to damp out, especially as they are high frequency ($f > 5$ Hz) and short wavelength.

Therefore, there probably exist some 2D effects, but much less pronounced than for Leibstadt (modelled) and Beznau (expected).

2.5.2 Summary of weights and parameters

Tab. 2-3: Summary of weights and computational parameters for the horizontal ground motion at Gösgen site

Weights for the median site amplification factor and corresponding aleatory variability for horizontal ground motion : <i>Site Goesgen</i>		
<i>Velocity profile</i>		
Irrelevant (one single profile)		
<i>Nonlinear properties</i>		
M1	M2	
0.65	0.35	
<i>Approaches</i>		
Deformation range (γ/γ_r) _{max}	RWF(SHAKE)	RWF(RVT)
< 1	0.48	0.32
> 1 and < 31.62	0.48 Red_LE[(γ/γ_r) _{max}]	0.32 Red_LE[(γ/γ_r) _{max}]
> 31.62	0.15 at high frequency	0.10 at high frequency
Fixed parameters for computing the frequency dependence of the relative SHAKE and RVT weights		
<i>RVT Subsets</i>		
Base case		
15/40=0.375		
<i>Magnitude / pga interpolation + extrapolations</i>		
Linear	SHAKE	RVT
Non-linear		
<i>See formulas</i>		
<i>P-SV sensitivity</i>		
No change on the median		
For the aleatory variability, consider three possibilities	$\sigma_{P-SV} = 0\%$ $\sigma_{\log 10P-SV} = 0.0$ Weighting = 0.3	$\sigma_{P-SV} = 20\%$ $\sigma_{\log 10P-SV} = 0.079$ Weighting = 0.4
$2D$ effects: $A_{2D} = I + C_{2D}(f, \zeta) = I + C_{2D}^0 \cdot A_0(f/f_0) \cdot \exp(-2\pi\zeta_{av} \cdot f l / \beta_m) \cdot \zeta_{av} = \sum_i h_i \cdot 0.3 (\gamma/\gamma_{rD}) / [1. + (\gamma/\gamma_{rD})] / h$		
Fixed parameters	$f_0 = 4.0$ Hz	$l = 550$ m
Alternative choice for parameters and corresponding weights	$C_{2D}^0 = 0$ weight 0.70	$\beta_m = 416$ m/s $h = 25$ m
For the aleatory variability, consider the associated aleatory variability	$\sigma_{2D} = 0\%$ $\sigma_{\log 102D} = 0.08$	$C_{2D}^0 = 0.20$ weight 0.30 $\sigma_{2D} = 20\%$ $\sigma_{\log 102D} = 0.18$

2.6 Leibstadt

2.6.1 Site-Specific Model Evaluations

2.6.1.1 Alternative velocity and NL material properties

Evaluation of alternative velocity profiles: The differences between L1 and L2 velocity profiles correspond to the cementation of the gravels below 30 m for L2 profile. According to the existing documentation and the discussion within the expert group (especially the indications from J. Studer), the cementing is very heterogeneous, and there is little chance that it is completely cemented from 30 to 50 m. I therefore assign a weight of 80% to the non-cemented case (L1) and 20% to the cemented case (L2).

Evaluation of alternative non-linear profiles: For the L1 profile, there are two options: Ishibashi & Zhang (M1), or Hardin & Drnevich (M2). As discussed above, the respective weights are 65% and 35%. For the L2 profile, there are again two options: Ishibashi & Zhang, or Hardin & Drnevich, but these options concern only the top non-cemented layer. The underlying cemented layer has fixed NL curves, with which I feel very uncomfortable, since it drops below the non-cemented (even the H&D one !) at high strains: it should be at least the same !. The consequence in Shake and RVT computations is that the strain is concentrated in this "cemented layer" unit for large pga, especially in the I&Z case, and it leads to results which seem unrealistic to me. Therefore, because of the unexpected behaviour of the nonlinear properties for this L2 profile, I will assign only a 25% weight to I&Z (M'1), and a 75% weight to H&D (M'2)

Final combined weights:

L1_M1	: 50% (0.80 x 0.65)
L1_M2	: 30 % (0.80 x 0.35)
L2_M'1	: 5 % (0.2 x 0.25)
L2_M'2	: 15 % (0.2 x 0.75)

2.6.1.2 Alternative 2D parameters

The two series of available computations (from D. Fäh and P.-Y. Bard) are consistent in exhibiting significant 2D effects, which are larger in case of waves coming from the N – NW (corresponding to forward diffraction on the river terrace). These computations may be approximately fitted with a C_{2D}^0 around 30%.

The maps and the various cross-sections (NPP_L_CENTRE, NPP_L_EW, NPP_L_NW-SE) all indicate close lateral variations linked with the river terrace:

- NS: the terrace is located 120 m to the north of the NPP site
- EW: the terrace is located 150 - 300 m to the west of the NPP (irregular topogr. to the west)
- NW-SE: the terrace is located about 100 m to the NW of the NPP site

In addition, the same terrace is bending, and is also present 350 m to the ENE of the NPP site. Considering such a structure, I anticipate some kind of 3D effects. I therefore include a sub-branch with larger values for C_{2D}^0 parameter .

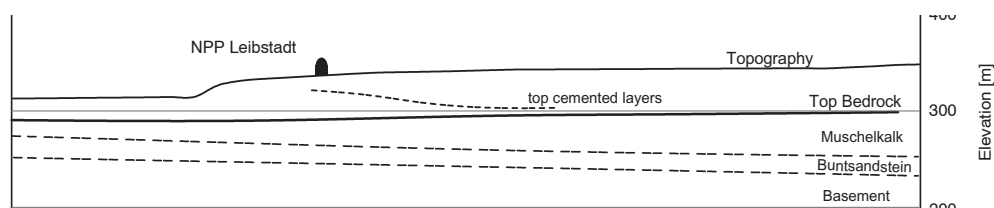


Fig. 2-2: NS cross-section through the Leibstadt NPP site (north is to the left)

2.6.2 Summary of weights and parameters

Tab. 2-4: Summary of weights and computational parameters for the horizontal ground motion at Leibstadt site

Weights for the median site amplification factor and corresponding aleatory variability for horizontal ground motion : Site Leibstadt			
<i>Velocity profile and NL properties</i>			
L1_M1	L1_M2	L2_M1	L2_M2
0.50	0.30	0.05	0.15
<i>Nonlinear properties</i>			
cf above			
<i>Approaches</i>			
Deformation range (γ/γ_r) _{max}	RWF(SHAKE)	RWF(RVT)	Linear (Base case RVT 0.05g) Non-linear
< 1	0.40	0.40	0.20 0
> 1 and < 31.62	0.40*Red_LE[(γ/γ_r) _{max}]	0.40*Red_LE[(γ/γ_r) _{max}]	0.10 Complement to 1, i.e., 0.9 0.8Red_LE[(γ/γ_r) _{max}] + sub-branching
> 31.62	0.125	0.125	0.0 0.75 + sub branching
Fixed parameters for computing the frequency dependence of the relative SHAKE and RVT weights			
		f1=0.5 Hz	f2=1.0 Hz
<i>RVT Subsets</i>			
Base case			
15/50=0.30		Random model 35/50=0.70	
<i>Magnitude / pga interpolation + extrapolations</i>			
Linear		SHAKE	RVT
		Non-linear	
<i>See formulas</i>			
<i>P-SV sensitivity</i>			
No change on the median			
For the aleatory variability, consider three possibilities	$\sigma_{p-sv} = 0\%$ $\sigma_{\log 10p-sv} = 0.0$ Weighting = 0.3	$\sigma_{p-sv} = 20\%$ $\sigma_{\log 10p-sv} = 0.079$ Weighting = 0.4	$\sigma_{p-sv} = 50\%$ $\sigma_{\log 10p-sv} = 0.176$ Weighting = 0.3
<i>2D effects: $A_{2D} = 1 + C_{2D}(f, \zeta) = 1 + C_{2D}^0 A_0(f/f_0) \exp(-2\pi\zeta_{av} f / \beta_m) \zeta_{av} = \sum_i h_i \cdot 0.3 (\gamma/\gamma_{ri}) / [1. + (\gamma/\gamma_{ri})] / h$</i>			
Fixed parameters	f0 = 2.0 Hz	l = 100 m	$\beta_m = 400$ m/s h = 50 m
Alternative choice for parameters and corresponding weights	$C_{2D}^0 = 0.00$ weight 0.10		$C_{2D}^0 = 0.30$ weight 0.60 $C_{2D}^0 = 0.60$ weight 0.30
For the aleatory variability, consider the associated aleatory variability	$\sigma_{2D} = 0\%$ $\sigma_{\log 102D} = 0.0$	$\sigma_{2D} = 20\%$ $\sigma_{\log 102D} = 0.08$	$\sigma_{2D} = 50\%$ $\sigma_{\log 102D} = 0.18$

2.7 Mühleberg

2.7.1 Site-Specific Model Evaluations

2.7.1.1 Alternative NL material properties

As already discussed above (section 2.3.1), I assign a 65% weight to the Ishibashi & Zhang curves (M1), and a 35% weight to the Hardin & Drnevich curves (M2)

2.7.1.2 Estimating NL amplification factors

For the Mühleberg case, no NL computation has been performed. Yet, there exist cases for which RVT base case strains lead to $(\gamma/\gamma_r)_{\max}$ values exceeding 1, especially in the case with material properties following the Hardin & Drnevich model. A special procedure is therefore to be applied to estimate the NL amplification factors; this estimation is automatically associated with a higher level of epistemic uncertainty. The subbranches for other cases where NL computations are available, are thus to be replaced by other subbranches with different NL amplification factor estimates, corresponding to a wider range (larger uncertainty).

The NL amplification factors are to be estimated from the corresponding RVT base case result, as follows :

$$AF_{NL}(f; pga, m) = AF_{RVTBC}(f; pga, m) \cdot F_{NL, M\ddot{u}hl}(f, C_{MNL})$$

with

$$F_{NL, M\ddot{u}hl}(f, C_{MNL}) = 1 + C_{MNL} E(f/3)$$

Where E is the already defined function: as the low strain fundamental frequency for Mühleberg is around 10 Hz, the consideration of the function $E(f/3)$ implicitly assumes that the fundamental frequency may be reduced down to 3 Hz, i.e., by a factor of 3. This is consistent with the "k" value introduced to account for the decrease of fundamental frequency in the NL subbranching described in section 2.3.3 ($k = 1. + 2 * [\log(pga/0.4) / \log(1.5/0.4)]$). The fundamental frequency reducing factor is uniformly set equal to 3 whatever the pga, simply because the epistemic uncertainty is larger here.

C_{MNL} takes several values, with different weights

$C_{MNL} = 2$	+ weight: 10%
$C_{MNL} = 1$	+ weight : 25%
$C_{MNL} = 0$	+ weight : 30%
$C_{MNL} = - 0.5$	+ weight : 25%
$C_{MNL} = - 0.667$	+ weight : 10%

2.7.1.2 Alternative 2D parameters

According to the cross-sections provided by PROSEIS, the topography and subsoil exhibit significant lateral variations since the NPP site is within a river valley having an EW "banana" shape". The most relevant cross-sections are those perpendicular to local valley axis, i.e., NPP_M_CENTRE (NS through the site), M_EAST (NNW-SSE east of the NPP) and M_WEST (NNE-SSW west of the NPP)

- The NS cross-section NPP_M_CENTRE exhibit a valley type topography, filled with thin quaternary layers over a total distance of about 700 m and a maximum thickness of about 15 m. The NPP site is located 200 m north of the southern edge of this sedimentary filling.

2.7.2 Summary of weights and parameters

Tab. 2-5: Summary of weights and computational parameters for the horizontal ground motion at Mühleberg site

Weights for the median site amplification factor and corresponding aleatory variability for horizontal ground motion : <i>Site Muehleberg</i>			
<i>Velocity profile</i>			
Irrelevant (One single profile)			
<i>Nonlinear properties</i>			
M1		M2	
0.65		0.35	
<i>Approaches</i>			
Deformation range $(\gamma/\gamma_r)_{max}$	RWF(SHAKE)	RWF(RVT)	Linear (Base case RVT 0.05g) Non-linear
< 1	0.48	0.32	0.20 0
> 1 and < 31.62	$0.48 * Red_LE[(\gamma/\gamma_r)_{max}]$	$0.32 * Red_LE[(\gamma/\gamma_r)_{max}]$	Complement to 1 = 0.9 + Subbranching
> 31.62	0.15	0.10	0.75 + sub branching
Fixed parameters for computing the frequency dependence of the relative SHAKE and RVT weights			
		f1=0.5 Hz	f2=1.0 Hz
<i>RVT Subsets</i>			
Base case			
15/40=0.375			
Random model			
25/40=0.625			
<i>Magnitude / pga interpolation + extrapolations</i>			
Linear	SHAKE	RVT	Non-linear
See formulas			
<i>P-SV sensitivity</i>			
No change on the median			
For the aleatory variability, consider three possibilities	$\sigma_{P-SV} = 0\%$ $\sigma_{log10P-SV} = 0.0$ Weighting = 0.3	$\sigma_{P-SV} = 20\%$ $\sigma_{log10P-SV} = 0.079$ Weighting = 0.4	$\sigma_{P-SV} = 50\%$ $\sigma_{log10P-SV} = 0.176$ Weighting = 0.3
<i>2D effects</i>			
$A_{2D} = I + C_{2D}(\zeta) = I + C_{2D}^0 A_0(f/f_0) \cdot exp(-2\pi\zeta_{av} f l / \beta_m) \cdot \zeta_{av} = \sum_i h_i \cdot 0.3 (\gamma/\gamma_r) / [1. + (\gamma/\gamma_r)] / h$			
Fixed parameters	f0 = 10.0 Hz	l = 200 m	$\beta_m = 400$ m/s h = 10 m
Alternative choice for parameters and corresponding weights	$C_{2D}^0 = 0.0$ weight 0.20	$C_{2D}^0 = 0.10$ weight 0.60	$C_{2D}^0 = 0.30$ weight 0.20
For the aleatory variability, consider the associated aleatory variability	$\sigma_{2D} = 0\%$ $\sigma_{log102D} = 0.0$	$\sigma_{2D} = 10\%$ $\sigma_{log102D} = 0.04$	$\sigma_{2D} = 30\%$ $\sigma_{log102D} = 0.114$

- The 2 other cross-sections are similar, with however a smaller lateral extent for the surficial soil layer (450 m), and similar thicknesses (up to 15 m). Along these directions, the soil layer edges are located 150 to 250 m away from the NPP.

Therefore, there probably exist some 2D effects, but less pronounced than for Leibstadt, and only at high frequency. I include a three-branch sub-tree with respective C_{2D}^0 coefficients and weights, respectively, of (0.0, 20%), (0.1, 60%), and (0.3, 20%)

3 MEDIAN AMPLIFICATION OF VERTICAL GROUND MOTION

3.1 Approach

I considered three different approaches to estimate the vertical ground motion:

- the first approach is simply to consider that site conditions do not affect the vertical ground motion: the amplification factor is equal to 1 for all frequencies. Such an approach is certainly wrong for an arbitrary site; however, as the four NPP sites all correspond to stiff soils, and as standard attenuation laws certainly merge rock and stiff soil sites in the "rock site" category because of poor geotechnical information, such a simple approach is not to be totally ruled out.
- the second approach is to use the V/H ratios observed in real strong motion data in combination with the estimated median horizontal ground motion to derive an estimation of the vertical ground motion.
- the third approach is to estimate the amplification factors with a 1D soil response analysis accounting for specific site properties. These results are available from SHAKE computations considering different pga levels and different degradation curves for the P wave velocity and damping.

In the third approach, the results depend on the computational parameters (velocity profiles, NL parameters, input signals), and might be modified by incident wavefield type, and possible 2D or 3D effects (in a similar way to what is considered for horizontal ground motion).

The weight of the first approach depends mainly on the similarity of the considered site to a rock site: It is, therefore, largest for the Mühleberg site (shallow stiff material).

The second approach presents – in my opinion – the advantage that it relies on real observations, which exhibit a dependence of the V/H ratio with magnitude and distance, especially for large events. I therefore assign this approach an increasing weight with increasing pga, especially as SHAKE type modelling for large pga is highly uncertain because of the lack of constraints for the degradation curves for P-wave velocity and damping.

3.2 Logic Tree Structure

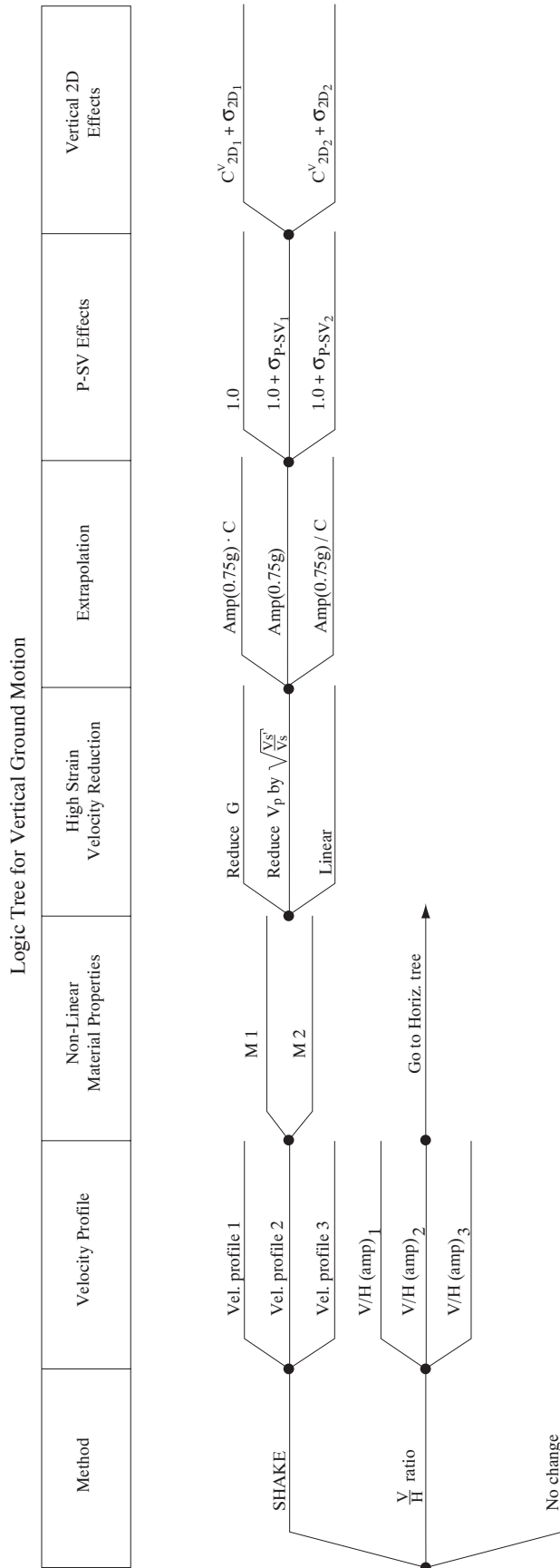


Fig. 3-1: Generic logic tree-structure for vertical ground motion

3.3 Model Evaluations Common to All Sites

3.3.1 Relative weighting between the three approaches

3.3.1.1 Weight of the 'no change' branch

The average S-wave velocities over the top 30 meters are comparable (353 to 416 m/s) for the three sites Beznau, Gösgen and Leibstadt, and significantly different for Mühleberg (> 600 m/s).

Therefore, the weight will be identical for the three first sites (20%) and larger for the fourth one (40%)

3.3.1.2 Relative weighting between V/H and SHAKE approaches

As mentioned in section 3.1, this relative weight is pga dependent. At large pga (> 0.75 g), I assign each of them an equal weight. At low pga, I consider the 1D, site specific approach more reliable for a site-specific estimate.

The assigned weights, displayed in Figure 3.3.1, are thus the following :

Beznau, Gösgen, Leibstadt:

- weight = $0.60 - 0.2 [pga / 0.75]$ for SHAKE approach: Maximum 0.6, minimum 0.40
- weight = $0.20 + 0.2 [pga / 0.75]$ for the V/H approach : Maximum 0.4, minimum 0.20

Mühleberg:

- weight = $0.40 - 0.1 [pga / 0.75]$ for SHAKE approach: Maximum 0.4, minimum 0.30
- weight = $0.20 + 0.1 [pga / 0.75]$ for the V/H approach]: Maximum 0.3, minimum 0.20

3.3.2 V/H approach

3.3.2.1 Estimation formula (after Borzorgnia & Campbell, EXT-RF-0246)

For a given (M, pga) pair, the hazard should be deaggregated (from what I understood, this deaggregation is readily available) to get the corresponding (M, R) pairs with their respective weights .

Then, for each (M,R) pair, estimate the V/H ratio with the B&C formulas:

$$\ln (V/H) = \ln (Y_V) - \ln (Y_H)$$

where Y_V and Y_H are the vertical and average horizontal components of PGA or PSA calculated from the near-source attenuation relations of Campbell and Bozorgnia (2002). These attenuation relations are given by

$$\ln Y = c_1 + f_1(M_W) + c_4 \ln \sqrt{f_2(M_W, r_{seis}, S)} + f_3(F) + f_4(S) + \varepsilon \quad (2)$$

where the magnitude scaling characteristics are given by

$$f_1(M_W) = c_2 M_W + c_3 (8.5 - M_W)^2, \quad (3)$$

the distance scaling characteristics are given by

$$f_2(M_W, r_{seis}, S) = r_{seis}^2 + g(S)^2 \left(\exp[c_8 M_W + c_9 (8.5 - M_W)^2] \right)^2 \quad (4)$$

in which the near-source effect of local site conditions is given by

$$g(S) = c_5 + c_6(S_{VFS} + S_{SR}) + c_7 S_{FR}, \tag{5}$$

the effect of faulting mechanism is given by

$$f_3(F) = c_{10} F_{RV} + c_{11} F_{TH}, \tag{6}$$

and the far-source effect of local site conditions is given by

$$f_4(S) = c_{12} S_{VFS} + c_{13} S_{SR} + c_{14} S_{FR}. \tag{7}$$

In the above equations, Y is either Y_V or Y_H in g ($g = 981 \text{ cm/sec}^2$); M_w is moment magnitude, r_{src} is the distance to seismogenic rupture in km; $S_{VFS} = 1$ for very firm soil, $S_{SR} = 1$ for soft rock, $S_{FR} = 1$ for firm rock, and $S_{VFS} = S_{SR} = S_{FR} = 0$ for firm soil; $F_{RV} = 1$ for reverse faulting, $F_{TH} = 1$ for thrust faulting, and $F_{RV} = F_{TH} = 0$ for strike-slip and normal faulting; and ϵ is a random error term with zero mean and standard deviation $\sigma_{\ln Y}$, where $\sigma_{\ln Y}$ is given by

$$\sigma_{\ln Y} = \begin{cases} c_{15} - 0.07M_w & \text{for } M_w < 7.4 \\ c_{15} - 0.518 & \text{for } M_w \geq 7.4 \end{cases} \tag{8}$$

The regression coefficients $c_1 - c_{15}$ are given in Table 3. A more detailed discussion of the attenuation relations and their mathematical basis is given in Campbell and Bozorgnia (2002).

Once the V/H ratio is estimated with these empirical relationships, then the vertical motion V is to be calculated by multiplying this (V/H) ratio by the median Horizontal ground motion derived as described in section 2.

3.3.2.2 Interpolation / extrapolation rules

The values for V/H ratio are given only for a limited set of frequencies / periods that do not necessarily correspond to the values selected for the horizontal amplification factors.

Some interpolation is thus needed: the recommended procedure is to estimate V/H for the two nearby periods / frequencies, and then use simple linear interpolation on the log values ($\ln(Y_V) - \ln(Y_H)$).

For the 0 Frequency (pga value), simply use the "COR PGA" coefficients

In case some extrapolation would be needed for very low frequencies below 0.25 Hz (period beyond 4 s), it is recommended to apply the V/H values derived for $T=4.0 \text{ s}$ / $f=0.25 \text{ Hz}$ [and for the same (M, R) – (M-pga) pair].

3.3.2.3 Parameters for the V/H approach

Tab. 3-1: Site categories and faulting parameters for applying the V/H approach

	Beznau	Gösgen	Leibstadt	Mühleberg
Vs30	400	416	353	662
Soil category	Very firm soil	Very firm soil	Very firm soil	Generic rock
S _{VFS}	1.0	1.0	1.0	0
S _{SR}	0.0	0.0	0.0	0.5
S _{FR}	0.0	0.0	0.0	0.5
Faulting category	Generic	Generic	Generic	Generic
F _{RV}	0.25	0.25	0.25	0.25
F _{TH}	0.25	0.25	0.25	0.25

Tab. 3-2: Coefficients and statistical parameters from the regression analysis of PGA and PSA response spectra

Period (sec)	c ₁	c ₂	c ₃	c ₄	c ₅	c ₆	c ₇	c ₈	c ₉	c ₁₀	c ₁₁	c ₁₂	c ₁₃	c ₁₄	c ₁₅	No.	r ²
Average Horizontal Component																	
Unc PGA	-2.896	0.812	0.000	-1.318	0.187	-0.029	-0.064	0.616	0	0.179	0.307	-0.062	-0.195	-0.320	1.028	960	0.955
Cor PGA	-4.033	0.812	0.036	-1.061	0.041	-0.005	-0.018	0.766	0.034	0.343	0.351	-0.123	-0.138	-0.289	0.940	443	0.949
0.05	-3.740	0.812	0.036	-1.121	0.058	-0.004	-0.028	0.724	0.032	0.302	0.362	-0.140	-0.158	-0.205	0.980	435	0.940
0.075	-3.076	0.812	0.050	-1.252	0.121	-0.005	-0.051	0.648	0.040	0.243	0.333	-0.150	-0.196	-0.208	1.004	439	0.923
0.10	-2.661	0.812	0.060	-1.308	0.166	-0.009	-0.068	0.621	0.046	0.224	0.313	-0.146	-0.253	-0.258	1.016	439	0.901
0.15	-2.270	0.812	0.041	-1.324	0.212	-0.033	-0.081	0.613	0.031	0.318	0.344	-0.176	-0.267	-0.284	1.049	439	0.862
0.20	-2.771	0.812	0.030	-1.153	0.098	-0.014	-0.038	0.704	0.026	0.296	0.342	-0.148	-0.183	-0.359	1.063	439	0.844
0.30	-2.999	0.812	0.007	-1.080	0.059	-0.007	-0.022	0.752	0.007	0.359	0.385	-0.162	-0.157	-0.585	1.069	439	0.859
0.40	-3.511	0.812	-0.015	-0.964	0.024	-0.002	-0.005	0.842	-0.016	0.379	0.438	-0.078	-0.129	-0.557	1.075	439	0.871
0.50	-3.556	0.812	-0.035	-0.964	0.023	-0.002	-0.004	0.842	-0.036	0.406	0.479	-0.122	-0.130	-0.701	1.081	439	0.890
0.75	-3.709	0.812	-0.071	-0.964	0.021	-0.002	-0.002	0.842	-0.074	0.347	0.419	-0.108	-0.124	-0.796	1.144	438	0.917
1.0	-3.867	0.812	-0.101	-0.964	0.019	0	0	0.842	-0.105	0.329	0.338	-0.073	-0.072	-0.858	1.176	438	0.935
1.5	-4.093	0.812	-0.150	-0.964	0.019	0	0	0.842	-0.155	0.217	0.188	-0.079	-0.056	-0.954	1.176	428	0.960
2.0	-4.311	0.812	-0.180	-0.964	0.019	0	0	0.842	-0.187	0.060	0.064	-0.124	-0.116	-0.916	1.176	405	0.971
3.0	-4.817	0.812	-0.193	-0.964	0.019	0	0	0.842	-0.200	-0.079	0.021	-0.154	-0.117	-0.873	1.176	333	0.976
4.0	-5.211	0.812	-0.202	-0.964	0.019	0	0	0.842	-0.209	-0.061	0.057	-0.054	-0.261	-0.889	1.176	275	0.978
Vertical Component																	
Unc PGA	-2.807	0.756	0	-1.391	0.191	0.044	-0.014	0.544	0	0.091	0.223	-0.096	-0.212	-0.199	1.107	941	0.964
Cor PGA	-3.108	0.756	0	-1.287	0.142	0.046	-0.040	0.587	0	0.253	0.173	-0.135	-0.138	-0.256	1.051	439	0.958
0.05	-1.918	0.756	0	-1.517	0.309	0.069	-0.023	0.498	0	0.058	0.100	-0.195	-0.274	-0.219	1.196	434	0.934
0.075	-1.504	0.756	0	-1.551	0.343	0.083	0.000	0.487	0	0.135	0.182	-0.224	-0.303	-0.263	1.216	436	0.910
0.10	-1.672	0.756	0	-1.473	0.282	0.062	0.001	0.513	0	0.168	0.210	-0.198	-0.275	-0.252	1.194	436	0.900
0.15	-2.323	0.756	0	-1.280	0.171	0.045	0.008	0.591	0	0.223	0.238	-0.170	-0.175	-0.270	1.160	436	0.899
0.20	-2.998	0.756	0	-1.131	0.089	0.028	0.004	0.668	0	0.234	0.256	-0.098	-0.041	-0.311	1.113	436	0.915
0.30	-3.721	0.756	0.007	-1.028	0.050	0.010	0.004	0.736	0.007	0.249	0.328	-0.026	0.082	-0.265	1.069	436	0.941
0.40	-4.536	0.756	-0.015	-0.812	0.012	0	0	0.931	-0.018	0.299	0.317	-0.017	0.022	-0.257	1.075	436	0.949
0.50	-4.651	0.756	-0.035	-0.812	0.012	0	0	0.931	-0.043	0.243	0.354	-0.020	0.092	-0.293	1.081	436	0.957
0.75	-4.903	0.756	-0.071	-0.812	0.012	0	0	0.931	-0.087	0.295	0.418	0.078	0.091	-0.349	1.144	435	0.962
1.0	-4.950	0.756	-0.101	-0.812	0.012	0	0	0.931	-0.124	0.266	0.315	0.043	0.101	-0.481	1.176	435	0.967
1.5	-5.073	0.756	-0.150	-0.812	0.012	0	0	0.931	-0.184	0.171	0.211	-0.038	-0.018	-0.518	1.176	420	0.973
2.0	-5.292	0.756	-0.180	-0.812	0.012	0	0	0.931	-0.222	0.114	0.115	0.033	-0.022	-0.503	1.194	395	0.977
3.0	-5.748	0.756	-0.193	-0.812	0.012	0	0	0.931	-0.238	0.179	0.159	-0.010	-0.047	-0.539	1.247	321	0.978
4.0	-6.042	0.756	-0.202	-0.812	0.012	0	0	0.931	-0.248	0.237	0.134	-0.059	-0.267	-0.606	1.285	274	0.980

3.3.3 SHAKE approach

Alike for the linear equivalent approach for the horizontal ground motion, several assumptions may be considered, corresponding to as many branches. In addition, one needs also to detail the interpolation / extrapolation procedures, especially as SHAKE computations for vertical motion are available only for magnitude 6 input signals, and a limited amount of cases.

3.3.3.1 Methods for determining non-linearity properties of P wave velocity and damping

SHAKE vertical amplification factors were computed with three different assumptions for NL degradation curves:

- M1 = considering the degradation only in the second lamé coefficient (shear modulus μ), with no modification on the other Lamé coefficient λ ,
- M2 = considering identical degradations on P and S wave velocities (and damping), which correspond to exactly similar degradations on the two Lamé coefficients λ and μ
- M3 (intermediate between M1 and M2) = considering a P wave degradation equal to the square root of the S-wave degradation

Given the lack of experimental results on such degradation curves, it is not easy to justify quantitative numbers for the respective weighting of these 3 assumptions. The following numbers are therefore very subjective:

- I consider the M2 assumption physically unrealistic, and I assign it a 0% weight.
- I consider the M1 case as the most satisfactory from a physical / mechanical viewpoint, and I assign it a 60% weight.
- The M3 intermediate case is given a weight of 20%
- finally, to be consistent with my approach for the horizontal motion, I also considered a 'linear' approach (corresponding to the amplification factor computed for $p_{ga} = 0.1$ g), and I assign it a relative weight of 20%

3.3.3.2 Interpolation for arbitrary values of p_{ga} and m

SHAKE vertical amplification factors were computed only for magnitude 6 input signals, and for three p_{ga} levels: 0.1, 0.4 and 0.75 g. Moreover, they are not available for all soil profiles

Other magnitude values

Since magnitude dependence is implicitly included in the V/H approach, and as we do not have any basis to guide the extrapolation of vertical amplification factors to other magnitudes, I prefer not to consider any magnitude dependence for this "SHAKE" approach branch.

p_{ga} interpolation

The proposed interpolation follows the logarithmic interpolation scheme proposed for the horizontal amplification factor:

$$AF_v(p_{ga}) = B_1 * AF_v(A_1, 6) + B_2 * AF_v(A_2, 6)$$

with

$$B_1 = (LA_2 - Lp_{ga}) / (LA_2 - LA_1)$$

$$B_2 = (Lp_{ga} - LA_1) / (LA_2 - LA_1)$$

where

$$Lp_{ga} = \log(p_{ga}) ; LA_1 = \log(A_1) ; LA_2 = \log(A_2)$$

A_1 and A_2 are the nearest p_{ga} values for which the vertical amplification factors AF_v are computed

Special case: Low p_{ga} values (< 0.1 g)

Simply consider the 0.1 g value: $AF_v(p_{ga}) = AF_v(0.1 \text{ g}, 6)$

3.3.3.3 Extrapolation for large values of p_{ga} (beyond 0.75 g)

This is a highly uncertain exercise: some strong motion recordings show that in some cases non-linear effects result in increased vertical amplification (e.g. Port Island vertical array in Kobé, Kushiro records). Therefore, I try several possibilities, with the assumption, however, that NL effects affect vertical ground motion essentially beyond the fundamental vertical resonance frequency f_v .

As for the horizontal component, the main idea is to base the estimates on the results computed for $p_{ga} = 0.75$ g, by multiplying them by an "uncertainty" function E_v which is assigned different values along each subbranch

$$AF_v(p_{ga}, m) = AF_v(0.75 \text{ g}, 6) \cdot E_v(f, f_v, C_v)$$

with

$$E_v(f, f_v, C_v) = 1. + C_v \cdot E(2f/f_v)$$

E is a function introduced to describe the frequency dependence of uncertainty, which is thought to be limited at low frequency, and larger at high frequency:

$$\begin{aligned} E(x) &= 0. && \text{for } x \leq 0.5 \\ E(x) &= \log(2x) / \log(2) && \text{for } 0.5 \leq x \leq 1.0 \\ E(x) &= 1. && \text{for } x > 1.0 \end{aligned}$$

f_v is the low strain, site dependent fundamental frequency for the vertical component (the value is given for each site). The multiplying factor 2 is introduced to account for the decrease of fundamental frequency at very large strains.

C_v is a 'correcting factor' which is uncertain, and takes different values for each subbranch. The values and weights are given below:

$$\begin{aligned} C_v &= 1 && \text{weight : 10\%} \\ C_v &= 0.5 && \text{weight : 20\%} \\ C_v &= 0 && \text{weight : 50\%} \\ C_v &= -0.3 && \text{weight : 20\%} \end{aligned}$$

[This extrapolation scheme is biased towards higher values, because of the few observations exhibiting such amplification on vertical component when the horizontal component is reduced by NL effects.]

3.3.3.4 Missing SHAKE computations

Vertical amplification factors have not been computed for all velocity profiles S_i and NL material properties M_j , but only for one set $S_0_M_0$. Therefore, a procedure to estimate them on the basis of the available H and V computations has to be introduced.

The basis for this procedure is the variations in the associated amplification factors for the horizontal motion, which are directly available from the SHAKE computations on the horizontal component:

$$\begin{aligned} V_{SHA,H} &= \text{Max}_f \{ |AF_{SHA,H}(f; pga, 6; S_i_M_j) / AF_{SHA,H}(f; pga, 6; S_0_M_0) - 1| \} \\ &\text{for } 0.3 f_0 < f < 3 f_0 \end{aligned}$$

$V_{SHA,H}$ therefore describes the maximum variations around the horizontal fundamental frequency from the "reference model" $S_0_M_0$ to the site model $S_i_M_j$ under consideration

This kind of 'extrapolation' automatically induces a new source of epistemic uncertainty; it is therefore associated with a new subbranching.

The procedure to estimate AF_v for all soil models $S_i_M_j$ is therefore defined as follows:

$$AF_v(f; pga, 6; S_i_M_j) = AF_v(f, pga, 6; S_0_M_0) \cdot E_v(f, f_v, V_v)$$

with

$$E_v(f, f_v, V_v) = 1. + V_v \cdot E(2f/f_v)$$

E is again the function introduced to describe the frequency dependence of uncertainty, which is thought to be limited at low frequency, and larger at high frequency:

$$\begin{aligned} E(x) &= 0. && \text{for } x \leq 0.5 \\ E(x) &= \log(2x) / \log(2) && \text{for } 0.5 \leq x \leq 1.0 \\ E(x) &= 1. && \text{for } x > 1.0 \end{aligned}$$

f_v is the low strain, site dependent fundamental frequency for the vertical component (the value is given for each site). The multiplying factor 2 is introduced to account for the decrease of fundamental frequency at very large strains.

V_v represents the variability from one set of profile / material $S_i_M_j$ to another. It is estimated from the "observed" variability $V_{SHA,H}$ on the computed horizontal amplification factor $AF_{SHA,H}$ with the following rules

$V_v = + 0.5 V_{SHA,H}$	-	weight : 30%
$V_v = 0.$	-	weight : 40%
$V_v = - 0.5 V_{SHA,H}$	-	weight : 30%

3.3.3.5 Effect of incident wavefield (wave type / incidence angle)

As for the horizontal motion, there is no branching, nor any systematic modification of amplification factor derived for vertically incident SH waves: Wave type (SV, P, SH, ...) and incidence / azimuth angles are thought to affect essentially the aleatory variability and not the average value.

3.3.3.6 2D / 3D effects

No specific computations has been performed to investigate the 2D or 3D effects on vertical motion. However, observations in many sites, as well as computations on "canonical models" show that 2D/3D effects generate Rayleigh waves that affect the vertical component *at frequencies corresponding to the vertical component resonant frequency (this may be controversial, as some may argue that it is a frequency which is simple twice the fundamental S-wave resonance frequency, in connection with troughs in the H/V ellipticity curves of Rayleigh waves)*.

Therefore, I also consider 2D-3D effects on the vertical component, in a way very similar to what is done for the horizontal component, with effects shifted however to higher frequencies. The formula is the same as for the horizontal components, except for the fundamental frequency; the damping term is not changed as it corresponds to Rayleigh waves, for which the S-wave characteristics (velocity and damping) are of primary importance. The approach is described below:

General formula:

The amplification factors derived with the SHAKE approach should be multiplied by a 2D factor A_{2D} defined as:

$$A_{2D}(f, \zeta_{av}) = 1 + C_{2D}(f, \zeta_{av})$$

with

$$C_{2D}(f, \zeta_{av}) = A(f, f_v) B_v(f, \zeta_{av})$$

where

f is the frequency

f_v is the fundamental frequency for the vertical component at the site under consideration

ζ_{av} is an average damping value in the surficial soils where surface waves diffracted on lateral heterogeneities are propagating.

Frequency dependence : $A(f, f_v)$

The results available in the scientific lieterature indicate that 2D and 3D effects appear only above the site fundamental frequency f_v . $A(f, f_v)$ is therefore defined as a ramp function on a logarithmic frequency axis:

$$A(f, f_v) = A_0(f/f_v)$$

with

$$A_0(x) = 0 \quad \text{for } x \leq 0.7$$

$$A_0(x) = -(\log(x/0.7)) / \log(0.7) \quad \text{for } 0.7 < x \leq 1$$

$$A_0(x) = 1 \quad \text{for } 1 < x$$

Geometrical / damping dependence : $B(f, \zeta_{av})$

The diffracted waves are generated on the lateral heterogeneities, and then propagate to the site: their amplitude at the site will therefore depend both on the distance to the heterogeneities, and on the damping values. The proposed model is given by

$$B_v(f, \zeta_{av}) = C_{2D}^v \cdot \exp(-2\pi\zeta_{av} f l / \beta_m)$$

Where

- C_{2D}^v represents in some way the amplitude of the diffracted waves (normalized to the incident wavefield) on the heterogeneity; it is also, approximately, the largest possible 2D effect at the site (corresponding to the low strain / very low damping case). *This value is uncertain, and, for each site, different values are proposed with different weights. These values are thought slightly smaller than the corresponding values for the horizontal component, because only Rayleigh waves are affecting vertical motion, while horizontal motion is affected by both Rayleigh and Love waves. One has however to keep in mind that these perturbations are also related to direct S-waves which carry more energy than P waves.*
- the last term $\exp(-2\pi\zeta_{av} f l / \beta_m)$ represents the amplitude decay due to the propagation from the heterogeneity to the site:

ζ_{av} is the average damping over the soil column: it is pga dependent because of NL material degradation. It is estimated as specified for the horizontal motion: see section 2.3.8.

l is the distance of the NPP site to the closest lateral heterogeneity

β_m still represents the average S-wave velocity in the soil column: it is kept unchanged with respect to the horizontal motion, because it is associated here with Rayleigh waves.

The tables presented in the next sections provide, for each NPP site, the values of f_v , C_{2D}^v , l , β_m and h , as well as the corresponding weighting. Three subbranches are introduced with different weights to account for the uncertainties in the parameter estimates (mainly indeed C_{2D}^v). One of the subbranch corresponds to $C_{2D}^v = 0$, as it is likely that the actual data on which are based at least partly the input motion estimates, do include some – unknown - amount of 2D/3D effects. The other values are based on the actual geological cross-sections at each site, and some subjective "expert judgement".

3.3.4 At-Depth Amplification Factors

The same basic approaches will be kept for motion at depth as described above for the surface motion; however, some changes will be introduced in the relative weights, since empirical V/H ratios are not available for motion at depth (neither outcropping nor within). The following sections are highlighting these changes.

3.3.4.1 No-Change Branch

Although I did consider to increase the relative weight of that branch, at least for the 'within bedrock' sites (BZ2, MZ2), I finally decided to keep the same weights as for the surface sites: the reason behind that choice is that the "no-change" branch does not take into account the fact that the sites are at depth.

3.3.4.2 Changes in the "V/H" Branch

The main issue comes from the fact that empirical V/H ratios are available only for surface sites. A secondary issue is that the deaggregation results may lead to distances as small as 3 km, and there are few empirical V/H data at such short distances.

The proposed depth corrections are based on several considerations:

- physically, this correction should be frequency dependent, since long wavelengths (low frequencies) should lead to very small changes from the surface values, while short wavelengths (high frequencies) should lead to much larger variability over short distances. Even though we are concerned here with outcropping motion and not with within motion.
- The nature of the soil is changing with depth (it becomes stiffer), and the "reference" surface V/H ratio should therefore take it into account.
- The results for this branch are more uncertain at depth than at the surface

I thus propose to introduce both a subbranching with three different depth corrections, and a frequency dependent weight.

The frequency dependence of the weight is described as follows. Let $w_{V/H,surf}$ be the weight of the V/H branch for the corresponding surface site [$w_{V/H,surf} = \text{Min} \{0.20 + 0.2 (pga/0.75), 0.4\}$ for Beznau, Gösigen, Leibstadt, $w_{V/H,surf} = \text{Min} \{0.20 + 0.1 (pga/0.75), 0.3\}$ for Mühleberg].

The weight, $w_{V/H,z}$, of the site located at depth z will be derived as follows:

$$w_{V/H,z} = w_{V/H,surf} \cdot (1 - 2z/\lambda) = w_{surf} \cdot (1 - 2z f / \beta_m) \quad \text{if} \quad f < \beta_m/2z$$

$$w_{V/H,z} = 0 \quad \text{if} \quad f \geq \beta_m/2z$$

with the β_m values being the average low strain velocities over the resonant layer, already specified in the elicitation summary for surface motion (i.e., 500 m/s at Beznau, 416 m/s at Gösigen, 400 m/s at Leibstadt, 400 m/s at Mühleberg)

This reduction of the weight may be thought as being very sharp ($w_{V/H,z} = 0.5 w_{V/H,surf}$ at around 10 Hz for Leibstadt, Mühleberg and Gösigen, and 12.5 Hz at Beznau), and the weight decrease should be scaled with $(1 - z/\lambda)$ rather than on $(1 - z/(\lambda/2))$. Indeed the choice of a 'decorrelation' distance of $\beta_m/2f$ was considered reasonable because of two opposite factors:

- on one hand, the S-wave velocity will decrease at high strains, and this should lead to a shorter "decorrelation" length
- on the other hand, the fact that only "outcropping" motion is of interest here should reduce the depth dependence of ground motion.

Important note: as the weight of the V/H branch is reduced at high frequencies, one must increase correlatively the weight of another branch: since the "no-change" branch does not take into account the depth dependence of ground motion, the weight of the "SHAKE" should be raised as follows: $w_{SHA,z} = w_{SHA,surf} + (w_{V/H,surf} - w_{V/H,z}) = w_{SHA,surf} + w_{V/H,surf} \cdot 2z f / \beta_m$ (limited to an upper value of $w_{SHA,surf} + w_{V/H,surf}$).

Subbranching for uncertainties and corresponding weights

Three different estimates are proposed :

- a) consider the V/H value derived from Bozorgnia & Campbell's relationships at the site surface (i.e., "very firm soil" for Beznau, Gösigen and Leibstadt, "generic rock" for Mühleberg)

- b) consider the V/H value derived from Bozorgnia & Campbell's relationships at "firm rock" surface sites (i.e., with $S_{VFS} = 0$, $S_{SR} = 0$, $S_{FR} = 1$).
- c) Apply corrections to the surface V/H ratios based on the computations by Fäh, as follows:

$$(V/H)(z) = (V/H)(z=0) \cdot \{ (V/H)_{Fäh}(z) / (V/H)_{Fäh}(z=0) \}$$

in that formula, $(V/H)(z=0)$ is the ratio derived from Bozorgnia & Campbell's relationships at the site surface (as in a), while the $(V/H)_{Fäh}(z)$ values should be the average V/H values derived, from each frequency of interest, from D. Fäh's computations using various source positions and mechanisms, for the site under study.

The corresponding relative weights are proposed:

$$\text{Approach a: } W_a = 0.5 (1 - z/h)$$

$$\text{Approach b: } W_b = 0.5 \cdot z/h$$

$$\text{Approach c: } W_c = 0.5$$

In this formulation, h is the thickness of the resonant layer, as described the elicitation summary for the surface motion ($h = 65$ m at Beznau, 25 m at Gösigen, 50 m at Leibstadt, and 10 m at Mühleberg)

Minimum distance for 'V/H' ratio

A close look at the (M, R) distribution of the data set used by Bozorgnia & Campbell (2002) [see their Figure 1], shows that while the density of data is diminishing for distances smaller than 8-10 km, there are still a few data at distances as low as 4-5 km for magnitudes between 5.8 and 7.3.

Therefore, I recommend to use a minimum distance of 6 km for the estimation of the V/H ratio. In other words, if the deaggregation study leads to distances smaller than 6 km, replace this value of distance by 6 km.

3.3.4.3 'SHAKE' branch

As mentioned in the previous section, the overall weighting of this branch is increased at high frequencies to compensate the reduced weight of the V/H branch.

The subbranches and their weights should be exactly the same as those described for the surface motion (subbranching for non-linearity properties of P wave velocity and damping, interpolation and extrapolation rules, estimates of missing SHAKE computations based on corresponding horizontal computations; however, consistent with what is proposed for horizontal motion (see above sections 2.3 and 2.4), slight changes are introduced in two respects.

3.3.4.4 Incident wavefield effects at depth

As for horizontal motion, and vertical motion at the surface, the incident wave field characteristics (wave type, incidence angle) are considered to affect only for the aleatory variability.

The following values are proposed for the additional aleatory variability σ_{PSV} , consistent with what was proposed for horizontal motion (section 2.3)

- For sites BZ1, GZ1, GZ2, LZ1, LZ2, MZ1, I propose to keep the same σ_{PSV} values as for the surface sites (vertical motion).
- For site MZ2, I propose to apply a value reduced by half : $0.5 \sigma_{PSV}$ (σ_{PSV} = value for the vertical motion at the corresponding surface site).

- For site BZ2, I propose to apply an intermediate value : $0.75 \sigma_{PSV}$ (σ_{PSV} = value for the vertical motion at the corresponding surface site).

3.3.4.5 2D/3D effects at depth

Considering again the 2D/3D modifications are carried essentially by surface waves, it is proposed to apply the same correcting factor $C(z)$ to the surface "overamplification" factor $A_{2D}(f, \zeta, z)$

$$A_{2D}(f, \zeta, z) = 1 + A(f, f_v) \cdot B_v(f, \zeta_{av}) \cdot C(z)$$

The $C(z)$ factor is estimated with exactly the same formula as for horizontal motion:

$$C(z) = \text{Max} \{ |\cos(\omega z/c)|, 0.2 \} \approx \text{Max} \{ |\cos(2\pi f z/\beta_m)|, 0.2 \}$$

Where β_m is the average shear wave velocity already specified for these 2D effects.

This 2D overamplification term should apply to all deep sites, *except* the deepest site MZ2 at Mühleberg ($(h=10 \text{ m} < z_2 = 14 \text{ m})$): for this particular, there is no subbranching for 2D effects (or, in other terms, 1 single branch with weight 100% for the value $C_{2D}^v = 0$).

3.4 Beznau

3.4.1 Site-Specific Model Evaluations

3.4.1.1 Alternative velocity profiles

The same weights as for the horizontal motion are to be applied.

3.4.1.2 Alternative 2D parameters

The same weights as for the horizontal motion are to be applied. The C_{2D}^v coefficients are slightly reduced to take into account the fact that only Rayleigh waves contribute to the vertical motion, keeping in mind however that these perturbations are also related to direct S-waves which carry more energy than P waves.

3.4.2 Summary of weights and parameters for Beznau

Tab. 3-3: Summary of weights and computational parameters for the vertical ground motion at Beznau site

Weights for the median site amplification factor and corresponding aleatory variability for vertical ground motion : Site Beznau	
Method	
No change	SHAKE
0.2	0.6 0.2 [pga/0.75] Min 0.4 0.2 + 0.2 [pga/ 0.75] - Max 0.40 V/H ratio
SHAKE BRANCH	
Velocity profile	
B1	B2
0.50	0.20 B3 0.30
Nonlinear properties	
Irrelevant (one single choice)	
High strain velocity reduction	
1) Reduce G	2) Reduce V_p by V_s/V_s 3) Reduce V_p by $(V_s/V_s)^{0.5}$ 4) Linear (method 1 0.10 g)
0.60	0 0.20 0.20
Extrapolation towards high shaking levels	
Multiply the vertical amplification factor obtained for pga = 0.75 g by $E_v(f, f_b, C_v) = 1. + C_v E(f/f_v)$	
$C_v = 1$	$C_v = 0.5$ $C_v = 0$ $C_v = -0.3$
0.10	0.20 0.50 0.20
P-SV sensitivity	
No change on the median	
For the aleatory variability, consider three possibilities	$\sigma_{P-SV} = 0\%$ $\sigma_{P-SV} = 20\%$ $\sigma_{P-SV} = 50\%$ $\sigma_{\log OP-SV} = 0.0$ $\sigma_{\log OP-SV} = 0.079$ $\sigma_{\log OP-SV} = 0.176$ Weighting = 0.3 Weighting = 0.4 Weighting = 0.3
2D effects :	
Fixed parameters	$A_{2D} = 1 + C_{2D}(f, \zeta_{av}) = 1 + C_{2D} A_0(f/f_v) \exp(-2\pi\zeta_{av} f l / \beta_m)$ $f_v = 15$ Hz $l = 300$ m $\beta_m = 500$ m/s $h = 65$ m
Alternative choice for parameters and corresponding weights	$C_{2D}^{V} = 0.0$ $C_{2D}^{V} = 0.15$ $C_{2D}^{V} = 0.40$ weight 0.10 weight 0.60 weight 0.30
For the aleatory variability, consider the associated aleatory variability	$\sigma_{2D} = 0\%$ $\sigma_{2D} = 20\%$ $\sigma_{2D} = 50\%$ $\sigma_{\log 02D} = 0.0$ $\sigma_{\log 02D} = 0.08$ $\sigma_{\log 02D} = 0.18$
V/H BRANCH : Parameters to apply in Bozorgnia & Campbell approach	
$S_{VFS} = 1.0$	$S_{SR} = 0.0$ $S_{FR} = 0.0$ $F_{RV} = 0.25$ $F_{TH} = 0.25$

3.5 Gösgen

3.5.1 Site-Specific Model Evaluations

3.5.1.1 Alternative material properties

The same weights as for the horizontal motion are to be applied.

3.5.1.2 Alternative 2D parameters

The same weights as for the horizontal motion should to be applied; however, considering the low values of the C_{2D}^V coefficients, together with the values of the propagation terms at high frequencies, it is considered reasonable to neglect 2D effects for vertical ground motion at Gösgen.

3.5.2 Summary of weights and parameters for Gösgen

Tab. 3-4: Summary of weights and computational parameters for the vertical ground motion at Gösgen site

Weights for the median site amplification factor and corresponding aleatory variability for vertical ground motion : Site Goesgen	
Method	
No change	SHAKE
0.2	0.6 0.2 [pga/0.75] Min 0.4 V/H ratio 0.2 + 0.2 [pga/0.75] - Max 0.40
<i>SHAKE BRANCH</i>	
<i>Velocity profile</i>	
Irrelevant (One single profile)	
<i>Nonlinear properties</i>	
M1	M2
0.65	0.35
<i>High strain velocity reduction</i>	
1) Reduce G	2) Reduce V_p by V_s/V_s
0.60	0 0.20
	3) Reduce V_p by $(V_s/V_s)^{0.5}$
	4) Linear (method 1 0.10 g)
	0.20
<i>Extrapolation towards high shaking levels</i>	
<i>Multiply the vertical amplification factor obtained for pga = 0.75 g by $E_v(f, f_v, C_v) = 1. + C_v E(f/f_v)$</i>	
$C_v = 1$	$C_v = 0$
0.10	0.50
	$C_v = -0.3$
	0.20
<i>P-SV sensitivity</i>	
No change on the median	
For the aleatory variability, consider three possibilities	$\sigma_{P-SV} = 0\%$ $\sigma_{\log_{10P-SV}} = 0.0$ Weighting = 0.3 $\sigma_{P-SV} = 20\%$ $\sigma_{\log_{10P-SV}} = 0.079$ Weighting = 0.4 $\sigma_{P-SV} = 50\%$ $\sigma_{\log_{10P-SV}} = 0.176$ Weighting = 0.3
<i>NO 2D effects for Gösgen (too high frequencies)</i>	
$A_{2D} = 1 + C_{2D}(f, \zeta_{av}) = 1 + C_{2D}^v A_0(f/f_v) \cdot \exp(-2\pi\zeta_{av} \cdot f / \beta_m)$	
Fixed parameters	$f_v = 20.0$ Hz $l = 550$ m $\beta_m = 416$ m/s $h = 25$ m
Alternative choice for parameters and corresponding weights	$C_{2D}^v = 0$, weight 1.00 $C_{2D}^v = 0.10$ weight 0.0
For the aleatory variability, consider the associated aleatory variability	$\sigma_{2D} = 0\%$ $\sigma_{\log_{102D}} = 0.0$ $\sigma_{2D} = 20\%$ $\sigma_{\log_{102D}} = 0.18$
<i>V/H BRANCH : Parameters to apply in Bozorgnia & Campbell approach</i>	
$S_{VFS} = 1.0$	$S_{SR} = 0.0$ $S_{FR} = 0.0$ $F_{RH} = 0.25$ $F_{TH} = 0.25$

3.6 Leibstadt

3.6.1 Site-Specific Model Evaluations

3.6.1.1 Alternative velocity and NL material properties

The same weights as for the horizontal motion are to be applied.

3.6.1.2 Alternative 2D parameters

The C_{2D}^v coefficients are slightly reduced with respect to C_{2D}^0 (horizontal motion case), while the corresponding weights are unchanged..

3.6.2 Summary of weights and parameters

Tab. 3-5: Summary of weights and computational parameters for the vertical ground motion at Leibstadt site

Weights for the median site amplification factor and corresponding aleatory variability for vertical ground motion : Site Leibstadt	
Method	
No change	SHAKE
0.2	0.6 0.2 [pga/0.75] V/H ratio 0.20 + 0.2 [pga/0.75]
SHAKE BRANCH	
Velocity profile and nonlinear properties	
L1_M1	L2_M1
0.50	0.05
L2_M2	L2_M2
	0.15
High strain velocity reduction	
1) Reduce G	3) Reduce V_p by $(V_s/N_s)^{0.5}$
0.60	0.20
	4) Linear (method 1 0.10 g) 0.20
Extrapolation towards high shaking levels	
Multiply the vertical amplification factor obtained for pga = 0.75 g by $E_v(f, f_v, C_v) = 1. + C_v E(f/f_v)$	
$C_v = 1$	$C_v = 0$
	$C_v = -0.3$
0.10	0.50
	0.20
P-SV sensitivity	
No change on the median	
For the aleatory variability, consider three possibilities	$\sigma_{P-SV} = 0\%$ $\sigma_{\log_{10}P-SV} = 0.0$ Weighting = 0.3 $\sigma_{P-SV} = 20\%$ $\sigma_{\log_{10}P-SV} = 0.079$ Weighting = 0.4 $\sigma_{P-SV} = 50\%$ $\sigma_{\log_{10}P-SV} = 0.176$ Weighting = 0.3
2D effects:	
$A_{2D} = 1 + C_{2D}(f, \zeta_{sav}) = 1 + C_{2D} A_0(f/f_v). \exp(-2\pi\zeta_{sav} f / \beta_m)$	
Fixed parameters	$f_v = 7.5$ Hz $l = 100$ m $\beta_m = 400$ m/s $h = 50$ m
Alternative choice for parameters and corresponding weights	$C_{2D}^v = 0.00$ weight 0.10 $C_{2D}^v = 0.25$ weight 0.60 $C_{2D}^v = 0.50$ weight 0.30
For the aleatory variability, consider the associated aleatory variability	$\sigma_{2D} = 0\%$ $\sigma_{\log_{10}2D} = 0.0$ $\sigma_{2D} = 20\%$ $\sigma_{\log_{10}2D} = 0.08$ $\sigma_{2D} = 50\%$ $\sigma_{\log_{10}2D} = 0.18$
V/H BRANCH : Parameters to apply in Bozorgnia & Campbell approach	
$S_{VFS} = 1.0$	$S_{SR} = 0.0$
	$S_{FR} = 0.0$
	$F_{RV} = 0.25$
	$F_{TH} = 0.25$

3.7 Mühleberg

3.7.1 Site-Specific Model Evaluations

3.7.1.1 Alternative NL material properties

The same weights as for the horizontal motion are to be applied.

3.7.1.2 Alternative 2D parameters

The C_{2D}^v coefficients are slightly reduced with respect to C_{2D}^0 (horizontal motion case).

3.7.2 Summary of weights and parameters

Tab. 3-6: Summary of weights and computational parameters for the horizontal ground motion at Mühleberg site

Weights for the median site amplification factor and corresponding aleatory variability for vertical ground motion: Site Muehleberg	
Method	
No change	SHAKE
0.4	0.4 0.1 [pga/0.75] Min 0.3 V/H ratio 0.2 + 0.1 [pga/0.75] - Max 0.30
SHAKE BRANCH	
Velocity profile	
Irrelevant (One single profile)	
Nonlinear properties	
M1	M2
0.65	0.35
High strain velocity reduction	
1) Reduce G	3) Reduce V_p by $(V_s'/N_s)^{0.5}$
0.60	0.20
	4) Linear (method 1 0.10 g) 0.20
Extrapolation towards high shaking levels	
Multiply the vertical amplification factor obtained for pga = 0.75 g by $E_v(f, f_v, C_v) = 1 + C_v E(f/f_v)$	
$C_v = 1$	$C_v = 0$
0.10	0.50
$C_v = -0.3$	
0.20	
P-SV sensitivity	
No change on the median	
For the aleatory variability, consider three possibilities	$\sigma_{P-SV} = 0\%$ $\sigma_{\log 10P-SV} = 0.0$ Weighting = 0.3 $\sigma_{P-SV} = 20\%$ $\sigma_{\log 10P-SV} = 0.079$ Weighting = 0.4 $\sigma_{P-SV} = 50\%$ $\sigma_{\log 10P-SV} = 0.176$ Weighting = 0.3
2D effects	
$A_{2D} = 1 + C_{2D}(f, f_{50\phi}) = 1 + C_{2D}^v A_{1D}(f/f_v) \cdot \exp(-2\pi f_{50\phi} f / \beta_m)$	
Fixed parameters	$f_0 = 20.0$ Hz $L = 200$ m $\beta_m = 400$ m/s $h = 10$ m
Alternative choice for parameters and corresponding weights	$C_{2D}^v = 0.0$ weight 0.10 $C_{2D}^v = 0.10$ weight 0.60 $C_{2D}^v = 0.20$ weight 0.30
For the aleatory variability, consider the associated aleatory variability	$\sigma_{2D} = 10\%$ $\sigma_{\log 102D} = 0.04$ $\sigma_{2D} = 10\%$ $\sigma_{\log 102D} = 0.04$ $\sigma_{2D} = 30\%$ $\sigma_{\log 102D} = 0.114$
V/H BRANCH : Parameters to apply in Bozorgnia & Campbell approach	
$S_{VFS} = 0.0$	$S_{SR} = 0.5$
	$S_{FR} = 0.5$
	$F_{RI} = 0.25$
	$F_{TH} = 0.25$

4 ALEATORY VARIABILITY OF HORIZONTAL GROUND MOTION

4.1 Approach

4.1.1 General comments

The approach is to follow the same logic tree as for the median horizontal ground motion. The aleatory variability needs to be estimated for each main approach

The aleatory variability on the horizontal amplification factors has several origins that are described below.

4.1.1.1 Variability in the input signal waveform (SH case): σ_{ISW}

Within the SHAKE approach, this variability is estimated through the standard deviation in amplification factors obtained for the 15 different input signals. It is represented, for each velocity profile, by the standard deviation $\sigma_{SHA}(A_i, M_j; f)$ which is frequency dependent.

Within the RVT approach, this variability corresponds to the "random phase" variability in the Base case, and should be estimated according to the technical note TP3-TN-0297_RVT_sigma.doc by N. Abrahamson, with the approximate formula

$$\sigma_{RVTBC}(A_i, M_j; f) = \sigma_{RVTBC}(M_j; f) = \sigma_{Inamp}, \text{ with:}$$

$$\sigma_{Inamp} = \frac{1.28}{2 \ln(f) + 2.3M - 10.74}$$

Comment: In this formula, σ_{Inamp} does not depend on the acceleration level; this is somewhat inconsistent with what is observed in the SHAKE results, for which, clearly, the standard deviation does increase, at least at frequencies beyond the fundamental frequency, with the acceleration level. I think this difference comes from the fact the RVT based formula proposed by N. Abrahamson does not take into account the additional variability due to the input dependent changes in shear modulus and damping.

Within the NL approach, Within the NL approach, this variability should be estimated as for the SHAKE approach, through the standard deviation in amplification factors obtained for the different input signals, $\sigma_{NL}(A_i, M_j)$. However, there are only 5 different input accelerograms, and I doubt the estimate is statistically meaningful.

Therefore, I simply assume that $\sigma_{NL}(A_i, M_j; f) = \sigma_{SHA}(A_i, M_j; f)$ (My feeling is that it is a lower bound).

4.1.1.2 Variability due to aleatory variations in soil profiles

Such a variability appears ONLY in the RVT computations, from the runs other than the base case: It is represented by the standard deviation $\sigma_{RVT}(A_i, M_j; f)$

4.1.1.3 Variability in incident waves (oblique incidence angle, SH, SV or P wave types)

It is represented by the standard deviation $\sigma_{\theta PSV}$, the estimates of which are given in the various summary tables . It is independent of acceleration level and magnitude. It has to be modulated by the frequency dependent 'envelope function' $A_0(f/f_0)$ [0 for $f < 0.7 f_0$, $-(\log(f/0.7f_0)) / \log(0.7)$ for $0.7 f_0 < f < f_0$, 1 for $f > f_0$]: the variability is increased only around and beyond the site fundamental frequency.

4.1.1.4 Variability of 2D/3D effects depending on incident wave azimuth / angle

It is represented by the standard deviation σ_{2D} , the estimates of which are given in the various summary tables . It is independent of acceleration level and magnitude. It has to be modulated by the frequency dependent 'envelope function' $E_\sigma(f; f_0, \zeta_{av}, l, \beta_m) = A_0(f/f_0) \exp(-2\pi\zeta_{av}fl/\beta_m)$

NB: In all those formulas, the standard deviation ' σ ' correspond to the standard deviation of the logarithm of the amplification factor

For internal consistency reasons, I chose to keep the same logic trees for the aleatory variability and median ground motion; the general formulas for aleatory variability on the amplification factors are given below.

4.1.2 Formulas for aleatory variability on horizontal ground motion

4.1.2.1 SHAKE and Non-Linear Cases

$$\sigma_{AF, H}^2(\text{pga}, m; f) = \sigma_{SHA}^2(\text{pga}, m; f) + \sigma_{\theta PSV}^2 + \sigma_{2D}^2 \cdot E_\sigma(f; f_0, \zeta_{av}, l, \beta_m)$$

4.1.2.2 RVT – Base Case

$$\begin{aligned} \sigma_{AF, H}^2(\text{pga}, m; f) &= \sigma_{RVTBC}^2(\text{pga}, m; f) + \sigma_{\theta PSV}^2 + \sigma_{2D}^2 \cdot E_\sigma(f; f_0, \zeta_{av}, l, \beta_m) \\ &= \sigma_{Inamp}^2(m; f) + \sigma_{\theta PSV}^2 + \sigma_{2D}^2 \cdot E_\sigma(f; f_0, \zeta_{av}, l, \beta_m) \end{aligned}$$

4.1.2.3 RVT – Other cases

$$\begin{aligned} \sigma_{AF, H}^2(\text{pga}, m; f) &= \sigma_{Inamp}^2(m; f) + \sigma_{RVT}^2(\text{pga}, m; f) + \sigma_{\theta PSV}^2 \\ &+ \sigma_{2D}^2 \cdot E_\sigma(f; f_0, \zeta_{av}, l, \beta_m) \end{aligned}$$

4.1.2.4 'Linear' Case

I assume the same standard deviation as from the SHAKE result

$$\sigma_{AF, H}^2(0.05g, m; f) = \sigma_{SHA}^2(0.1g, 6; f) + \sigma_{\theta PSV}^2 + \sigma_{2D}^2 \cdot E_\sigma(f; f_0, \zeta_{av}, l, \beta_m)$$

4.1.3 Comments

Scepticism with such a formulation

These formulas lead to significant standard deviation, which will add to the "input", rock motion standard deviation. It seems right from a mathematical viewpoint given the way the site motion

is estimated, but it seems wrong from a physical viewpoint given the observed standard deviations on ground motion for different site categories.

Consequences for magnitude / acceleration interpolation

To be correct, these formulas should include a dependence on magnitude, acceleration and frequency as derived from the SHAKE or RVT cases. To be consistent with my formulation for the median, I should therefore include some interpolation and extrapolation scheme for estimating the values of $\sigma_{\text{SHA}}^2(\text{pga}, m; f)$ and $\sigma_{\text{RVT}}^2(\text{pga}, m; f)$ for arbitrary acceleration and magnitude values.

Instead, I selected a simplified interpolation procedure. The basic reasons for using this simplified procedure that are a) some reluctance to consider the mathematical formulas really representative of the actual world and b) a personal bias according which most of the uncertainties in the final result is coming from the epistemic uncertainty, and not from the aleatory variability. I therefore do not want to have too complex a model of the aleatory variability.

4.2 Logic Tree Structure

Since I chose to keep the same logic tree structures as for the median ground motion, the logic tree is the same (see Figure 2.1).

There is one difference, however, related to the incident wavefield: I assumed the incident wavefield does not affect the median ground motion, but that it does affect the aleatory variability. The logic tree for aleatory variability thus includes a sub-branching corresponding to different values for σ_{OPSV}^2 . This subbranching includes one branch with $\sigma_{\text{OPSV}}^2 = 0$, because a certain amount of variability associated with incident wave type is already included in the 'rock' ground motion estimate.

4.3 Evaluations Common to All Sites

4.3.1 Special indications for interpolating the standard deviations

From the computed standard deviations on the SHAKE results, one can notice a significant dependence on acceleration level beyond the fundamental frequency.

To simplify the computation procedure, I consider the following:

- A magnitude dependence of $\sigma_{\text{AF, H}}^2$ only from the magnitude dependence of the $\sigma_{\text{RVTBC}}^2(\text{pga}, m; f) = \sigma_{\text{Inamp}}^2(m; f)$ term (therefore only along the RVT branch)
- An acceleration dependence only from the SHAKE (and NL) terms $\sigma_{\text{SHA}}^2(\text{pga}, 6; f)$

The formulas to be used are detailed in the two next sections for SHAKE and RVT cases.

4.3.1.1 Interpolation of SHAKE standard deviations for arbitrary (pga, m) values

Suppose one has to compute the SHAKE standard deviation σ_{SHA} for arbitrary values of pga and m. I consider here only magnitude 6 results, and I interpolate for different acceleration values as described below:

Let $A_1 < \text{pga} < A_2$ be the two nearest peak accelerations for which the amplification factor is known with SHAKE computations, then the estimation formula for any soil column is:

$$\sigma_{SHA}(pga, m) = B_1 * \sigma_{SHA}(A_1, 6) + B_2 * \sigma_{SHA}(A_2, 6)$$

with

$$B_1 = (LA_2 - Lpga) / (LA_2 - LA_1)$$

$$B_2 = (Lpga - LA_1) / (LA_2 - LA_1)$$

where

$$Lpga = \log(pga) ; LA_1 = \log(A_1) ; LA_2 = \log(A_2)$$

Special cases:

a) $pga < 0.1$ g: simply consider the corresponding variability computed at 0.1 g, i.e,

$$\sigma_{SHA}(pga, m) = \sigma_{SHA}(0.1g, 6)$$

b) $pga > 0.75$ g: simply consider the corresponding variability computed at 0.75 g, i.e,

$$\sigma_{SHA}(pga, m) = \sigma_{SHA}(0.75g, 6)$$

These standard deviations values are to be applied along all the SHAKE and NL branches, even when the 'SHAKE' median amplification factors are estimated on the basis of the RVT base case amplification factors (interpolations for intermediate pga and m values).

4.3.1.2 Interpolation of RVT standard deviation values for arbitrary (pga, m) values

Suppose one has to compute the standard deviation σ_{RVT} corresponding to RVT approach for arbitrary values of pga and m.

The magnitude dependence will come only from the RVT base case with N. Abrahamson formula:

$$\ln amp = \frac{1.28}{2 \ln(f) - 2.3M - 10.74}$$

The acceleration dependence will come only from the observed standard deviation for the other soil profiles and magnitude 6 : $\sigma_{RVT}(pga, 6; f)$. There is some interpolation needed:

$$\sigma_{RVT}(pga, m) = B_1 * \sigma_{RVT}(A_1, 6) + B_2 * \sigma_{RVT}(A_2, 6)$$

with

$$B_1 = (LA_2 - Lpga) / (LA_2 - LA_1)$$

$$B_2 = (Lpga - LA_1) / (LA_2 - LA_1)$$

where

$$Lpga = \log(pga) ; LA_1 = \log(A_1) ; LA_2 = \log(A_2)$$

Special cases:

a) $pga < 0.05$ g: simply consider the corresponding variability computed at 0.05 g, i.e,

$$\sigma_{RVT}(pga, m) = \sigma_{RVT}(0.05g, 6)$$

b) $pga > 1.5$ g: simply consider the corresponding variability computed at 1.5 g, i.e,

$$\sigma_{RVT}(pga, m) = \sigma_{RVT}(1.5g, 6)$$

Summary

- RVT –Base Case : $\sigma_{RVTBC}^2(pga, m; f) = \sigma_{\ln amp}^2(m; f)$
- RVT –Other cases: $\sigma_{RVT,Other}^2(pga, m; f) = \sigma_{\ln amp}^2(m; f) + \sigma_{RVT}^2(pga, 6; f)$

4.3.2 Variability associated with the incident wavefield

Some indications on the variability $\sigma_{\theta_{PSV}}$ can be found in the documents showing the sensitivity of amplification factors to incidence or azimuth angle and/or wave types.

From these, I propose three different values for $\sigma_{\theta_{PSV}}$ with associated weights :

$\sigma_{\theta_{PSV}} = 0$	+	weight 30%
$\sigma_{\theta_{PSV}} = 20\%$	+	weight 40%
$\sigma_{\theta_{PSV}} = 50\%$	+	weight 30%

4.4 Beznau

See values in section 2.4

4.5 Gösgen

See values in section 2.5

4.6 Leibstadt

See values in section 2.6

4.7 Mühleberg

See values in section 2.7

5 ALEATORY VARIABILITY OF VERTICAL GROUND MOTION

5.1 Approach

The approach is again to follow the same logic tree as for the median vertical ground motion. The aleatory variability need therefore to be estimated for each main approach:

- no change approach
- SHAKE approach
- V/H approach

5.1.1 'No change' Approach: no additional aleatory variability

$$\sigma_{AF,V}^2(A_i; f) = 0 \text{ since } AF_V = 1.$$

5.1.2 SHAKE Approach

The formula is similar to the one used for the horizontal motion, excepted for the fact that the magnitude dependence is not accounted for here, because of the lack of available model calculations

$$\sigma_{AF,V}^2(pga; f) = \sigma_{SHA,V}^2(pga; f) + \sigma_{0PSV}^2 + \sigma_{2D}^2 \cdot E_{\sigma}(f; f_v, \zeta, l, \beta_m)$$

As outlined in this formula, the aleatory variability on the vertical amplification factors has several origins:

5.1.2.1 Variability in the input signal waveform (SH case): σ_{ISW}

This variability is estimated through the standard deviation in amplification factors obtained for the 15 different input signals. It is represented, for each velocity profile, by the standard deviation $\sigma_{SHA,V}(pga; f)$ which is frequency dependent.

5.1.2.2 Variability in incident waves (oblique incidence angle, SH, SV or P-wave types)

It is represented by the standard deviation σ_{0PSV} , the estimates of which are given in the various summary tables. It is independent of acceleration level and magnitude. It has to be modulated by the frequency dependent 'envelope function' $A_0(f/f_v)$, where f_v is the fundamental frequency for vertical motion.

5.1.2.3 Variability of 2D/3D effects depending on incident wave azimuth / angle

It is represented by the standard deviation σ_{2D} , the estimates of which are given in the various summary tables. It is independent of acceleration level and magnitude. It has to be modulated by the frequency dependent 'envelope function' $E_{\sigma}(f; f_v, \zeta_{av}, l, \beta_m) = A_0(f/f_v) \exp(-2\pi\zeta_{av}fl/\beta_m)$

NB: In all those formulas, the standard deviation " σ " correspond to the standard deviation of the logarithm of the amplification factor

5.1.3 V/H Approach

$$\sigma_{AF,V}^2(pga,m; f) = \sigma_{V/H}^2(f,m) + \sigma_{AF,H}^2(pga,m;f) + 2 \text{Cor}(H, V/H)$$

with

- $\sigma^2_{V/H}$ is estimated with the following formula
 - $\sigma_{\ln(V/H)} = c_{15} - 0.07 M_w$ for $M_w < 7.4$,
 - $\sigma_{\ln(V/H)} = c_{15} - 0.518$ for $M_w > 7.4$,
 - with c_{15} given in Table 4
- $\text{Cor}(H, V/H)$ is estimated from N. Abrahamson's technical note
- $\sigma^2_{AF,H}$ is estimated from the horizontal component, including the P-SV and 2D variabilities, that need not to be considered twice.

In case $\text{Cor}(H, V/H)$ and $\sigma^2_{V/H}$ are not directly available, I propose to simply approximate $\sigma^2_{AF,V}$ (pga, m; f) by $\sigma^2_{AF,H}$ (pga,m; f); it is not correct from a mathematical viewpoint, but I think it is correct from a physical viewpoint.

Tab. 5-1: Statistical bias in predicted value of vertical-to-horizontal (V/H) ratio

Period (sec)	No.	Bias in ln V/H	Bias (Factor)	c_{15}
Unc. PGA	941	-0.0121	0.99	0.87
Cor. PGA	439	-0.0074	0.99	0.85
0.05	432	0.0003	1.00	0.94
0.075	436	-0.0081	0.99	0.95
0.10	436	-0.0098	0.99	0.97
0.15	436	-0.0110	0.99	0.97
0.20	436	-0.0100	0.99	0.97
0.30	436	-0.0094	0.99	0.97
0.40	436	-0.0074	1.00	0.97
0.50	436	-0.0044	1.00	0.97
0.75	435	-0.0057	0.99	0.97
1.0	435	-0.0033	1.00	0.97
1.5	419	-0.0183	0.98	0.97
2.0	393	-0.0292	0.97	0.97
3.0	313	-0.0370	0.96	0.97
4.0	262	0.0055	1.01	0.97

5.2 Logic tree structure

Since I chose to keep the same logic tree structures as for the median ground motion, the logic tree is the same (see Figure 3.1).

As with the horizontal component, there is one difference related to the incident wavefield: I assumed the incident wavefield does not affect the median ground motion, but that does affect only the aleatory variability. The logic tree for aleatory variability thus includes a sub-branching corresponding to different values for $\sigma^2_{\theta_{PSV}}$. This subbranching includes one branch with

$\sigma_{\theta\text{PSV}}^2 = 0$, because a certain amount of variability associated with incident wave type is already included in the "rock" ground motion estimate.

5.3 Evaluations common to all sites

5.3.1.1 Interpolation of SHAKE standard deviations for arbitrary (pga, m) values

Suppose one has to compute the SHAKE standard deviation σ_{SHA} for arbitrary values of pga and m. I consider here only magnitude 6 results, and I interpolate for different acceleration values as described below:

Let $A_1 < \text{pga} < A_2$ be the two nearest peak accelerations for which the amplification factor is known with SHAKE computations.

Then the estimation formula for any soil column is:

$$\sigma_{\text{SHA},V}(\text{pga}, m) = B_1 * \sigma_{\text{SHA},V}(A_1, 6) + B_2 * \sigma_{\text{SHA},V}(A_2, 6)$$

with

$$B_1 = (LA_2 - L\text{pga}) / (LA_2 - LA_1)$$

$$B_2 = (L\text{pga} - LA_1) / (LA_2 - LA_1)$$

where

$$L\text{pga} = \log(\text{pga}); LA_1 = \log(A_1); LA_2 = \log(A_2)$$

Special cases:

- a) $\text{pga} < 0.1$ g: simply consider the corresponding variability computed at 0.1 g, i.e.,
 $\sigma_{\text{SHA},V}(\text{pga}, m) = \sigma_{\text{SHA},V}(0.1\text{g}, 6)$
- b) $\text{pga} > 0.75$ g: simply consider the corresponding variability computed at 0.75 g, i.e.,
 $\sigma_{\text{SHA},V}(\text{pga}, m) = \sigma_{\text{SHA},V}(0.75\text{g}, 6)$

5.3.2 Variability associated with the incident wavefield

Some indications on the variability $\sigma_{\theta\text{PSV}}$ can be found in the documents showing the sensitivity of amplification factors to incidence or azimuth angle and/or wave types.

From these, I propose the three same different values for $\sigma_{\theta\text{PSV}}$ with associated weights:

$\sigma_{\theta\text{PSV}} = 0$	+	weight 30%
$\sigma_{\theta\text{PSV}} = 20\%$	+	weight 40%
$\sigma_{\theta\text{PSV}} = 50\%$	+	weight 30%

5.4 Beznau

See values in section 3.4

5.5 Gosgen

See values in section 3.5

5.6 Leibstadt

See values in section 3.6

5.7 Mühleberg

See values in section 3.7

6 MAXIMUM GROUND MOTIONS

Evaluating the maximum possible ground motion at a given site is not a simple task. As far as site effects are concerned, the only source of limitations in the ground motion lies in the maximum strains that a given soil can withstand, and beyond which it fails. While such a failure is conceivable – and actually is a real phenomenon - for tangential stresses and strains – roughly corresponding to horizontal motion -, it is much less obvious for normal (compressive) stresses and strains – mainly corresponding to vertical motion in a first, rough approximation.

6.1 Horizontal Component

6.1.1 Evaluation of Proponent Models

There has been basically two different approaches proposed

- estimating the maximum pga from the maximum possible strains, and associating a normalized response spectrum (Pecker's document 'Evaluation of maximum ground motions'+ estimates of associated spectra, TP3-TN-0358).
- estimating the maximum spectral ordinate for each frequency/period, on the basis of observed maximum ground motion throughout the world (empirical approach, TP3-TN-0359).

6.1.1.1 Estimation of maximum pga's

Basically, this approach is based on an estimate of the (depth dependent) shear strength, and an estimate of the yield shear strain. The first one is derived from cohesion and friction parameters of the soil, while the second one is estimated to be around 2% to 3%.

The subsequent estimate of the maximum acceleration comes from a modal representation of the soil response, with appropriately adjusted shear wave velocities and damping.

This approach provides maximum pga estimates that seem 'reasonable' (Table 3 p.27 of Pecker's document, TP3-TN-0358); however, it relies on several assumptions that may not be correct

- at failure, the soil velocity profile follows a power law depth dependence, derived from the shear strength profile and the assumption of quasi constant strain over the whole profile. One may indeed prefer a totally different approach where the strain is localized at a given depth, with a very sharp reduction of elastic parameters at this very depth
- the shear strength under dynamic excitation is similar to the shear strength under static load. This may be correct, but I am not totally convinced. The range of "plausible" friction angles under dynamic loading may exceed the range of 'plausible' friction angles under static loading
- the yield strain (2-3%) under dynamic excitation is similar to the yield strain under static load. Again, this may be correct but I am not totally convinced; however, the sensitivity study included in A. Pecker's report shows that the influence on pga is almost negligible. There is, however, an influence on the spectral shape (lower frequencies for larger yield strain).
- at failure, the modal approach may still be used to estimate the peak strains and accelerations. I heard in the past many structural and geotechnical engineers totally reject such an

assumption when applied to civil engineering concrete structures and soil geotechnical structures as well.

- The maximum values significantly depend on the number of modes taken into account (they are larger for a lower number of modes, as was shown in earlier's version of A. Pecker's report).

Therefore, my confidence on the results of such an approach is limited and I will consider some subbranching with different scaling factors to introduce a significant amount of epistemic uncertainty on the values issued by such an approach – which has the great advantage of providing some estimate which does bear some physical / mechanical basis.

Moreover, the history of geotechnical earthquake engineering since the late sixties shows a systematic trend to overemphasize the beneficial effects of non-linear behavior, trends which led to significant corrections for example after the Mexico City and Loma Prieta events. Although I do not identify in this approach a clear bias, I will deliberately introduce in this subbranching a slight bias to account for such a observed trend. Another reason for introducing such a bias is the fact that some NL computations for Beznau led to peak ground motions significantly larger than the estimates given by this approach (>2.1g to be compared with 1.3 g).

6.1.1.2 Maximum recorded horizontal motion (TP3-TN-0359)

This approach is purely empirical and simply looks at the maximum ground motion ever recorded for each frequency. The only link between this approach and site conditions is through the soil categorization in 4 different site classes.

Clearly, such an approach can only provide some "qualitative" indication on a "lower bound" for such a maximum ground motion, since such "maximum" motions can only increase with the increasing number of instruments and seismic events., In additiona, such an approach is clearly not site-specific, since sites are grouped in very gross site categories.

This approach presents the advantage to be totally free of any underlying model, and may therefore reflect, in some way, the level of maximum ground motion that one may reasonably anticipate, irrespective of any other considerations on the regional seismic hazard and local site conditions.

Since I am not convinced of some of the underlying assumptions of the Pecker's model, I trust a little bit more such a purely empirical approach; however, I will introduce some sub-branching to allow some larger values for the maximum ground motions, since future events can only raise the values listed in Ripperger and Fäh's document

On the other hand, when analyzed in detail, the 'maximum' observed envelope spectrum exhibits several spectral peaks which are very probably related with several individual records: there is a good chance that the next unusually large record will fill some of the spectral troughs, as I do not see any physical reason while some frequencies would correspond to a relatively smaller possible ground motion than neighboring frequencies. I therefore introduce an 'enveloping' of the Ripperger & Fäh's maximum spectra, which may be obtained in two ways.

Let $S_{\max, \text{obs}}(f)$ be the 'observed' maximum spectral acceleration for frequency f , as derived from from TP3-TN-0359, and $S_{\max, \text{env}}(f)$ the "enveloped" maximum spectral acceleration.

$S_{\max, \text{env}}(f)$ is simply derived by smoothing the observed maximum spectra $S_{\max, \text{obs}}(f)$ with a smoothing process going thorough main local maxima and strong enough to remove all peaks but one. More specifically, the algorithm is the following:

1. find the 'meaningful' local maxima in the intermediate frequency band: for instance, for the 'soil' observed maximum ground motion, these maxima are the following (Figure) for the horizontal spectrum, these maxima occur at 0.5-0.6 Hz, 3 Hz, 10 Hz, 20 Hz for the vertical spectrum, these maxima occur at 0.6 Hz, 1.4 Hz, 2.2 Hz, 4.3 Hz, 9 Hz, 20 Hz

2. fit a 7th order polynomial through these maxima and the spectra at low and high frequencies

6.1.2. Logic Tree Structure

My logic tree starts with two main branches, one for Pecker's estimate of pga, the other one for Fähr's estimate of maximum ground motion.

6.1.2.1 Pecker's approach branch

Uncertainty in pga values

I consider that the maximum pga estimates given in Table 3 p.27 of Pecker's document are highly uncertain.

To represent this epistemic uncertainty, I therefore introduce a subbranching with four branches with different scaling factors: the first three are symmetric and are representative of the uncertainties in the model, while the fourth one is intended to introduce a bias in the estimate. The 'plausible values' recommended in the WS3a workshop to take into account the variability in shear strength due to variability in friction angle were from 0.85 to 1.25; considering the comment on dynamic vs static parameter, I will increase a little bit this range to $1/\sqrt{2}$ (0.707) to $\sqrt{2}$ (1.414); and the fourth branch has a scaling factor which is chosen so as to exceed the ratio between the max pga computed in NL runs for Beznau and the estimate given following Pecker's approach (i.e., $21.5/13 = 1.65$). As these NL runs were performed only for a limited set of accelerograms, the maximum value for the scaling factor is taken equal to a factor of 2. The final scaling factors are therefore : 0.707, 1.0, 1.414 and 2.0.

Associated spectra

Given the PGA, one must then associate an acceleration spectrum, anchored to such pga values. Two approaches are possible:

- applying the normalized spectra derived from linear computations with the associated shear modulus and damping values (TP3-TN-0358, May 2003): as the standard deviations on these normalized spectral shapes are also significant (up to a factor of 2 for low frequencies – 0.5 to 1 Hz -, the spread in anchoring accelerations is also intended to take into account, at least partly, this variability in spectral shapes.
- applying the normalized spectra deduced from the existing strong motion records (i.e., the solid black line ('soil') spectra on top of Figure 3 of TP3-TN-0359, divided by the corresponding PHA.

I use both approaches with equal weights.

6.1.2.2 Fähr's approach branch

This approach provides directly estimates over the whole spectrum. I will therefore simply keep the 'soil' maximum spectra displayed in Figure 3 top (solid black line), and introduce a subbranching into four branches, where the spectral ordinate values are multiplied, respectively, by scaling factors 1.0, 1.2, 1.5 and 2.0. The first branch implicitly considers the present day ever observed maximum spectral ordinates to be the true maxima: it has obviously little chances to be true, and it will be attributed a rather low weight. The two other scaling factor values, which can be only indicative, are derived from an analysis of the increase of the maximum values with time over the last decades: there were sharp increase in the late seventies (with factors up to 3-4 in the high-frequency range), while in the two last decades, the increase was smaller and affecting only intermediate and low frequencies, with jump factors smaller than 2 and typically in the range around 1.5.

Considering that in the last two decades, the number of accelerometers has drastically increased, and several magnitude around 7 events have been recorded at very close stations: I do not anticipate jumps in the maximum ground motion by factors as high as what occurred in the seventies with the San Frenando and Imperial Valley events. Also, the enveloping/smoothing procedure adopted for the observed maximum spectra should reduce the jumps with future earthquakes.

6.1.3 Weights for Maximum Ground Motions

6.1.3.1 Pecker / Fäh weights

For all sites, I assign a 50 % weight for Pecker's approach, and a 50% weight for Fäh's approach, in order to give equal consideration to purely empirical, non site-specific estimates and those based on site specific mechanical considerations.

6.1.3.2 Pecker's branch: uncertainty in pga values.

For each site, I consider the following base pga values :

Beznau: 13 m/s² - Gösgen : 14 m/s² - Leibstadt: 16 m/s² - Mühleberg: 16 m/s² -

Each of these values is multiplied along each subbranch by factors 0.707, 1.0, 1.414 and 2.0, with respective weights of 15%, 65%, 15%, and 5%.

6.1.3.3 Pecker's branch: associated spectra.

There are two possibilities : normalized spectra from 1D soil response (TP3-TN-0358), and soil normalized spectra from Figure 3 top of TP3-TN-0359.

The corresponding weights are, respectively 50% for the former, and 50% for the latter.

6.1.3.4 Fäh's branch: uncertainty in spectral values.

There are four branches corresponding to scaling factors 1.0, 1.2, 1.5 and 2.0, respectively.

The corresponding weights are, respectively, 20%, 50%, 25% and 5%.

6.2 Maximum horizontal ground motions at depth

6.2.1 Discussion of models used for surface ground motion

Two different approaches have been used for the surface motion:

- estimating the maximum pga from the soil strength, and associating a normalized response spectrum.
- estimating the maximum spectral ordinate for each frequency/period, on a purely empirical basis (observed maximum ground motion throughout the world).

Both approaches were already discussed in some detail for surface motion; a few other considerations should be added for ground motion at depth.

In addition, it is not easy to understand what is really, or should be, a "maximum outcropping motion" at depth, and how one could measure it or compute it.

6.2.1.1 Estimation of maximum pga's based on soil strength

Basically, this approach is based on an estimate of the (depth dependent) shear strength, and an estimate of the yield shear strain. The first one is derived from cohesion and friction parameters of the soil, while the second one is estimated to be around 2% to 3%. The subsequent estimate of the maximum acceleration comes from a modal representation of the soil response, with appropriately adjusted shear wave velocities and damping.

A discussion on the underlying assumptions of that approach led me to have only a limited confidence in its results, and therefore to consider a subbranching with different scaling factors to introduce a significant amount of epistemic uncertainty on the values issued by such an approach.

For ground motion at depth, I consider the confidence of such an approach is even more limited. Considering that the velocity profile at failure exhibits a gradient with a positive exponent, the maximum ground motion values found at depth with such an approach for the 4 sites are systematically lower than the values at the surface. Meanwhile, amongst the very few experimental vertical array data corresponding to soil failure, the Kobe Port Island array clearly showed that the ground motion at depth was significantly larger than at the surface (the horizontal pga is almost twice larger at 16 m depth than at the surface) : such a result can be reproduced only with models including some kind of strain localization, which is not the case of the Pecker's soil strength approach.

As a consequence, I decided to

- a) decrease the weight of this approach for motion at depth; this decrease will be exceptionally sharp at sites BZ2 and MZ2: this soil strength approach is not applicable for rock sites, and its weight is thus 0 in those 2 cases.
- b) modify the weighting of the subbranches, so as to introduce a larger bias towards higher pga values.

6.2.1.2 Maximum recorded horizontal motion (TP3-TN-0359)

This purely empirical approach simply takes into account the maximum ground motion ever recorded for each frequency. Its additional limitations for the present case of ground motion at depth, come from the fact that the vast majority of recorded data are surface data.

Several approaches can be imagined to (try to) overcome these limitations:

- a) Just consider the surface maximum ground motion, without any depth correction factor, and enlarge the uncertainty of the scaling factors in the subbranching introduced to take into account the data set limitations.
- b) introduce a "depth correction" factor similar to the depth correction factor used in liquefaction analyses ("rd(z)" factor in Seed and Idriss classical approach): I finally rejected this possibility, since maximum ground motion should be associated with soil failure, and the "rd(z)" function is definitely not known, and certainly very different in the case of failure from what is found after quasi-elastic wave propagation analyses.
- c) Consider the overall envelope of ever recorded ground motion on any type of site (soft soil, stiff soil, rock, ...).
- d) Consider a weighted average of maximum ground motion ever recorded on soil and rock, respectively.

I finally decided to consider choices a) and d), the relative weighting between soil and rock envelope spectra being related to the relative depth of the site with respect to the total thickness of sediments at the site.

In addition, given the results from the very few recorded array data at failed soils (Port Island, Kobe event of 1995; Wildlife Liquefaction array, California Superstition Hills event 1987), I decided to increase the bias to larger values in the sub-branching for scaling factors on soil spectra (modifying the weights).

Additional details:

For surface motion, an 'enveloping' of the Ripperger & Fäh's maximum spectra, was introduced, and the procedure to obtain that enveloping detailed for the maximum spectra on 'soil' sites (see elicitation summary for surface motion). A similar enveloping should be applied to the maximum spectra obtained for rock sites "rock sites"

6.2.2 Logic Tree Structure and weights

As for surface motion, my logic tree starts with two main branches, one for Pecker's estimate of p_{ga} , the other one for Fäh's estimate of maximum ground motion.

6.2.2.1 Pecker's approach branch

For surface motion, its weight was set equal to 50% ; considering its physical inability to represent soil failure and strain localization at some particular depth, I will decrease this weight to 40% (sites within soil units) and 0% (sites within rock units), as listed in Table 4.1:

Uncertainty in p_{ga} values

I start for the maximum p_{ga} estimates given in Table 3 p.27 of Pecker's document (i.e., 13 m/s^2 for Beznau, 14 m/s^2 for Gösigen, 16 m/s^2 for Leibstadt, and 16 m/s^2 for Mühleberg).

To represent the epistemic uncertainty on these values for the surface motion, I introduced a subbranching into 4 branches with different scaling factor values, respectively 0.707, 1.0, 1.414 and 2.0, which were assigned, respectively, the following weights: 15%, 65%, 15%, and 5%.

For the depth sites for which this approach is kept, I keep the same subbranching into 4 branches with the same scaling factor values. But I change their respective weights, in order to increase the bias towards larger values, corresponding to the occurrence of failure at an intermediate depth. Since this bias should increase with depth, these weights, as listed in Table 4.1, are set equal to 10%, 60%, 20%, and 10%, for the intermediate depth site, and to 10%, 50%, 25%, and 15% for the deepest.

6.2.2.1.2 – Associated spectra

Two approaches were selected to associate an acceleration spectrum, anchored to such p_{ga} values:

- applying the normalized spectra derived from linear computations with the associated shear modulus and damping values (TP3-TN-0358, May 2003).
- applying the normalized spectra deduced from the existing strong motion records (i.e., the solid black line ('soil') spectra on top of Figure 3 of TP3-TN-0359, divided by the corresponding PHA.

For the surface motion, I assigned equal weight to each approach; for motion at depth, considering again that the linear equivalent approach is not very satisfactory because of the absence of any strain localization, I decrease the weight from 50% to 40% for the intermediate depth site, and to 30% for the deepest site (when applicable).

6.2.2.2 Fähr's empirical approach branch

There is one major difference with respect to the surface motion case: in order to account for the fact that some sites at depth are located within rock units, I introduced another subbranching.

Subbranching for soil and rock envelope spectra

The weights of each branch are very much site-dependent. Their values for each site at depth are listed in Table 4.1. These values were obtained in the following way:

$$W(\text{soil envelope spectrum}) = 1 - z/h$$

$$W(\text{rock envelope spectrum}) = z/h$$

Where z the depth of the site, and h is the thickness of the alluvial cover over rock. The h values considered for each site were 10 m for Beznau (opalinuston), 25 m for Gösigen, 50 m for Leibstadt, and 10 m for Mühleberg.

Subbranching for scaling factors

Along each of these 2 branches, one should consider an uncertain scaling factor as for surface motion. The same values of scaling factors (1., 1.2, 1.5 and 2.0) are considered.

Along the 'rock' spectrum branch, the same weights as for surface motion are considered (i.e., 20%, 50%, 25% and 5%, respectively), because they represent the fact that the observed maxima can be only a lower bound for the "true" maxima.

Along the 'soil' spectrum branch, the weights were assigned different values, in order to increase the bias towards higher motion: this increase is introduced to represent, in some way, the possibility of soil failure at some depth. This increase is thus larger for deeper sites (Leibstadt, Gösigen). The weights for each site are listed in Table 4.1.

Tab. 6-1: Weights for maximum horizontal ground motion at depth

Site	BZ1	BZ2	GZ1	GZ2	LZ1	LZ2	MZ1	MZ2
<i>Pecker's soil strength approach</i>								
W (Pecker)	40%	0%	40%	40%	40%	40%	40%	0%
<i>Scaling factors</i>								
W (0.707)	10%	-	10%	10%	10%	10%	10%	-
W (1.0)	60%	-	60%	50%	60%	50%	60%	-
W (1.414)	20%	-	20%	25%	20%	25%	20%	-
W (2.0)	10%	-	10%	15%	10%	15%	10%	-
<i>Associated spectra</i>								
LE approach (TP3-TN-0358)	40%	-	40%	30%	40%	30%	40%	-
Empirical shapes (soil)	60%	-	60%	70%	60%	70%	60%	
<i>Fähr's empirical approach</i>								
W (Fähr)	60%	100%	60%	60%	60%	60%	60%	100%
<i>Relative weighting between soil and rock envelope spectrum</i>								
W (soil)	40%	0%	80%	60%	90%	80%	30%	0%
W (rock)	60%	100%	20%	40%	10%	20%	70%	100%

<i>Scaling factors for soil envelope spectrum</i>								
W (1.0)	15%	10%	15%	10%	15%	10%	15%	10%
W(1.2)	45%	40%	45%	40%	45%	40%	45%	40%
W(1.5)	30%	35%	30%	35%	30%	35%	30%	35%
W(2.0)	10%	15%	10%	15%	10%	15%	10%	15%
<i>Scaling factors for rock envelope spectrum</i>								
W (1.0)	20%							
W(1.2)	50%							
W(1.5)	25%							
W(2.0)	5%							

6.3 Vertical Component

6.3.1 Evaluation of Proponent Models

There is only one approach proposed, based on observed maximum ground motion. As discussed in the specialized meeting in Nice on April 12, 2003, there is no straightforward physical mechanism that would limit the vertical ground motion, except may be for downgoing motion because of the small tensile strength of most soils.

The main basis for maximum vertical ground motion is therefore the spectra on bottom frame of Figure 3 of TP3-TN-0359, where I consider only the "solid black line" spectrum corresponding to 'soil' class.

6.3.2 Logic Tree Structure

The logic tree structure is thus consistent with what is proposed for the horizontal ground motion, with considering only the 'Fäh's approach' branch, with three subbranches to take into account the limited set of strong motion data presently available throughout the world. The multiplying coefficients are again 1.0, 1.2 and 1.5...

6.3.3 Weights for Maximum Ground Motions

There are four branches corresponding to scaling factors 1.0, 1.2, 1.5 and 2.0, respectively.

The corresponding weights are, respectively, 20%, 50%, 25% and 5%.

6.4 Maximum vertical ground motions at depth

6.4.1 Chang in the models

Only one approach was proposed for the surface motion, based on observed maximum ground motion, since there is no straightforward physical mechanism that would limit the vertical ground motion.

The same approach is kept for the maximum ground motion at depth except for the fact that, as for the horizontal motion, one must also consider the 'rock' envelope spectrum for maximum vertical ground motion (Figure 3 of TP3-TN-0359).

6.4.2 Logic Tree Structure and weights

The logic tree structure is thus consistent with what is proposed for the horizontal ground motion, with considering only the 'Fäh's approach' branch, with two subbranching levels

- a first one with two branches for rock and soil envelope spectra; the weights were derived as for the corresponding branch on the horizontal ground motion, i.e., based on the z/h value.
- the second one with four subbranches to take into account the limited set of strong motion data presently available throughout the world. The scaling factors are again 1.0, 1.2, 1.5 and 2.0, with respective weights 20%, 50%, 25% and 5%.

Tab. 6-2: Weights for maximum vertical ground motion at depth (*Fäh's empirical approach*)

Site	BZ1	BZ2	GZ1	GZ2	LZ1	LZ2	MZ1	MZ2
<i>Relative weighting between soil and rock envelope spectrum</i>								
W (soil)	40%	0%	80%	60%	90%	80%	30%	0%
W(rock)	60%	100%	20%	40%	10%	20%	70%	100%
<i>Scaling factors for all envelope spectra (soil and rock)</i>								
W (1.0)	20%							
W(1.2)	50%							
W(1.5)	25%							
W(2.0)	5%							

7 REFERENCES

- Bozorgnia, Y. & Campell, K.W. 2002: Vertical-to-Horizontal Response Spectral Ratio and the Vertical Design Spectrum. Submitted to Earthquake Spectra, March 8, 2002.
- PEGASOS EXT-RF-0246: Bozorgnia, Y. & Campell, K.W. 2002: Vertical-to-Horizontal Response Spectral Ratio and the Vertical Design Spectrum. Submitted to Earthquake Spectra, March 8, 2002.
- PEGASOS TP3-ASW-0024: Hölker, A.: Matlab software package and databases for the computation of the SP3 / site amplification models.
- PEGASOS TP3-TN-0297: Abrahamson, N.: Aleatory variability of site amplification factors for the RVT approach.
- PEGASOS TP3-TN-0340: Bard, P.-Y. 2003: A short note on the reliability of SHAKE amplification factors at low frequencies (20.3.2003).
- PEGASOS TP3-TN-0354: Pecker, A. 2003: Evaluation of Maximum Ground Motions.
- PEGASOS TP3-TN-0358: Bard, P.Y.: Response spectra associated with maximum peak ground acceleration for the 4 PEGASOS sites.
- PEGASOS TP3-TN-0359: Rippberger, J. & Fäh, D. 2003: Maximum Recorded Horizontal and Vertical Ground Motions.
- PEGASOS TP3-TN-0401: Hölker, A.: Summarizing the SP3 site effect models to Soil hazard Input Files (SIFs).

APPENDIX 1 EG3-HID-0050 SITE AMPLIFICATION AT THE SURFACE AND EMBEDDED LAYER DEPTHS FINAL MODEL P.-Y. BARD

A1.1 Introduction

This document describes the implementation of Pierre-Yves Bard's models of site amplification at the surface, mean and maximum building depths (Table 1) as well as his assessment of maximum possible ground motions at the four Swiss NPP sites: Beznau, Gösgen, Leibstadt and Mühleberg. The purpose of this document is to translate the expert's evaluation of amplification factors into a Soil hazard Input File (SIF) for the hazard computation software (SOILHAZP) and to provide the expert with the necessary information to review the results of his model.

The implementation of Pierre-Yves Bard's model is based on his elicitation summaries EG3-EXM-0029 of October 2nd, 2003 (site effects at the surface), of October 30th (maximum ground motion at the surface) and of December 23th (embedded layers).

The following document and software are directly linked to this HID:

- TP3-TN-0401: A technical note describing the computational steps performed to create the soil hazard input files (SIFs)
- TP3-ASW-0024: The software used to implement the SP3 models

This HID consists of four sub-sections:

- A description of the computational steps leading to the development of amplification factor spectra and their associated aleatory variabilities for each site and combination of magnitudes, input PGAs and ground motion types.
- A description of the expert's assessment of maximum ground motion spectra.
- A summarized description of creation of SIFs for site amplification, the associated aleatory variability. A detailed description is available in the technical note TP3-TN-0401.
- The generalized logic tree for horizontal ground motion at the surface.

The implementation of Pierre-Yves Bard's model was done by the SP3 TFI Team at Proseis using Matlab R13. The complete implementation is archived as TP3-ASW-0024. It consists of a software module and a database.

Tab. A-1: Mean and maximum building depth for the four Swiss NPP sites

	Beznau	Gösgen	Leibstadt	Mühleberg
Mean building depth	6 m	5 m	5 m	7 m
Max. building depth	15 m	9 m	10 m	14 m

A1.2 Site amplification and its aleatory variability

In this section the key-elements of Pierre-Yves Bard's model are outlined, the crucial aspects are detailed, and the results are illustrated by means of a single example figure per computational step. Figures showing the results for all cases and sites are available as an electronic appendix in PDF format. The logic tree architecture is not reviewed here completely, since it is detailed in the elicitation summaries. However, the generalized logic tree for horizontal ground motion at the surface is given at the end of this HID. Finally it shall be noticed, that the results given in this section are an intermediate product, since they are summarized to discrete fractiles and associated with spectral accelerations before being used as an input for the soil hazard computations.

A1.2.1 Amplification of horizontal ground motion

The characteristic elements of Pierre-Yves Bard's model are:

- In the first two levels of the logic tree all possible combinations of velocity profiles and material models for the considered site are detailed.
- Five alternative approaches to the simulation of site amplification are considered: (1 and 2) RVT with and without (base case) randomization of the velocity profile; (3) the average of the SHAKE simulations for 15 representative ground motions; (4) the average of the true non-linear (NL) simulations for 5 representative ground motions; and (5) the "linear case", which is in fact an RVT base case simulation for a PGA level of 0.05 g.
- The weights assigned to the alternative approaches depend on the site under consideration and the deformation range, this being derived from the strain depth profiles of the RVT simulation for a particular PGA level.
- Linear interpolation is used to obtain RVT amplification factors for intermediate magnitudes and PGA levels. To estimate SHAKE and NL amplification factors for intermediate magnitudes and PGA levels, the proximity of available SHAKE or NL simulation to corresponding RVT base case simulations is quantified. This proximity is then used to derive a scaling factor to be applied to the RVT base case at the magnitude and PGA level of interest.
- In cases with PGA levels above 1.5 g and / or magnitudes above 7, a set of uncertainty factors is applied to the considered RVT, SHAKE, or NL simulation for PGA = 1.5 g and magnitude 7. The NL simulations for a PGA of 2.5 g at Beznau and Gösgen are not considered.
- P-SV effects are considered to be irrelevant regarding the median site amplification.
- 2D effects are considered to be relevant at all sites. Three alternative factors are used to modify the site amplification to include these in the model.
- To estimate NL amplification factors at depth for outcropping motion (which are not available from the database), two alternatives based on SHAKE simulations for magnitude 6 at 0.4 g and 0.75 g are used:

$$(1) \quad AF_{NL,depth,outcrop} = AF_{NL,surface} \bullet \frac{AF_{SHAKE,depth,outcrop}}{AF_{SHAKE,surface}}$$

$$(2) \quad AF_{NL,depth,outcrop} = AF_{NL,depth,within} \bullet \frac{AF_{SHAKE,depth,outcrop}}{AF_{SHAKE,depth,within}}$$

- In contrast to the surface layer the above correction of the non-linear amplification factors and a frequency and depth dependent deamplification of the 2D effects is applied in the case of embedded layer depths.

Any resulting amplification factor is based on either RVT, SHAKE, or NL simulations, to which different 2D effects factors or uncertainty factors have been applied (in the case of extrapolation). Central to Pierre-Yves Bard's model is the weighting of the RVT, SHAKE, or NL simulations, which is linked to the frequency and the deformation range, which is in turn dependant on the site, PGA level and magnitude.

The example in Figure A-1 shows the assessment of alternative amplification factors considered for the mean building depth at NPP Beznau for the case of a magnitude 6 earthquake with PGA on rock of 1.5 g. For corresponding figures showing the results for all other cases and sites see the *Bard.AF AVar.<site>.HM<depth>.pdf* files in the appendix. Figure A-2 shows the weighted geometric mean amplification factors for mean building depth in Beznau as function of PGA on rock and frequency. For the other sites and magnitudes see the *Bard.SiteModAF.<site>.HM<depth>.pdf* files.

A1.2.2 Aleatory variability of amplification of horizontal ground motion

Pierre-Yves Bard develops the aleatory variability of the amplification of horizontal ground motion using a tree parallel in essence to that of the site amplification. The models of amplification and aleatory variability are, however, not completely correlated, since the weights of the final branch tips are different. Beside this, there are two more differences: The epistemic uncertainty of P-SV effects is explicitly considered for the aleatory variability, while it is not for site amplification. In the case of extrapolation of amplification factors, the uncertainty factors applied to amplification are neglected regarding the aleatory variability. In the case of embedded layer depths the aleatory variability due to PSV effects was reduced for the maximum depths at Beznau and Mühleberg when compared with the surface case.

The resulting uncertainties are the square root of the sums of the squared variabilities of the underlying amplification factors, the P-SV sensitivities and the 2D effects.

Figure A-3 shows an assement of the aleatory variability, corresponding to the site amplification case shown in Figure A-1. For the results of all other cases and sites please see the *Bard.AF AVar.<site>.HM<depth>.pdf* files in the appendix. For the plots of mean aleatory variability corresponding to that in Figure A-2, see the *Bard.SiteModAVar.<site>.HM<depth>.pdf* files.

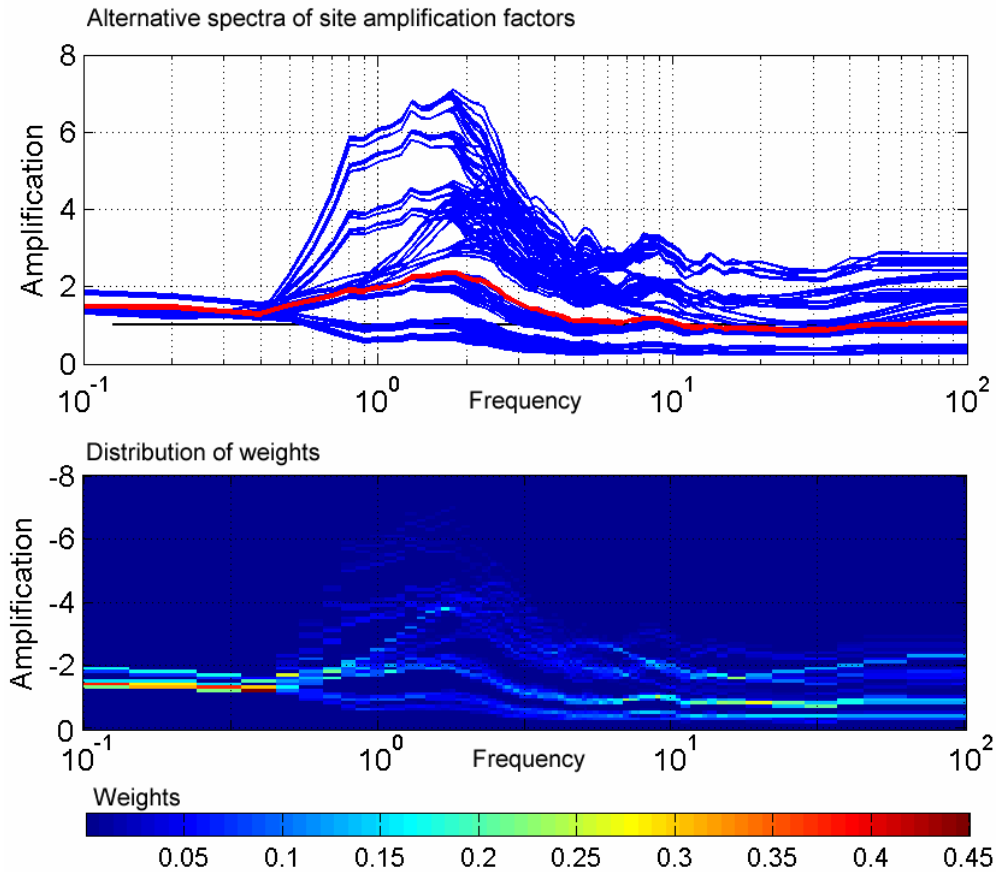


Fig. A-1: Site amplifications factors for horizontal ground motion at the mean building depth of NPP Beznau for the case of a magnitude 6 earthquake with PGA on rock of 1.5 g
 The upper plot shows the alternative amplification factors (blue curves) and their weighted mean (red curve). The lower plot shows the distribution of weights in the amplification-frequency space. Corresponding plots are available for all sites and cases in the appendix: See the *Bard.AF_AVar.<site>.HM<depth>.pdf* files.

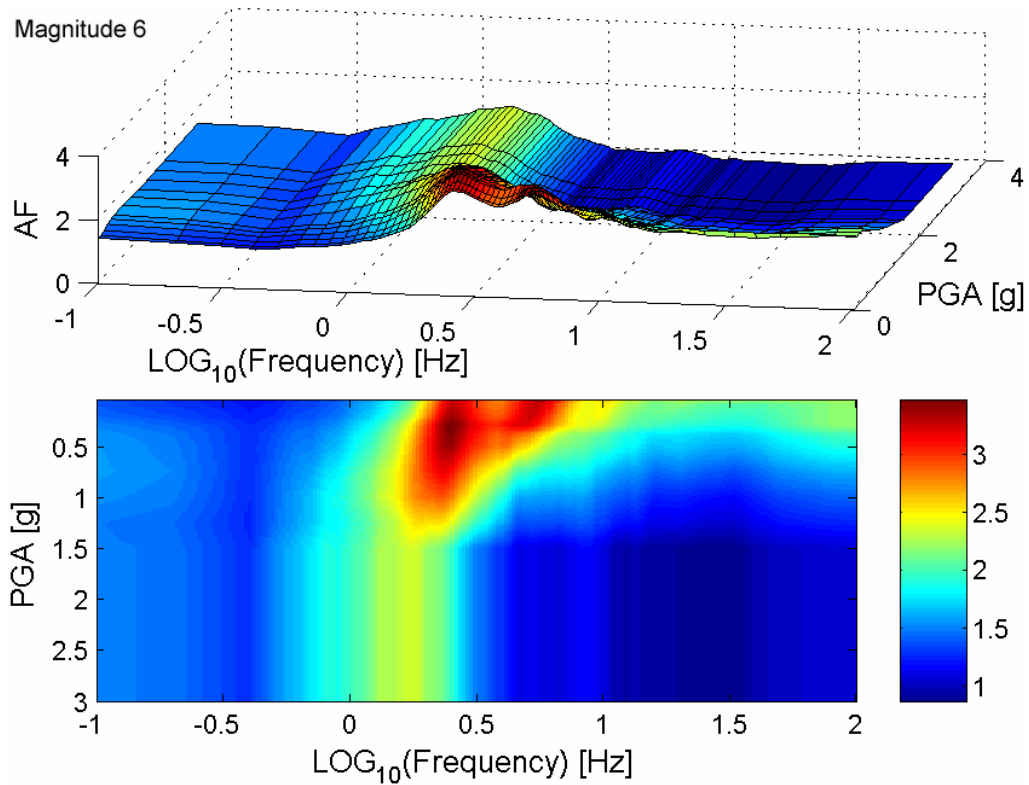


Fig. A-2: Weighted geometric mean amplification factors (AF as function of PGA on rock and frequency) for horizontal ground motion of a magnitude 6 scenario at mean building depth of NPP Beznau

Corresponding plots are available for all sites and cases in the appendix: See the *Bard.SiteModAF.<site>.HM<depth>.pdf* files.

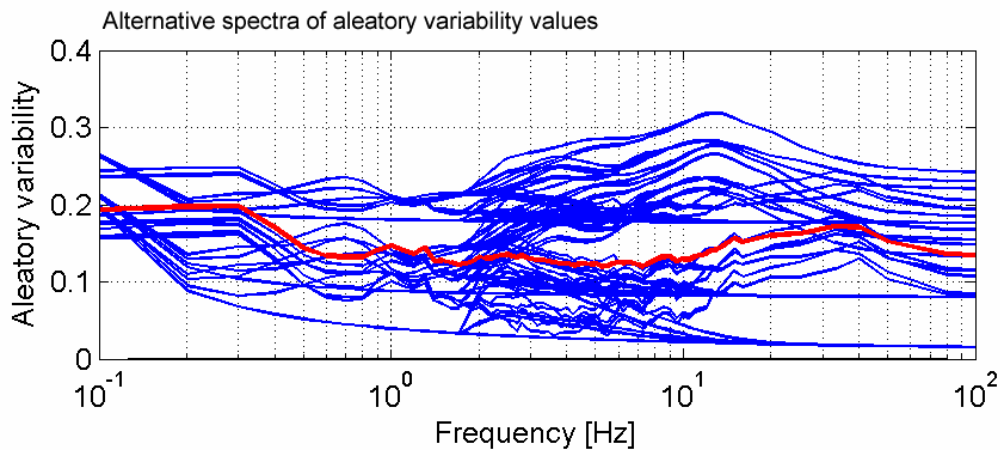


Fig. A-3: Aleatory variability of amplifications factors for horizontal ground motion at the mean building depth of NPP Beznau for the case of a magnitude 6 earthquake with PGA on rock of 1.5 g

The blue curves correspond to the alternative aleatory variabilities and the red curve is the weighted mean aleatory variability. Corresponding plots are available for all sites and cases in the appendix: See the *Bard.AF_AVar.<site>.HM<depth>.pdf* files in the appendix.

A1.2.3 Amplification of vertical ground motion

The development of amplification factors for vertical ground motion is based on three approaches: (1) V/H ratios which are applied to amplification factors for horizontal ground motion; (2) SHAKE simulations of P-wave propagation; (3) the possibility that there are no site effects for P-waves ("no change" branch). These alternatives are developed in the first level of the logic tree.

The V/H ratio approach: PY Bard uses the Borzorgnia and Campbell (2002) model (EXT-RF-0246) to calculate V/H ratios for arbitrary combinations of magnitude and distance to the rupture. The obtained V/H ratios are then applied to all amplification spectra arising from the horizontal ground motion model. The distance term, was obtained through a deaggregation of the final rock hazard results and 10 km were found. This distance, from which the main contribution to hazard is located, is considered as representative rupture distance to be used for the V/H ratio approach. This is valid for all four sites. In the case of the embedded layers, a frequency dependent reduction of the weight (compared with the surface case) of the V/H approach was introduced and additional sub-branching to account for higher epistemic uncertainty was implemented.

The SHAKE approach: A logic tree for SHAKE simulations of P-wave amplification was developed by Pierre-Yves Bard. The characteristic elements are similar to those of the model of horizontal ground motion:

- All combinations of velocity profiles and material models are considered. SHAKE amplification factors for those combinations for which no simulations are available are estimated on the basis of ratios of the corresponding SHAKE simulations for horizontal ground motion.
- Two different P-wave degradation methods are considered, as well as a linear case, which is always taken to be the corresponding SHAKE model for $PGA = 0.1$ g.
- In the case of extrapolation of SHAKE simulations to PGA levels above 0.75 g alternative factors are applied to account for uncertainty.
- Only for the aleatory variability is P-SV sensitivity considered.
- Alternative factors to account for 2D effects are considered.
- In the case of embedded layer depths, a frequency and depth dependent reduction of 2D effects is implemented.

Figures showing the assessment of amplification factors for vertical ground motion (corresponding to Figure A-1) are available in the files *Bard.AF.AVar.<site>.VM<depth>.pdf*. Figures showing mean site amplification factors as function of frequency and PGA on rock (corresponding to Figure A-2) are available in the *Bard.SiteModAF.<site>.VM<depth>.pdf* files.

A1.2.4 Aleatory variability of amplification of vertical ground motion

As with the horizontal case, aleatory variability of vertical ground motion is developed in a logic tree parallel to that for site amplification, but it differs in the weights of the final branch tips.

In the case of the V/H approach the squared aleatory variability is the sum of the squared uncertainty of the V/H ratios and the squared aleatory variability of the amplification factors of horizontal ground motion to which the ratios were applied. In case of the SHAKE approach the squared aleatory variability is the sum of the squared uncertainty of the SHAKE simulation, the P-SV effects, and the 2D effects. In the case of the "no change" branch, the aleatory variability of site effects is zero.

Plots of the assessment of aleatory variability of vertical ground motion are available in *Bard.AF_AVar.<site>.VM<depth>.pdf* and figures showing mean aleatory variability as function of frequency and PGA on rock are given in the *Bard.SiteModAVar.<site>.VM<depth>.pdf* files.

A1.2.5 Parameter ranges

Pierre-Yves Bard's model of horizontal and vertical ground motion has been computed for the input PGAs (on rock) of 0.05, 0.1, 0.2, 0.03, 0.4, 0.5, 0.75, 1.0, 1.25, 1.5, 1.75, 2.0, 3.0 g and magnitudes 5, 6 and 7. All SP3 expert models are computed for a set of 76 spectral frequencies. These frequencies are 0.1, 0.2, 0.3, 0.4, 0.5, 0.6, 0.7, 0.8, 0.9, 1, 1.1, 1.2, 1.3, 1.4, 1.5, 1.6, 1.7, 1.8, 1.9, 2, 2.1, 2.2, 2.3, 2.4, 2.5, 2.6, 2.7, 2.8, 2.9, 3, 3.15, 3.3, 3.45, 3.6, 3.8, 4, 4.2, 4.4, 4.5, 4.6, 4.7, 4.8, 5, 5.1, 5.25, 5.5, 5.75, 6, 6.25, 6.5, 6.75, 7, 7.25, 7.5, 7.75, 8, 8.5, 9, 9.5, 10, 10.5, 11, 12, 12.5, 13, 13.5, 15, 16, 20, 25, 33, 40, 50, 80 and 100 Hz.

A1.3 Maximum ground motion at the surface

A1.3.1 Horizontal ground motion

Pierre-Yves Bard developed 12 alternative maximum ground motion spectra for the surface and a 4 or 16 alternative maximum ground motion spectra for the embedded layer depths. Each of the alternatives is assigned a weight.

The maximum ground motion model considers maximum PGAs modeled by Pecker (TP3-TN-0354), estimated spectral shapes by Bard (TP3-TN-0358), and the upper envelope of empirical spectra of maximum ground motions on soil and rock by Ripperger and Fäh (TP3-TN-0359).

Figures showing the maximum (horizontal and vertical) ground motions for all sites are available in the appendix in the file *Bard.MaxGM.AllSites.HMall.pdf*. Figure A-4 shows the alternative maximum horizontal ground motion spectra for NPP Beznau at mean building depth as an example.

A1.3.2 Vertical ground motion

The model of maximum vertical ground motion is identical to that of the horizontal component, except that only the empirical spectra for vertical ground motion by Ripperger & Fäh (TP3-TN-0359) are considered. The resulting alternative spectra are available in the appendix in *Bard.MaxGM.AllSites.HMall.pdf*.

A1.4 Soil hazard input files (SIFs)

The compilation of SIFs of the site amplification factors and their aleatory variability requires two computational steps, whereas the results of maximum ground motion assessment are used directly as shown in Figure A-4. The two computational steps are firstly the association of site amplification factors and their aleatory variability with spectral accelerations of the underlying input motions, and secondly summarizing site amplification and variability to a set of discrete fractiles. Both steps are outlined below and described in detail in the techn. note TP3-TN-0401.

A1.4.1 Associating site amplification factors with input spectral accelerations

The amplification factors and their aleatory variability (Section 2) are modeled for a set of input shaking levels (PGA on rock), a set of magnitudes, and a set of frequencies.

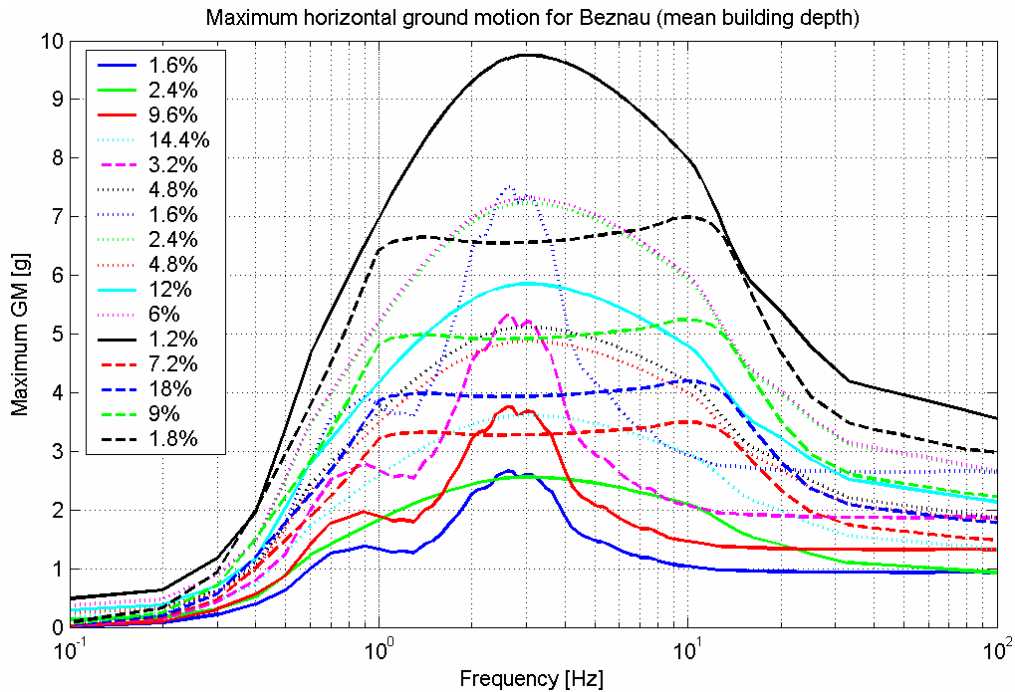


Fig. A-4: Assessment of alternative maximum horizontal ground motion spectra and corresponding weights for the mean building depth of NPP Beznau

Identical plots for the other Swiss NPP sites and other layers at Beznau can be found in the appendix.

In order to apply them to the rock hazard results, which are modeled for different spectral accelerations on rock and combinations of magnitudes and distances, the amplification factors must be associated with a spectral acceleration corresponding to the particular input shaking level (PGA) and considered frequency. The spectral acceleration is derived from the spectral shape of the input motion, which underlies the simulation of the amplification factors (figures 1 and 2 in TP3-TN-0401). In this first step, every single amplification factor is assigned a spectral acceleration (on rock) to which it can be applied.

A1.4.2 Summarizing epistemic uncertainty

The epistemic uncertainty in the expert's assessments of site amplification and aleatory variability is expressed by the branch tips and weights. For the soil hazard computations these branch tips are summarized to 17 discrete fractiles of both site amplification and aleatory variability, which is necessary in order to interpolate the data for any spectral acceleration and magnitude occurring in the rock hazard results. By using discrete fractiles no assumptions are made regarding the shape of the distribution of epistemic uncertainties. The 17 fractiles used are: 0.13 %, 0.62 %, 2.28 %, 5 %, 10 %, 20 %, 30 %, 40 %, 50 %, 60 %, 70 %, 80 %, 90 %, 95 %, 97.72 % (2 sigma), 99.38 % (2.5 sigma), and 99.87 % (3 sigma).

For the soil hazard computations these fractiles are associated with a weight and are considered as alternative models in the same way, as the original results from the branch tips represent alternative models each of which associated a weight.

A1.4.3 Plots of the soil hazard input files

Figure A-5 shows an example of the SIF of site amplification for horizontal ground motion of 4 Hz at Beznau at mean building depth. Plots showing the SIFs for site amplification and aleatory

variability in all cases (sites and spectral frequencies) are available as PDF files in the appendix: *Bard.SIFaf.<site>.<motion-depth>.pdf* and *Bard.SIFavar.<site>.<motion-depth>.pdf*

A1.5 Logic tree

The general logic tree for horizontal ground motion is given in Figure A-6. The logic tree structure shown applies to all sites. Differences between the sites are the weightings of individual branches parameters for the computation of various effects (P-Sv, 2D, etc.).

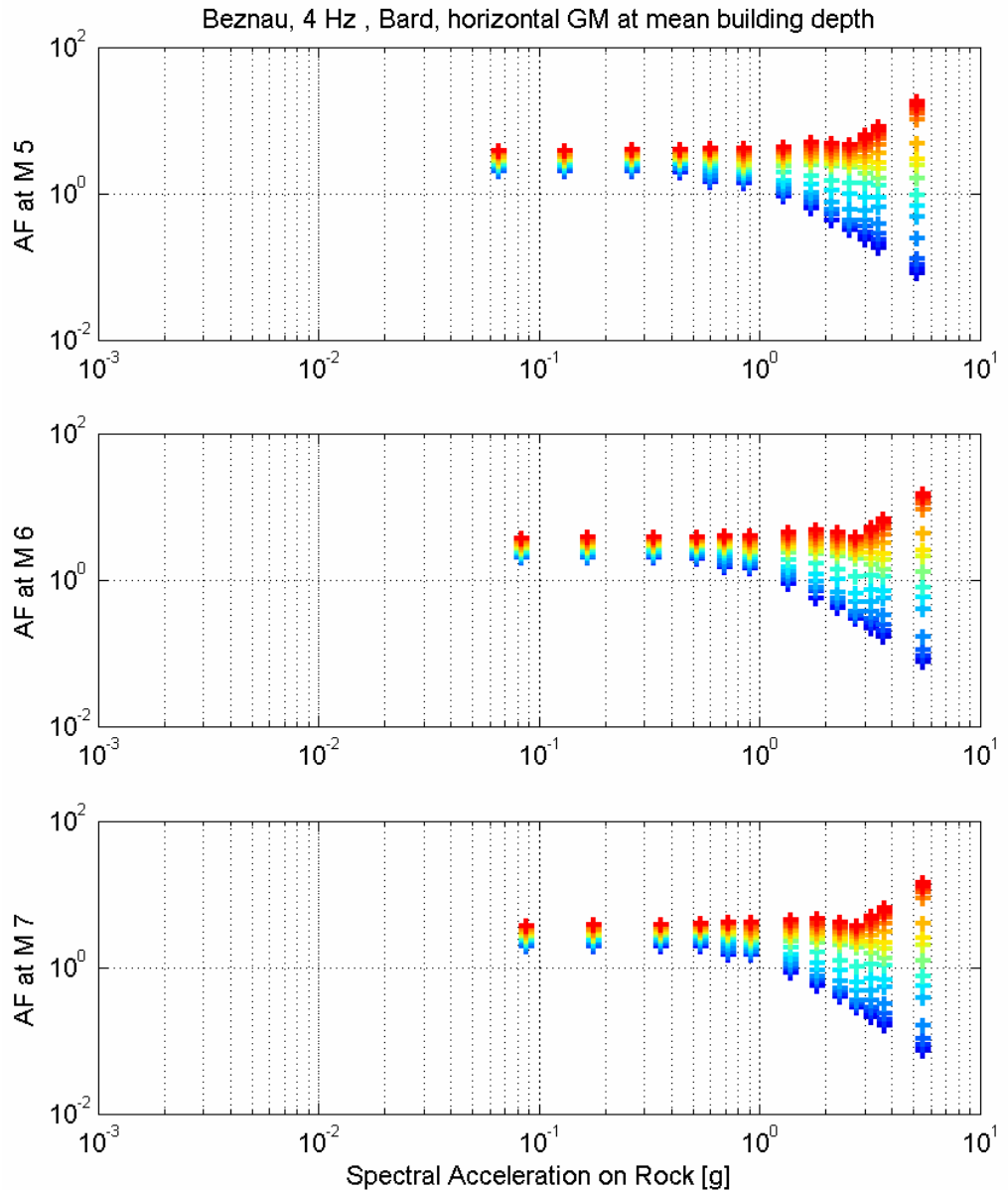


Fig. A-5: Summarized model of site amplification factors for ground motion of 4 Hz at mean building depth at NPP Beznau and earthquake magnitudes 5, 6 and 7

The crosses represent the results of the expert model after summarizing the epistemic uncertainty to 17 fractiles. The color-coding corresponds to these fractiles.

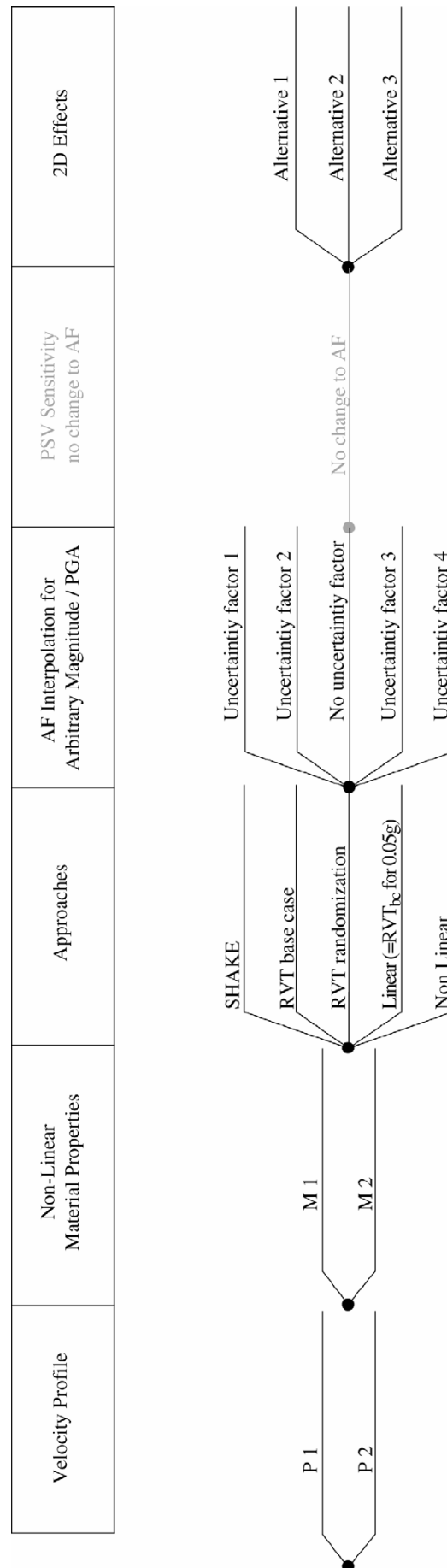
Linear interpolation and nearest neighbor extrapolation respectively will be performed in the hazard software to obtain amplification factors for any spectral acceleration on rock and any considered earthquake magnitude. The full set of figures is available in the appendix in the files *Bard.SIFaf.<site>.<motion-depth>.pdf* and *Bard.SIFavar.<site>.<motion-depth>.pdf*.

Fig. A-6: Bard's general logic tree for horiz. ground motion at the surface

A1.6 Appendix

The appendix is available only in electronic form on CD-ROM. All figures are stored as PDF files. The files are named according to the convention:

<expert>.<content>.<site><motion><depth>.pdf. Contents are *AF_AVAR* (assessment of site amplification and aleatory variability), *SiteModAF* (mean site amplification factors), *SiteModAvar* (mean aleatory variability), *SIFaf* (amplification factors as input to the soil hazard computations), *SIFavar* (parameterized aleatory variability as input to the soil hazard computations), and Max-GM (maximum ground motion, also input to the soil hazard computations). Motions are *HM* for horizontal ground motion and *VM* for vertical ground motion. Depth codes are *surf* for surface, *d1* for mean building depth and *d2* for the maximum building depth.



Part II:

Site Response Characterisation, Elicitation Summary

Dr. Donat Fäh

Schweizerischer Erdbebendienst (SED)
Institut für Geophysik ETH Zürich
Zürich – Switzerland

Probabilistische Erdbeben-Gefährdungs-Analyse für die KKW-Stand Orte
in der Schweiz (PEGASOS)

SP3 Site Response Characterisation

Elicitation Summary

Donat Fäh

Schweizerischer Erdbebendienst (SED)
Institut für Geophysik ETH Zürich
Zürich – Switzerland



TABLE OF CONTENTS

TABLE OF CONTENTS	1
LIST OF TABLES	3
LIST OF FIGURES	4
1 INTRODUCTION	7
2 MEDIAN AMPLIFICATION OF HORIZONTAL GROUND MOTION	7
2.1 Approach	7
2.2 Logic Tree Structure	9
2.3 Model Evaluations Common to All Sites	10
2.3.1 Factor for the 1D modeling uncertainty	10
2.3.2 Soil profile and material properties	14
2.3.3 Factor for correction of non-vertical incidence	14
2.3.4 Existence of 2D effects and application of a general correction factor	16
2.3.5 Existence and correction factor for 3-D effects	20
2.3.6 Correction for parametric uncertainty	20
2.4 Beznau	22
2.4.1 Logic Tree for Beznau	22
2.4.2 Site-Specific Model Evaluations	22
2.5 Gösgen	23
2.5.1 Logic Tree for Gösgen	23
2.5.2 Site-Specific Model Evaluations	23
2.6 Leibstadt	27
2.6.1 Logic Tree for Leibstadt	27
2.6.2 Site-Specific Model Evaluations	27
2.7 Mühleberg	29
2.7.1 Logic Tree for Mühleberg	29
2.7.2 Site-Specific Model Evaluations	29
3 MEDIAN AMPLIFICATION OF VERTICAL GM	33
3.1 Approach	33
3.2 Logic Tree Structure	33
3.3 Model Evaluations Common to All Sites	34
3.3.1 Concept A based on H/V ratios	34
3.3.2 Concept B based on the computations for the vertical component	35
3.3.3 Concept C based on the SP2 vertical ground motion estimate	35
3.4 Beznau	35
3.4.1 Logic Tree for Beznau	35
3.5 Gösgen	36
3.5.1 Logic Tree for Gösgen	36
3.6 Leibstadt	36
3.6.1 Logic Tree for Leibstadt	36
3.7 Mühleberg	38
3.7.1 Logic Tree for Mühleberg	38
4 ALEATORY VARIABILITY OF HORIZONTAL GROUND MOTION	39

4.1	Approach	39
4.2	Logic Tree Structure	39
5	ALEATORY VARIABILITY OF VERTICAL GROUND MOTION	41
5.1	Approach	41
5.2	Logic tree structure	41
6	MAXIMUM GROUND MOTIONS	41
6.1	Horizontal Component	41
6.1.1	Logic Tree Structure	43
6.1.2	Evaluation of Proponent Models	43
6.1.3	Weights for Maximum Ground Motions	43
6.2	Vertical Component	45
6.2.1	Logic Tree Structure	45
7	AMPLIFICATIONS AT INTERMEDIATE DEPTH LEVELS 2 AND 3	47
7.1	Median amplification for the horizontal component	47
7.2	Median amplification for the vertical component	49
7.3	Aleatory variability	52
7.4	Maximum Ground Motion	52
8	REFERENCES	55
APPENDIX 1 EG3-HID-0052 SITE AMPLIFICATION AT THE SURFACE AND EMBEDDED LAYER DEPTHS FINAL MODEL D. FÄH		57
A1.1	Introduction	57
A1.2	Site amplification and its aleatory variability	58
A1.2.1	Amplification of horizontal ground motion	58
A1.2.2	Aleatory variability of amplification of horizontal ground motion	60
A1.2.3	Amplification of vertical ground motion	60
A1.2.4	Aleatory variability of amplification of vertical ground motion	61
A1.2.5	Parameter ranges	61
A1.3	Maximum ground motion at the surface	62
A1.3.1	Horizontal ground motion	62
A1.3.2	Vertical ground motion	62
A1.4	Soil hazard input files (SIFs)	64
A1.4.1	Associating site amplification factors with input spectral accelerations	64
A1.4.2	Summarizing epistemic uncertainty	64
A1.4.3	Plots of the soil hazard input files	64
A1.5	Logic tree for horizontal ground motion	64
A1.6	Appendix	67

LIST OF TABLES

Tab. 2-1:	Ground motion level at which RVT shows a strong v_s reduction	9
Tab. 2-2:	Maximum strains in % obtained from the SHAKE runs (TP3-TN-0212 Part 7) for ground motion level 0.4 and 0.75 g	9
Tab. 2-3:	Correction factors for the different frequency ranges and ground motion Level 1	12
Tab. 2-4:	Correction factors for the different frequency ranges and ground motion Level 1	12
Tab. 2-5:	Correction factors for the different frequency ranges and ground motion Level 2	13
Tab. 2-6:	Correction factors for the different frequency ranges and ground motion Level 2	13
Tab. 2-7:	First correction factors for the different frequency ranges and ground motion Level 3	14
Tab. 2-8:	Correction factors for the different frequency ranges and ground motion Level 3	14
Tab. 2-9:	Correction factor $F_{nvi_dist}^1$ for non-vertical incidence of SH waves	15
Tab. 2-10:	Correction factor $F_{nvi_dist}^2$ for non-vertical incidence, total horizontal component, applied for frequencies above $f_0/2$	15
Tab. 2-11:	Correction factor $F_{nvi_dist}^2$ for non-vertical incidence, total horizontal component, applied for frequencies below $f_0/2$	16
Tab. 2-12:	Estimated probabilities for 2D effects at the different NPP sites	18
Tab. 2-13:	Probabilities for close (P_{close}) and distant sources (P_{dist})	19
Tab. 2-14:	Best estimate and range of the fundamental frequency of resonance, f_0 , and estimated error, Err , used to compute the second correction factor of the parametric uncertainty	22
Tab. 2-15:	Definitions of the level of ground motion for site Beznau	22
Tab. 2-16:	Definitions of the level of ground motion for site Gösgen	25
Tab. 2-17:	Definitions of the level of ground motion for site Leibstadt	27
Tab. 2-18:	Definitions of the level of ground motion for site Mühleberg.	29
Tab. 6-1:	Factors applied to the PGA values in order to compute the maximum spectral acceleration for the horizontal component at a given frequency	42
Tab. 6-2:	Factors applied to the PGA values in order to derive the spectral shape of the maximum spectral acceleration for the vertical component at a given frequency	46
Tab. A-1:	Mean and maximum building depth for the four Swiss NPP sites	57
Tab. A-2:	PGAs (on rock) for which Donat Fähr's model has been computed	62

LIST OF FIGURES

Fig. 2-1:	Logic tree for NPP site Leibstadt, used to estimate the median amplification of the horizontal ground motion.	11
Fig. 2-2:	Average ratio between results obtained with modal summation and RVT at the lowest shaking level, as a function of the normalized frequency f/f_0	17
Fig. 2-3:	Treatment of the parametric uncertainty	21
Fig. 2-4:	Logic tree for NPP site Beznau, used to estimate the median amplification of the horizontal ground motion.	24
Fig. 2-5:	Logic tree for NPP site Gösigen, used to estimate the median amplification of the horizontal ground motion	26
Fig. 2-6:	Logic tree for NPP site Leibstadt, used to estimate the median amplification of the horizontal ground motion	28
Fig. 2-7:	Logic tree for NPP site Mühleberg, used to estimate the median amplification of the horizontal ground motion	30
Fig. 3-1:	Logic tree for NPP site Leibstadt, used to estimate the median amplification of the vertical ground motion	33
Fig. 3-2:	$H(\text{rock})/V(\text{rock}) * V(\text{soil})/H(\text{soil})$ computed for the different NPP sites	35
Fig. 3-3:	Logic tree for NPP site Beznau, used to estimate the median amplification of the vertical ground motion	36
Fig. 3-4:	Logic tree for NPP site Gösigen, used to estimate the median amplification of the vertical ground motion	37
Fig. 3-5:	Logic tree for NPP site Leibstadt, used to estimate the median amplification of the vertical ground motion	37
Fig. 3-6:	Logic tree for NPP site Mühleberg, used to estimate the median amplification of the vertical ground motion	38
Fig 6-1:	Derivation of the spectral shapes for maximum ground motion from the maximum observed ground motion summarized (TP3-TN-0359)	42
Fig. 6-2:	Shapes of the spectra for maximum ground motions for the horizontal and vertical component, normalized to PGA	43
Fig. 6-3:	Frequency dependent logic tree used to estimate the maximum spectral acceleration for the horizontal component	44
Fig.6-4:	Maximum spectral acceleration and maximum peak acceleration of all the records (from report TP3-TN-0359)	45
Fig. 6-5:	Frequency dependent logic tree used to estimate the maximum spectral acceleration for the vertical component	46
Fig. 7-1:	Ratio between amplification for outcropping motion obtained with the RVT base case and amplification for ground motion obtained with the non-linear run	48
Fig. 7-2:	Logic tree for NPP site Mühleberg, used to estimate the median amplification of the horizontal ground motion at the elevation level 3	50
Fig. 7-3:	Logic tree for NPP site Leibstadt, used to estimate the median amplification of the vertical ground motion at depth	51

Fig. 7-4:	$H_s(\text{rock})/V_s(\text{rock}) * V(\text{soil})/H(\text{soil})$ shown for the Beznau NPP site for the three elevation levels	51
Fig. 7-5:	Logic tree for NPP site Mühleberg, used to estimate the median amplification of the vertical ground motion at the elevation level 3	52
Fig. 7-6:	Frequency dependent logic tree used to estimate the maximum spectral acceleration for the horizontal component at depth	53
Fig. 7-7:	Frequency dependent logic tree used to estimate the maximum spectral acceleration for the vertical component at depth	54
Fig. A-1:	Site amplifications factors for horizontal ground motion at the mean building depth of NPP Beznau for the case of a magnitude 6 earthquake with PGA on rock of 1.5 g	59
Fig. A-2:	Weighted arithmetic mean amplification factors (AF as function of PGA on rock and frequency) for horizontal ground motion of a magnitude 6 scenario at mean building depth of NPP Beznau	60
Fig. A-3:	Aleatory variability of amplifications factors for horizontal ground motion at the mean building depth of NPP Beznau for the case of a magnitude 6 earthquake with PGA on rock of 1.5 g	61
Fig. A-4:	Alternative maximum ground motion spectra for NPP Beznau	63
Fig. A-5:	Distribution of alternative maximum horizontal ground motion amplitudes at 4 Hz for NPP Beznau	63
Fig. A-6:	Summarized model of site amplification factors for ground motion of 4 Hz at mean building depth at NPP Beznau and earthquake magnitudes 5, 6 and 7	65
Fig. A-7:	General logic tree for horizontal ground motion	66

1 INTRODUCTION

This elicitation summary describes a possible way to estimate the amplification of seismic waves during strong earthquakes at the four NPP sites in Switzerland. This includes an estimate of the aleatory variability, and of the maximum possible ground motion. The amplification function is different at the NPP sites, and depends on the ground motion level, the magnitude, and the characteristics and geometry of the soft sediment cover. Epistemic uncertainty is introduced in order to account for the uncertainties of the model parameters and the modelling techniques.

2 MEDIAN AMPLIFICATION OF HORIZONTAL GROUND MOTION

2.1 Approach

This part describes the general concept to estimate amplification at a specific site with the logic tree approach. Details will be given in the following chapters. Measurements of shear moduli and damping curves as a function of strain have not been performed for the soils at the NPP sites. This introduces a high level of uncertainty concerning their behaviour during strong shaking. Therefore a scheme is developed based on only four levels of ground motion, and the possible physical models that approximate the behaviour of the soils at that ground motion level. At a certain level the site can behave in different ways. This is treated with different branches in the logic tree. The ground motion levels and the related physical models are as follows:

Level 1: The physical model is based on the equivalent linear theory.

Level 2: Non-linear behaviour or equivalent linear models are used.

Level 3: Only non-linear behaviour of the soils is expected.

Level 4: The soil column is expected to fail.

For example at Level 2, the site response can be either non-linear or described by an equivalent-linear model with different degrees of non-linear behaviour.

Computations are available for a broad range of ground motion parameters with Random Vibration Theory (RVT), SHAKE and truly non-linear (SUMDES, modified by Geodeco) methods. All computations are listed in report TP3-TN-0250. The starting point in the logic tree are the results obtained from these one-dimensional modelling techniques. All other effects are treated with correction factors.

All these one-dimensional computations have some advantages (+) and disadvantages (-). They are summarized in the following list:

1. RVT is always used without soil randomisation, because the randomisation leads to a reduction in the amplification factor due to the averaging of results from different velocity structures.
 - + RVT is using an attenuation model to define ground motion.

- + Result corresponds to a large number of SHAKE runs.
 - RVT uses stationary random signals, which is not correct at low frequency.
 - RVT has to define the signal duration, which is unknown for large magnitudes.
 - RVT with point source approximation over-predicts amplification at low frequencies (< 2 Hz).
 - Parameter selection does not correspond to Bay's (2002) attenuation model (stress-drop used in RVT is 120 bar). A high stress-drop is used in RVT computations, which results in a high input ground-motion. The required PGA of the input motion is obtained by reducing the distance, which means that the distance to the source is often smaller than 10 km.
2. SHAKE is used for different scaled seismograms as input:
- ± No source model is needed (No source effects included).
 - + "Realistic" time signals are used that are based on observation.
 - The ground motion level of the input is high when compared to Bay's (2002) attenuation law, which is valid for bedrock conditions.
 - Input motions might be affected by site effects (e.g. record from the Gemona site used in the computation).
 - There is only a limited number of input time-series.
 - There is no high frequency content in the input ground motion. Amplification factors can only be used up to a certain frequency.
3. Non-linear computation (SUMDES)
- + results are valid for high strain levels
 - Some parameters used in the modelling are unknown, and had to be estimated.
 - There is no high frequency content in the input ground motion. Amplification factors can only be used up to a certain frequency.
 - Input motion might be affected by site effects.

Based on an evaluation of the advantages and disadvantages, RVT has been selected as the basic method to treat equivalent linear models. A correction term takes into account the differences between RVT and SHAKE results.

The magnitude dependence of the amplification factor is taken into account stepwise for given magnitude ranges. Three ranges are selected $M = 5 - 6$, $M = 6 - 7$, $M = 7 - 8$. Most computations performed to estimate site amplifications are applying a high input ground-motion for the given magnitude.

The equivalent linear model is considered to be not valid anymore when a strong reduction of the average shear-wave velocity, v_s , of the soils is observed (TP3-TN-0212, Part 2). Elastoplastic behaviour should limit the v_s reduction. Table 2-1 is giving a qualitative summary for the RVT computations where a strong v_s reduction is observed. Then we change to ground motion Level 2. In Level 2, non-linear behaviour becomes important, and this is treated for each NPP site differently.

Tab. 2-1: Ground motion level at which RVT shows a strong v_s reduction
 b: Beznau; g: Gösgen; l: Leibstadt; m: Mühleberg.

PGA range in g	Magnitude 5	Magnitude 6	Magnitude 7
– 0.05			
0.05 – 0.1			
0.1 – 0.2			
0.2 – 0.4		l	ll
0.4 – 0.8		glllll	glllll
0.8 – (1.6)	gglllllmm	bbbgggllllllllmm	bbbbbgggllllllllmm
Failure of soil column			

When the strain reaches 0.5 – 1 %, the modelling with an equivalent-linear model becomes unrealistic and we have to move to Level 3. In order to estimate this limit, maximum strain has been considered. Maximum strain is available for SHAKE runs (TP3-TN-0212, Part 7) and RVT computations. Maximum strains obtained with SHAKE are always larger than in the RVT runs by a factor of about 2. Table 2-2 summarizes the maximum strains obtained from the SHAKE runs (TP3-TN-0212, Part 7) for ground motion PGA level 0.4 and 0.75 g.

In what concerns Level 4, Report TP-TN-0205 evaluates the maximum shear strain as a function of depth with a non-linear model, for an extreme case with input motion of PGA = 1.5 g at site Gösgen. Maximum shear strain at site Gösgen is 4 %, mean values are at about 0.5 %. In the non-linear computations with SUMDES (TP3-TB-0048) for Gösgen, one input motion produced complete failure of the soil column. This is Level 4 ground motion with very large displacements, where the modelling results do not give the correct answer. A general discussion is given in the chapter on maximum ground motion where this transition to Level 4 is discussed

Tab. 2-2: Maximum strains in % obtained from the SHAKE runs (TP3-TN-0212 Part 7) for ground motion level 0.4 and 0.75 g

Site	Model 1	Model 2	Model 3	Model 4
Beznau	0.1–0.5 / 0.1–1.3	0.1–0.3 / 0.1–1.3	0.1–0.3 / 0.2–1.1	
Gösgen	0.1 / 0.1–0.25	0.1–0.2 / 0.1–2.0		
Leibstadt	0.1 / 0.1–0.4	0.1–0.8 / 0.1–2.0	0.1 / 0.1–0.3	0.1–0.9 / 0.1–2.5
Mühleberg	0.02 / 0.02–0.06	0.02 / 0.02–0.12		

2.2 Logic Tree Structure

This section describes the general logic tree, which is applicable to all sites, and discusses its organization. The example for NPP site Leibstadt is used to explain the different branches of the tree. The logic tree is given in Figure 2-1.

The pair PGA / Magnitude (as discretized in Table 2-1) is the parameter to decide in which Ground Motion Level to start the logic tree. This is different for the NPP sites, and is given in the chapter of the respective site. The discussion provided in section 2.1 provides the base for the decision. The ground motion levels and physical model for the different NPP sites are as follows:

Level 1: BASE: RVT without soil randomization (low strain) for all sites.

For a given PGA, the next lower ground motion level of the RVT run is selected.

Level 2: For Beznau and Gösgen:

BASE: non-linear (at 0.4 and 0.75 g) with an effective stress approach taking into account pore pressure build-up and cyclic mobility effects, and RVT without soil randomization (at 0.3 and 0.4 g).

For Leibstadt:

BASE: non-linear (at 0.4 g and 0.75 g) without pore pressure build-up (TP-TB-0048), and RVT without soil randomization (at 0.2 and 0.3 g).

For Mühleberg:

For this site no non-linear computations have been performed. Moreover the site's fundamental frequency of resonance has not been measured. At PGA levels in the 1.0 – 1.5 g range, we observe strong v_s -reductions in some of the RVT runs. These v_s reductions are allowed to occur in the equivalent linear approach, because almost no information on the thickness and composition of the soft soils is available for this site.

BASE: RVT without soil randomization (at 0.5, 0.75, 1.0, 1.25 and 1.5 g)

Level 3: BASE: non-linear (at 0.4, 0.75 and 1.5 g) with and without pore-pressure build-up, depending on the site. The equivalent-linear model is not valid anymore. Mühleberg has no Level 3.

Level 4:

failure of the soil column; Gösgen and Leibstadt (with cemented layer) are expected to be the first sites to do so.

Computed amplification factors from RVT, SHAKE and truly non-linear (SUMDES, modified by Geodeco) methods are used in the branch "Composition". All other effects are treated with correction factors in the following branches. These branches and factors are discussed in the next chapter. The validity of this evaluation is limited to frequencies above 0.45 Hz.

2.3 Model Evaluations Common to All Sites

This section describes the corrections applied to the amplifications in the logic tree that are common to all sites. The correction factors are in most cases very simple functions, i.e. constant values over a certain frequency band. This is intentional and reflects the very large uncertainty of the correction factors.

2.3.1 Factor for the 1D modeling uncertainty

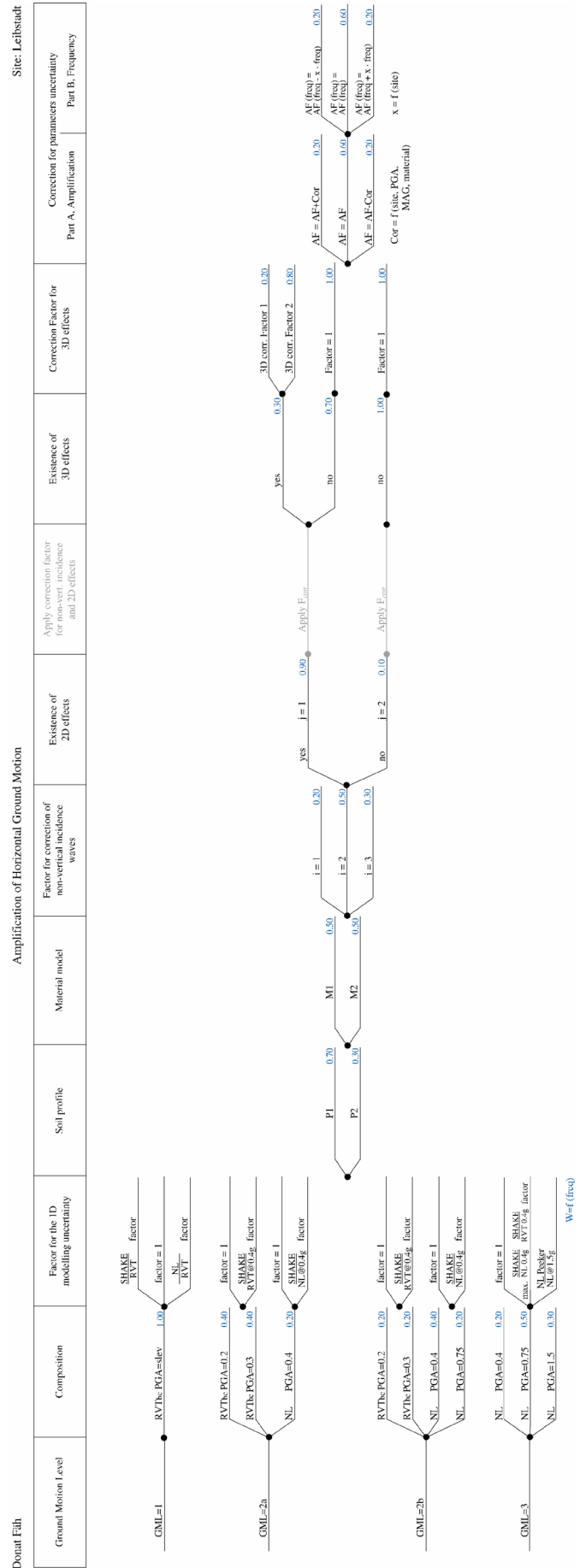
A numerical modelling technique is always based on a physical model and some assumptions, and therefore has limits for the applicability. The factor for the 1D modelling uncertainty accounts for the differences that can result when different numerical modelling techniques are applied. Different frequency bands with different levels of uncertainty are distinguished:

$0.45 \text{ Hz} < f < f_0/2$: At low frequencies, amplification should not go to 1. Amplification factors obtained from RVT go to one at low frequency, and are therefore less reliable than SHAKE results.

$f_0/2 < f < 2f_0$: Frequency range around the fundamental mode of resonance.

$2f_0 < f$: In the high-frequency range, the effect of the first higher mode of resonance may or may not appear.

Fig. 2-1: Logic tree for NPP site Leibstadt, used to estimate the median ampl. of the horizontal ground motion.



The fundamental frequency of resonance f_0 is determined from the H/V ambient vibration measurements at the NPP sites (Beznau: $f_0 = 2.5$ Hz; Gösigen: $f_0 = 4.7$ Hz; Leibstadt: $f_0 = 2.2$ Hz; Mühleberg: $f_0 = 12$ Hz (estimated due to the high variability of the measurements)).

Ratios between SHAKE and RVT (without soils randomization), non-linear and RVT, and SHAKE and non-linear are used to estimate the 1D modelling uncertainty in LEVEL 1 and 2. This has been performed using the computations for all magnitudes and sites. The selected correction factors are summarized in Tables 2-3 to 2-6 for the two ground motion levels. Very simple, constant correction factors are taken. For all sites and magnitudes the same correction factors are applied. The basis for the selection of weights of the branches in the logic tree are the advantages and disadvantages of the computational methods, the problems of RVT at low frequencies and the level of non-linear behavior as discussed in chapter 2.1. The weights in Level 1 are as follows:

Level 1: SHAKE/RVT at 0.1 and 0.4 g and non-linear/RVT at 0.4 g

Logic tree for the frequency range $0.45 \text{ Hz} < f < f_0/2$:

- 0.3----- SHAKE/RVT factor
- 0.4----- 1.0
- 0.3----- non-linear/RVT factor

Logic tree for the frequency range $f_0/2 < f < 2f_0$ and $2f_0 < f$:

- 0.2----- SHAKE/RVT factor
- 0.6----- 1.0
- 0.2----- non-linear/RVT factor

RVT computations are given a lower weight at low frequencies.

Tab. 2-3: Correction factors for the different frequency ranges and ground motion **Level 1**
 SHAKE/RVT is obtained from the computations at 0.1 g and 0.4 g.

SHAKE/RVT	$0.45\text{Hz} < f < f_0/2$	$f_0/2 < f < 2f_0$	$2f_0 < f$
Beznau	1.20	1.05	1.10
Gösigen	1.25	1.15	1.15
Leibstadt	1.15	1.05	1.15
Mühleberg	1.05	0.95	--
Selected Factor	1.20	1.05	1.15

Tab. 2-4: Correction factors for the different frequency ranges and ground motion **Level 1**
 Non-linear/RVT is obtained from the computations at 0.4 g.

Non-linear/RVT	$0.45 \text{ Hz} < f < f_0/2$	$f_0/2 < f < 2f_0$	$2f_0 < f$
Beznau	1.15	0.80	0.85
Gösigen	1.05	0.90	0.80
Leibstadt	1.10	1.00	0.90
Mühleberg	--	--	--
Selected Factor	1.10	0.90	0.85

The weights of the branches in the logic tree in Level 2 are as follows:

Level 2: Comparison at 0.4 g

RVT Branch for the frequency range $0.45 \text{ Hz} < f < f_0/2$

----0.5---- 1.0

----0.5---- **SHAKE/RVT at 0.4 g**

RVT Branch for the frequency range $f_0/2 < f < 2f_0$ and $2f_0 < f$

----0.7---- 1.0

----0.3---- **SHAKE/RVT at 0.4 g**

Non-linear Branch

----0.7---- 1.0

----0.3---- **SHAKE/non-linear for 0.4 g**

Tab. 2-5: Correction factors for the different frequency ranges and ground motion **Level 2**
SHAKE/RVT is obtained from the computations at 0.4 g.

SHAKE/RVT	$0.45 \text{ Hz} < f < f_0/2$	$f_0/2 < f < 2f_0$	$2f_0 < f$
Beznau	1.20	1.05	1.15
Gösgen	1.25	1.10	1.15
Leibstadt	1.10	1.10	1.25
Mühleberg	1.05	1.00	--
Selected Factor	1.15	1.10	1.15

Tab. 2-6: Correction factors for the different frequency ranges and ground motion **Level 2**
SHAKE/non-linear is obtained from the computations at 0.4 g.

SHAKE/Non-linear	$0.45 \text{ Hz} < f < f_0/2$	$f_0/2 < f < 2f_0$	$2f_0 < f$
Beznau	1.00	1.25	1.25
Gösgen	1.05	1.30	1.30
Leibstadt	1.00	1.05	1.10
Mühleberg	--	--	--
Selected Factor	1.00	1.25	1.25

In Level 3, two factors are included and they are summarized in Tables 2-7 and 2-8. The first corresponds to the maximum factor obtained in Level 2. The second factor is an uncertainty estimate between Pecker's non-linear computation (TP3-TN-0205) and the results obtained with program SUMDES, including pore pressure build-up. The weights of the branches in the logic tree in Level 3 are as follows:

Level 3:

Non-linear Branch

----0.6---- 1.0

----0.2---- MAX (SHAKE/non-linear for 0.4 g, SHAKE/RVT at 0.4 g)

----0.2---- Pecker / (non-linear with pore pressure build-up) for 1.5 g

Tab. 2-7: First correction factors for the different frequency ranges and ground motion **Level 3**

The maximum from Level 2 is taken.

MAX	$0.45 \text{ Hz} < f < f_0/2$	$f_0/2 < f < 2f_0$	$2f_0 < f$
Selected Factor	1.20	1.30	1.30

Tab. 2-8: Correction factors for the different frequency ranges and ground motion **Level 3**

Pecker / non-linear (NL) is obtained from the computations at 1.5g including pore pressure build-up in the modelling.

Pecker/NL	$0.45 \text{ Hz} < f < f_0/2$	$f_0/2 < f < 2f_0$	$2f_0 < f$
Selected Factor	0.95	1.0	1.50

2.3.2 Soil profile and material properties

The equivalent-linear models (modulus and damping curves) are equally weighted, because no reliable field measurements are available for the NPP sites. For the different NPP sites, soil profiles are weighted according the following list. The reason in case of an unequal weighting is provided in the comment line. The models (profiles) are defined in report TP3-TN-0166.

Beznau:

Beznau	Weight	Comment
Model 1	0.4	Realistic layering (high frequency)
Model 2	0.2	
Model 3	0.4	Explains H/V ratios and phase-velocities

Gösgen: one profile

Leibstadt:

Leibstadt	Weight	Comment
Model 1	0.7	H/V shows no cemented layer
Model 2	0.3	

Mühleberg: one profile

2.3.3 Factor for correction of non-vertical incidence

In general, the incidence of seismic waves is non-vertical. This is due to the fact that the sources are located at a certain distance from the site and different wave types exist with different incidence angles. RVT, SHAKE and all non-linear computations are restricted to the vertical incidence of SH waves. Therefore a factor is applied that accounts for these restrictions. Three cases are treated for the case that the sources are distant: a correction of non-vertical incidence of SH waves ($i = 1$ in Figure 2-1), a correction for PSV wave propagation by selection of a factor for the total horizontal component ($i = 2$), and no correction ($i = 3$) by assuming vertical incidence due to a velocity gradient in the bedrock at the site. We introduce the following definitions for the correction factors:

$F_{nvi_dist}^i$ = correction factor for non-vertical incidence from a distant source

and distinguish the three cases $I = 1,2,3$:

$F_{nvi_dist}^1$ = factor for SH case (fac1)
 $F_{nvi_dist}^2$ = factor for SH+PSV case (fac2)
 $F_{nvi_dist}^3$ = 1 no correction

1. Correction factor $F_{nvi_dist}^1$ for SH waves

The correction factors are computed using ratios between modal summation and RVT results for SH wave propagation (TP3-TN-0167). For RVT the lowest shaking level (Magnitude 5, PGA = 0.05 g) is taken (linear case). Results with modal summation results are available for Beznau, Gösigen and Leibstadt. For site Mühleberg the factor is estimated. Two frequency ranges are considered $[0.5 \cdot f_0, 2 \cdot f_0]$ $[0.5 \cdot f_0, 4 \cdot f_0]$ to estimate a constant factor, and one factor is then selected. The first higher mode amplification is not present anymore in the mode summation result.

Comparison between plane-wave 1D non-vertical incidence (TP3-TN-0186) and mode summation shows comparable results, and confirm the effect of non-vertical incidence (TP3-TN-0283). This correction factor is applied only for distant sources. For the definition and treatment of distant and close sources see section 2.3.4. The correction factors given in Table 2-9 are different for the NPP sites, and are applied for all ground motion levels. The weights in the logic tree are the same for the different sites.

Tab. 2-9: Correction factor $F_{nvi_dist}^1$ for non-vertical incidence of SH waves

Mean Reduction factor	$f_0/2 < f < 2f_0$	$f_0/2 < f < 4f_0$	Applied factors for $f_0/2 < f$
Beznau $f_0 = 2.5$ Hz	0.90	0.95	0.9
Gösigen $f_0 = 4.7$ Hz	0.8	-	0.8
Leibstadt $f_0 = 2.2$ Hz	0.95	0.90	0.9
Mühleberg $f_0 [8 - 15]$ Hz]	-	-	0.95

2. Correction factor $F_{nvi_dist}^2$ for the total horizontal component (SH+PSV)

The PSV waves do not dominate the results (TP3-TN-0167), but they influence the shape of amplification for the horizontal component (peak is lower, but broader) when compared to SH waves only. For RVT, the lowest shaking level (Magnitude 5, PGA = 0.05 g) is taken (linear case) as a reference to compute the correction factor. Results with modal summation are available for Beznau, Gösigen and Leibstadt. The ratio between modal summation and RVT is shown in Figure 2-2. The mean correction factors for the different frequency ranges are provided in Tables 2-10 and 2-11. For site Mühleberg the factor is estimated.

Tab. 2-10: Correction factor $F_{nvi_dist}^2$ for non-vertical incidence, total horizontal component, applied for frequencies above $f_0/2$

Mean Reduction factor	$f_0/2 < f < 2f_0$	$f_0/2 < f < 4f_0$	Applied factors for $f_0/2 < f$
Beznau $f_0 = 2.5$ Hz	0.85	0.90	0.85
Gösigen $f_0 = 4.7$ Hz	0.80	-	0.8
Leibstadt $f_0 = 2.2$ Hz	0.95	0.90	0.9
Mühleberg $f_0 [8 - 15]$ Hz]	-	-	0.95

Tab. 2-11: Correction factor $F_{nvi_dist}^2$ for non-vertical incidence, total horizontal component, applied for frequencies below $f_0/2$

Mean Amplification factor	$f_0/5 < f < f_0/2$
Beznau $f_0 = 2.5$ Hz	1.2
Gösgen $f_0 = 4.7$ Hz	1.0
Leibstadt $f_0 = 2.2$ Hz	1.2
Mühleberg $f_0 [8 - 15]$ Hz	1.0

This factor is applied only for distant sources. For the definition and treatment of distant and close sources see section 2.3.4. The correction factors are different for the NPP sites, and are applied for all ground motion levels. The weights in the logic tree are the same for the different sites. The largest weight is assigned to the case where both SH and P-SV waves are involved due to the fact that in most cases the incident wave-field is a superposition of SH and P-SV waves. An intermediate weight is given to the case where we assume a velocity gradient in the bedrock, and therefore an almost vertical incidence of waves.

2.3.4 Existence of 2D effects and application of a general correction factor

Two dimensional amplification effects may play an important role and are treated in this section. We distinguish between two cases, in the first case 2D effects are assumed to occur ($j = 1$), and in the second case 2D effects are excluded ($j = 2$).

Two-dimensional computations were performed only for site Leibstadt. In these computations we distinguish between distant sources (> 20 km) that are either shallow or deep (TP3-TN-0168), and sources that are close or located below the site (TP3-TN-0186). For the distant sources we moreover distinguish between sources to the north and sources to the south, because the computed amplification levels are different for the two cases.

The factors for distant sources are computed from the ratios between the 2D SH-wave computations (TP3-TN-0168) and the modal summation results (SH component in report TP3-TN-0167). We introduce the following notation:

$P_{ND} = 0.4$	probability of the earthquake located to the north and deep (ND)
$P_{NS} = 0.1$	probability of the earthquake located to the north and shallow (NS)
$P_{SD} = 0.4$	probability of the earthquake located to the south and deep (SD)
$P_{SS} = 0.1$	probability of the earthquake located to the south and shallow (SS)
$F_{ND} = 2-D$	factor for earthquakes located to the north and deep (ND)
$F_{NS} = 2-D$	factor for earthquakes located to the north and shallow (NS)
$F_{SD} = 2-D$	factor for earthquakes located to the south and deep (SD)
$F_{SS} = 2-D$	factor for earthquakes located to the south and shallow (SS)

The factor as function of frequency for the four cases is simplified as follows:

2-D factor for earthquakes located to the north and deep (ND)

$f < f_0/2$: $F_{ND} = 1.0$
$f_0/2 < f < f_0$: ramp from $F_{ND} = 1.0$ to $F_{ND} = 1.3$
$f_0 < f < 4f_0$: $F_{ND} = 1.3$
$4f_0 < f < 6f_0$: ramp from $F_{ND} = 1.3$ to $F_{ND} = 1.0$
$6f_0 < f$: $F_{ND} = 1.0$

2-D factor for earthquakes located to the north and shallow (NS)

$f < f_0/2$: FNS = 1.0

$f_0/2 < f < f_0$: ramp from FNS = 1.0 to FNS = 1.7

$f_0 < f < 4f_0$: FNS = 1.7

$4f_0 < f < 6f_0$: ramp from FNS = 1.7 to FNS = 1.0

$6f_0 < f$: FNS = 1.0

2-D factor for earthquakes located to the south and deep (SD)

$f < f_0/2$: FSD = 1.0

$f_0/2 < f < f_0$: ramp from FSD = 1.0 to FSD = 1.2

$f_0 < f < 4f_0$: FSD = 1.2

$4f_0 < f < 6f_0$: ramp from FSD = 1.2 to FSD = 1.0

$6f_0 < f$: FSD = 1.0

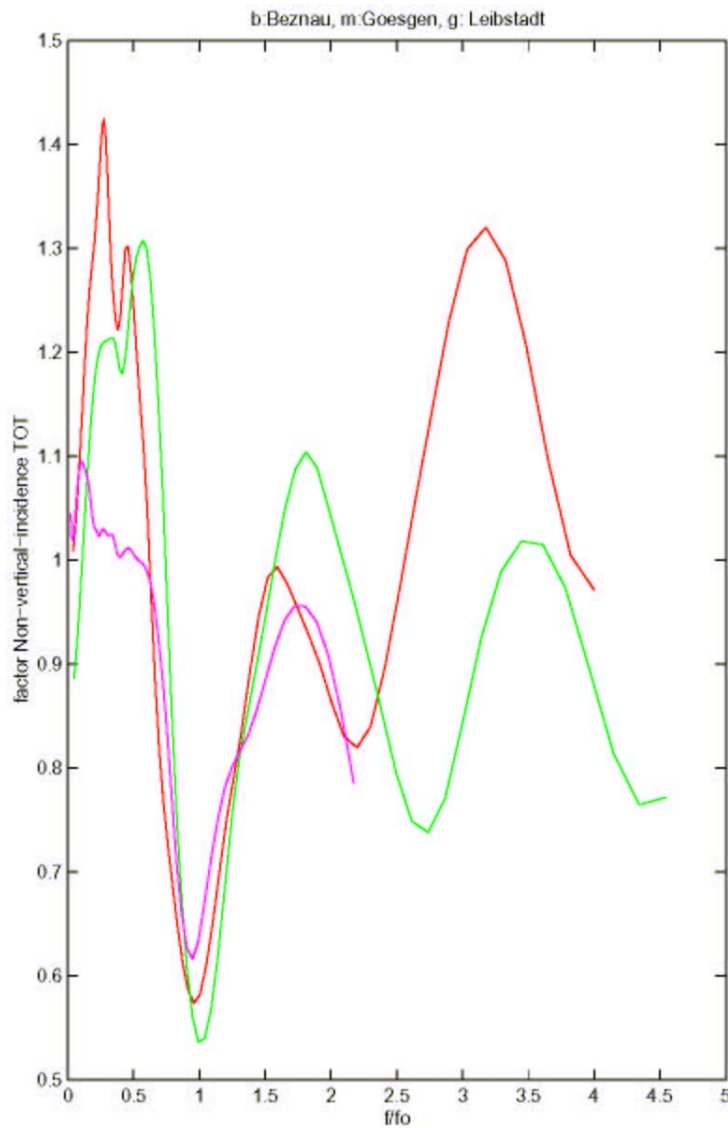


Fig. 2-2: Average ratio between results obtained with modal summation and RVT at the lowest shaking level, as a function of the normalized frequency f/f_0

2-D factor for earthquakes located to the south and shallow (SS)

- $f < f_0/2$: FSS = 1.0
- $f_0/2 < f < f_0$: ramp from FSS = 1.0 to FSS = 0.9
- $f_0 < f < 4f_0$: FSS = 0.9
- $4f_0 < f < 6f_0$: ramp from FSS = 0.9 to FSS = 1.0
- $6f_0 < f$: FSS = 1.0

where f_0 is fundamental frequency of resonance, as defined in section 2.3.1. These factors are valid for all shaking levels. The probabilities P_{ND} , P_{NS} , P_{SD} , and P_{SS} for sources to be shallow or deep, and the location to the north or south are unknown and they are estimated to be 0.4, 0.1, 0.4, and 0.1.

The factors for close sources are computed from the ratios between the 2D and 1D computations (TP3-TN-0186) for vertically incident SH waves. The cases for -30° , 0° , $+30^\circ$ incidence and for the low strain level are included. The correction factor as a function of frequency is simplified as follows:

F_{2D_close} : correction factor for 2D effects from a close source

- $f < f_0/2$: $F_{2D_close} = 1.0$
- $f_0/2 < f < f_0$: ramp from $F_{2D_close} = 1.0$ to $F_{2D_close} = 1.25$
- $f_0 < f < 4f_0$: $F_{2D_close} = 1.25$
- $4f_0 < f < 6f_0$: ramp from $F_{2D_close} = 1.25$ to $F_{2D_close} = 1.0$
- $6f_0 < f$: $F_{2D_close} = 1.0$

For Gösigen, Beznau and Mühleberg no computations have been performed in order to estimate 2D effects. The results from site Leibstadt are applied to these sites. 2D effects have to be expected for Beznau and Gösigen, but are less probable for Mühleberg. The expressions "north" and "south" in these cases do not express geographical directions but refer only to the different cases in the Leibstadt-site computations. The functions are adapted to the different sites by selection of the appropriate fundamental frequency of resonance f_0 defined in section 2.3.1. The probability for 2D effects is controlled by the branches $j = 1$ (2D effects) and $j = 2$ (no 2D effects). The probabilities for the different NPP sites are estimated and given in Table 2-12. The basis for the different probabilities of 2D effects at the different sites is the topographical feature and the subsurface geometry. The more pronounced the 2D geometry is, the higher is the probability for 2D wave propagation effects.

Tab. 2-12: Estimated probabilities for 2D effects at the different NPP sites

	$j = 1$ (2D effects)	$j = 2$ (no 2D effects)
Beznau	0.8	0.2
Gösigen	0.5	0.5
Leibstadt	0.9	0.1
Mühleberg	0.1	0.9

Hazard computations in the PEGASOS project are performed in two steps: source and attenuation are treated together in the first step, and site effects are treated separately in the second step. The probability that a source of a certain magnitude is distant (P_{dist}) or close (P_{close}) depends on the results of the hazard de-aggregation in the first step. Without knowing the final hazard results, the probabilities are estimated based on one hand on the non-final sensitivity studies, and on the other hand on the expert discussion during the SP1 workshops. The probabilities are provided in Table 2-13 for the two distance ranges.

Tab. 2-13: Probabilities for close (P_{close}) and distant sources (P_{dist})

The magnitude 5 earthquakes contribute more to the hazard for close distances.

	Magnitude 5 – 6	Magnitude 6 – 7	Magnitude 7 – 8
Source closer than 20 km or below the site	0.8	0.5	0.2
Source distance > 20 km	0.2	0.5	0.8

We can now approximate all cases discussed in section 2.3.3 and 2.3.4 to one mean correction factor F_{corr}^{ij} for non-vertical incidence and 2D effects. The parameters i ($i=1,2,3$) and j ($j=1,2$) have been defined in the previous sections.

$$F_{corr}^{ij} = P_{dist} * (F_{nvi_dist}^i * F_{2D_dist}^j) + P_{close} * (F_{nvi_close} * F_{2D_close}^j)$$

where

- (a) P_{dist} = probability that earthquake is distant
 P_{close} = probability that earthquake is close
- (b) $F_{nvi_dist}^i$ = correction factor for non-vertical incidence from a distant source
 $F_{nvi_dist}^1$ = fac1 for SH case
 $F_{nvi_dist}^2$ = fac2 for SH+PSV case
 $F_{nvi_dist}^3$ = 1 no correction
- (c) $F_{2D_dist}^j$ = correction factor for 2D effects from a distant source
 $F_{2D_dist}^1$ = $PND * FND + PNS * FNS + PSD * FSD + PSS * FSS$ for 2D effects = yes
 $F_{2D_dist}^2$ = 1 for 2D effects = no

where:

- PND = probability of the earthquake located to the north and deep (ND)
 PNS = probability of the earthquake located to the north and shallow (NS)
 PSD = probability of the earthquake located to the south and deep (SD)
 PSS = probability of the earthquake located to the south and shallow (SS)
 FND = 2-D factor for earthquakes located to the north and deep (ND)
 FNS = 2-D factor for earthquakes located to the north and shallow (NS)
 FSD = 2-D factor for earthquakes located to the south and deep (SD)
 FSS = 2-D factor for earthquakes located to the south and shallow (SS)
- (d) F_{nvi_close} = correction factor for non-vertical incidence from a close source
 F_{nvi_close} = 1
- (e) $F_{2D_close}^1$ = correction factor for 2D effects from a close source
 $F_{2D_close}^2$ = 1 for 2D effects = no

The correction factors are applied for all ground motion levels. The variability induced by the different cases is included in the total aleatory variability, discussed in section 4.

2.3.5 Existence and correction factor for 3-D effects

Constructive interference of waves may occur in structures with a 3D geometry that permits the 3D focusing of seismic waves. This is taken into considerations only for site Leibstadt and Beznau, and the branches "2D-effects-YES" ($j=1$). For these sites the geometry of the soft sediment could cause 3D resonance effects. No 3D computations have been performed for the NPP sites, and the correction factors and probabilities are estimated. The basis for the different weights of 3D effects at the different sites is the topographical feature and the subsurface geometry. The more pronounced the 3D geometry is, the higher is the weight for 3D wave propagation effects. The correction factors are based on a geometrical superposition of two propagating waves.

Logic tree for Leibstadt:

2D effects YES ----0.3-----3D YES ---0.2---- Factor 1
 ---0.8---- Factor 2
 2D effects YES ----0.7-----3D NO ---Factor is 1.0

Logic tree for Beznau:

2D effects YES ----0.1-----3D YES ---0.2---- Factor 1
 ---0.8---- Factor 2
 2D effects YES ----0.9-----3D NO ---Factor is 1.0

The factors Factor 1 and Factor 2 as function of frequency are again simplified by a similar function as introduced in section 2.3.4:

Definition of Factor 1:

$f < f_0/2$: Factor 1 = 1.0
 $f_0/2 < f < f_0$: ramp from Factor 1 = 1.0 to Factor 1 = 1.4
 $f_0 < f < 4f_0$: Factor 1 = 1.4
 $4f_0 < f < 6f_0$: ramp from Factor 1 = 1.4 to Factor 1 = 1.0
 $6f_0 < f$: Factor 1 = 1.0

Definition of Factor 2:

$f < f_0/2$: Factor 2 = 1.0
 $f_0/2 < f < f_0$: ramp from Factor 2 = 1.0 to Factor 2 = 1.2
 $f_0 < f < 4f_0$: Factor 2 = 1.2
 $4f_0 < f < 6f_0$: ramp from Factor 2 = 1.2 to Factor 2 = 1.0
 $6f_0 < f$: Factor 2 = 1.0

The correction factors are applied for all ground motion levels.

2.3.6 Correction for parametric uncertainty

two steps are applied at the end of the logic tree that account for the uncertainties of the soil parameters. This last part of the logic tree is outlined in Figure 2-3.

Part A: Amplification

Sediment S-wave velocity, moduli and thickness, used in the computations, have a considerable uncertainty at all sites. This has an effect on the amplitudes of the amplification, and it is accounted for with this first factor for the parametric uncertainty. The one-sigma level of the

soil randomization with RVT is used to quantify this uncertainty. Not all RVT runs are taken, but only those that show a clear amplification peak around the fundamental frequency of resonance, within the interval given in Table 2-14 (second column). In general, the one-sigma level is increasing with shaking (but not always). Level 2 and 3 are treated differently, still based on the soil randomization with RVT. The definition is as follows:

For Level 1: RVT's ± one-sigma-level at the given shaking (PGA and magnitude)

For Levels 2 & 3: MAX (RVT one-sigma-level at all shaking-levels and magnitudes in Level 1)

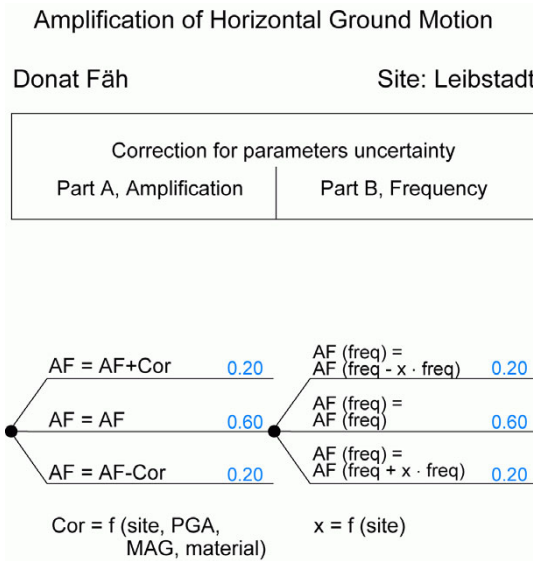


Fig. 2-3: Treatment of the parametric uncertainty

At each frequency, the three branches are:

- AF = AF-Cor RVT's (base-case minus one-sigma level in soil randomization)/base-case
- AF = AF no correction
- AF = AF+Cor RVT's (base-case plus one-sigma level in soil randomization)/base-case

For the non-linear branch: The base case corresponds to the non-linear computation, and the one-sigma level is taken to be the maximum of the RVT one-sigma levels of the different models for the specific site, at all shaking-levels and magnitudes in Level 1.

Part B: Frequency

The models used within the project for the different sites are based on the measurement of the fundamental frequency of resonance with the H/V spectral ratio. This fundamental frequency of resonance, fo, has a certain error both for the field measurement and when determined for the theoretical models. The error in a field-measurement is of the order of 10 – 20 %, depending on the site. The estimated error for all sites is given in Table 2-14.

Tab. 2-14: Best estimate and range of the fundamental frequency of resonance, f_0 , and estimated error, Err, used to compute the second correction factor of the parametric uncertainty

Error-Table	f_0 interval	Estimated error Err
Beznau $f_0 = 2.5$ Hz	[2.2 – 2.9 Hz]	20 %
Gösigen $f_0 = 4.7$ Hz	[4.5 – 5.1 Hz]	15 %
Leibstadt $f_0 = 2.2$ Hz	[2.0 – 2.4 Hz]	10 %
Mühleberg f_0 not measured	[8 – 15 Hz]	30 %

In order to account for this uncertainty the following correction factors are included in the logic tree:

$AF(f-x f) = \text{Value}(f-x f) / \text{Value}(f)$: Amplification factor taken at frequency $\text{freq}-x \text{ freq}$

$AF(f) = 1.0$: Amplification factor taken at frequency freq

$AF(f+x f) = \text{Value}(f+x f) / \text{Value}(f)$: Amplification factor taken at frequency $\text{freq}+x \text{ freq}$

The parameter x is defined as $x = \text{Err} / 100$, with Err given in Table 2-14, and f is the frequency.

2.4 Beznau

2.4.1 Logic Tree for Beznau

The logic tree for site Beznau with the weights and branches is given in Figure 2-4.

2.4.2 Site-Specific Model Evaluations

The ground motion levels for Beznau are defined in Table 2-15. The discussion is provided in section 2.1. The PGA-range in the first column is for the reference ground motion on bedrock with S-wave velocity of 2000 m/s at the surface.

Tab. 2-15: Definitions of the level of ground motion for site Beznau

PGA range in g	Magnitude 5 – 6	Magnitude 6 – 7	Magnitude 7 – 8
– 0.05	Level 1	Level 1	Level 1
0.05 – 0.1	Level 1	Level 1	Level 1
0.1 – 0.2	Level 1	Level 1	Level 1
0.2 – 0.4	Level 1	Level 2a	Level 2a
0.4 – 0.8	Level 2a	Level 2b	Level 2b
0.8 – (1.6)	Level 2b	Level 3	Level 3
Failure of soil column			Level 4

The ground motion levels, physical model and weights in the logic tree for site Beznau are as follows:

Weight:

Level 1	--1.0--	For a given PGA/Magnitude, the next lower ground motion level of the RVT run is selected (RVT without soil randomization).
Level 2a	--0.4--	RVT without soil randomization at 0.3 g and the given magnitude.
	--0.4--	RVT without soil randomization at 0.4 g and the given magnitude.
	--0.2--	Non-linear at 0.4 g (with pore pressure build-up and cyclic mobility effects). In the high frequency range extrapolated. Extrapolation above 50 Hz from the mean in the range [30 Hz, 50 Hz].
	--0.0--	Non-linear at 0.75 g (with pore pressure build-up and cyclic mobility effects).. In the high frequency range extrapolated. Extrapolation above 50 Hz from the mean in the range [30 Hz 50 Hz].
Level 2b	--0.2--	RVT without soil randomization at 0.3 g and the given magnitude.
	--0.2--	RVT without soil randomization at 0.4 g and the given magnitude.
	--0.4--	Non-linear at 0.4 g (with pore pressure build-up and cyclic mobility effects). In the high frequency range extrapolated. Extrapolation above 50 Hz from the mean in the range [30 Hz, 50 Hz].
	--0.2--	Non-linear at 0.75 g (with pore pressure build-up and cyclic mobility effects). In the high frequency range extrapolated. Extrapolation above 50 Hz from the mean in the range [30 Hz, 50 Hz].
Level 3	--0.2--	Non-linear at 0.4 g (with pore pressure build-up and cyclic mobility effects). In the high frequency range extrapolated. Extrapolation above 50 Hz from the mean in the range [30 Hz, 50 Hz].
	--0.5--	Non-linear at 0.75 g (with pore pressure build-up and cyclic mobility effects). In the high frequency range extrapolated. Extrapolation above 50 Hz from the mean in the range [30 Hz, 50 Hz].
	--0.3--	Non-linear at 1.50 g (with pore pressure build-up and cyclic mobility effects). In the high frequency range extrapolated. Extrapolation above 50 Hz from the mean in the range [30 Hz, 50 Hz].

The basis for the selection of weights of the branches in the logic tree is the advantages and disadvantages of the computational methods and the level of non-linear behavior as discussed in chapter 2.1.

2.5 Gösgen

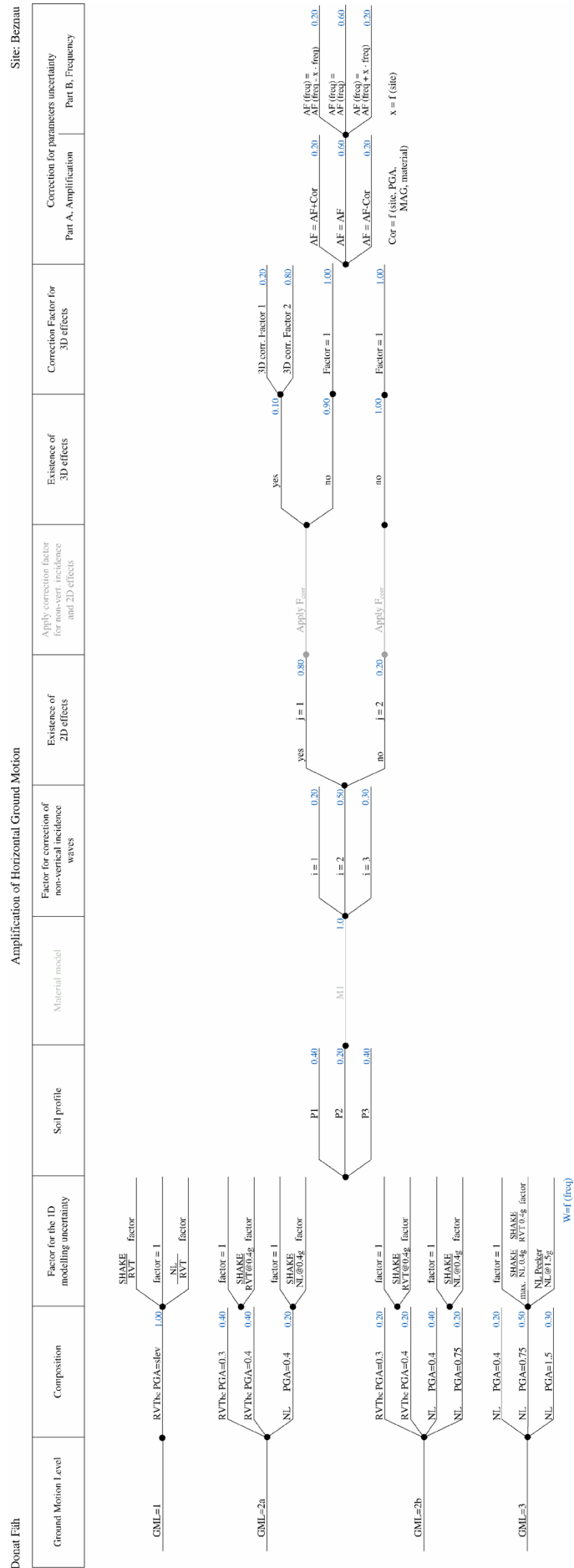
2.5.1 Logic Tree for Gösgen

The logic tree for site Gösgen with the weights and branches is given in Figure 2-5.

2.5.2 Site-Specific Model Evaluations

The ground motion levels for Gösgen are defined in Table 2-16. The discussion is provided in section 2.1. The PGA-range in the first column is for the reference ground motion on bedrock with S-wave velocity of 2000 m/s at the surface.

Fig. 2-4: Logic tree for the site Beznau, used to estimate the median amplification of the horizontal ground motion.



Tab. 2-16: Definitions of the level of ground motion for site Gösgen

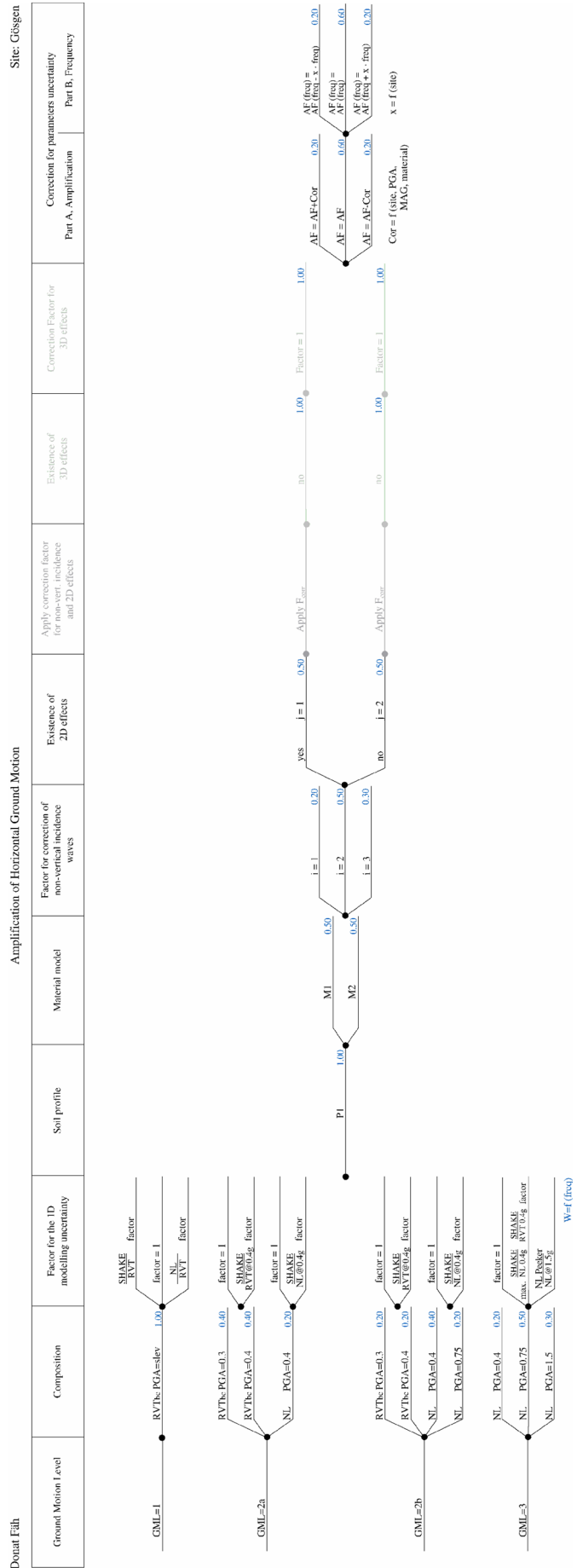
PGA range in g	Magnitude 5 – 6	Magnitude 6 – 7	Magnitude 7 – 8
– 0.05	Level 1	Level 1	Level 1
0.05 – 0.1	Level 1	Level 1	Level 1
0.1 – 0.2	Level 1	Level 1	Level 1
0.2 – 0.4	Level 2a	Level 2a	Level 2a
0.4 – 0.8	Level 2b	Level 2b	Level 2b
0.8 – (1.6)	Level 2b	Level 3	Level 3
Failure of soil column			Level 4

The ground motion levels, physical model and weights in the logic tree for site Gösgen are the same as for Beznau and are as follows:

Weight:

- Level 1 --1.0-- For a given PGA/Magnitude, the next lower ground motion level of the RVT run is selected (RVT without soil randomization).
- Level 2a --0.4-- RVT without soil randomization at 0.3 g and the given magnitude.
--0.4-- RVT without soil randomization at 0.4 g and the given magnitude.
--0.2-- Non-linear at 0.4 g (with pore pressure build-up and cyclic mobility effects). In the high frequency range extrapolated. Extrapolation above 50 Hz from the mean in the range [30 Hz, 50 Hz].
--0.0-- Non-linear at 0.75 g (with pore pressure build-up and cyclic mobility effects). In the high frequency range extrapolated. Extrapolation above 50 Hz from the mean in the range [30 Hz, 50 Hz].
- Level 2b --0.2-- RVT without soil randomization at 0.3 g and the given magnitude.
--0.2-- RVT without soil randomization at 0.4 g and the given magnitude.
--0.4-- Non-linear at 0.4 g (with pore pressure build-up and cyclic mobility effects). In the high frequency range extrapolated. Extrapolation above 50 Hz from the mean in the range [30 Hz, 50 Hz].
--0.2-- Non-linear at 0.75 g (with pore pressure build-up and cyclic mobility effects). In the high frequency range extrapolated. Extrapolation above 50 Hz from the mean in the range [30 Hz, 50 Hz].
- Level 3 --0.2-- Non-linear at 0.4 g (with pore pressure build-up and cyclic mobility effects). In the high frequency range extrapolated. Extrapolation above 50 Hz from the mean in the range [30 Hz, 50 Hz].
--0.5-- Non-linear at 0.75 g (with pore pressure build-up and cyclic mobility effects). In the high frequency range extrapolated. Extrapolation above 50 Hz from the mean in the range [30 Hz, 50 Hz].
--0.3-- Non-linear at 1.50 g (with pore pressure build-up and cyclic mobility effects). In the high frequency range extrapolated. Extrapolation above 50 Hz from the mean in the range [30 Hz, 50 Hz].

Fig. 2-5: Logic tree for the site Gösgen, used to estimate the median amplification of the horizontal ground motion



Donat Fäh

Amplification of Horizontal Ground Motion

Site: Gösgen

Ground Motion Level	Composition	Factor for the 1D modelling uncertainty	Soil profile	Material model	Factor for correction of non-vertical incidence waves	Existence of 2D effects	Apply correction factor for non-vertical incidence and 2D effects	Existence of 3D effects	Correction Factor for 3D effects	Correction for parameters uncertainty Part A, Amplification	Correction for parameters uncertainty Part B, Frequency
GML=1		SHAKE RVT factor factor = 1 NL RVT factor									
GML=2h		RVTb: PGA=0.3 RVTb: PGA=0.4 NL: PGA=0.4									
GML=2b		RVTb: PGA=0.3 RVTb: PGA=0.4 NL: PGA=0.4 NL: PGA=0.75									
GML=3		NL: PGA=0.4 NL: PGA=0.75 NL: PGA=1.5									

2.6 Leibstadt

2.6.1 Logic Tree for Leibstadt

The logic tree for site Leibstadt with the weights and branches is given in Figure 2-6.

2.6.2 Site-Specific Model Evaluations

The ground motion levels for Leibstadt are defined in Table 2-17. The discussion is provided in section 2.1. The PGA-range in the first column is for the reference ground motion on bedrock with S-wave velocity of 2000 m/s at the surface.

Tab. 2-17: Definitions of the level of ground motion for site Leibstadt

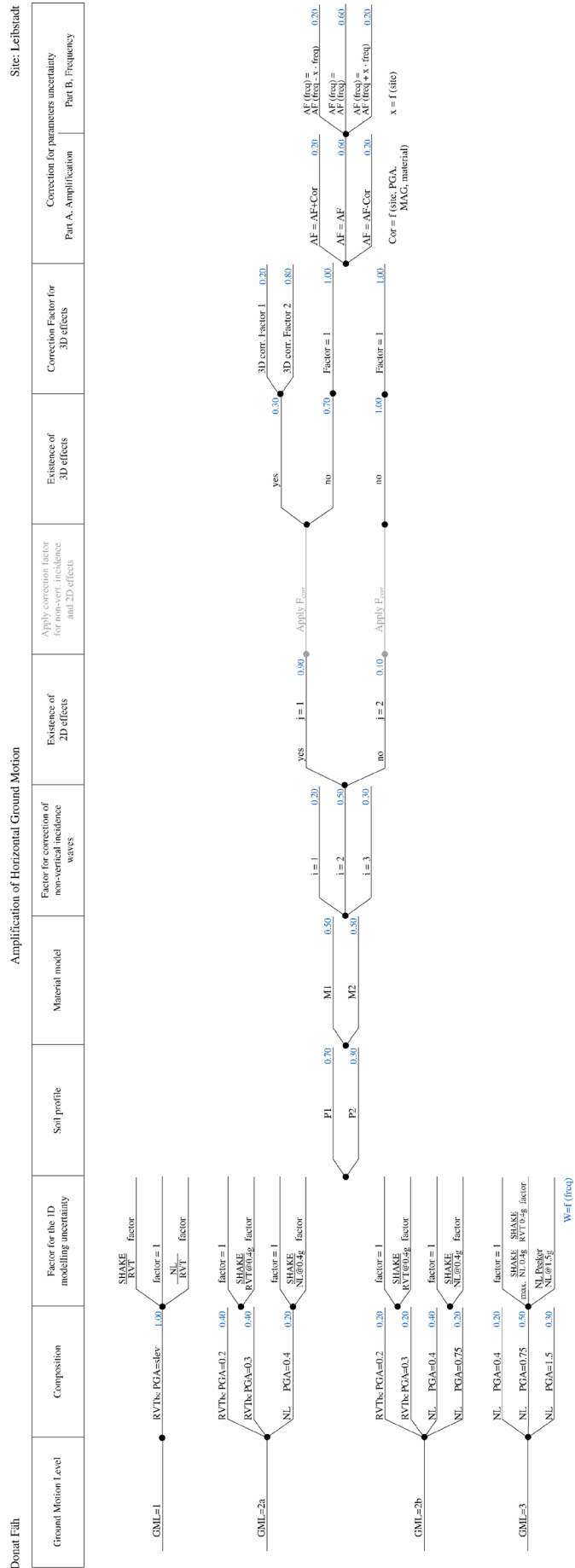
PGA range in g	Magnitude 5 – 6	Magnitude 6 – 7	Magnitude 7 – 8
– 0.05	Level 1	Level 1	Level 1
0.05 – 0.1	Level 1	Level 1	Level 1
0.1 – 0.2	Level 1	Level 1	Level 1
0.2 – 0.4	Level 1	Level 2a	Level 2a
0.4 – 0.8	Level 2a	Level 2b	Level 2b
0.8 – (1.6)	Level 2b	Level 3	Level 3
Failure of soil column			Level 4

The ground motion levels, physical model and weights in the logic tree for site Leibstadt are as follows:

Weight:

- Level 1 --1.0-- For a given PGA/Magnitude, the next lower ground motion level of the RVT run is selected (RVT without soil randomization).
- Level 2a --0.4-- RVT without soil randomization at 0.2 g and the given magnitude.
- 0.4-- RVT without soil randomization at 0.3 g and the given magnitude.
- 0.2-- Non-linear at 0.4 g (without pore pressure build-up). In the high frequency range extrapolated. Extrapolation above 50 Hz from the mean in the range [30 Hz, 50Hz].
- 0.0-- Non-linear at 0.75 g (without pore pressure build-up). In the high frequency range extrapolated. Extrapolation above 50 Hz from the mean in the range [30 Hz, 50 Hz].
- Level 2b --0.2-- RVT without soil randomization at 0.2 g and the given magnitude.
- 0.2-- RVT without soil randomization at 0.3 g and the given magnitude.
- 0.4-- Non-linear at 0.4 g (without pore pressure build-up). In the high frequency range extrapolated. Extrapolation above 50 Hz from the mean in the range [30 Hz, 50 Hz].
- 0.2-- Non-linear at 0.75 g (without pore pressure build-up). In the high frequency range extrapolated. Extrapolation above 50 Hz from the mean in the range [30 Hz, 50 Hz].

Fig. 2-6: Logic tree for the site Leibstadt, used to estimate the median amplification of the horizontal ground motion



- Level 3 --0.2-- Non-linear at 0.4 g (without pore pressure build-up). In the high frequency range extrapolated. Extrapolation above 50 Hz from the mean in the range [30 Hz, 50 Hz].
- 0.5-- Non-linear at 0.75 g (without pore pressure build-up). In the high frequency range extrapolated. Extrapolation above 50 Hz from the mean in the range [30 Hz, 50 Hz].
- 0.3-- Non-linear at 1.50 g (without pore pressure build-up). In the high frequency range extrapolated. Extrapolation above 50 Hz from the mean in the range [30 Hz, 50 Hz].

2.7 Mühleberg

2.7.1 Logic Tree for Mühleberg

The logic tree for site Mühleberg with the weights and branches is given in Fig. 2-7. The reference structures used to define ground motion attenuation in the working group SP2 is very close to the Mühleberg structure. The ground motion estimate obtained from SP2 is therefore an alternative to the entire tree developed for Mühleberg. However, the weight for this branch is smaller due to the fact that the bedrock is probably altered. This additional branch in the logic tree is only applied for Mühleberg.

Additional branch in the logic tree for Mühleberg:

- 0.7----- entire tree developed for Mühleberg
- 0.3----- SP2 ground motion and aleatory uncertainty

2.7.2 Site-Specific Model Evaluations

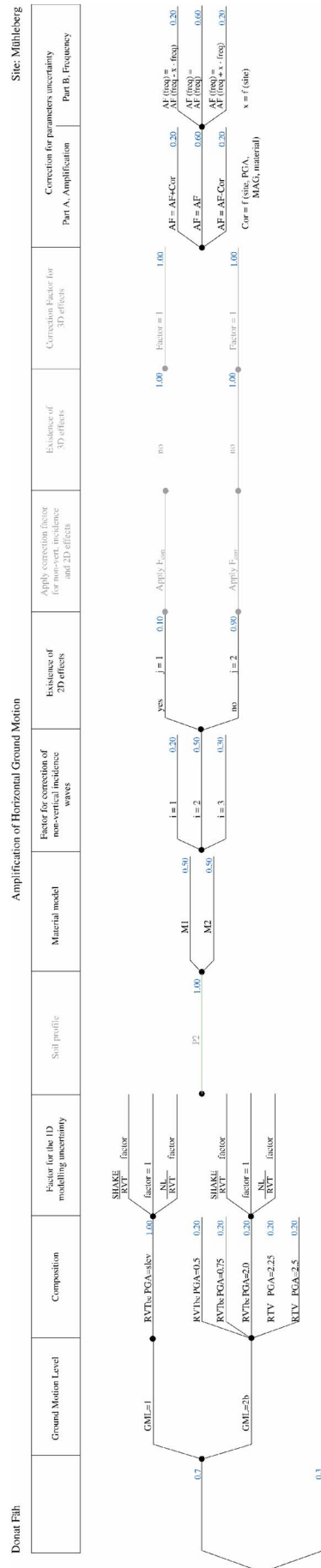
The ground motion levels for Mühleberg are defined in Table 2-18. The discussion is provided in section 2.1. The PGA-range in the first column is for the reference ground motion on bedrock with S-wave velocity of 2000 m/s at the surface.

Tab. 2-18: Definitions of the level of ground motion for site Mühleberg.

PGA range in g	Magnitude 5 – 6	Magnitude 6 – 7	Magnitude 7 – 8
– 0.05	Level 1	Level 1	Level 1
0.05 – 0.1	Level 1	Level 1	Level 1
0.1 – 0.2	Level 1	Level 1	Level 1
0.2 – 0.4	Level 1	Level 1	Level 1
0.4 – 0.8	Level 1	Level 1	Level 1
0.8 – 1.6	Level 2	Level 2	Level 2

For this site no non-linear computations have been performed. Moreover the site's fundamental frequency of resonance has not been measured. At PGA levels in the 1.0 – 1.5 g range, we observe strong v_s -reductions in some of the RVT runs. These v_s reductions are allowed to occur in the equivalent linear approach, because almost no information on the thickness and composition of the soft soils is available for this site. The weights in the branches are therefore taken to be equal. The ground motion levels, physical model and weights in the logic tree for site Mühleberg are as follows:

Fig. 2-7: Logic tree for the site Mühleberg, used to estimate the median amplification of the horizontal ground motion



- Level 1 --1.0 -- For a given PGA/Magnitude, the next lower ground motion level of the RVT run is selected (RVT without soil randomization).
- Level 2 --0.2 -- RVT without soil randomization at 0.50 g and the given magnitude.
--0.2 -- RVT without soil randomization at 0.75 g and the given magnitude.
--0.2 -- RVT without soil randomization at 1.00 g and the given magnitude.
--0.2 -- RVT without soil randomization at 1.25 g and the given magnitude.
--0.2 -- RVT without soil randomization at 1.50 g and the given magnitude.
- Level 3 not realized.

3 MEDIAN AMPLIFICATION OF VERTICAL GM

3.1 Approach

Very few computations have been performed to estimate the amplification on the vertical component. All computations are based on the idea that amplification on the vertical component is only due to amplification of P waves. This is certainly incorrect because S waves and surface waves in the PSV case can contribute significantly to the ground motion on the vertical component. The resulting uncertainty caused by the lack of reliable computations is accounted for by an increased epistemic uncertainty.

Three main branches of the logic tree are proposed to estimate the amplification for the vertical component of motion: A) a branch based on H/V spectral ratios and the results for the median amplification of the horizontal component, B) a branch based on the computations performed for the vertical component with program SHAKE, and C) and a branch based on the vertical ground motion estimate proposed by SP2, without the 2000m/s correction factor for bedrock conditions.

3.2 Logic Tree Structure

This section describes the general logic tree, which is applicable to all sites, and discusses its organization. The example for NPP site Leibstadt is used to explain the different branches of the tree. The logic tree is given in Figure 3-1.

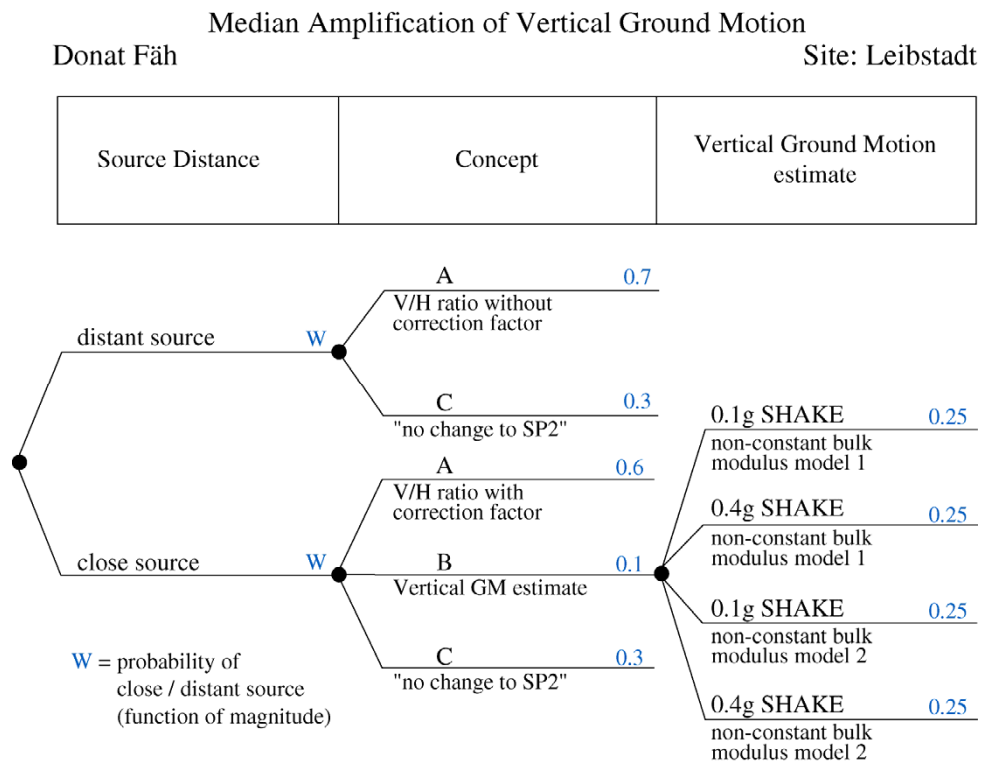


Fig. 3-1: Logic tree for NPP site Leibstadt, used to estimate the median amplification of the vertical ground motion

These branches and factors are discussed in the next chapter. The probabilities P_{dist} and P_{close} are defined in section 2.3.4 and are the same for all sites. The validity of this evaluation is limited to frequencies above 0.45 Hz.

3.3 Model Evaluations Common to All Sites

3.3.1 Concept A based on H/V ratios

We develop a V/H ratio for the different sites and an H/V ratio for rock, and multiply these ratios with the amplification obtained from the horizontal component defined in chapter 2. This is a concept that includes all epistemic uncertainties discussed for the horizontal component, and adds in the logic tree of the horizontal component one branch at the end of the tree. The estimate for the amplification on the vertical component is as follows:

$$V(\text{soil})/V(\text{rock}) = H(\text{rock})/V(\text{rock}) * V(\text{soil})/H(\text{soil}) * \text{Amplification}(\text{horizontal})$$

$$\text{Amplification}(\text{horizontal}) = H(\text{soil})/H(\text{rock}) \quad \text{amplification of the horizontal component at the end of each branch.}$$

$V(\text{soil})/H(\text{soil})$: V/H-ratio for the soil

$H(\text{rock})/V(\text{rock})$: H/V-ratio for rock

The product $H(\text{rock})/V(\text{rock}) * V(\text{soil})/H(\text{soil})$ is computed with the mode summation method, and the structures given in report TP3-TN-0167. The result is shown in Figure 3-2. The approximation is assumed to be valid for all ground-motion levels. With this approach, the vertical component is strongly related to the horizontal component. For Mühleberg, the "Gösgen"-curve is taken and the frequency axis is transformed by a factor of 2.5.

As proposed by Bozorgnia & Campell (2002), I introduce an effect on the V/H ratio that is due to the source distance. The V/H ratio has a distinct peak at large frequencies in the near-source region. The high-amplitude, high-frequency vertical ground motion that are observed in near-source seismograms are most likely generated by S-to-P conversion within the transition zone between the underlying bedrock and overlying softer sediments. This S-to-P conversion in the near-field cannot be taken into account with mode summation methods, due to the high phase-velocity of the almost vertically propagating P-waves. In the near-field, the curves obtained from the modelling with modal summation are therefore corrected. The correction factor is derived from the simplified V/H curves proposed for firm rock and very firm soil by Bozorgnia & Campell (2002, Fig. 7 in their publication). The logic tree obtained for the horizontal component is extended for the vertical component applying two different factors depending on the source distance:

$$P_{\text{dist}} \text{ (probability that earthquake is distant) } \text{ ---- } H(\text{rock})/V(\text{rock}) * V(\text{soil})/H(\text{soil})$$

$$P_{\text{close}} \text{ (probability that earthquake is close) } \text{ ---- } \textit{factor} * H(\text{rock})/V(\text{rock}) * V(\text{soil})/H(\text{soil})$$

The probabilities P_{dist} and P_{close} are defined in section 2.3.4. The *factor* as a function of frequency is derived by using the V/H curves proposed for firm rock and very firm soil by Bozorgnia & Campell (2002). Once again this function is simplified to the following form:

$$f < f_p/2 \quad : \quad \textit{factor} = 1.0$$

$$f_p/2 < f < f_p \quad : \quad \textit{ramp from factor} = 1.0 \text{ to } \textit{factor} = 1.4$$

$$f_p < f \quad : \quad \textit{factor} = 1.4$$

where the fundamental frequency for P-waves f_p is given for the different sites as follows: for Beznau $f_p = 9.5$ Hz; for Gösgen $f_p = 20$ Hz; for Leibstadt $f_p = 7.0$ Hz; for Mühleberg: $f_p = 30$ Hz (estimated).

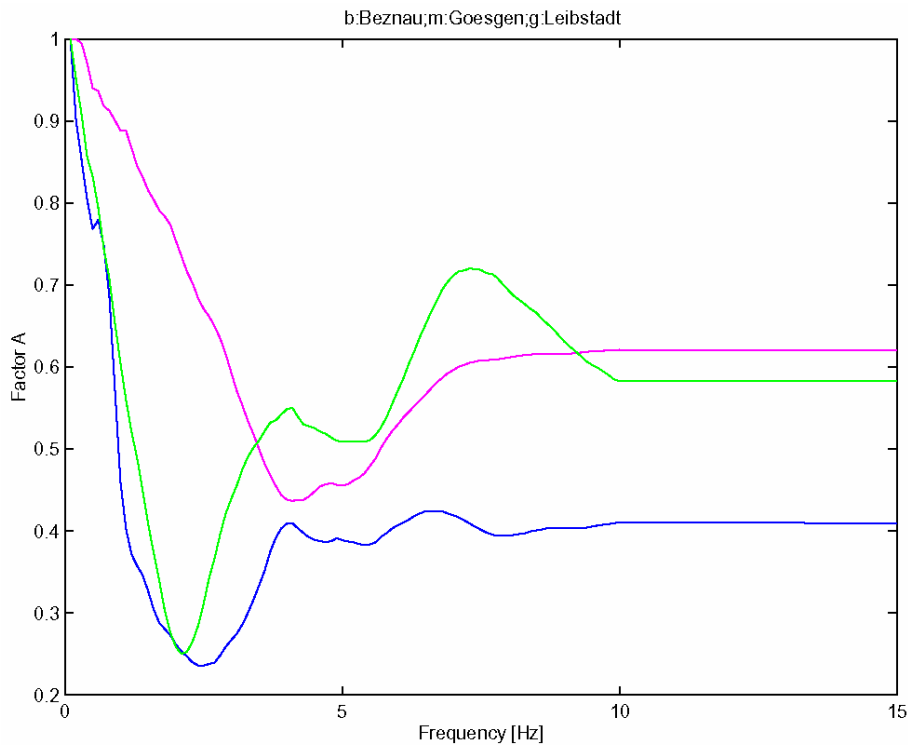


Fig. 3-2: $H(\text{rock})/V(\text{rock}) * V(\text{soil})/H(\text{soil})$ computed for the different NPP sites

3.3.2 Concept B based on the computations for the vertical component

It is assumed that the vertical component is amplified due the amplification of vertical incident P-waves, assuming a source below the site. We can then use the SHAKE results, where three cases are available. The case with constant bulk modulus is used for the sites with a water table close to the ground surface. This is for Mühleberg at 3.25 m, for Beznau at 3.0 m, and for Gösgen 5.0 m. Leibstadt is treated differently with the two cases with non-constant bulk modulus.

3.3.3 Concept C based on the SP2 vertical ground motion estimate

The reference structures of the SP2 attenuation models are similar to the structures of Beznau, Gösgen, and Leibstadt, and very close to the Mühleberg structure. By assuming that the vertical component of motion is not affected by site-effects, we can take the ground motion estimate for the vertical component obtained from SP2.

3.4 Beznau

3.4.1 Logic Tree for Beznau

The logic tree for site Beznau with the weights and branches is given in Figure 3-3. Low weight is given to the branch based on the computations for the vertical component due to fact that

vertical components contain S- and surface-wave energy. High weight is given to the branch based on H/V ratios that relates the vertical component to the large number of computations for the horizontal component.

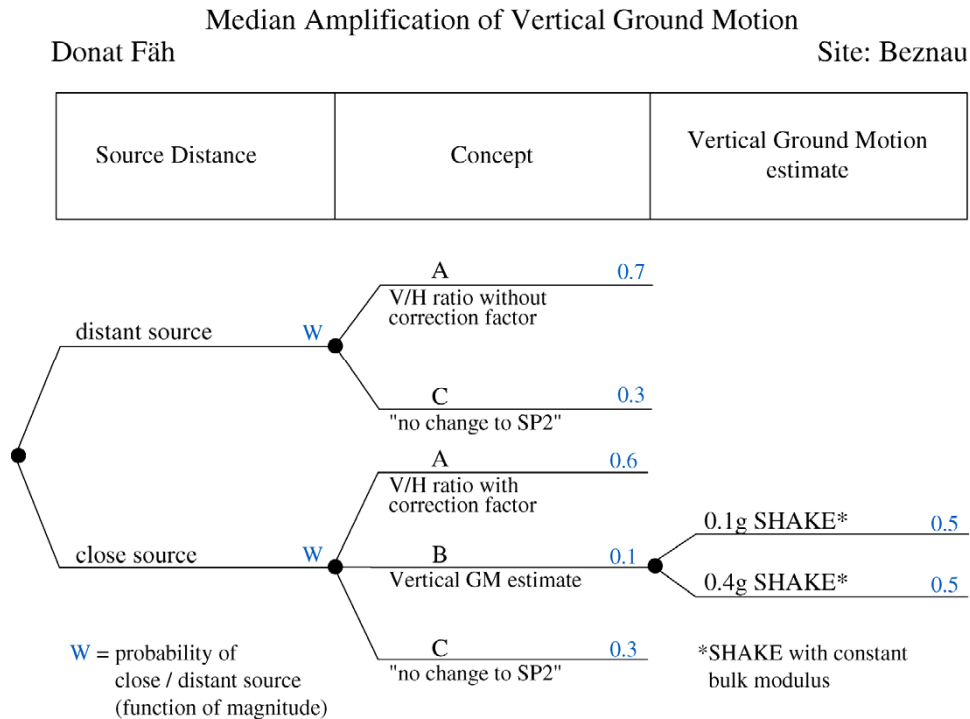


Fig. 3-3: Logic tree for NPP site Beznau, used to estimate the median amplification of the vertical ground motion

3.5 Gösgen

3.5.1 Logic Tree for Gösgen

The logic tree for site Gösgen with the weights and branches is given in Figure 3-4. Low weight is given to the branch based on the computations for the vertical component. High weight is given to the branch based on H/V ratios.

3.6 Leibstadt

3.6.1 Logic Tree for Leibstadt

The logic tree for site Leibstadt with the weights and branches is given in Figure 3-5. Low weight is given to the branch based on the computations for the vertical component. High weight is given to the branch based on H/V ratios.

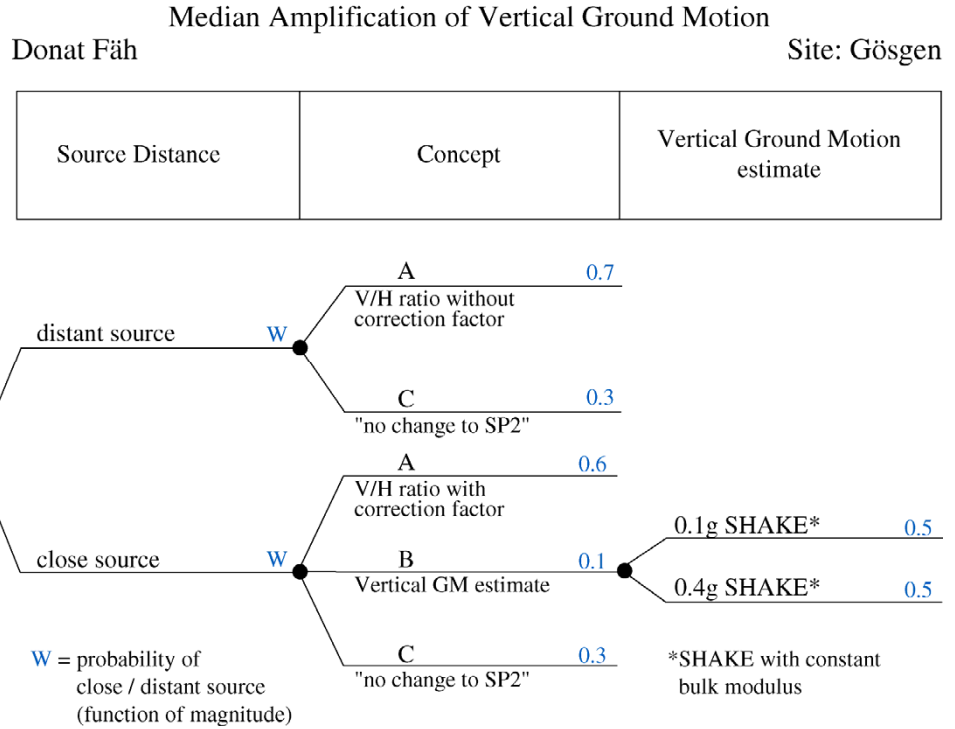


Fig. 3-4: Logic tree for NPP site Gösgen, used to estimate the median amplification of the vertical ground motion

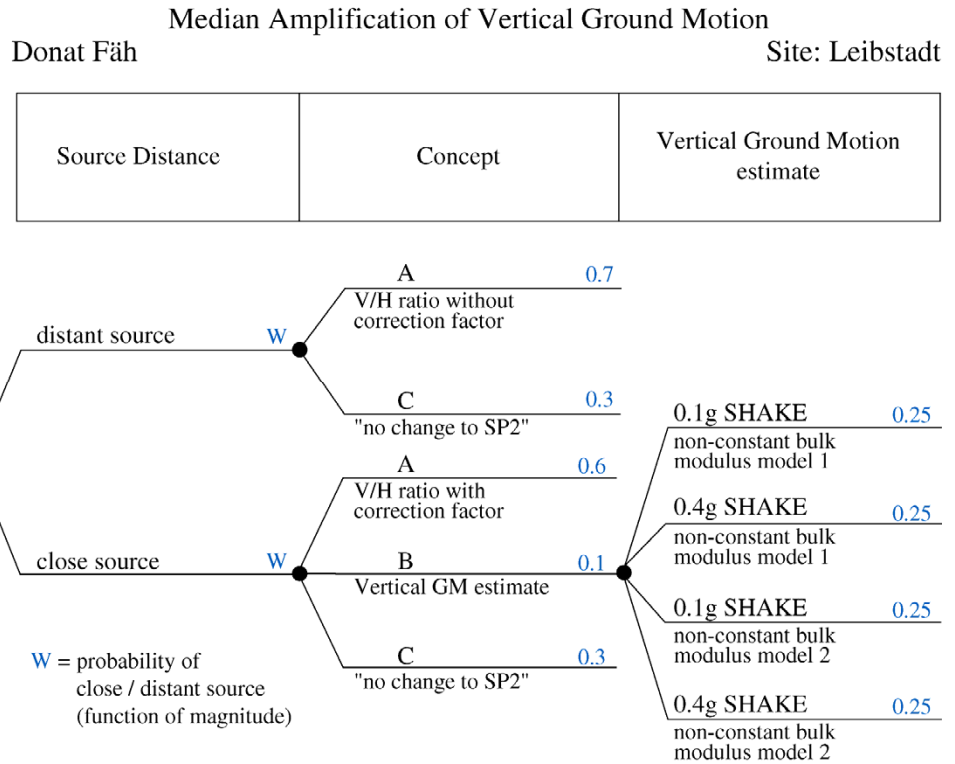


Fig. 3-5: Logic tree for NPP site Leibstadt, used to estimate the median amplification of the vertical ground motion

3.7 Mühleberg

3.7.1 Logic Tree for Mühleberg

The logic tree for site Mühleberg with the weights and branches is given in Figure 3-6. Low weight is given to the branch based on the computations for the vertical component. High weight is given to the branch based on the SP2 vertical ground motion estimate.

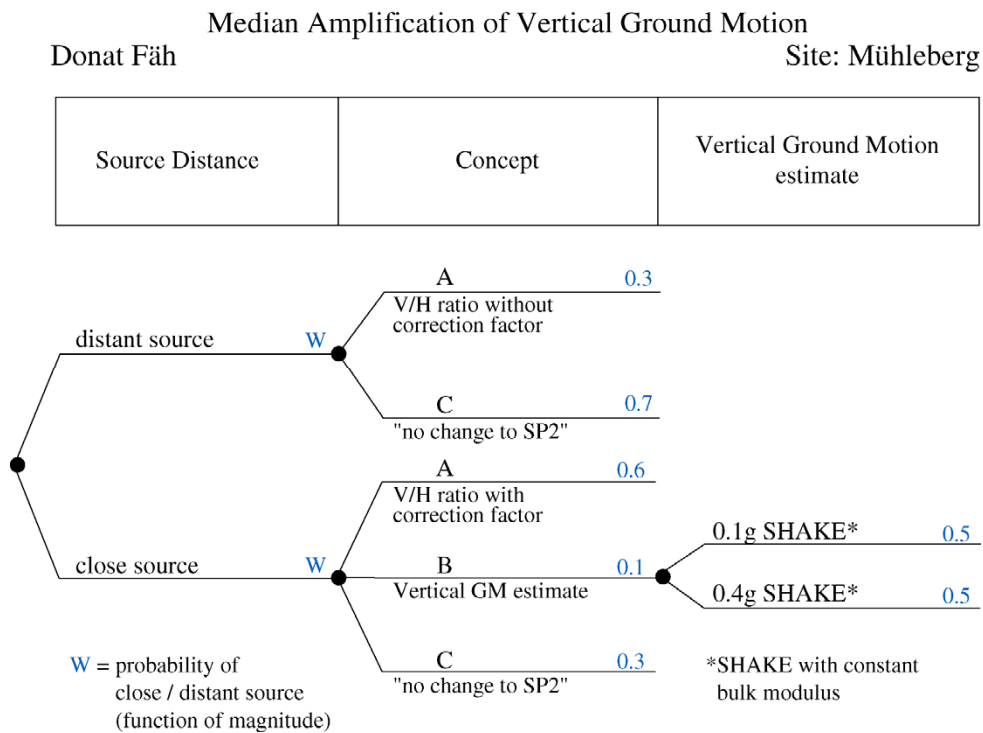


Fig. 3-6: Logic tree for NPP site Mühleberg, used to estimate the median amplification of the vertical ground motion

4 ALEATORY VARIABILITY OF HORIZONTAL GROUND MOTION

4.1 Approach

The computation of the aleatory variability is completely based on the logic tree approach for the horizontal component, as defined in section 2.2. Each complete branch of the logic tree uses as a base the computed amplification factors either from RVT or truly non-linear methods at a specific PGA level. This is defined in the branch "Composition", and referred to as the base computation. At the end of each branch we can define the total aleatory variability as the sum of a) the variability of the base computation, and b) the variability of the mean correction factor F_{corr}^{ij} .

- a) The variability of the base computation for the horizontal component is defined for each Level as follows:

For Level 1: Aleatory variability of the corresponding RVT run base-case.

For Level 2 & 3: 1) RVT is the base computation: The max. aleatory variability from all RVT runs at all shaking-levels and magnitudes in Level 1 is taken.

2) Non-linear is the base computation: The aleatory variability from the corresponding non-linear computation is taken.

- b) The variability of the mean correction factor F_{corr}^{ij} for non-vertical incidence and 2D effects defined in section 2.3.4. The variability is given as follows:

$$\begin{aligned} \sigma_{2D}^2 = & \left(\log (F_{\text{nvi_dist}}^i * F_{\text{ND}}) - \log (F_{\text{corr}}^{ij}) \right)^2 P_{\text{dist}} * P_{\text{ND}} \\ & + \left(\log (F_{\text{nvi_dist}}^i * F_{\text{NS}}) - \log (F_{\text{corr}}^{ij}) \right)^2 P_{\text{dist}} * P_{\text{NS}} \\ & + \left(\log (F_{\text{nvi_dist}}^i * F_{\text{SD}}) - \log (F_{\text{corr}}^{ij}) \right)^2 P_{\text{dist}} * P_{\text{SD}} \\ & + \left(\log (F_{\text{nvi_dist}}^i * F_{\text{SS}}) - \log (F_{\text{corr}}^{ij}) \right)^2 P_{\text{dist}} * P_{\text{SS}} \\ & + \left(\log (F_{\text{nvi_close}} * F_{\text{2D_close}}^j) - \log (F_{\text{corr}}^{ij}) \right)^2 P_{\text{close}} \end{aligned}$$

4.2 Logic Tree Structure

The logic tree structure corresponds to the one for the horizontal component defined in chapter 2. For the different sites there are no differences in the computation of the aleatory variability. For site Mühleberg, one branch of the logic tree is the ground motion estimate obtained from the SP2 working group. For this branch, the aleatory variability corresponds to the estimate of working group SP2.

5 ALEATORY VARIABILITY OF VERTICAL GROUND MOTION

5.1 Approach

The logic tree structure corresponds to the one for the vertical component defined in chapter 3. For concept A defined in chapter 3, the computation of the aleatory variability of the vertical component corresponds exactly to the one of the horizontal component described in chapter 4. For the SHAKE computations used in concept B, the aleatory variability is defined from the corresponding SHAKE run. For concept C the aleatory variability corresponds to the estimate of working group SP2.

5.2 Logic tree structure

For the different sites there are no differences in the way to compute of the aleatory variability. The differences between the sites are describes in chapter 3 in the logic tree of the vertical component.

6 MAXIMUM GROUND MOTIONS

This part provides an estimate of the possible maximum ground motion for the horizontal and vertical component. As a base the recommendations by Pecker et al. (TP3-TN-0354, 2003) and the maximum observed ground motions (TP3-TN-0359, 2003) are used to derive the logic tree. Since theoretical and numerical results have a high uncertainty caused by the lack of experience and observations, the epistemic uncertainty is very high.

6.1 Horizontal Component

The maximum peak ground accelerations (PGA) estimated by Pecker et al. (TP3-TN-0354, 2003) are as follows: for Beznau 20 m/s², for Gösigen 15 m/s², for Leibstadt 15 m/s², and for Mühleberg 16 m/s². No estimate of the maximum spectral acceleration as a function of frequency is provided. Therefore the spectral shapes are derived from the maximum observed ground motion summarized in report TP3-TN-0359. This is illustrated in Figure 6-1. Two possible shapes of the spectra are taken into account for the horizontal component, as is shown in Figure 6-2. The high plateau value derived from the observed maximum ground motions (see Figure 6-1) accounts for small-frequency-band peaks in possible response spectra. Only one shape is proposed for all NPP sites, because at high ground motion levels non-linear effects will cause energy transfer between different frequencies, which makes the behaviour unpredictable. Factors are applied to the PGA values in order to compute the maximum spectral acceleration for the horizontal component at a given frequency. The factors are given in Table 6-1. For intermediate frequencies, linear interpolation is proposed. The amplification factors are the same for all sites.

PGA values higher than those proposed by Pecker et al. (2003) cannot be excluded, and some of the non-linear computations also support this statement. This accounts for additional effects such as 2D/3D effects, when the failure introduces a solid-liquid interface that is able to trap S-

wave energy. For this reason the logic tree also includes a branch with maximum PGA values that are twice the values proposed by A.Pecker et al..

Tab. 6-1: Factors applied to the PGA values in order to compute the maximum spectral acceleration for the horizontal component at a given frequency

Factor 1 defines a flatter spectrum than Factor 2.

Frequency [Hz]	Factor 1	Factor 2
0.45	1.5	2.0
1.0	2.0	3.0
2.5	2.5	4.0
5.0	2.5	4.0
10.	2.0	3.0
20.	1.5	2.0
50.	1.0	1.0
100.	1.0	1.0

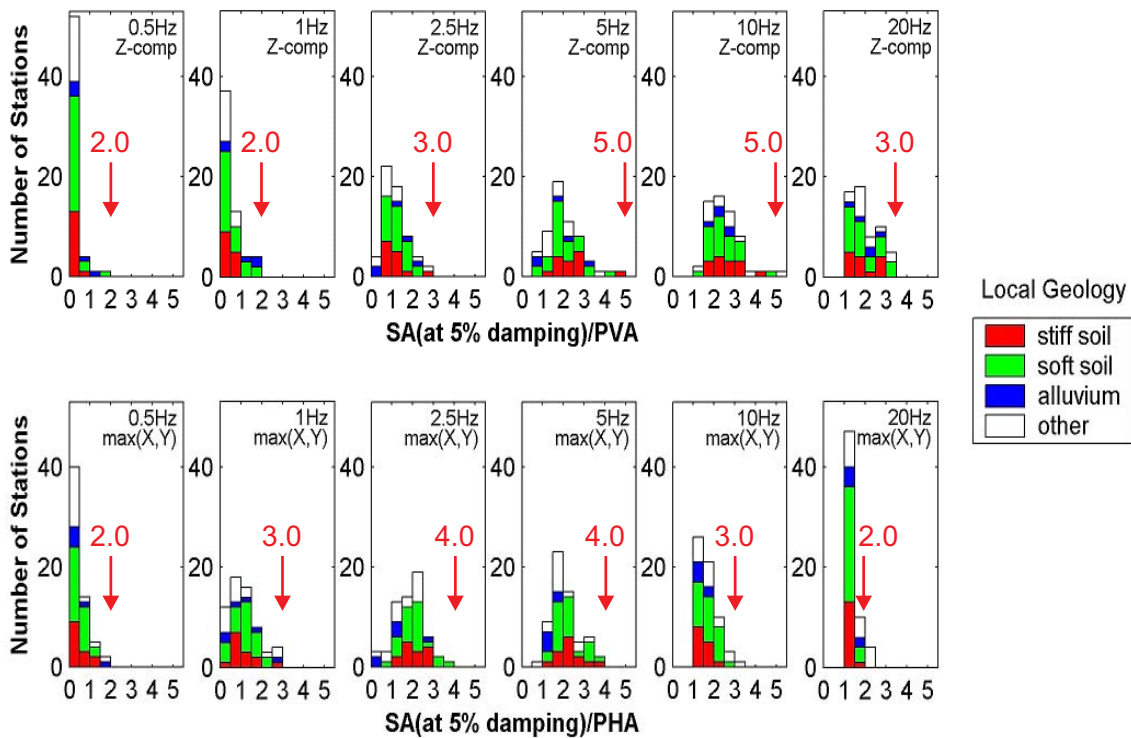


Fig 6-1: Derivation of the spectral shapes for maximum ground motion from the maximum observed ground motion summarized (TP3-TN-0359)

In case that a spectral acceleration is larger than the maximum value proposed in the logic tree, the computation is not removed. The spectral acceleration value assigned in such cases corresponds to a value between 50 % and 100 % of the maximum spectral acceleration. The reason is that at a specific site, a certain level of ground motion is recorded before the failure of the soil column. This cannot be included directly in the soil hazard computation. The spikes in

the maximum ground motion are therefore replaced by a ramp function between 50 % and 100 % of the maximum spectral acceleration defined here.

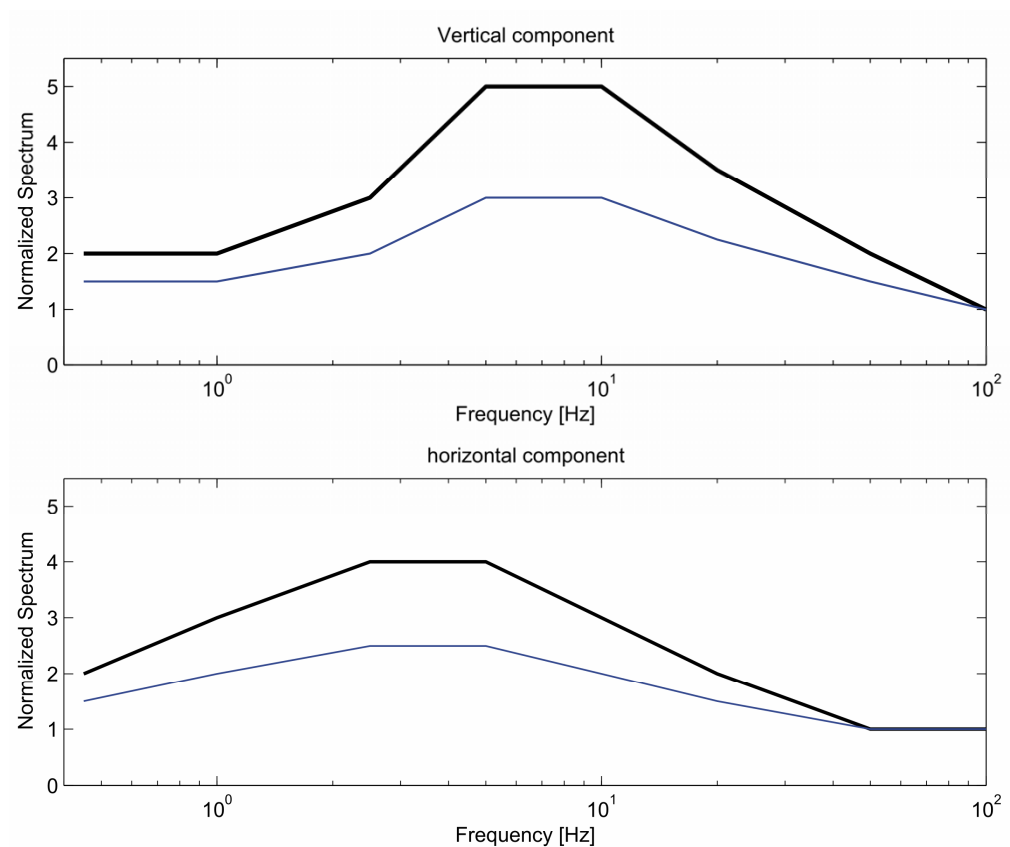


Fig. 6-2: Shapes of the spectra for maximum ground motions for the horizontal and vertical component, normalized to PGA

6.1.1 Logic Tree Structure

The logic tree for all sites with the weights and branches is given in Figure 6-3. The basis for the weights is given in section 6.1.3.

6.1.2 Evaluation of Proponent Models

Betbeder's model is considered to provide values that are too low. All other methods are considered to be valuable estimates of the maximum ground motion. The number of independent estimates of maximum ground motion is not sufficient to further reduce the maximum PGA.

6.1.3 Weights for Maximum Ground Motions

The weights are provided in Figure 6-3. Higher weight is given to the estimate proposed by Pecker et al. (2003) and the flat spectral shape (Factor 1). The PGA values from the Pecker et al. (2003) model are preferred over the factor of 2 increased values because they are based on the computed soil strengths. The spectral shape of the lowest maximum ground motion in Figure 6-2 corresponds approximately the maximum observed ground motions shown in Figure 6-4. For the higher PGA value, the flat spectrum is therefore preferred. It is noticed that the plateau of the spectrum for the vertical component is higher than for the horizontal, and shifted in the frequency range to higher frequencies. Since observations most probably will not cover all

possible values, we have to expect a change of the graphs in Figure 6-4 to higher values. This is accounted for by the different spectra in Figure 6-2.

- 0.7--- $\text{MAX(PGA)} = 1.0 \cdot \text{PGA}$ by Pecker et al. (2003)
 - 0.3--- Factor 1 applied to obtain the maximum spectral acceleration
 - If the actual value is larger than the maximum spectral acceleration, the following values are assigned
 - 0.2--- Resulting spectral acceleration is 55 % of the maximum
 - 0.2--- Resulting spectral acceleration is 65 % of the maximum
 - 0.2--- Resulting spectral acceleration is 75 % of the maximum
 - 0.2--- Resulting spectral acceleration is 85 % of the maximum
 - 0.2--- Resulting spectral acceleration is 95 % of the maximum
 - 0.7--- Factor 2 applied to obtain the maximum spectral acceleration
 - If the actual value is larger than the maximum spectral acceleration, the following values are assigned
 - 0.2--- Resulting spectral acceleration is 55 % of the maximum
 - 0.2--- Resulting spectral acceleration is 65 % of the maximum
 - 0.2--- Resulting spectral acceleration is 75 % of the maximum
 - 0.2--- Resulting spectral acceleration is 85 % of the maximum
 - 0.2--- Resulting spectral acceleration is 95 % of the maximum
- 0.3--- $\text{MAX(PGA)} = 2.0 \cdot \text{PGA}$ by Pecker et al. (2003)
 - 0.8--- Factor 1 applied to obtain the maximum spectral acceleration
 - If the actual value is larger than the maximum spectral acceleration, the following values are assigned
 - 0.2--- Resulting spectral acceleration is 55 % of the maximum
 - 0.2--- Resulting spectral acceleration is 65 % of the maximum
 - 0.2--- Resulting spectral acceleration is 75 % of the maximum
 - 0.2--- Resulting spectral acceleration is 85 % of the maximum
 - 0.2--- Resulting spectral acceleration is 95 % of the maximum
 - 0.2--- Factor 2 applied to obtain the maximum spectral acceleration
 - If the actual value is larger than the maximum spectral acceleration, the following values are assigned
 - 0.2--- Resulting spectral acceleration is 55 % of the maximum
 - 0.2--- Resulting spectral acceleration is 65 % of the maximum
 - 0.2--- Resulting spectral acceleration is 75 % of the maximum
 - 0.2--- Resulting spectral acceleration is 85 % of the maximum
 - 0.2--- Resulting spectral acceleration is 95 % of the maximum

Fig. 6-3: Frequency dependent logic tree used to estimate the maximum spectral acceleration for the horizontal component

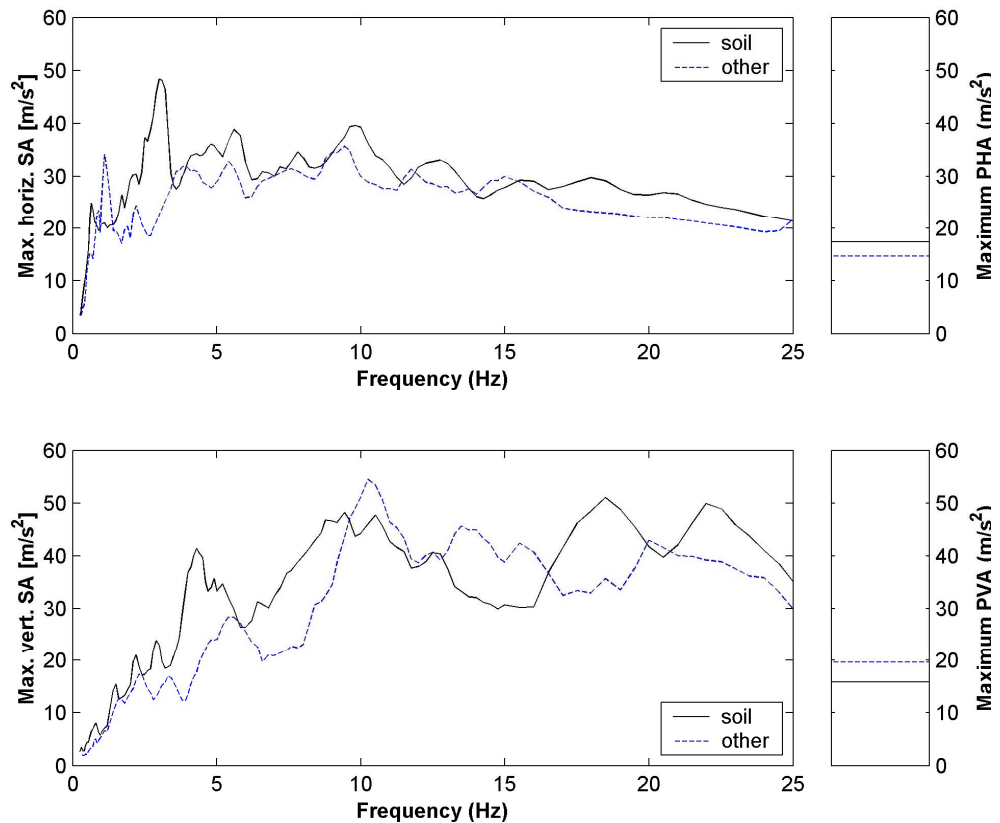


Fig.6-4: Maximum spectral acceleration and maximum peak acceleration of all the records (from report TP3-TN-0359)

Top: Maximum horizontal SA and maximum peak horizontal acceleration (PHA).
 Bottom: Maximum vertical SA and maximum peak vertical acceleration (PVA).
 Solid black line: local geology is "stiff soil", "soft soil" or "alluvium". Dashed blue line: local geology is "rock", "very soft soil" or unknown.

6.2 Vertical Component

No computations are available for estimating the maximum ground motion on the vertical component. Therefore, the logic tree structure for the maximum vertical ground motion is proposed to be similar to the one for the horizontal component. The maximum peak ground accelerations (PGA) estimated by Pecker et al. (2003) are assumed to be also valid estimates for the vertical component, because at these limits non S-wave energy is seen on the vertical component. The spectral shapes are derived from the maximum observed ground motion summarized in report TP3-TN-0359 for the vertical component. Two possible shapes of the spectra are taken into account. Factors are applied to the PGA values in order to compute the maximum spectral acceleration for the vertical component at a given frequency. The factors are given in Table 6-2. For intermediate frequencies, linear interpolation is proposed. The amplification factors are the same for all sites.

6.2.1 Logic Tree Structure

The logic tree for the vertical component for all sites with the weights and branches is given in Figure 6-5. The basis for the weights is similar to the horizontal component, and explained in section 6.1.3. The weights for the highest ground motion level is increased, due to the fact that P-wave energy still can pass a liquefied layer.

Tab. 6-2: Factors applied to the PGA values in order to derive the spectral shape of the maximum spectral acceleration for the vertical component at a given frequency

Frequency [Hz]	Factor 3	Factor 4
0.45	1.5	2.0
1.0	1.5	2.0
2.5	2.0	3.0
5.0	3.0	5.0
10.	3.0	5.0
20.	2.25	3.5
50.	1.5	2.0
100.	1.0	1.0

---0.3--- MAX(PGA)=1.0*PGA by Pecker et al. (2003)

--0.3--- Factor 3 applied to obtain the maximum spectral acceleration

If the actual value is larger than the maximum spectral acceleration, the following values are assigned

---0.2--- Resulting spectral acceleration is 55 % of the maximum

---0.2--- Resulting spectral acceleration is 65 % of the maximum

---0.2--- Resulting spectral acceleration is 75 % of the maximum

---0.2--- Resulting spectral acceleration is 85 % of the maximum

---0.2--- Resulting spectral acceleration is 95 % of the maximum

--0.7--- Factor 4 applied to obtain the maximum spectral acceleration

If the actual value is larger than the maximum spectral acceleration, the following values are assigned

---0.2--- Resulting spectral acceleration is 55 % of the maximum

---0.2--- Resulting spectral acceleration is 65 % of the maximum

---0.2--- Resulting spectral acceleration is 75 % of the maximum

---0.2--- Resulting spectral acceleration is 85 % of the maximum

---0.2--- Resulting spectral acceleration is 95 % of the maximum

---0.7--- MAX(PGA)=2.0*PGA by Pecker et al. (2003)

--0.7--- Factor 3 applied to obtain the maximum spectral acceleration

If the actual value is larger than the maximum spectral acceleration, the following values are assigned

---0.2--- Resulting spectral acceleration is 55 % of the maximum

---0.2--- Resulting spectral acceleration is 65 % of the maximum

---0.2--- Resulting spectral acceleration is 75 % of the maximum

---0.2--- Resulting spectral acceleration is 85 % of the maximum

---0.2--- Resulting spectral acceleration is 95 % of the maximum

--0.3--- Factor 4 applied to obtain the maximum spectral acceleration

If the actual value is larger than the maximum spectral acceleration, the following values are assigned

---0.2--- Resulting spectral acceleration is 55 % of the maximum

---0.2--- Resulting spectral acceleration is 65 % of the maximum

---0.2--- Resulting spectral acceleration is 75% of the maximum

---0.2--- Resulting spectral acceleration is 85 % of the maximum

---0.2--- Resulting spectral acceleration is 95 % of the maximum

Fig. 6-5: Frequency dependent logic tree used to estimate the maximum spectral acceleration for the vertical component

7 AMPLIFICATIONS AT INTERMEDIATE DEPTH LEVELS 2 AND 3

The project specified that the amplification has to be estimated for outcropping motion. The difficulty is that the concept of outcropping motion (only up-going waves) does not exist in nature and has nothing to do with real ground motion observed at elevation 2 and 3. Outcropping motion is defined by the up-going waves only:

$$2 * (\text{ground motion of the up-going wave}) / (\text{ground motion on bedrock at the surface})$$

These amplification factors are provided for the computations with SHAKE and RVT. It is, however, not possible to directly relate the non-linear ground motion at depth with the outcropping motion. There is also no direct relation to scale the non-linear result with the computations using SHAKE and RVT. Surface wave propagation and 2D or 3D effects cannot be handled by the concept of outcropping motion. However, these effects will also contribute to the up-going waves. For this reason, they will be included also in the intermediate depth levels.

7.1 Median amplification for the horizontal component

The logic trees proposed for the surface are also applied to the intermediate depth levels with a series of changes. For the RVT branches, the outcropping motion amplification is taken at the respective depth levels.

The non-linear runs provided the "within layer" ground motion at depth and not the outcropping ground motion. Therefore, the non-linear-case amplification factors have to be corrected with the available information, in order to obtain the outcropping motion amplification. Two types of ratios of motion at depth to the surface motion obtained with SHAKE and RVT can be used to scale the ground motions from the non-linear runs. However, physical phenomena between linear-equivalent and non-linear modeling might be very different. I therefore select two procedures a) and b) for the correction of the non-linear amplification factors:

- a) We can expect comparable results between RVT or SHAKE and the non-linear calculation at low level of shaking, if the ratio between incident wave and total wave-field is assumed to be the same for the different modeling schemes. What we can compute are the following ratios (at PGA of 0.4 g, site-specific and at each elevation level separately):

$$\text{Rat1} = (\text{amplification RVT}) / (\text{amplification non-linear})$$

$$\text{Rat2} = (\text{amplification SHAKE}) / (\text{amplification non-linear})$$

The ratios are a function of frequency, with the following definitions:

amplification RVT: for the outcropping motion in the base case

amplification SHAKE: for the outcropping motion

amplification non-linear: for the ground motion

With these ratios the non-linear amplification factors can be corrected so that it approximates the amplification for outcropping motion. The ratios RAT1 and RAT2 have been provided by Proseis and an example is given in Figure 7-1. It is evident that the amplification factors for outcropping motion are larger at high frequencies than the amplification factors for ground motion, due to the intrinsic attenuation of the waves in surface part of the soft sediments.

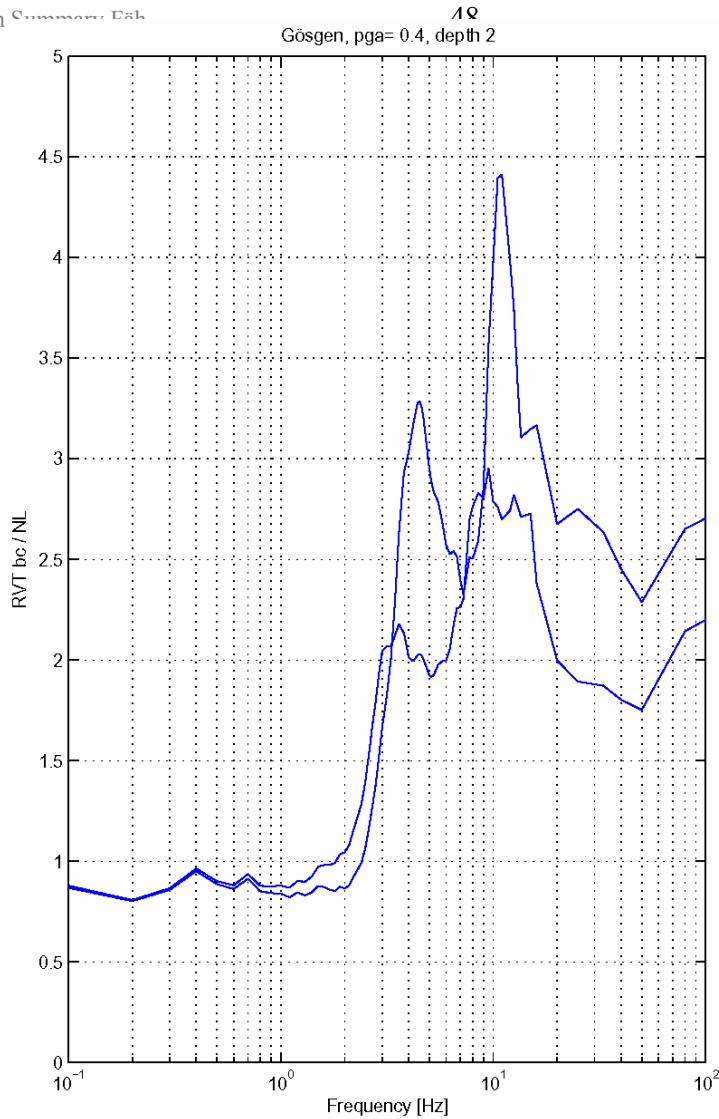


Fig. 7-1: Ratio between amplification for outcropping motion obtained with the RVT base case and amplification for ground motion obtained with the non-linear run
 PGA level is 0.4 g. The example is for the two models for site Gösgen at depth level 2.

b) For the SHAKE computations the amplification factors for ground motion and outcropping motion are available. With their ratio, we can correct the non-linear amplification factors:

$$RAT3 = (\text{SHAKE outcropping motion}) / (\text{SHAKE ground motion})$$

RAT3 is computed for each model and PGA level. If no SHAKE computations exist at a certain PGA level, the ratio from the closest PGA level is selected.

For the non-linear branches in the logic trees, the ground-motion amplification factor at depth is taken and multiplied by the factors RAT1, RAT2 and RAT3, defined above. The weight of the correction term RAT3 is taken higher, because this term does not include corrections due to different modeling techniques. The weights to the branches are as follows:

- 0.2----- apply factor RAT1
- 0.2----- apply factor RAT2
- 0.6----- apply factor RAT3

This introduces an epistemic uncertainty, due to the lack of the outcropping motion in the non-linear case.

The wave propagation effects other than vertically incident SH wave (2D-effects, inclined wave effects, PSV case) were only computed for the surface. Except for Mühleberg, all intermediate layers are in the soft sediments and the other wave propagation effects have to be taken into account also at the embedded layers. Since there are no specific computations performed concerning these wave propagation effects, no change to the scheme for the surface is proposed. For the Mühleberg case we cannot exclude that the bedrock is altered in the upper few meters, and therefore, we also keep the scheme for the surface layer. Elevation 3 for Mühleberg is located in the bedrock, and we make an exception for the weights in the branches. The weights of the branches are slightly changed when compared to the surface, as shown in Figure 7-2.

7.2 Median amplification for the vertical component

Also for the vertical component we keep the same procedure as for the surface layer (see Figure 7-3), including some modifications for the concept A and B.

For concept A, we use the same procedure as for the surface layer. The estimate for the amplification on the vertical component is obtained from the estimate of the horizontal component as follows:

$$V(\text{soil})/V_s(\text{rock}) = H_s(\text{rock})/V_s(\text{rock}) * V(\text{soil})/H(\text{soil}) * \text{Amplification}(\text{horizontal})$$

Amplification(horizontal) = $H(\text{soil})/H_s(\text{rock})$: amplification of the horizontal component at the end of each branch.

$V(\text{soil})/H(\text{soil})$: V/H-ratio for the soil

$H_s(\text{rock})/V_s(\text{rock})$: H/V-ratio for rock. The subscript "s" stands for surface layer.

The product $H_s(\text{rock})/V_s(\text{rock}) * V(\text{soil})/H(\text{soil})$ is computed with the mode summation method, exactly in the same way as described in report TP3-TN-0167, but for the layers at depth. An example of the comparison of the factors obtained at the three levels is shown in the Figure 7-4. The factors have been provided to Proseis.

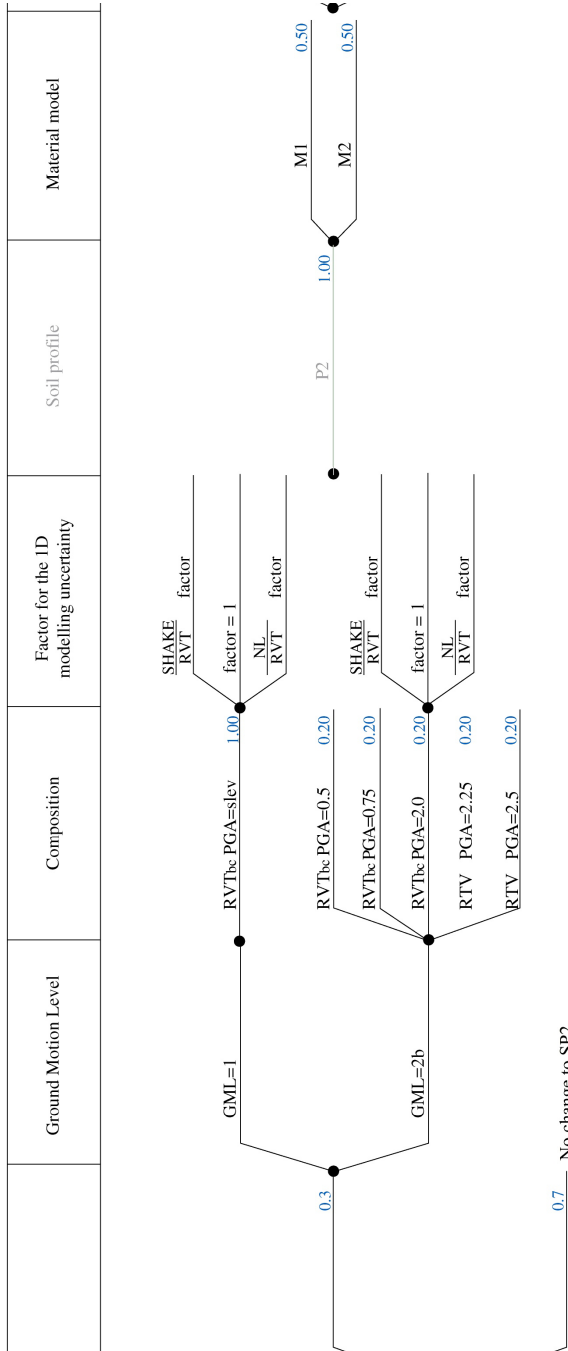
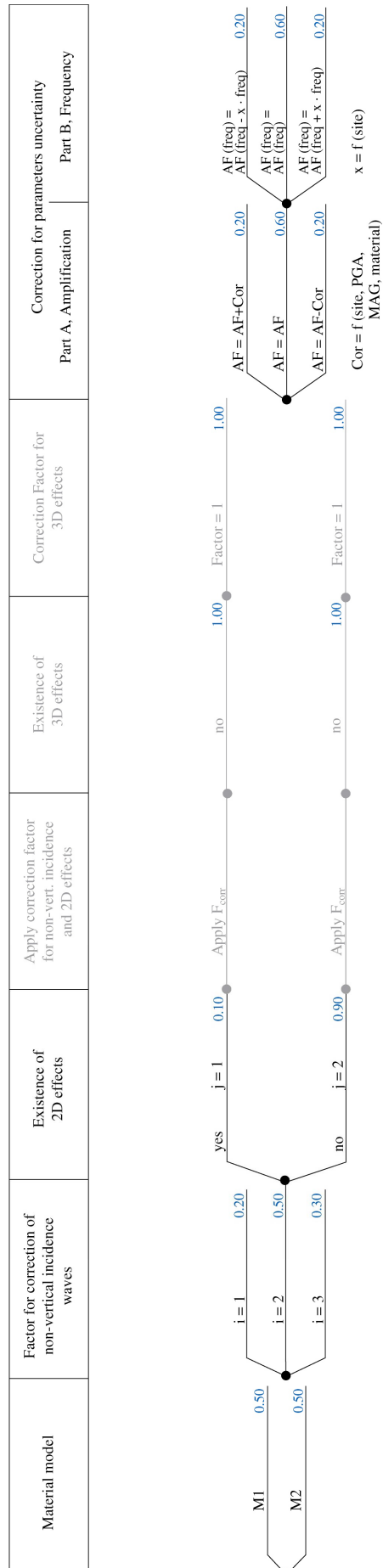


Fig. 7-2: Logic tree for NPP site Mühleberg, used to estimate the median amplification of the horiz. ground motion at the elevation level 3.

[The logic tree is cut in two parts; the start is on the left above and the continuation is shown on the right]

Site: Mühleberg

Amplification of Horizontal Ground Motion



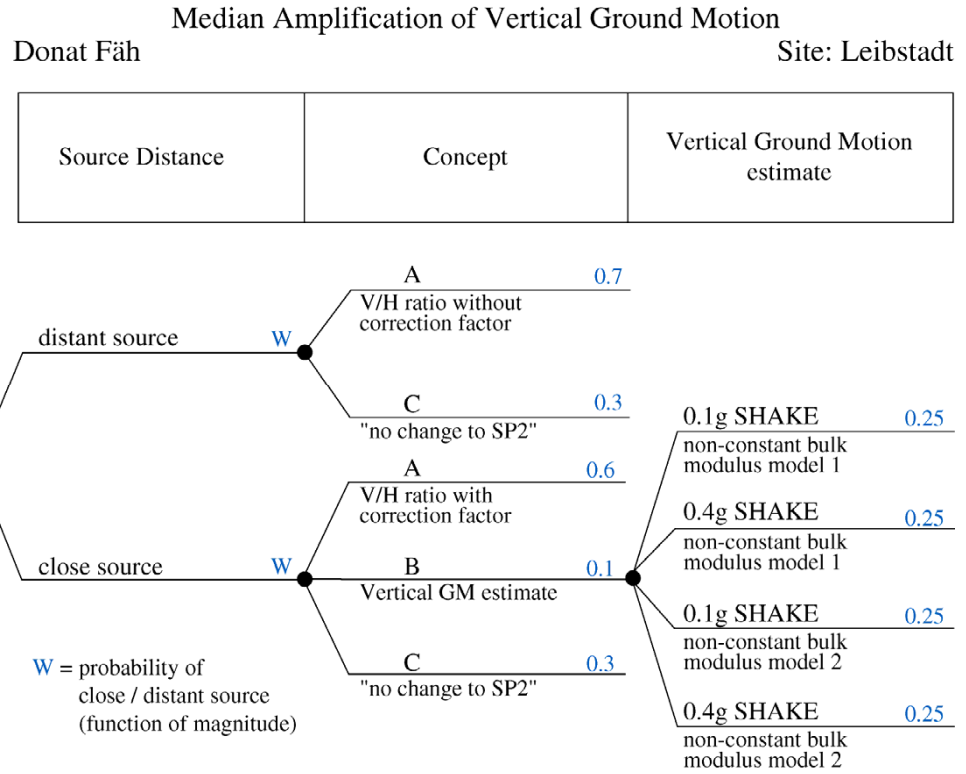


Fig. 7-3: Logic tree for NPP site Leibstadt, used to estimate the median amplification of the vertical ground motion at depth

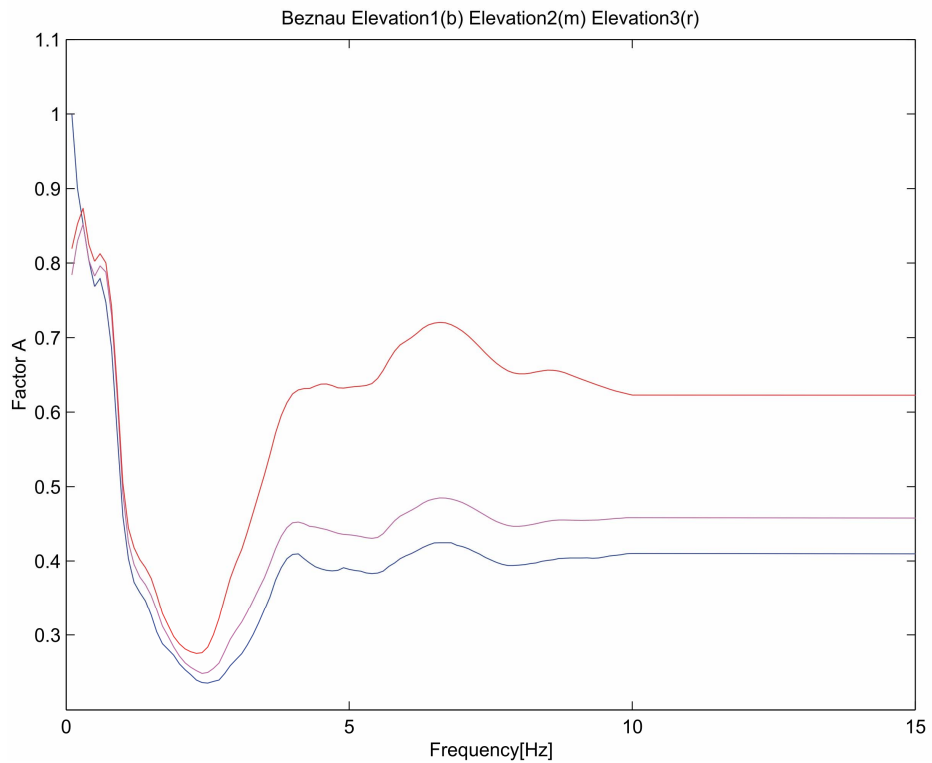


Fig. 7-4: $H_s(\text{rock})/V_s(\text{rock}) * V(\text{soil})/H(\text{soil})$ shown for the Beznau NPP site for the three elevation levels

For concept B (SHAKE branches), the computations for outcropping motion at the different elevation levels are used. Because elevation level 3 for Mühleberg is located in the bedrock, we make an exception for the weights in the branches. The weights of the branches are changed as is shown in Figure 7-5 to give more weight to the "no change to SP2" branch since Mühleberg is located in the bedrock.

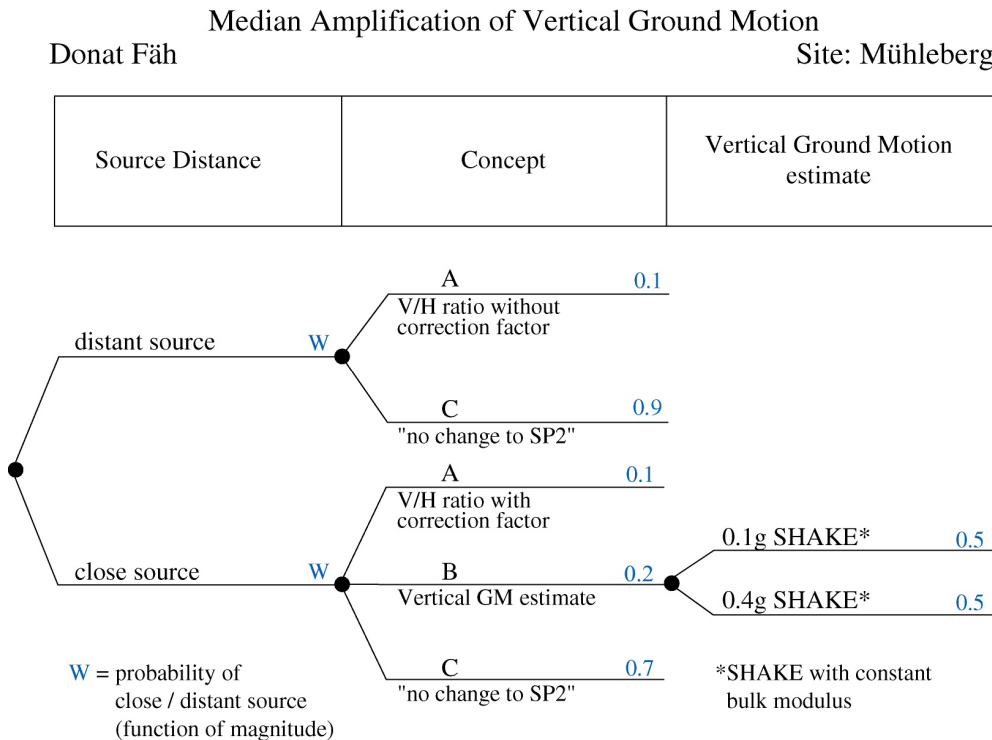


Fig. 7-5: Logic tree for NPP site Mühleberg, used to estimate the median amplification of the vertical ground motion at the elevation level 3

7.3 Aleatory variability

Aleatory variability of the ground motion amplification at depth is computed in the same way as for the surface level, assuming that aleatory variability of outcropping amplification factors are equal to the aleatory variability of the ground motion amplification.

7.4 Maximum Ground Motion

For the layers at depth the same procedure is applied as for the surface level, using the estimates of Pecker et al. (2003) for PGA at the surface. The same four spectral shapes are used. With high probability, the failure occurs in the upper 5 meters of the sediments. Failure introduces a reflecting solid liquid interface. Maximum ground motion is therefore expected to be larger at depth than at surface. This can be seen from the non-linear runs in some of the computations (Pecker's presentation "Maximum ground motion at depth" of October 20, 2003). The expected higher values at depth will be accounted for by giving different weights to the four possible spectra. The weights are provided in Figure 7-6 for the horizontal ground motion and Figure 7-7 for the vertical ground motion. The weights for the high-PGA spectra were increased compared to the surface level because the layers that may be liquefied are above the intermediate depth levels 2 and 3.

- 0.5--- $\text{MAX(PGA)}=1.0*\text{PGA}$ by Pecker et al. (2003)
 - 0.3--- Factor 1 applied to obtain the maximum spectral acceleration
 - If the actual value is larger than the maximum spectral acceleration, the following values are assigned
 - 0.2--- Resulting spectral acceleration is 55 % of the maximum
 - 0.2--- Resulting spectral acceleration is 65 % of the maximum
 - 0.2--- Resulting spectral acceleration is 75 % of the maximum
 - 0.2--- Resulting spectral acceleration is 85 % of the maximum
 - 0.2--- Resulting spectral acceleration is 95 % of the maximum
 - 0.7--- Factor 2 applied to obtain the maximum spectral acceleration
 - If the actual value is larger than the maximum spectral acceleration, the following values are assigned
 - 0.2--- Resulting spectral acceleration is 55 % of the maximum
 - 0.2--- Resulting spectral acceleration is 65 % of the maximum
 - 0.2--- Resulting spectral acceleration is 75 % of the maximum
 - 0.2--- Resulting spectral acceleration is 85 % of the maximum
 - 0.2--- Resulting spectral acceleration is 95 % of the maximum
- 0.5--- $\text{MAX(PGA)}=2.0*\text{PGA}$ by Pecker et al. (2003)
 - 0.8--- Factor 1 applied to obtain the maximum spectral acceleration
 - If the actual value is larger than the maximum spectral acceleration, the following values are assigned
 - 0.2--- Resulting spectral acceleration is 55 % of the maximum
 - 0.2--- Resulting spectral acceleration is 65 % of the maximum
 - 0.2--- Resulting spectral acceleration is 75 % of the maximum
 - 0.2--- Resulting spectral acceleration is 85 % of the maximum
 - 0.2--- Resulting spectral acceleration is 95 % of the maximum
 - 0.2--- Factor 2 applied to obtain the maximum spectral acceleration
 - If the actual value is larger than the maximum spectral acceleration, the following values are assigned
 - 0.2--- Resulting spectral acceleration is 55 % of the maximum
 - 0.2--- Resulting spectral acceleration is 65 % of the maximum
 - 0.2--- Resulting spectral acceleration is 75 % of the maximum
 - 0.2--- Resulting spectral acceleration is 85 % of the maximum
 - 0.2--- Resulting spectral acceleration is 95 % of the maximum

Fig. 7-6: Frequency dependent logic tree used to estimate the maximum spectral acceleration for the horizontal component at depth

- 0.2--- MAX(PGA)=1.0*PGA by Pecker et al. (2003)
 - 0.3--- Factor 3 applied to obtain the maximum spectral acceleration
 - If the actual value is larger than the maximum spectral acceleration, the following values are assigned
 - 0.2--- Resulting spectral acceleration is 55 % of the maximum
 - 0.2--- Resulting spectral acceleration is 65 % of the maximum
 - 0.2--- Resulting spectral acceleration is 75 % of the maximum
 - 0.2--- Resulting spectral acceleration is 85 % of the maximum
 - 0.2--- Resulting spectral acceleration is 95 % of the maximum
 - 0.7--- Factor 4 applied to obtain the maximum spectral acceleration
 - If the actual value is larger than the maximum spectral acceleration, the following values are assigned
 - 0.2--- Resulting spectral acceleration is 55 % of the maximum
 - 0.2--- Resulting spectral acceleration is 65 % of the maximum
 - 0.2--- Resulting spectral acceleration is 75 % of the maximum
 - 0.2--- Resulting spectral acceleration is 85 % of the maximum
 - 0.2--- Resulting spectral acceleration is 95 % of the maximum
- 0.8--- MAX(PGA)=2.0*PGA by Pecker et al. (2003)
 - 0.7--- Factor 3 applied to obtain the maximum spectral acceleration
 - If the actual value is larger than the maximum spectral acceleration, the following values are assigned
 - 0.2--- Resulting spectral acceleration is 55 % of the maximum
 - 0.2--- Resulting spectral acceleration is 65 % of the maximum
 - 0.2--- Resulting spectral acceleration is 75 % of the maximum
 - 0.2--- Resulting spectral acceleration is 85 % of the maximum
 - 0.2--- Resulting spectral acceleration is 95 % of the maximum
 - 0.3--- Factor 4 applied to obtain the maximum spectral acceleration
 - If the actual value is larger than the maximum spectral acceleration, the following values are assigned
 - 0.2--- Resulting spectral acceleration is 55 % of the maximum
 - 0.2--- Resulting spectral acceleration is 65 % of the maximum
 - 0.2--- Resulting spectral acceleration is 75 % of the maximum
 - 0.2--- Resulting spectral acceleration is 85 % of the maximum
 - 0.2--- Resulting spectral acceleration is 95 % of the maximum

Fig. 7-7: Frequency dependent logic tree used to estimate the maximum spectral acceleration for the vertical component at depth

8 REFERENCES

- Bay, F., Fäh, D., Malagnini, L. & Giardini, D. 2003: Spectral Shear-Wave Ground Motion Scaling for Switzerland. *Bull. Seism. Soc. Am.* 93, 414-429.
- Bozorgnia, Y. & Campell, K.W. 2002: Vertical-to-Horizontal Response Spectral Ratio and the Vertical Design Spectrum. Submitted to *Earthquake Spectra*, March 8, 2002.
- Pecker, A., Koller, M. & Studer, J.: Evaluation of Maximum Ground Motions; Report Nr.2, 14.04.2003 (PEGASOS TP3-TN-0354)
- PEGASOS TP3-ASW-0024: Hölker, A.: Matlab software package and databases for the computation of the SP3 / site amplification models.
- PEGASOS TP3-TB-0048: Pelli, F. 2002: Nonlinear Site Response Analyses for Beznau, Gösigen, Leibstadt.
- PEGASOS TP3-TN-0166: Koller, M. 2002: PEGASOS Soil Profiles for Supporting Computations.
- PEGASOS TP3-TN-0167: Fäh, D. 2002: Spectral Amplification for SH-and PSV waves at sites Beznau Gösigen and Leibstadt.
- PEGASOS TP3-TN-0168: Fäh, D. 2002: Two dimensional modelling of SH-wave amplification. Rev. 1.
- PEGASOS TP3-TN-0186: Bard, P.Y. 2002: 2D SH computations for the Leibstadt nuclear power plant site Amplification factors in the low and high strain cases.
- PEGASOS TP3-TN-0205: Pecker, A. 2002: Gösigen Nuclear Power Plant Site, True Nonlinear Site Response Analysis.
- PEGASOS TP3-TN-0212: Travasarou, T. 2002: Visualisation and Comparison of RVT and SHAKE Results.
- PEGASOS TP3-TN-0250: Tinic, S. 2002: Overview of the supporting computations.
- PEGASOS TP3-TN-0283: Hölker, A.: Comparison of Bard's and Fäh's P-SV computations (SH case).
- PEGASOS TP3-TN-0354: Pecker, A. 2003: Evaluation of Maximum Ground Motions.
- PEGASOS TP3-TN-0359: Rippberger, J. & Fäh, D. 2003: Maximum Recorded Horizontal and Vertical Ground Motions.
- PEGASOS TP3-TN-0401: Hölker, A.: Summarizing the SP3 site effect models to Soil hazard Input Files (SIFs).

APPENDIX 1 EG3-HID-0052 SITE AMPLIFICATION AT THE SURFACE AND EMBEDDED LAYER DEPTHS FINAL MODEL D. FÄH

A1.1 Introduction

This document describes the implementation of Donat Fäh's models of site amplification at the surface, mean and maximum building depths (Table 1) as well as his assessment of maximum possible ground motions at the four Swiss NPP sites: Beznau, Gösgen, Leibstadt and Mühleberg. The purpose of this document is to translate the expert's evaluation of amplification factors into a Soil hazard Input File (SIF) for the hazard computation software (SOILHAZP) and to provide the expert with the necessary information to review the results of his model.

The implementation of Donat Fäh's model is based on the July 11th 2003 (surface) and November 17th (embedded layers) versions of his elicitation summary (EG3-ES-0041) and additional clarifications. It includes the post WS5 modifications of the maximum ground motion assessment, dated Feb. 4th 2004, and replaces EG3-HID-0049 .

The following document and software are directly linked to this HID:

- TP3-TN-0401: A technical note describing the computational steps performed to create the soil hazard input files (SIFs)
- TP3-ASW-0024: The software used to implement the SP3 models

This HID consists of three sub-sections:

- A description of the computational steps leading to the development of amplification factor spectra and their associated aleatory variabilities for each site and combination of magnitudes, input PGAs and ground motion types.
- A description of the expert's assessment of maximum ground motion spectra.
- A summarized description of creation of SIFs for site amplification, the associated aleatory variability. A detailed description is available in the technical note TP3-TN-0401.
- The generalized logic tree for horizontal ground motion at the surface.

The implementation of Donat Fäh's model was done by the SP3 TFI Team at Proseis using Matlab R13. The complete implementation is archived as TP3-ASW-0024. It consists of a software module and a database.

Tab. A-1: Mean and maximum building depth for the four Swiss NPP sites

	Beznau	Gösgen	Leibstadt	Mühleberg
Mean building depth	6 m	5 m	5 m	7 m
Max. building depth	15 m	9 m	10 m	14 m

A1.2 Site amplification and its aleatory variability

In this section the key-elements of Donat Fäh's model are outlined, the crucial aspects are detailed, and the results are illustrated by means of a single example figure per computational step. Figures showing the results for all cases and sites are available as an electronic appendix in PDF format. Generally Donat Fäh's models are defined only for frequencies larger than 0.45 Hz, although for technical reasons site amplification factors for frequencies as low as 0.1 Hz are shown. The logic tree architecture is not reviewed here, since it is detailed in the elicitation summary. A displayed of the generalized logic tree for horizontal ground motion, however, is given at the end of this HIS. Finally it shall be noticed, that the results given in this section are an intermediate product, since they are summarized to discrete fractiles and associated with spectral accelerations before being used as an input for the soil hazard computations.

A1.2.1 Amplification of horizontal ground motion

The characteristic elements of Donat Fäh's model are:

- Depending on the selection of site, earthquake magnitude and PGA level (on rock) a so-called ground motion level is defined. Depending on the value of this ground motion level, different combinations of alternative approaches (NL and RVT at different PGA levels) are then selected for use.
- In the second level of the logic tree, alternative factors are defined to account for the uncertainty in the 1D modeling. Depending on the approach (RVT or NL) underlying a particular branch, these uncertainty factors are ratios of SHAKE to RVT, NL to RVT, SHAKE to NL, or between the NL models of Pelli and Pecker.
- In the third and fourth levels of the logic tree, all possible combinations of velocity profiles and material models for the considered site are detailed.
- The 5th level defines three alternatives to account for non-vertical incidence of waves.
- In the 6th level the existence of 2D effects is considered. Branches on which 2D effects are considered to be relevant become more detailed on two subsequent logic tree levels, as 3D effects are then considered.
- In the case of embedded layer depths and NL simulations being used for a particular branch, three kind of ratios are applied to correct the "within" (total) motion, which was modeled in the NL simulations, to "outcrop" (only the up-going wave) motion, which is requested by the project. The three kind of ratios, which are applied, are (1) $RVT_{\text{outcrop motion}} / NL_{\text{within motion}}$, (2) $SHAKE_{\text{outcrop motion}} / NL_{\text{within motion}}$, and (3) $SHAKE_{\text{outcrop motion}} / SHAKE_{\text{within motion}}$.
- The two final levels account for the parametric uncertainty. In the last but one level the amplification factors are shifted in three ways and in the last level the frequency is shifted in three ways. This results in a smearing filter which is applied to all amplification factors.
- For the case of Mühleberg, there is a "no site effects" branch considered as an alternative, which is by-passing the entire model for site effects.

Any resulting amplification factor is based on either RVT (outcrop motion) or NL (within motion) simulations, to which factors for the 1D modeling uncertainty, non-vertical incidence waves, 2D effects, 3D effects, and parametric uncertainty have been applied. In the case of NL simulations also correction factors for outcropping motion have been applied.

The differences between the site effect models for the surface and embedded layer depths are the "outcrop motion" to "within motion" ratios, which are applied to the NL simulations and modified weights of some branch tips.

The example in Figure A-1 shows the assessment of alternative amplification factors considered for the mean building depth at NPP Beznau for the case of a magnitude 6 earthquake with PGA on rock of 1.5g. For corresponding figures showing the results for all other cases and sites see the *Faeh.AF AVar.<site>.HM<depth>.pdf* files in the appendix. Figure A-2 shows the weighted arithmetic mean amplification factors for mean building depth in Beznau as function of PGA on rock and frequency. For the other sites and magnitudes see the *Faeh.SiteModAF.<site>.HM<depth>.pdf* files.

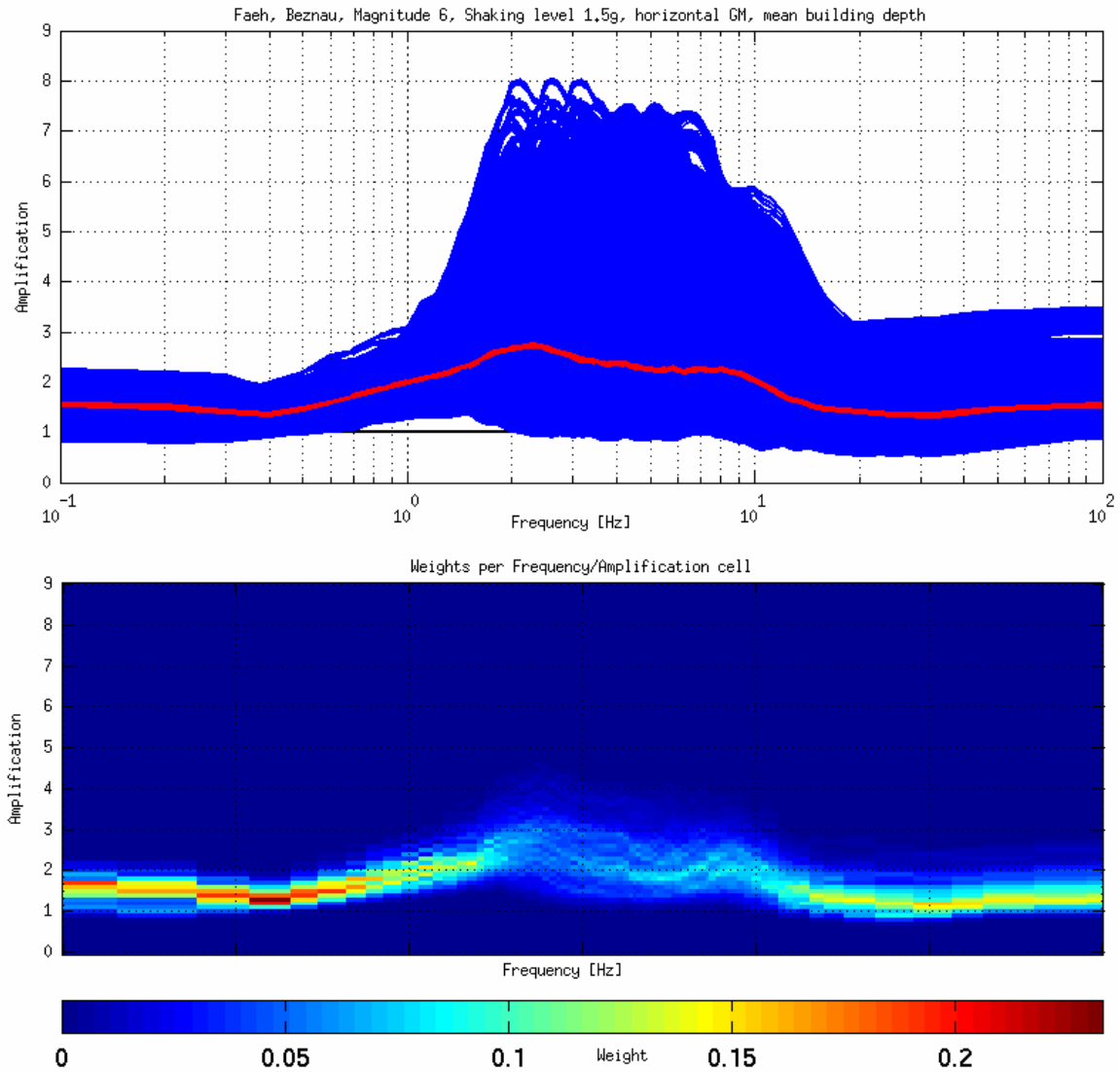


Fig. A-1: Site amplifications factors for horizontal ground motion at the mean building depth of NPP Beznau for the case of a magnitude 6 earthquake with PGA on rock of 1.5 g

The upper plot shows the alternative amplification factors (blue curves) and their weighted mean (red curve). The lower plot shows the distribution of weights in the amplification-frequency space. Corresponding plots are available for all sites and cases in the appendix: See the *Faeh.AF AVar.<site>.HM<depth>.pdf* files.

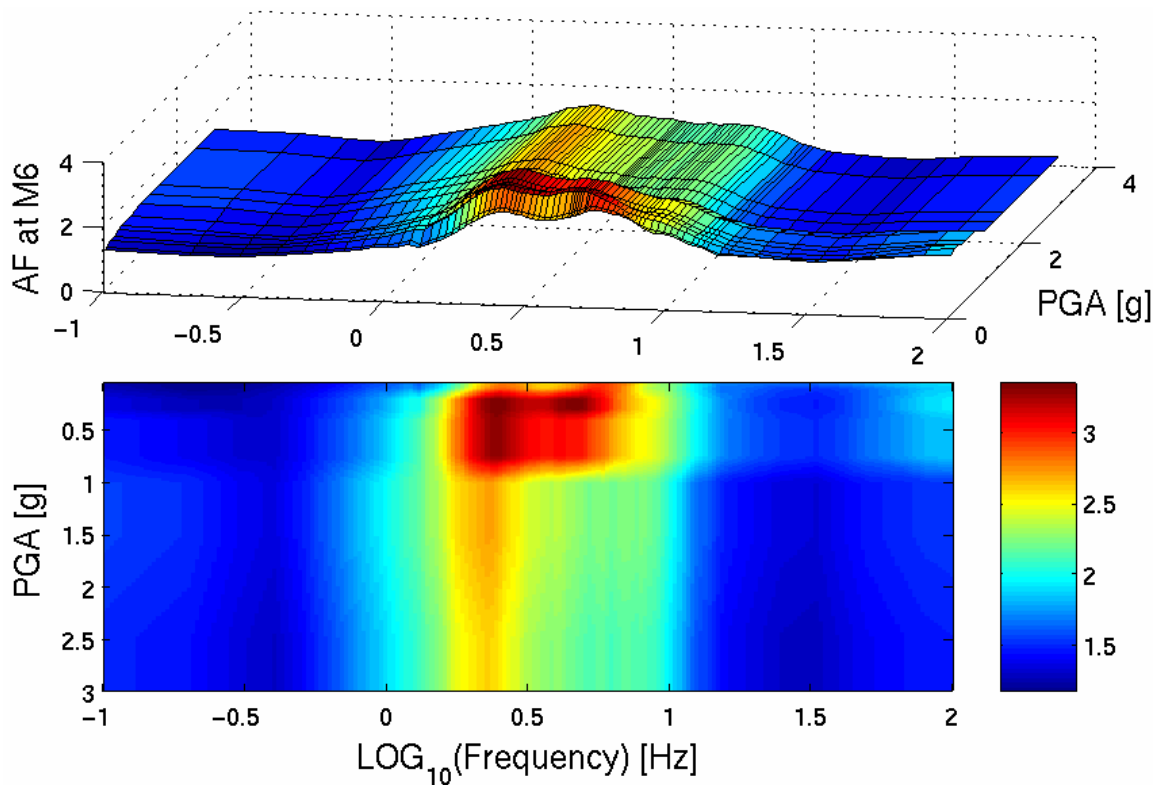


Fig. A-2: Weighted arithmetic mean amplification factors (AF as function of PGA on rock and frequency) for horizontal ground motion of a magnitude 6 scenario at mean building depth of NPP Beznau

Corresponding plots are available for all sites and cases in the appendix: See the *Faeh.SiteModAF.<site>.HM<depth>.pdf* files.

A1.2.2 Aleatory variability of amplification of horizontal ground motion

Donat Fäh develops the aleatory variability of the amplification of horizontal ground motion using a logic tree parallel to that for the site amplification. The aleatory variability for a particular branch is the sum of the variabilities of the base model (RVT or NL) and a combined uncertainty due to non-vertical incidence waves and 2D effects. The aleatory variability for the surface layer and embedded layers are considered to be equal.

Figure A-3 shows an assessment of the aleatory variability, corresponding to the site amplification case shown in figure 1. For the results of all other cases and sites please see the *Faeh.AF_AVar.<site>.HM<depth>.pdf* files in the appendix. For the plots of mean aleatory variability corresponding to that in figure 2, see the *Faeh.SiteModAVar.<site>.HM<depth>.pdf*

A1.2.3 Amplification of vertical ground motion

The development of amplification factors for vertical ground motion is based on two alternatives: "close" or "distant" hypocenter. In both cases the possibilities of "no site effects" and V/H ratios applied to the model for amplification of horizontal ground motion are considered. In case of a nearby hypocenter the SHAKE simulations for amplification of vertical ground motion are also considered as an alternative. The V/H ratios were supplied by D. Fäh and derived for the embedded layers as described in TP3-TN-0167 for the surface case. The site effects model for the surface and embedded layers differ in the V/H ratios, the motion type of the SHAKE simulations (surface and outcrop), and in some weights in the Mühleberg model.

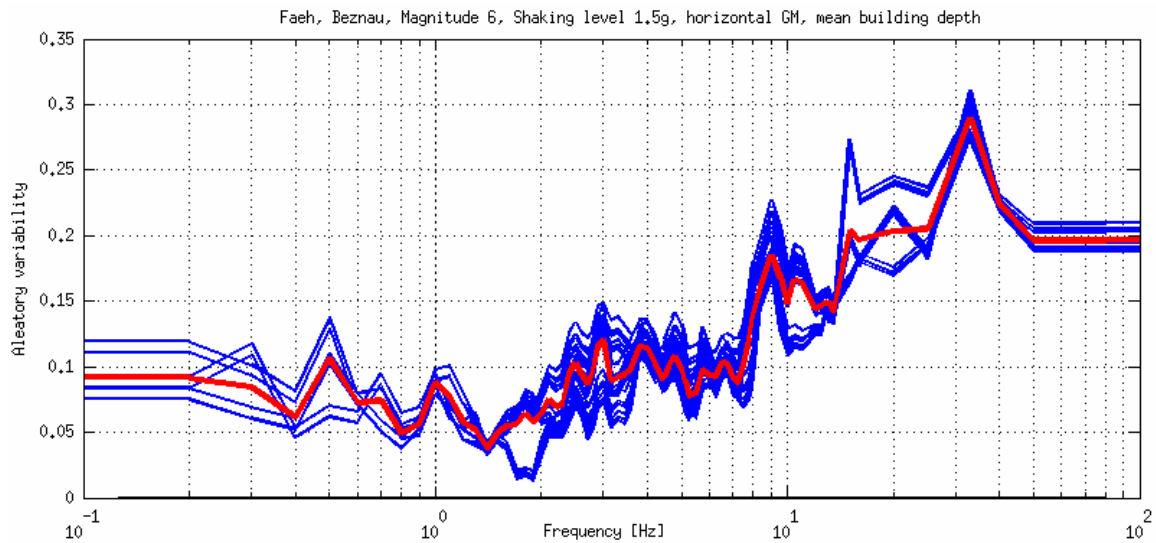


Fig. A-3: Aleatory variability of amplifications factors for horizontal ground motion at the mean building depth of NPP Beznau for the case of a magnitude 6 earthquake with PGA on rock of 1.5 g

The blue curves correspond to the alternative aleatory variabilities and the red curve is the weighted mean aleatory variability. Corresponding plots are available for all sites and cases in the appendix: See *Faeh.AF_AVar.<site>.HM<depth>.pdf* files in the appendix.

Figures showing the assessment of amplification factors for vertical ground motion (corresponding to Figure A-1) are available in the files *Faeh.AF_AVar.<site>.VM<depth>.pdf*. Figures showing mean site amplification factors as function of frequency and PGA on rock (corresponding to Figure A-2) are available in the *Faeh.SiteModAF.<site>.VM<depth>.pdf* files.

A1.2.4 Aleatory variability of amplification of vertical ground motion

The aleatory variability of vertical ground motion is developed in the same logic tree as the amplification factors. In case of "no site effects" the aleatory variability (of the site effects) is zero. In case of applying V/H ratios, the aleatory variability of vertical ground motion is equal to that of the horizontal ground motion. In the case of P-wave SHAKE models the aleatory variability is equal to that associated with the particular SHAKE simulation. Finally, there are no differences in the aleatory variability for the embedded layers and the surface layer.

Plots of the assessment of aleatory variability of vertical ground motion are available in *Faeh.AF_AVar.<site>.VM<depth>.pdf* and figures showing mean aleatory variability as function of frequency and PGA on rock are given in the *Faeh.SiteModAVar.<site>.VM<depth>.pdf* files.

A1.2.5 Parameter ranges

Donat Fähr's model of horizontal and vertical ground motion has been computed for the input PGAs (on rock) shown in Table A-2 and magnitudes 5, 6 and 7. All SP3 expert models are computed for a set of 76 spectral frequencies. These frequencies are 0.1, 0.2, 0.3, 0.4, 0.5, 0.6, 0.7, 0.8, 0.9, 1, 1.1, 1.2, 1.3, 1.4, 1.5, 1.6, 1.7, 1.8, 1.9, 2, 2.1, 2.2, 2.3, 2.4, 2.5, 2.6, 2.7, 2.8, 2.9, 3, 3.15, 3.3, 3.45, 3.6, 3.8, 4, 4.2, 4.4, 4.5, 4.6, 4.7, 4.8, 5, 5.1, 5.25, 5.5, 5.75, 6, 6.25, 6.5, 6.75,

7, 7.25, 7.5, 7.75, 8, 8.5, 9, 9.5, 10, 10.5, 11, 12, 12.5, 13, 13.5, 15, 16, 20, 25, 33, 40, 50, 80 and 100 Hz. However, Donat Fäh's models are not applicable for frequencies below 0.45 Hz.

Tab. A-2: PGAs (on rock) for which Donat Fäh's model has been computed

PGA	Horizontal ground motion												Vertical ground motion														
	Beznau			Gösgen			Leibstadt			Mühleberg			Beznau			Gösgen			Leibstadt			Mühleberg					
[g]	srf	d1	d2	srf	d1	d2	srf	d1	d2	srf	d1	d2	srf	d1	d2	srf	d1	d2	srf	d1	d2	srf	d1	d2	srf	d1	d2
0.05	x	x	x	x	x	x	x	x	x	x	x	x	x	x	x	x	x	x	x	x	x	x	x	x			
0.10	x	x	x	x	x	x	x	x	x	x	x	x	x	x	x	x	x	x	x	x	x	x	x	x			
0.20	x	x	x	x	x	x	x	x	x	x	x	x	x	x	x	x	x	x	x	x	x	x	x	x			
0.30	x	x	x	x	x	x	x	x	x	x	x	x	x	x	x	x	x	x	x	x	x	x	x	x			
0.40	x	x	x	x	x	x	x	x	x	x	x	x	x	x	x	x	x	x	x	x	x	x	x	x			
0.50	x	x	x	x	x	x				x	x	x	x	x	x	x	x					x	x	x			
0.75	x	x	x	x	x	x	x	x	x	x	x	x	x	x	x	x	x	x	x	x	x	x	x	x			
1.00	x	x	x	x	x	x	x	x	x	x	x	x	x	x	x	x	x	x	x	x	x	x	x	x			
1.25	x			x			x			x						x						x	x	x			
1.50	x	x	x	x	x	x	x	x	x	x	x	x	x	x	x	x	x	x	x	x	x	x	x	x			
2.50	x	x	x	x	x	x	x	x	x	x	x	x			x			x				x					
3.00	x			x			x			x																	

A1.3 Maximum ground motion at the surface

A1.3.1 Horizontal ground motion

Donat Fäh developed four alternative spectra for maximum horizontal ground motion each associated with a certain weight. These spectra are based on two alternative synthetic spectra, which were derived from observed spectra in TP3-TN-0359, and on the site-specific, but two times differently scaled maximum PGA values modeled by A. Pecker (TP3-TN-0354).

Each of the four spectra is subdivided into 11 separate spectra, which range from 50 % to 100 % of the original amplitudes and which are associated weights increasing from 1/66 to 11/66 of the weight of the original spectra.

Figure A-4 shows the alternative maximum ground motion spectra for NPP Beznau and the horizontal component as an example. Figure A-5 shows the corresponding distribution of weights for 4 Hz. Figures showing the maximum (horizontal and vertical) ground motions for all sites are available in the appendix in the files *Faeh.MaxGM.<site>.HM.pdf*.

A1.3.2 Vertical ground motion

The development of alternative spectra for maximum vertical ground motion correspond to that of horizontal ground motion except that the shape of the synthetic spectra is different. As for the horizontal case, figures showing the maximum ground motions for all sites are available in the appendix in *Faeh.MaxGM.<site>.VM.pdf*.

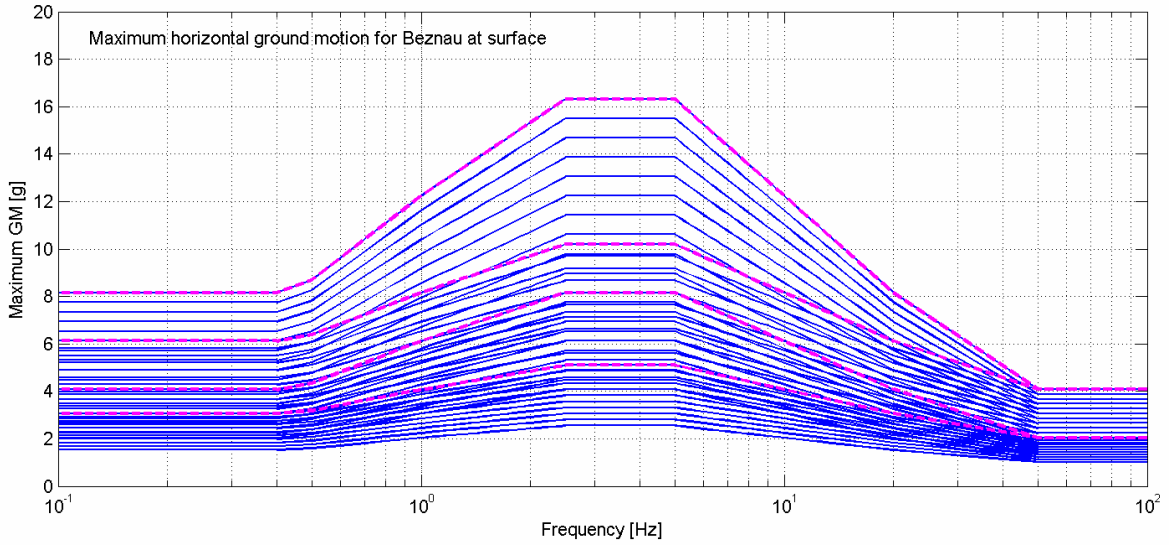


Fig. A-4: Alternative maximum ground motion spectra for NPP Beznau

Four basic spectra, which are indicated by dashed magenta lines, have been defined in D. Fäh's elicitation summary. Each of the four basic spectra is subdivided into 11 separate spectra, which range from 50 % to 100 % of the original amplitudes. Corresponding weights are shown in figure 5 for the 4 Hz case.

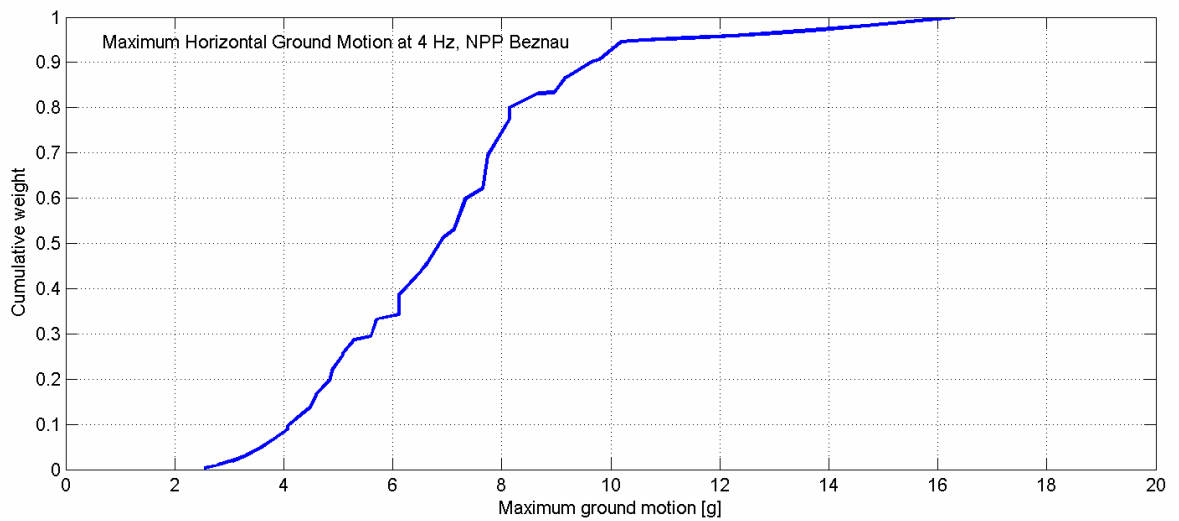


Fig. A-5: Distribution of alternative maximum horizontal ground motion amplitudes at 4 Hz for NPP Beznau

A1.4 Soil hazard input files (SIFs)

The compilation of SIFs of the site amplification factors and their aleatory variability requires two computational steps, whereas the results of maximum ground motion assessment are used directly as shown in figures 4 and 5. The two computational steps are firstly the association of site amplification factors and their aleatory variability with spectral accelerations of the underlying input motions, and secondly summarizing site amplification and variability to a set of discrete fractiles. Both steps are outlined below and described in detail in the technical note TP3-TN-0401.

A1.4.1 Associating site amplification factors with input spectral accelerations

The amplification factors and their aleatory variability (Section 2) are modeled for a set of input shaking levels (PGA on rock), a set of magnitudes, and a set of frequencies. In order to apply them to the rock hazard results, which are modeled for different spectral accelerations on rock and combinations of magnitudes and distances, the amplification factors must be associated with a spectral acceleration corresponding to the particular input shaking level (PGA) and considered frequency. The spectral acceleration is derived from the spectral shape of the input motion, which underlies the simulation of the amplification factors (figures 1 and 2 in TP3-TN-0401). In this first step, every single amplification factor is assigned a spectral acceleration (on rock) to which it can be applied.

A1.4.2 Summarizing epistemic uncertainty

The epistemic uncertainty in the expert's assessments of site amplification and aleatory variability is expressed by the branch tips and weights. For the soil hazard computations these branch tips are summarized to 17 discrete fractiles of both site amplification and aleatory variability, which is necessary in order to interpolate the data for any spectral acceleration and magnitude occurring in the rock hazard results. By using discrete fractiles no assumptions are made regarding the shape of the distribution of epistemic uncertainties. The 17 fractiles used are: 0.13 %, 0.62 %, 2.28 %, 5 %, 10 %, 20 %, 30 %, 40 %, 50 %, 60 %, 70 %, 80 %, 90 %, 95 %, 97.72 % (2 sigma), 99.38 % (2.5 sigma), and 99.87 % (3 sigma).

For the soil hazard computations these fractiles are associated with a weight and are considered as alternative models in the same way, as the original results from the branch tips represent alternative models each of which associated a weight.

A1.4.3 Plots of the soil hazard input files

Figure A-6 shows an example of the SIF of site amplification for horizontal ground motion of 4 Hz at Beznau at mean building depth. Plots showing the SIFs for site amplification and aleatory variability in all cases (sites and spectral frequencies) are available as PDF files in the appendix: *Faeh.SIFaf.<site>.<motion-depth>.pdf* and *Faeh.SIFavar.<site>.<motion-depth>.pdf*

A1.5 Logic tree for horizontal ground motion

Figure A-7 shows the generalized logic tree structure for horizontal ground motion at all sites. The structure applies to all sites, however for Mühleberg there is an additional "no change" branch, i.e. a soil amplification factor of 1, bypassing the entire model with a certain weight.

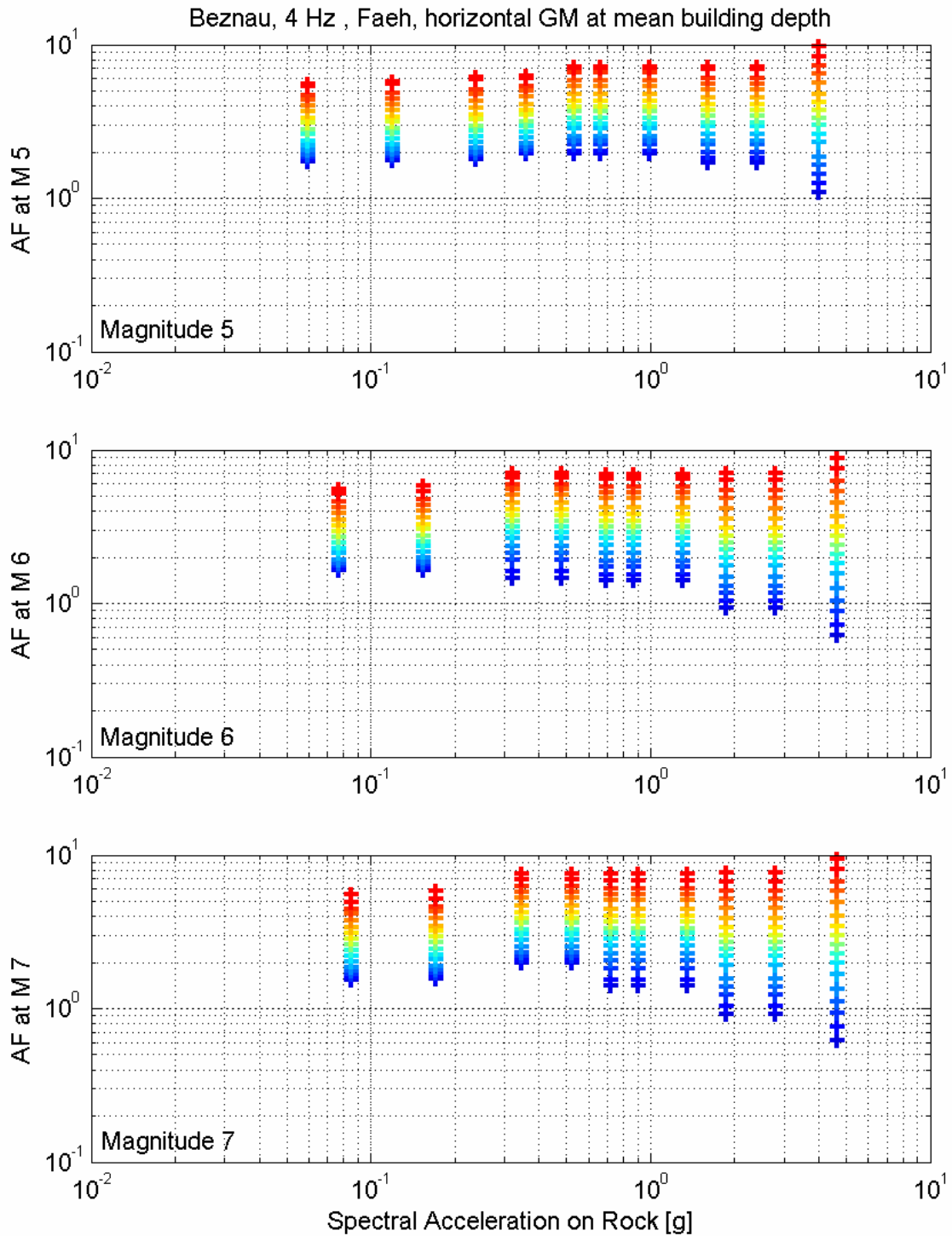
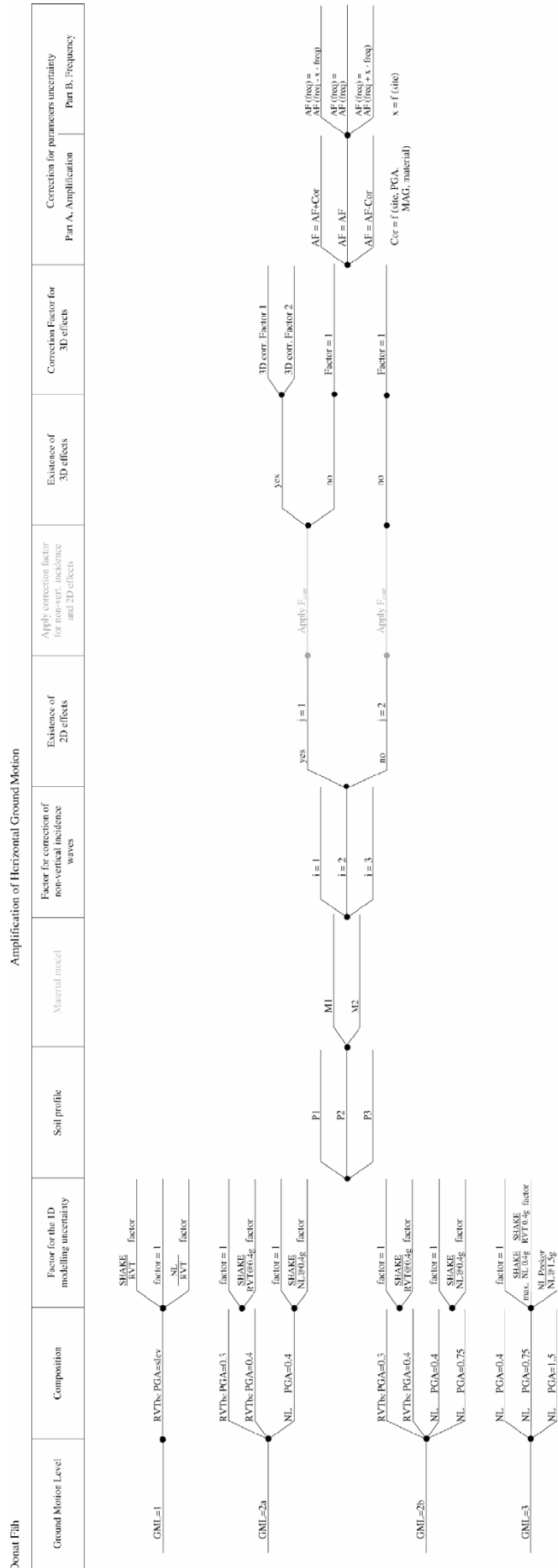


Fig. A-6: Summarized model of site amplification factors for ground motion of 4 Hz at mean building depth at NPP Beznau and earthquake magnitudes 5, 6 and 7

The crosses represent the results of the expert model after summarizing the epistemic uncertainty to 17 fractiles. The color-coding corresponds to these fractiles. Linear interpolation and nearest neighbor extrapolation respectively will be performed in the hazard software to obtain amplification factors for any spectral acceleration on rock and any considered earthquake magnitude. The full set of figures is available in the appendix in the files *Faeh.SIFaf.<site>.<motion-depth>.pdf* and *Faeh.SIFavar.<site>.<motion-depth>.pdf*.

Fig. A-7: General logic tree for horiz. ground motion

A feature of Donat Fähr's logic tree model is, that there are four different entry points depending on the ground motion level being considered. Moreover, but only for Mühleberg there is an additional "no change" branch bypassing the entire model with a certain weight.



A1.6 Appendix

The appendix is available only in electronic form on CD-ROM. All figures are stored as PDF files. The files are named according to the convention: *<expert>.<content>.<site>.<motion><depth>.pdf*. Contents are *AF_AVAR* (assessment of site amplification and aleatory variability), *SiteModAF* (mean site amplification factors), *SiteModAvar* (mean aleatory variability), *SIFaf* (amplification factors as input to the soil hazard computations), *SIFavar* (parameterized aleatory variability as input to the soil hazard computations), and *MaxGM* (maximum ground motion, also input to the soil hazard computations). Motions are *HM* for horizontal ground motion and *VM* for vertical ground motion. Depth codes are *surf* for surface, *d1* for mean building depth and *d2* for the maximum building depth.

Part III:

Site Response Characterisation, Elicitation Summary

Prof. Dr. Alain Pecker

Géodynamique et Structure,
Bagnaux – France

Probabilistische Erdbeben-Gefährdungs-Analyse für die KKW-Stand Orte
in der Schweiz (PEGASOS)

SP3 Site Response Characterisation

Elicitation Summary

Alain Pecker

Géodynamique et Structure,
Bagnex – France



TABLE OF CONTENTS

TABLE OF CONTENTS	1
LIST OF TABLES	4
LIST OF FIGURES	5
1 INTRODUCTION	7
2 MEDIAN AMPLIFICATION OF HORIZONTAL GROUND MOTION	9
2.1 Approach	9
2.2 Logic Tree Structure	10
2.3 Model Evaluations Common to All Sites	11
2.3.1 SHAKE and RVT runs	11
2.3.2 Non-linear calculations of site amplification	13
2.3.3 Magnitude dependence of site amplification	13
2.3.4 Effect of inclined waves	15
2.3.5 2D effects	15
2.3.6 3D effects	15
2.4 Beznau	16
2.4.1 Logic Tree for Beznau	16
2.4.2 Site-Specific Model Evaluations	17
2.4.2.1 Alternative velocity profiles	17
2.4.2.2 Alternative non-linear properties	17
2.5 Gösgen	17
2.5.1 Logic Tree for Gösgen	17
2.5.2 Site-Specific Model Evaluations	19
2.5.2.1 Alternative non-linear properties	19
2.6 Leibstadt	20
2.6.1 Logic Tree for Leibstadt	20
2.6.2 Site-Specific Model Evaluations	21
2.6.2.1 Alternative velocity profiles	21
2.6.2.2 Alternative non-linear properties	21
2.6.2.3 2D amplification	21
2.7 Mühleberg	22
2.7.1 Logic Tree for Mühleberg	22
2.7.2 Site-Specific Model Evaluations	22
2.7.2.1 Alternative non-linear properties	22
3 MEDIAN AMPLIFICATION OF VERTICAL GROUND MOTION	25
3.1 Approach	25
3.2 Logic Tree Structure	25
3.3 Model Evaluations Common to All Sites	25
3.4 Beznau	26
3.4.1 Logic Tree for Beznau	26
3.4.2 Site-Specific Model Evaluations	26
3.5 Gösgen	27
3.5.1 Logic Tree for Gösgen	27
3.5.2 Site-Specific Model Evaluations	27

3.6	Leibstadt	27
3.6.1	Logic Tree for Leibstadt	27
3.6.2	Site-Specific Model Evaluations	27
3.7	Mühleberg	28
3.7.1	Logic Tree for Mühleberg	28
3.7.2	Site-Specific Model Evaluations	29
4	ALEATORY VARIABILITY OF HORIZONTAL GROUND MOTION	31
4.1	Approach	31
4.2	Logic Tree Structure	31
4.3	Evaluations Common to All Sites	31
4.4	Beznau	31
4.4.1	Logic Tree for Beznau	31
4.4.2	Site-Specific Model Evaluations	31
4.5	Gösgen	32
4.5.1	Logic Tree for Gösgen	32
4.5.2	Site-Specific Model Evaluations	32
4.6	Leibstadt	33
4.6.1	Logic Tree for Leibstadt	33
4.6.2	Site-Specific Model Evaluations	33
4.7	Mühleberg	33
4.7.1	Logic Tree for Mühleberg	33
4.7.2	Site-Specific Model Evaluations	33
5	ALEATORY VARIABILITY OF VERTICAL GROUND MOTION	35
5.1	Approach	35
5.2	Logic tree structure	35
5.3	Evaluations common to all sites	35
5.4	Beznau	35
5.4.1	Logic Tree for Beznau	35
5.5	Gösgen	36
5.5.1	Logic Tree for Gösgen	36
5.6	Leibstadt	37
5.6.1	Logic Tree for Leibstadt	37
5.7	Mühleberg	37
5.7.1.	Logic Tree for Mühleberg	37
6	MAXIMUM GROUND MOTIONS	39
6.1	Horizontal Component	39
6.1.1	Evaluation of Proponent Models	39
6.1.1.1	Maximum peak ground acceleration	39
6.1.1.2	Response spectra	40
6.1.2	Logic Tree Structure	40
6.1.3	Weights for Maximum Ground Motions	43
6.2	Vertical Component	43

7	GROUND MOTION AT DEPTH	45
7.1	Median amplification of horizontal ground motion	45
7.2	Median amplification of vertical ground motion	47
7.3	Aleatory variability of horizontal ground motion	47
7.4	Aleatory variability of vertical ground motion	47
7.5	Maximum horizontal ground motion	48
7.6	Maximum vertical ground motion	48
8	REFERENCES	49
APPENDIX 1	EG3-HID-0051 SITE AMPLIFICATION AT THE SURFACE AND EMBEDDED LAYER DEPTHS FINAL MODEL A. PECKER	51
A1.1	Introduction	51
A1.2	Site amplification and its aleatory variability	52
A1.2.1	Amplification of horizontal ground motion	52
A1.2.2	Aleatory variability of amplification of horizontal ground motion	52
A1.2.3	Amplification of vertical ground motion	54
A1.2.4	Aleatory variability of amplification of vertical ground motion	54
A1.2.5	Parameter ranges	54
A1.3	Maximum ground motion at the surface	55
A1.3.1	Horizontal ground motion	55
A1.3.2	Vertical ground motion	55
A1.4	Soil hazard input files (SIFs)	55
A1.4.1	Associating site amplification factors with input spectral accelerations	56
A1.4.2	Summarizing epistemic uncertainty	56
A1.4.3	Plots of the soil hazard input files	56
A1.5	Logic tree for horizontal ground motion	56
A1.6	Appendix	57

LIST OF TABLES

Tab. 1:	Maximum peak ground accelerations of the NPP sites according to Pecker's and Betbeder's models	39
Tab. 2:	First three theoretical natural frequencies of the NPP sites	40
Tab. 3:	Mean and maximum building depths for the NPP sites	45
Tab. A-1:	Mean and maximum building depth for the four Swiss NPP sites	51

LIST OF FIGURES

Fig. 1:	Generic logic tree for mean horizontal motion	10
Fig. 2:	Example of interpolation – Gösgen site, frequency 1.3 Hz	13
Fig. 3:	Effect of magnitude on amplification factors – Gösgen site – 0.75 g	14
Fig. 4:	Effect of magnitude on amplification factors – Gösgen site – 0.40 g	14
Fig. 5:	Effect of magnitude on amplification factors – Gösgen site – 0.10 g	15
Fig. 6:	Logic Tree for Beznau	16
Fig. 7:	Mobilized friction angle versus pga – Beznau	17
Fig. 8:	Logic tree fro Gösgen	18
Fig. 9:	Mobilized friction angle versus pga – Gösgen-Material 2	19
Fig. 10:	Mobilized friction angle versus pga – Gösgen-Material 1	19
Fig. 11:	Logic Tree for Leibstadt	20
Fig. 12:	Mobilized friction angle versus pga – Leibstadt-Material 2	21
Fig. 13:	Mobilized friction angle versus pga – Leibstadt-Material 1	22
Fig. 14:	Logic Tree for Mühleberg	23
Fig. 15:	Mobilized friction angle versus pga – Mühleberg-Material 2	24
Fig. 16:	Mobilized friction angle versus pga – Mühleberg -Material 1	24
Fig. 17:	Logic Tree with median site amplification for vertical ground motion – Beznau	26
Fig. 18:	Logic Tree with median site amplification for vertical ground motion – Gösgen	27
Fig. 19:	Logic Tree with median site amplification for vertical ground motion – Leibstadt	28
Fig. 20:	Logic Tree with median site amplification for vertical ground motion – Mühleberg	28
Fig. 21:	Logic Tree with aleatory variability for amplification of horizontal ground motion for Beznau	32
Fig. 22:	Logic Tree with aleatory variability for amplification of horizontal ground motion for Gösgen	32
Fig. 23:	Logic Tree with aleatory variability for amplification of horizontal ground motion for Leibstadt	33
Fig. 24:	Logic Tree with aleatory variability for amplification of horizontal ground motion for Mühleberg	34
Fig. 25:	Logic Tree with aleatory variability for amplification of vertical ground motion for Beznau	36
Fig. 26:	Logic Tree with aleatory variability for amplification of vertical ground motion for Gösgen	36
Fig. 27:	Logic Tree with aleatory variability for amplification of vertical ground motion for Leibstadt	37

Fig. 28:	Logic Tree with aleatory variability for amplification of vertical ground motion for Mühleberg	38
Fig. 29:	Normalized spectral shape for Beznau	41
Fig. 30:	Normalized spectral shape for Gösgen	41
Fig. 31:	Normalized spectral shape for Leibstadt	42
Fig. 32:	Normalized spectral shape for Mühleberg	42
Fig. 33:	Gösgen – Depth 5 m – Rock acceleration 1.5 g	46
Fig. 34:	Gösgen – Depth 9 m – Rock acceleration 1.5 g	46
Fig. A-1:	Site amplifications factors for horizontal ground motion at the mean building depth of NPP Beznau for the case of a magnitude 6 earthquake with PGA on rock of 1.5 g	53
Fig. A-2:	Weighted arithmetic mean amplification factors (AF as function of PGA on rock and frequency) for horizontal ground motion of a magnitude 6 scenario at mean building depth of NPP Beznau	53
Fig. A-3:	Aleatory variability of amplifications factors for horizontal ground motion at the mean building depth of NPP Beznau for the case of a magnitude 6 earthquake with PGA on rock of 1.5 g	54
Fig. A-4:	Assessment of maximum horizontal ground motion at the surface layer of NPP Beznau	55
Fig. A-5:	Summarized model of site amplification factors for ground motion of 4 Hz at mean building depth at NPP Beznau and earthquake magnitudes 5, 6 and 7	57
Fig. A-6:	General logic tree structure for horizontal ground motion	58

1 INTRODUCTION

This report presents the evaluation of the site response characterization at the location of the 4 Swiss Nuclear Power Plants. This evaluation is given in terms of frequency dependent amplification factors which, applied to the bedrock response spectrum, yields the ground surface response spectrum. The amplification factors are provided for the vertical motion and for the horizontal ground motion.

According to the project requirements these amplification factors are estimated following several approaches which, based on our evaluation of their reliability and fit for purpose, have been assigned different weights in a logic tree structure. In addition to the median estimate of the amplification factors, the aleatory variability is also provided following again a logic tree approach.

Finally, since the rock hazard model coming from the work of Experts groups 1 and 2 may lead to strong earthquake scenarios with very high rock accelerations, the maximum motion that any of the studied soil sites can transmit to the ground surface has been evaluated based on the ultimate shear resistance capacity of the soil strata.

All the evaluations presented in this report are based on the results of the calculations and studies carried out by various entities, whom reports were made available to us. It must be noted that, although the results presented in the numerous reports look reliable, no in depth check of the results have been performed by us.

2 MEDIAN AMPLIFICATION OF HORIZONTAL GROUND MOTION

2.1 Approach

The available data for the evaluation of the amplification factors consists of:

- 1D RVT runs
- 1D SHAKE runs
- Parametric studies to study the influence of P-SV waves
- 2D runs at one site
- Non linear analysis

An evaluation of the results is required to assign a degree of confidence to each of the methods. This has been done on the basis of currently admitted practice, past experience and robustness of the different methods as briefly explained below. More details are given for each site in the relevant paragraphs.

Basically, for the 1D amplification studies, the dominant factor used to assign different weights to the different models is the induced shear strain. It is known that equivalent linear analyses are only valid up to a certain level of ground shaking. When the input level becomes too high, answers from SHAKE cease to be reliable because non linear behavior can no longer be approximated by equivalent linear model and, in addition, damping is overestimated especially for the medium to high frequency range (Mohammadioun & Pecker 1984, Martin 1975, Assimaki et al. 2000). The usually accepted domain of validity of the equivalent linear approximation is for strains smaller than 0.1 % to 0.5 %. Beyond that fact, the shape of the G / G_{\max} curves may have a profound influence on the results and governs their validity. They cannot be chosen independently of the soil type, soil resistance and state of stresses. It was therefore checked that the strength mobilized (or equivalently the induced stress) within the soil profile did not exceed the available resistance; when this situation happens, the calculations are no longer considered reliable. For all those situations where the strains goes beyond a given threshold, the non linear calculations were deemed more appropriate to define the amplification factors. In the logic tree these thresholds in terms of induced shear strain have been converted to thresholds in peak ground acceleration to relate them to input parameters.

With regards to the other alternatives offered by the various calculations most of the results were considered as part of the aleatory variability: 2D calculations were only used when specific results were available because no reliable scientifically based methods are available to estimate its impact in the absence of specific calculations; P-SV calculations are also considered part of the aleatory variability because the calculations presented in the data base already incorporate a degree of aleatory variability due to the location of the source, depth of the focus, etc.

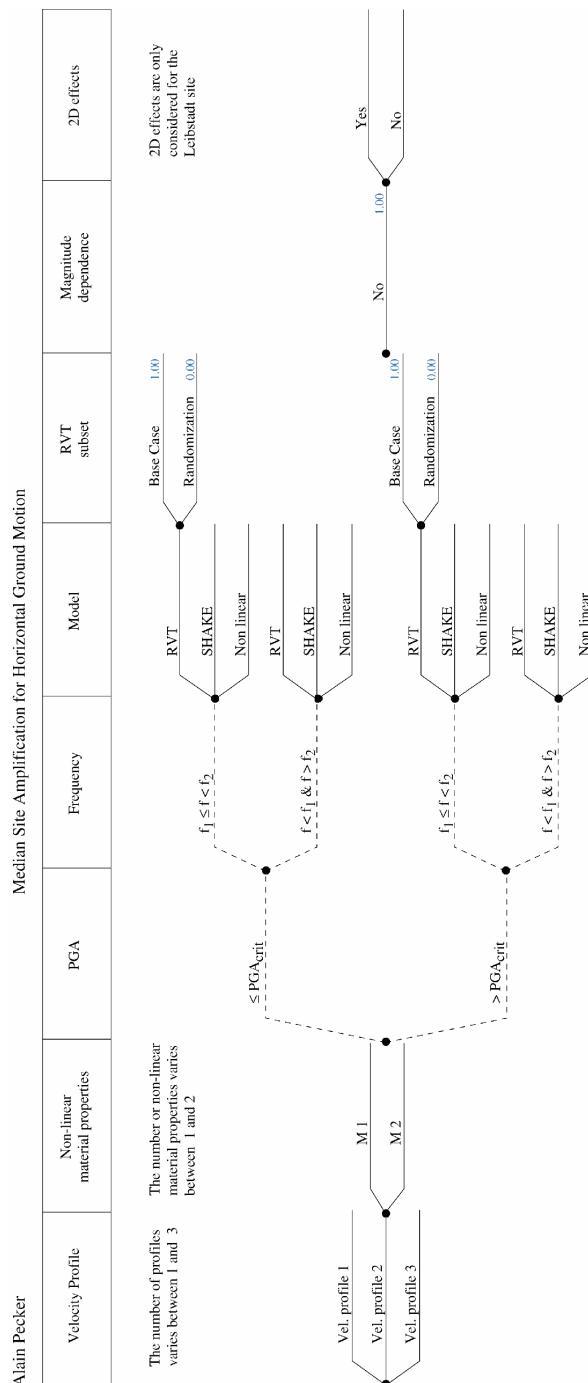
Most of the variability was attributed to variability in the input motion, reflected in all the runs (SHAKE, RVT, non linear); additional variability coming from the other factors was considered less significant; in particular randomization of the soil profiles in the RVT runs was thought to be unrealistic based on the study by Assimaki et al. (2002).

2.2 Logic Tree Structure

The general structure of the logic tree common to all sites is shown in figure 1 for the horizontal ground motion.

The first branches relate to the site data: velocity profiles and material characteristics; the next branch is based on the pga values, but as explained above is actually related to the induced shear strain. The next branches differentiate for frequencies "around" the fundamental frequency of the soil profile where all analyses seem reliable and frequencies above or below it where the RVT runs are not as accurate as the other methods. Basically the logic tree stops at the end of these branches except for Leibstadt where alternatives are considered for the 2D amplifications based on the available amplification studies.

Fig. 1: Generic logic tree for mean horizontal motion



2.3 Model Evaluations Common to All Sites

2.3.1 SHAKE and RVT runs

Both models are based on the equivalent linear approximation. The usually accepted domain of validity of this model is for strains smaller than 0.1% to 0.5%.

Another factor used for evaluating the reliability of the SHAKE runs is, as already quoted previously, the shape of the G/G_{\max} curves which may have a profound influence on the results and governs their validity. The G/G_{\max} versus γ curve is another way to present the shear stress – shear strain curve $\tau = f(\gamma)$. Therefore it cannot be chosen independently of the soil type, soil resistance and state of stresses.

In the SHAKE and RVT analyses, two material models have been used: Ishibashi – Zhang and Hardin – Drnevich. The former one accounts for the state of stresses since different curves are provided for different vertical effective overburden but none of them reflects the soil resistance or the soil type.

In order to assess the validity of those models, for each site and each material model, the curves G/G_{\max} have been rearranged in the following way:

The shear stress at any depth is:

$$(1) \quad \tau = G \gamma$$

which may be written as:

$$(2) \quad \tau = \frac{G}{G_{\max}} G_{\max} \gamma$$

At any depth under the assumption of vertically propagating shear waves, which is the assumption made in the SHAKE or RVT runs, the maximum shear stress is expressed as a function of the vertical effective stress σ'_v and of the soil friction angle ϕ' :

$$(3) \quad \tau_{\max} = \sigma'_v \tan \phi'$$

Equation (2) can be written in a similar format:

$$(4) \quad \tau = \sigma'_v \tan \Psi$$

with:

$$(5) \quad \tan \Psi = \frac{G_{\max}}{\sigma'_v} \frac{G}{G_{\max}} \gamma$$

Comparing equations (4) and (5), Ψ can be interpreted as the mobilized friction angle at a given strain level ($\Psi \leq \phi'$). Using the curves G/G_{\max} provided for each model, Ψ (eq. 5) can be drawn as a function of γ . As soon as Ψ exceed ϕ' the model is no longer valid, which sets another threshold on the shear strain, or equivalently on the pga.

Comparing the results of RVT runs without randomization to SHAKE results, it appears that the RVT runs look accurate in predicting the resonant frequency of the profile. Away from the peak the agreement is poor between both types of analysis, especially for the low magnitudes. When the magnitude increases the agreement becomes better in a frequency band centered around the peak, typically 0.8 Hz to 8 – 10 Hz.

In the low frequency range, the RVT runs invariably indicate an amplification of 1.0 which is not correct. In that frequency range the amplification should be equal to the ratio of the ground surface displacement divided by the rock displacement. A typical value would be in the range 1.2 to 1.5 depending on the profile stiffness, which is correctly predicted by the SHAKE runs. This has been confirmed by the analysis carried out by Bard (2003) on the time histories used in the SHAKE runs. Therefore, more weight will be attributed to the SHAKE runs in the low and high frequency range.

The variability shown by the SHAKE and RVT runs is coming from the variability in the input motions and in addition, for the RVT runs only, from the variability (randomization) in the soil properties. The first type of variability is fully accounted for in the logic tree. However, given the fact that the soil model is one dimensional, the effect of the variability in the soil properties due to the soil randomization is clearly overestimated. Recent studies (Assimaki et al. 2002) have shown that for 2D situations the effect of variability of soil properties on surface ground response spectra is negligible except in the high frequency range. Consequently, soil randomization will not be considered in the model. One alternative would have been to isolate the RVT runs that were randomized on the layer thickness only; however, the number of such runs is not sufficient to derive a meaningful statistical parameter.

With regards to interpolation between missing cases the following approach is followed. Since all cases are computed for the RVT runs, no interpolation is needed for those runs. Their results are used to fit a polynomial equation through all the data points: if n is the number of data points the degree of the polynomial equation is $(n - 1)$. This polynomial equation is obtained for each frequency as a function of the pga. For the SHAKE analyses, interpolations between calculated cases should be made on the basis of the RVT runs without randomization : the same polynomial function is used with the three SHAKE data points but is anchored at the appropriate level to minimize the quantity A .

$$(6) \quad A = \left[\sum_{i=1}^3 (b_i - \lambda p_i)^2 \right]^{1/2}$$

where:

b_i = amplification function from SHAKE for p.g.a1 = i

p_i = value of the polynomial function for p.g.a = i

λ = scaling factor

Further on, the amplification factors for the SHAKE runs will be taken not directly from the calculated data points but from the interpolated polynomial equation. It has been checked, at random, that the difference between the two sets of values is minimum and should not affect the validity of the results. An example of the interpolated polynomial equation for the RVT and SHAKE runs is given in Figure 2.

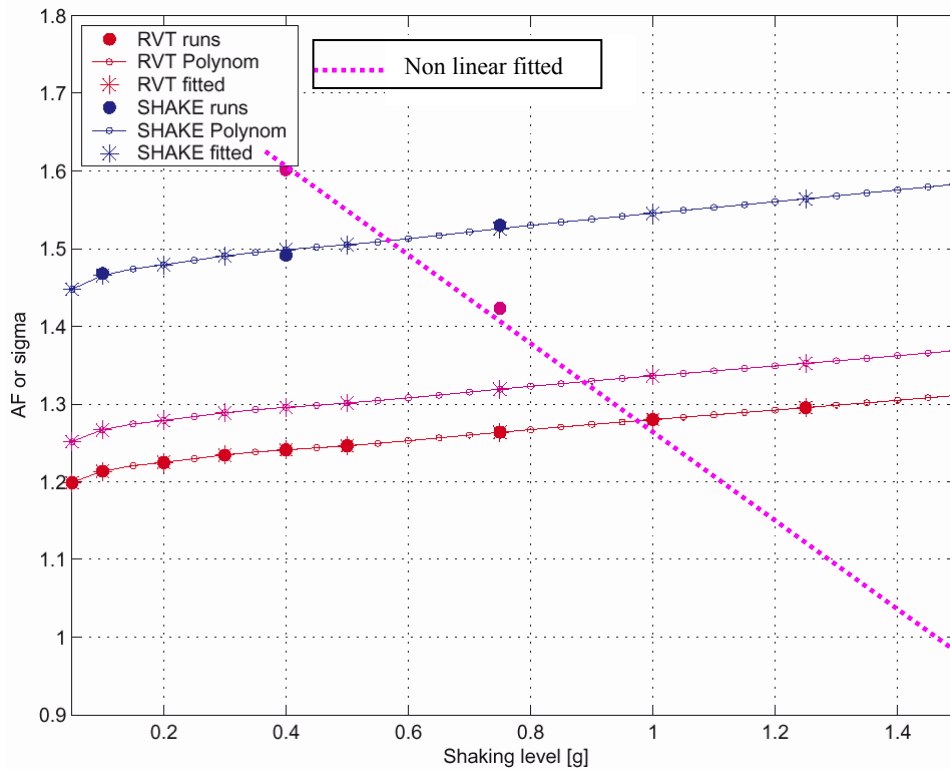


Fig. 2: Example of interpolation – Gösgen site, frequency 1.3 Hz

2.3.2 Non-linear calculations of site amplification

The non linear calculations are only available for pga greater than 0.4 g. Consequently, below that threshold no weight is attributed to the non linear calculations. Above the threshold value of 0.4 g a significant weight is attributed to the non linear analyses on the grounds that equivalent linear analyses are less reliable (see section 2.3.1). The non linear calculations which are referred to are the second set of calculations performed by Geodeco, in which the presence of the water table is taken into account (PEGASOS TP3-TN-0353). The first set; which implicitly assumed a dry soil is to be disregarded except for Leibstadt (PEGASOS TP3-TB-0048).

The non linear calculations are performed for only three levels of pga. For the missing runs interpolation shall be carried out frequency by frequency; due to the small number of available runs and to the obvious difference in behavior between the equivalent linear and non linear runs (see Figure 2), a simple linear interpolation scheme of the amplification function versus pga is chosen.

2.3.3 Magnitude dependence of site amplification

As illustrated in figures 3 to 5 for Gösgen, magnitude dependence from the SHAKE runs is almost negligible for frequencies higher than 1.0 Hz. In the low frequency range, it is also negligible for magnitudes higher than 6.0. Only the simulations for magnitude 5.0 earthquake show a noticeable dependence. A similar behavior has been noticed for the other sites with even less pronounced effect for Mühleberg. The only noticeable exception is Leibstadt for profile 2 which includes the presence of the cemented layer.

The RVT runs do not show any magnitude dependence.

Those results are in line with recently developed attenuation relationships which exhibits the same magnitude dependence for rock sites and soil sites; therefore, the amplification that would be computed from those relationships is magnitude independent.

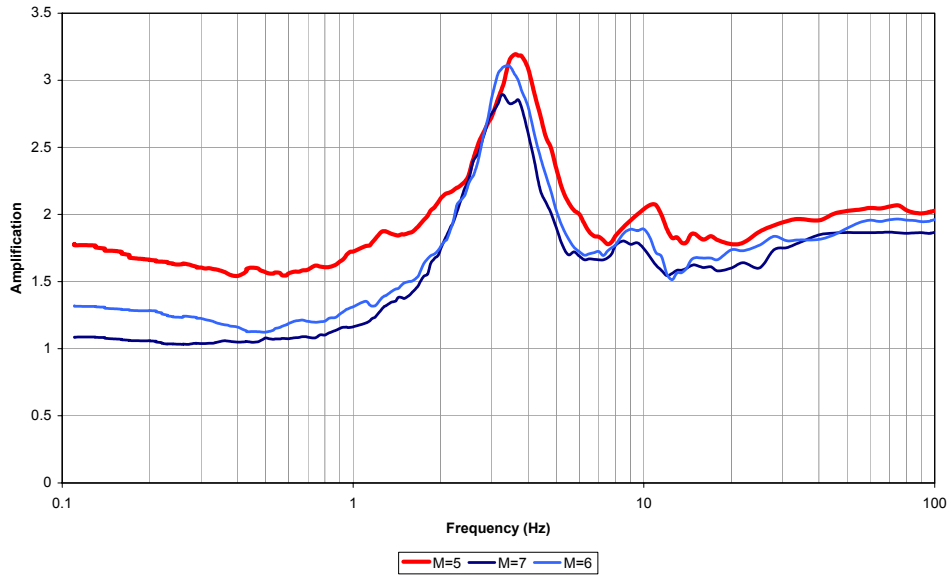


Fig. 3: Effect of magnitude on amplification factors – Gösgen site – 0.75 g

As a conclusion, I will not consider any magnitude dependence for the amplification. The amplification shall be computed as the arithmetic mean of the amplifications for the three magnitudes.

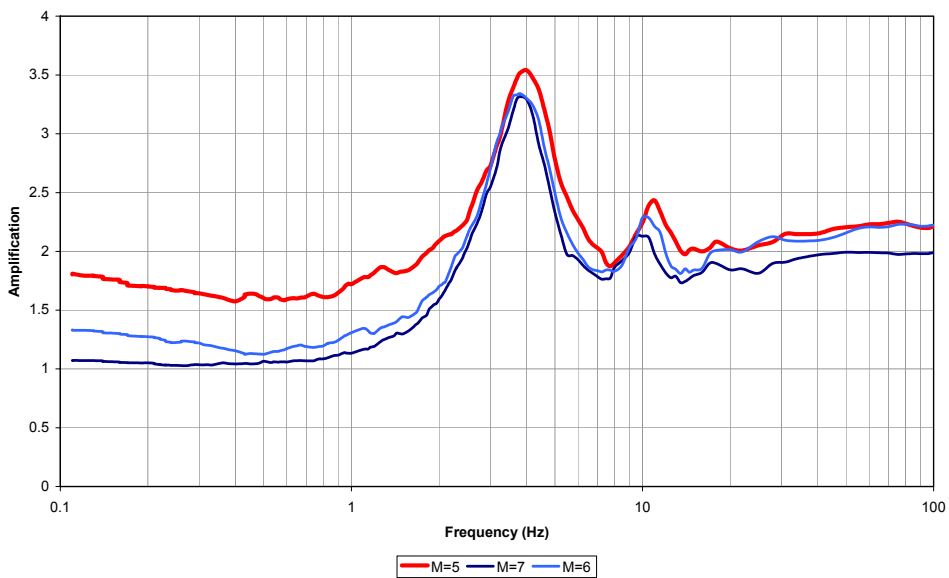


Fig. 4: Effect of magnitude on amplification factors – Gösgen site – 0.40 g

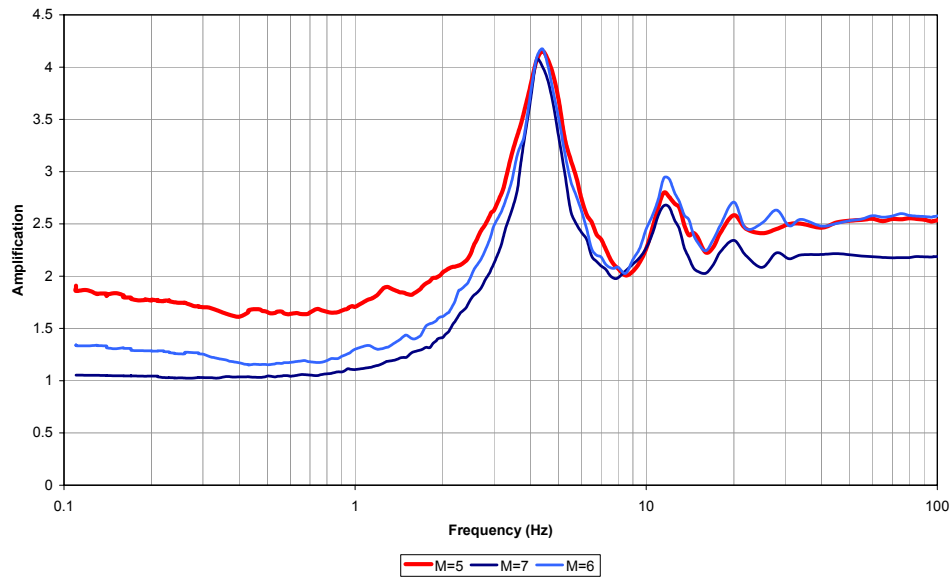


Fig. 5: Effect of magnitude on amplification factors – Gösgen site – 0.10 g

2.3.4 Effect of inclined waves

P-SV waves analyses have been carried out for three sites: Beznau, Gösgen and Leibstadt. The studies by Fäh took into account random factors such as fault distance, depth, strike angle, dip, duration (PEGASOS TP3-TN-0167). The variation exhibited by the results seem to be covered by the other studies. Since these studies include parametric studies on random variables, they are more useful to estimate the aleatory contribution to the results. In addition, results obtained by Bard (PEGASOS TP3-RF-0310) are in agreement with those by Fäh.

2.3.5 2D effects

This effect has been studied for Leibstadt by both Bard and Fäh. The study by Fäh cannot be used: the amplification is said to be calculated from the rock motion, which is obtained by replacing the soil layers by rock in the model. My understanding is that the topographic effect is included in the calculation of the rock motion and results are therefore not directly comparable to those of the 1D runs.

The study by Bard does not show a significant effect of the 2D topography. Since the Leibstadt site has been chosen as the site being the most likely to evidence 2D topographic effect, it can be concluded that this effect has indeed a minor impact on the results. Variations covered by the other parametric studies largely encompass the 2D effect: the amplification due to 2D effect is less than 50 % for small shaking level and decreases to less than 20 % for moderate shaking level.

2.3.6 3D effects

No calculations have been performed to assess the 3D effect. However, based on the small impact of the 2D topography for Leibstadt, which is believed to be the site where the strongest topographic effect should be noticed, the effect of 3D topography is neglected. In addition, I am not aware of well established standard to estimate a priori this effect.

2.4 Beznau

2.4.1 Logic Tree for Beznau

The Logic Tree for Beznau is represented in Figure 6.

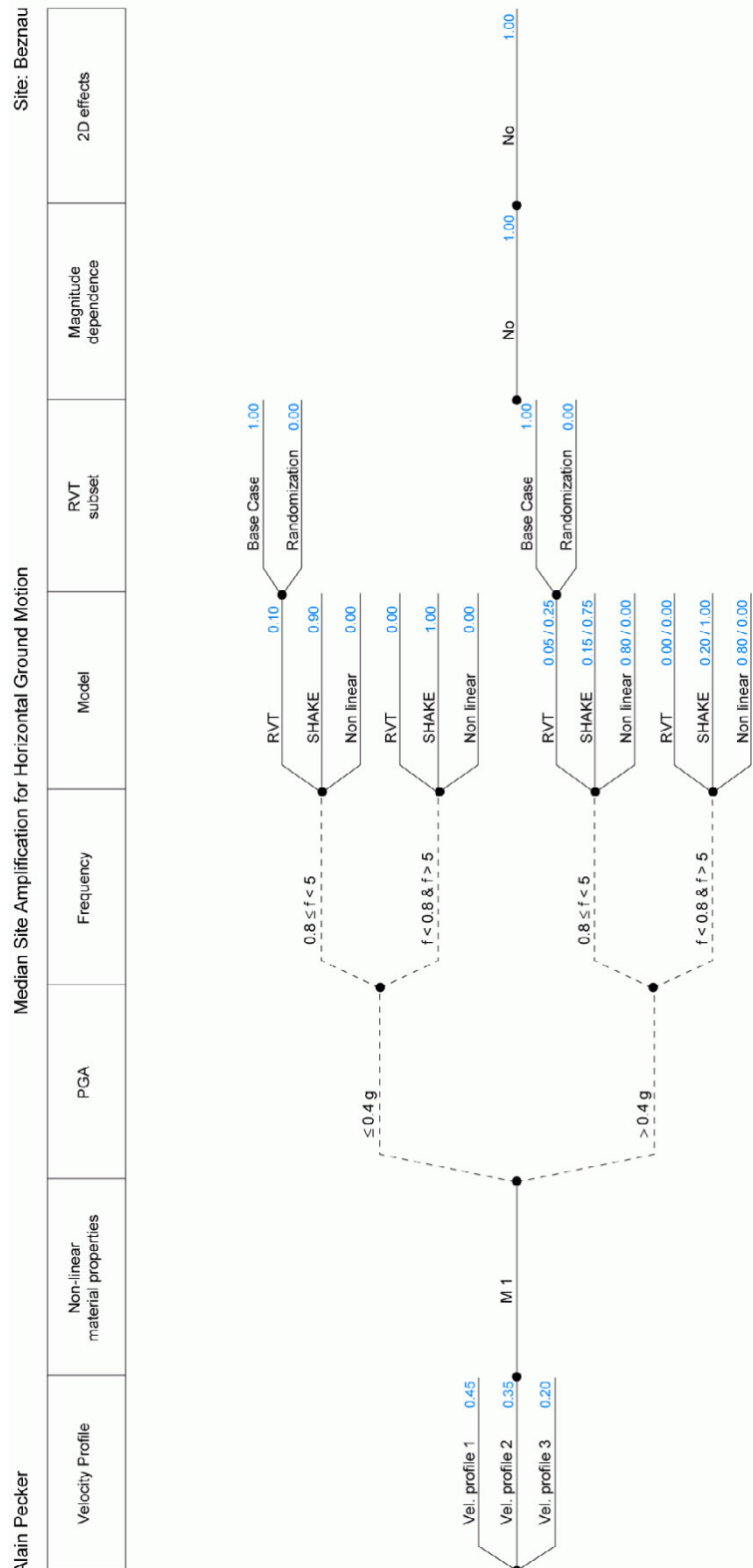


Fig. 6: Logic Tree for Beznau

2.4.2 Site-Specific Model Evaluations

2.4.2.1 Alternative velocity profiles

Three velocity profiles are considered. The first one is based on cross hole measurements within the shallow layers. The second one results from the inversion of the H/V ratio from one station. The third one comes from the inversion of the H/V ratio from a surface array. The last profile gives thick layers with constant velocity and a high velocity value at the ground surface. The first two profiles are given the largest weights because they have more realistic "smooth" profiles. Of these two smooth profiles, profile 1 is preferred because it comes directly from measurements.

2.4.2.2 Alternative non-linear properties

Only one material model, which is site specific is considered.

The top 9 m consist of gravels and sandy gravel in a medium dense to dense state; the friction angle should not be larger than 40 – 45°. The water table is at 3.0 m depth. Following the procedure described in Section 2.3.1, the mobilized friction angle is plotted versus pga in Figure 7. Figure 7 shows that the range of validity of the material model, which is site specific, is up to strains of the order of 0.3 to 0.4 %.

The SHAKE runs are therefore valid up to a peak ground acceleration of 0.4 g (strains smaller than 0.3 – 0.4 %).

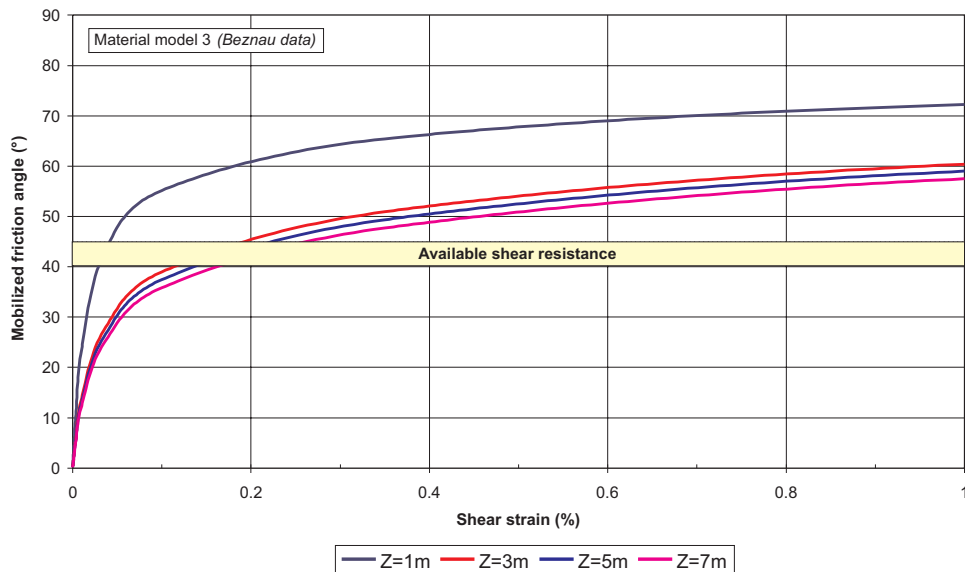


Fig. 7: Mobilized friction angle versus pga – Beznau

2.5 Gösgen

2.5.1 Logic Tree for Gösgen

Figure 8 shows the Logic Tree for Gösgen.

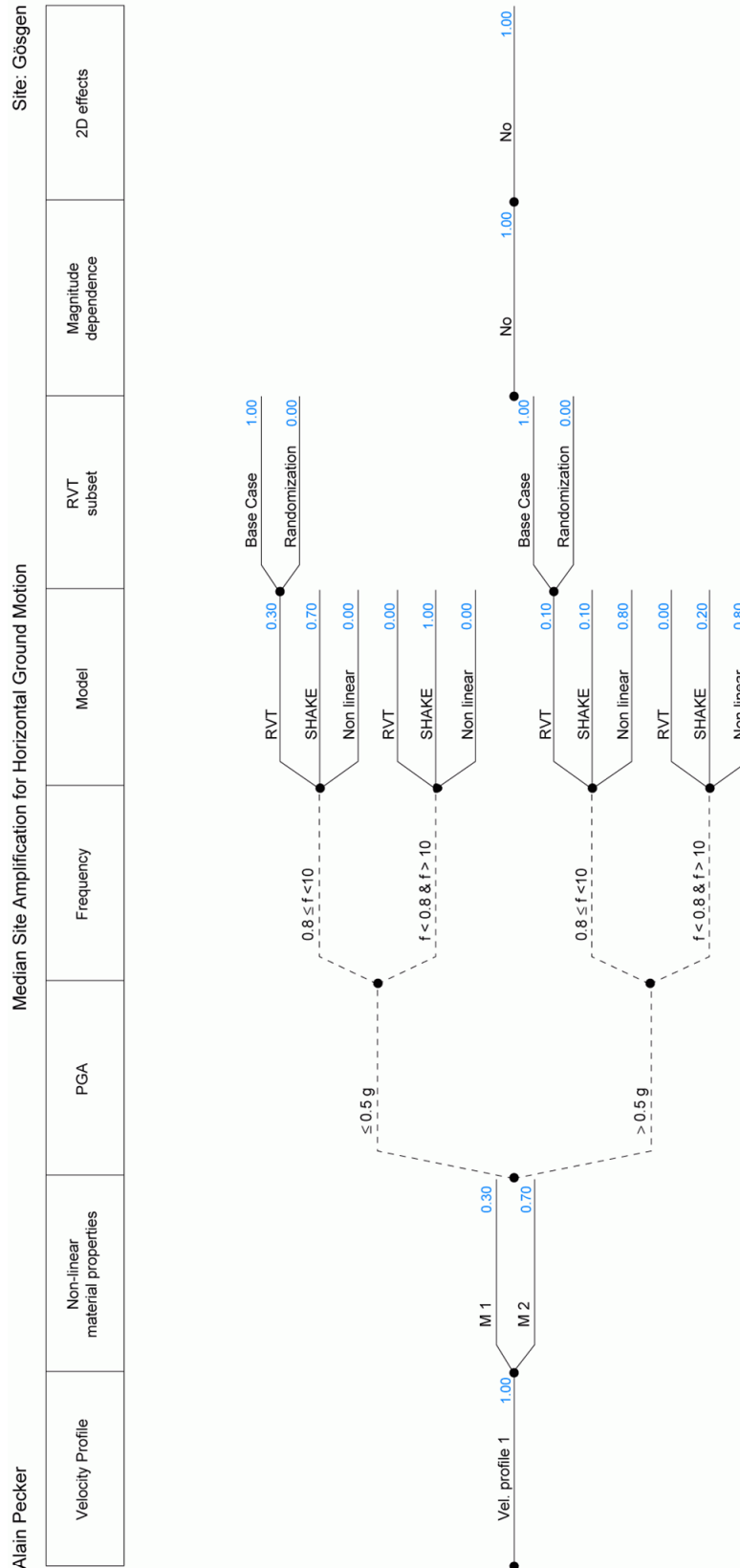


Fig. 8: Logic tree fro Gösgen

2.5.2 Site-Specific Model Evaluations

2.5.2.1 Alternative non-linear properties

Only one shear wave velocity profile is considered.

Down to 26 m the profile is composed of sands and gravels in a medium dense state; the friction angle should not exceed 38° to 42°. The water table is at 5.0 m depth. Figures 9 and 10 show that the Hardin – Drnevich model is appropriate, except for the very first layer, but that the Ishibashi model cannot be considered reliable beyond strains of the order of 0.1 %.

Based on the comments made in 2.3.1, more weight is attributed to the M2 model (Hardin – Drnevich). SHAKE runs with the M2 model are valid up to peak ground accelerations of 0.75 g (strains smaller than 0.2 %) as shown in Figures 9 and 10.

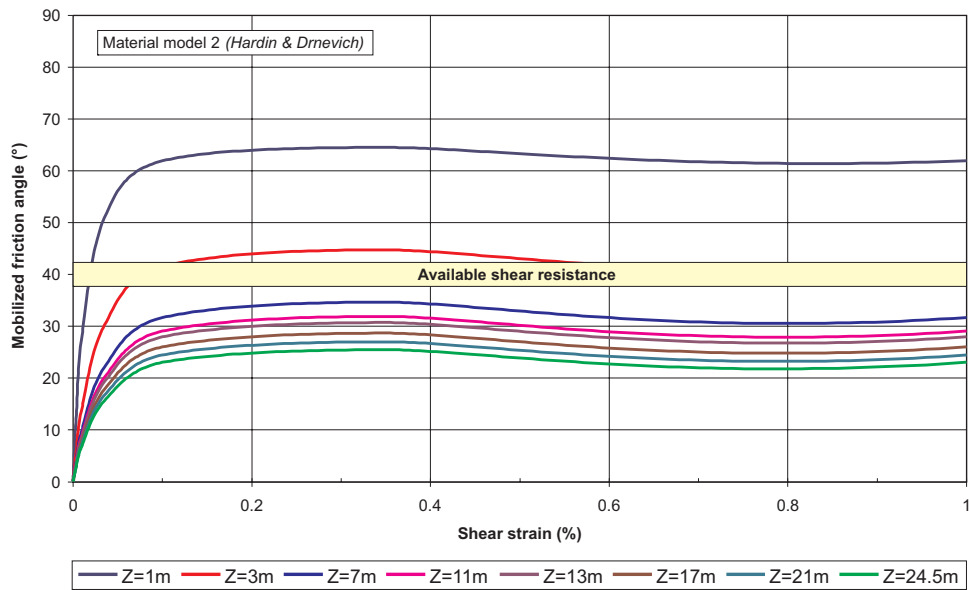


Fig. 9: Mobilized friction angle versus pga – Gösgen-Material 2

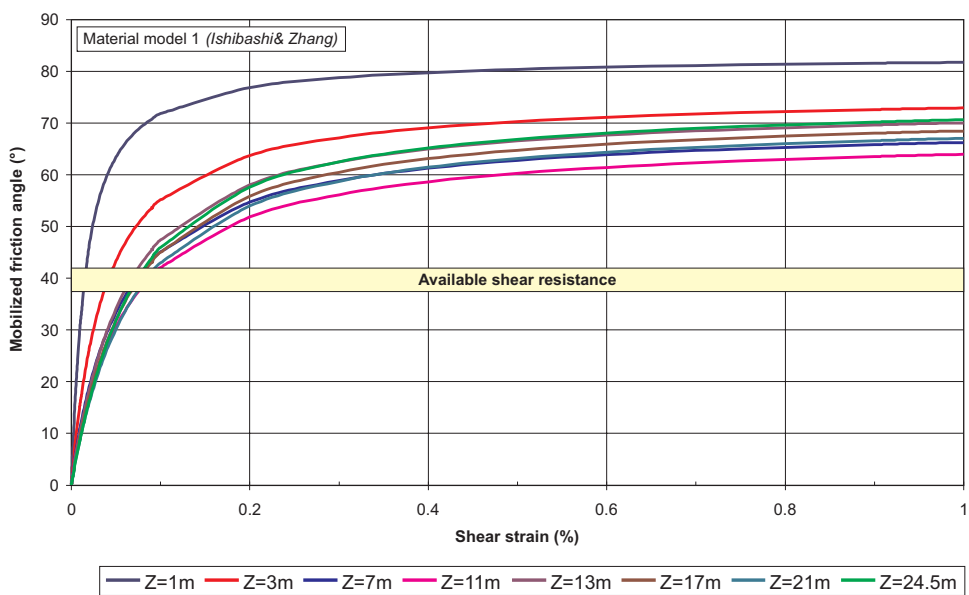


Fig. 10: Mobilized friction angle versus pga – Gösgen-Material 1

2.6 Leibstadt

2.6.1 Logic Tree for Leibstadt

The Logic Tree for Leibstadt is shown in Figure 11.

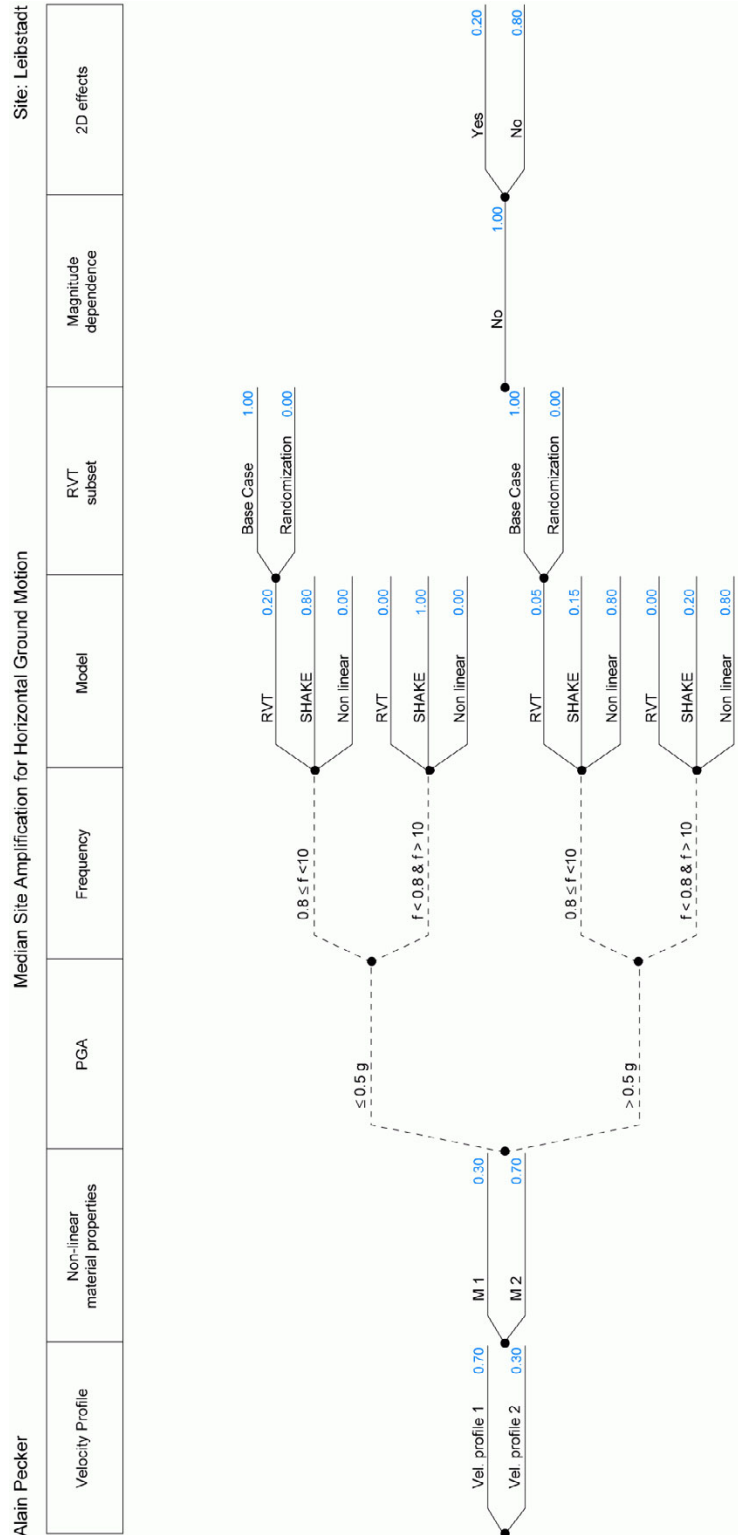


Fig. 11: Logic Tree for Leibstadt

2.6.2 Site-Specific Model Evaluations

2.6.2.1 Alternative velocity profiles

Two profiles are considered depending of the degree of cementation of a layer. The profile with the cemented layer (P2) does not match the measured H / V ratio, therefore the profile without the cemented layer (P1) is preferred.

2.6.2.2 Alternative non-linear properties

Two material models are considered.

Only profile P1 (without cemented layer) is considered; down to 50 m the profile consists of sands and gravels in a medium dense state. An upper bound for the friction angle should be in the range 35° to 40°. The water table is at 25.5 m depth. Figures 12 and 13 show that the Hardin – Drnevich model is valid up to 1 % strain, except for the very first layer but that the Ishibashi model cannot be considered reliable beyond strains of the order of 0.2 %.

Based on the comments made in Section 2.3.1., material model M2 (Hardin – Drnevich) is preferred. SHAKE runs with the M2 model may be valid up to peak ground accelerations of 0.5 g (strains less than 0.2 %) as shown in Figures 12 and 13.

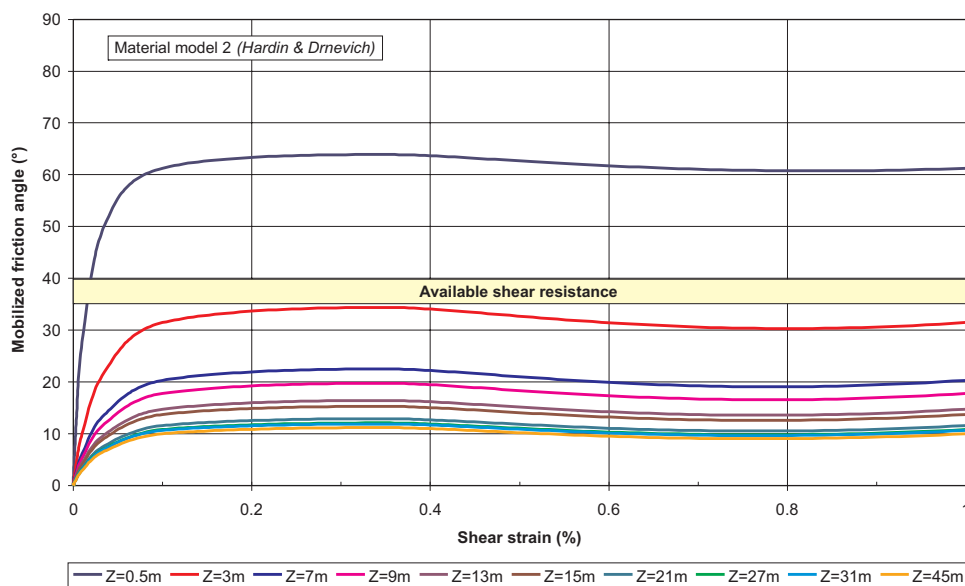


Fig. 12: Mobilized friction angle versus pga – Leibstadt-Material 2

2.6.2.3 2D amplification

For that site the amplification shall be computed as the mean of the amplifications computed at receivers 10 to 19 in PEGASOS TP3-TN-0186. Only the curves corresponding to the high strain case with vertical incidence need to be considered (red curves in figure 30 of this document).

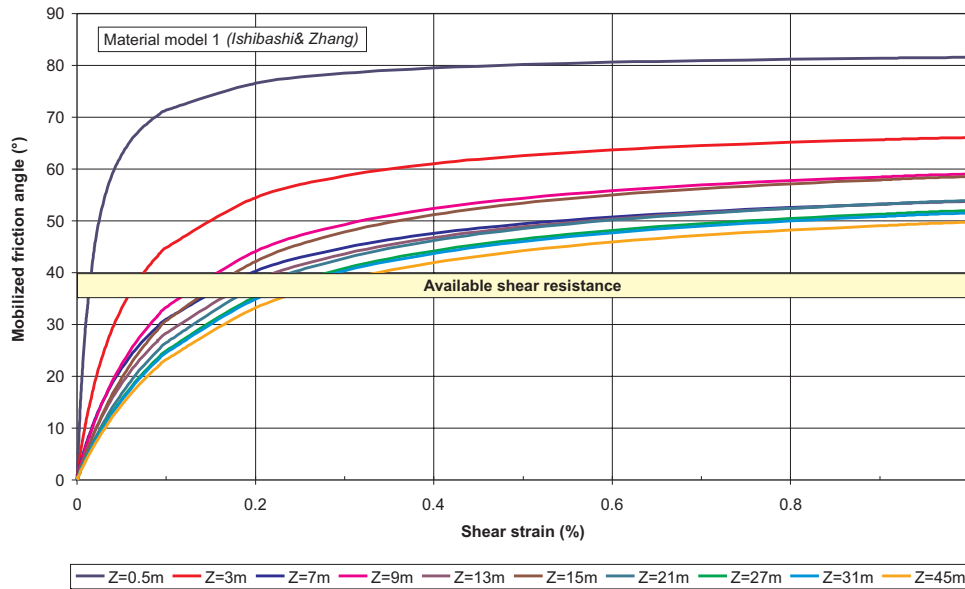


Fig. 13: Mobilized friction angle versus pga – Leibstadt-Material 1

2.7 Mühleberg

2.7.1 Logic Tree for Mühleberg

Figure 14 shows the Logic Tree for Mühleberg.

2.7.2 Site-Specific Model Evaluations

2.7.2.1 Alternative non-linear properties

Two material models are considered.

The top 9 m represent a layer of dense gravels as evidenced from the shear wave velocity profile; therefore the friction angle could be as high as 45° to 50° . The water table is at 3.25 m depth. The curves in Figures 15 and 16 show that the Hardin – Drnevich curves may be adequate, with the possible exception of the top layer but that the Ishibashi – Zhang model overestimates the soil resistance; beyond strains of 0.05 % it is no longer valid.

Based on the comments made in Section 2.3.1., material model M2 is preferred. SHAKE runs with the M2 model may be valid up to peak ground accelerations of 0.75 g (strains less than 0.08 %) as shown in Figures 15 and 16.

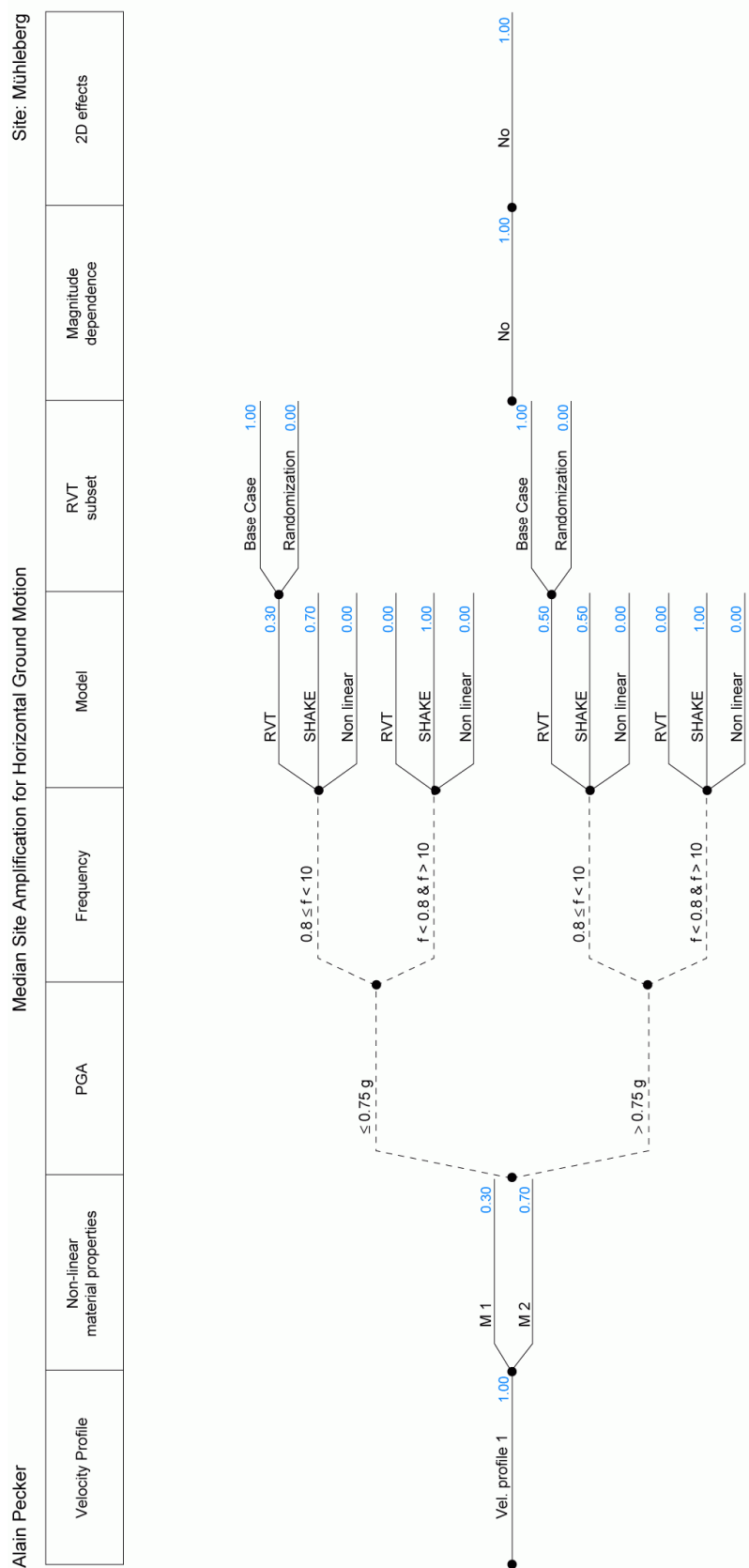


Fig. 14: Logic Tree for Mühleberg

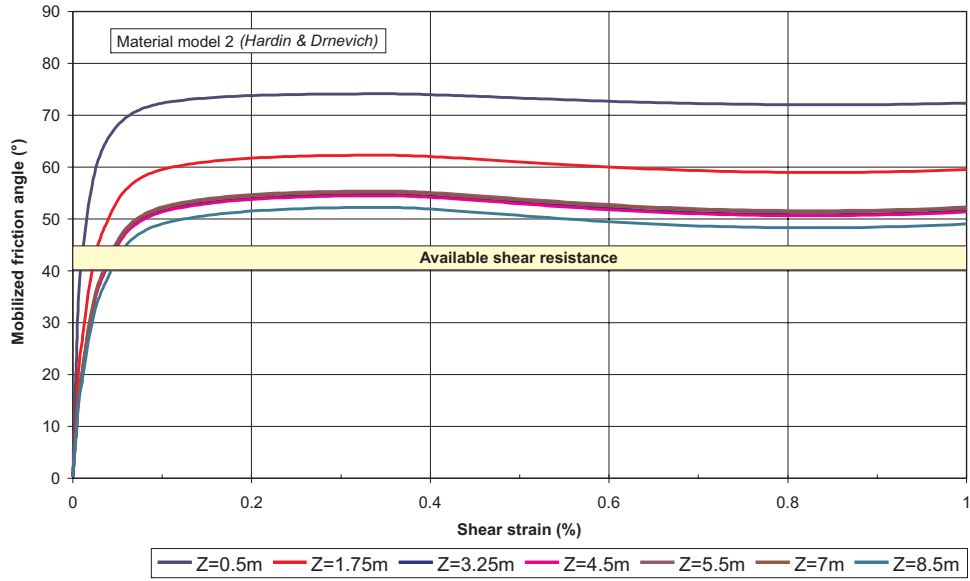


Fig. 15: Mobilized friction angle versus pga – Mühleberg-Material 2

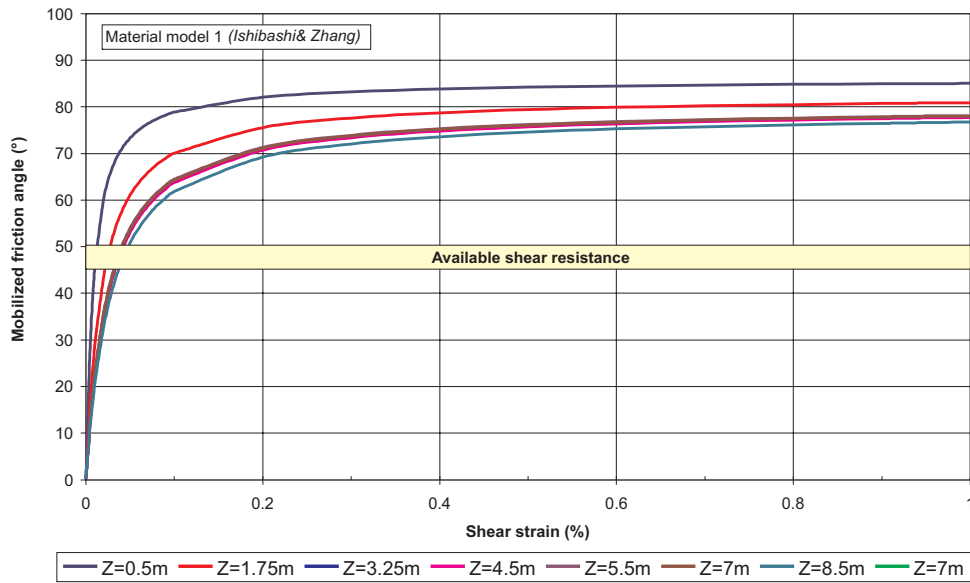


Fig. 16: Mobilized friction angle versus pga – Mühleberg-Material 1

3 MEDIAN AMPLIFICATION OF VERTICAL GROUND MOTION

3.1 Approach

The logic tree for the vertical motions considers alternatives based on the no amplification choice and amplifications computed from SHAKE runs using various assumptions on the reduction of the dilatational wave velocity due to the induced strain.

3.2 Logic Tree Structure

For the mean amplification of the vertical ground motion the rationale for assigning the weights is based on the physics of the phenomenon. In saturated soils the P waves travel through the water; the bulk modulus of the soil skeleton may be slightly affected by the induced shear strain but the overall bulk modulus, which is the sum of the soil skeleton bulk modulus and of the water bulk modulus, will be almost unaffected. In a dry soil, the propagation of P waves is controlled by the skeleton properties:

$$(7) \quad \rho V_p^2 = K + \frac{4}{3}G$$

Those properties are influenced by the shear strain but the bulk modulus K to a lesser extent than the shear modulus G.

Therefore amplifications based on calculations assuming a constant bulk modulus or no amplification at all were attributed the highest degree of confidence. Statistical correlations based on V/H ratios are not considered appropriate: the horizontal motion is much more material dependent than the vertical one and the uncertainty introduced by using indiscriminate correlations is too large.

3.3 Model Evaluations Common to All Sites

For all sites only two branches are considered:

- a no amplification branch for which the weight depends on the stiffness of the soil profile and its capability of developing a non linear behavior. For stiffer sites, a higher weight will be attributed to that branch
- a branch for which amplification is computed based on three assumptions of the reduction in the dilatational wave velocity: constant bulk modulus, reduction proportional to the reduction in the shear wave velocity, reduction proportional to the square root of the reduction in the shear wave velocity. As argued in chapter 3.2 more weight is given to the constant bulk modulus assumption and zero weight is given to the reduction proportional to the reduction in V_s .

As for the horizontal motion, no magnitude dependence is considered in the logic tree. Amplification factors are computed as the arithmetic mean for the three magnitudes.

Effect of P-SV waves are not considered and their effect is part of the aleatory variability.

3.4 Beznau

3.4.1 Logic Tree for Beznau

The Logic Tree with median site amplification for the vertical motions for Beznau is shown in Figure 17.

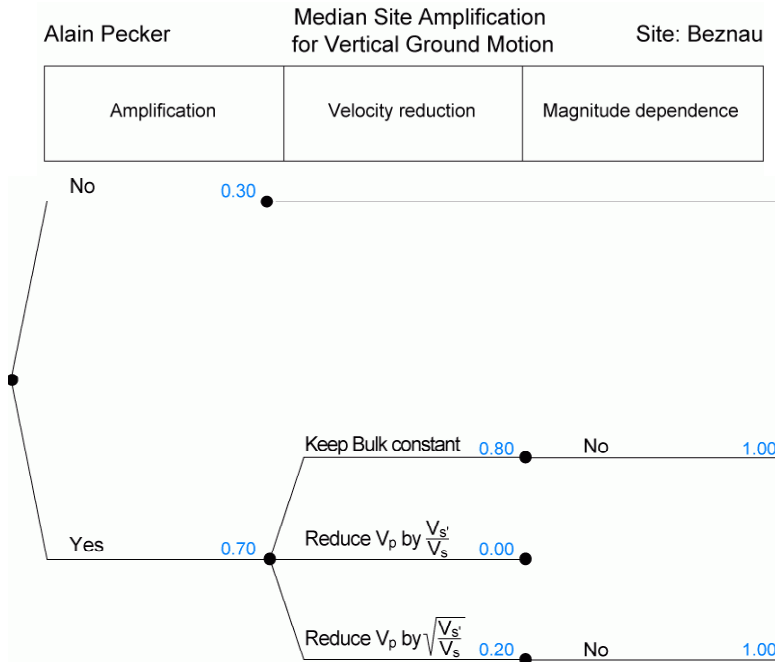


Fig. 17: Logic Tree with median site amplification for vertical ground motion – Beznau

3.4.2 Site-Specific Model Evaluations

The water table at Beznau is at 3.0 m below the ground surface. Consequently the option with a constant bulk modulus is favored. Because the site should develop significant non linearities under horizontal excitation, the weight attributed to the no amplification assumption is limited.

3.5 Gösgen

3.5.1 Logic Tree for Gösgen

Figure 18 shows the Logic Tree with median site amplification for vertical motions for Gösgen.

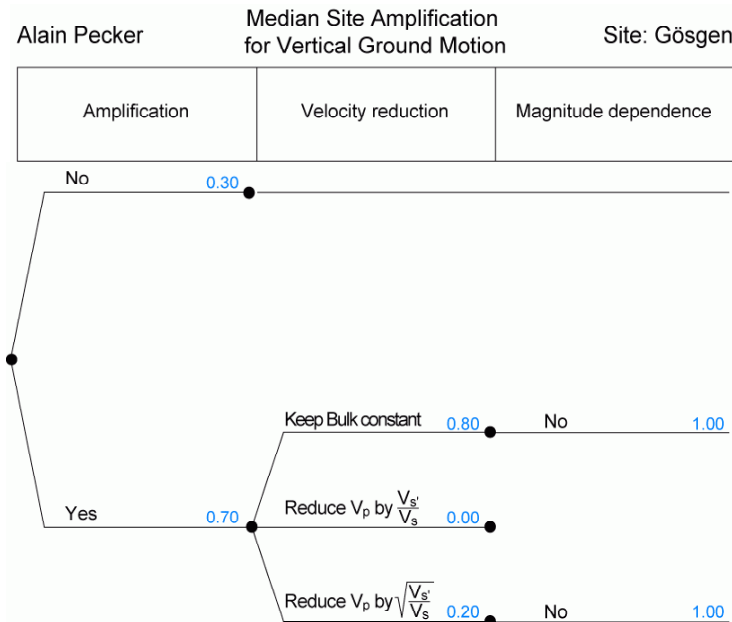


Fig. 18: Logic Tree with median site amplification for vertical ground motion – Gösgen

3.5.2 Site-Specific Model Evaluations

The site is very similar to Beznau with a water table depth of 5.0 m. Therefore, the same weights are attributed to the branches of the logic tree.

3.6 Leibstadt

3.6.1 Logic Tree for Leibstadt

Figure 19 shows the Logic Tree with median site amplification for vertical ground motion for Leibstadt.

3.6.2 Site-Specific Model Evaluations

For this site the water table is deep at 25.5 m below the ground surface. In addition, the soil profile consists of medium dense sand in which strong non linear behavior is expected. Therefore, the no amplification branch is given a reduced weight and the amplification branch is equally shared between the two possible choices which correspond to two possible assumptions for the reduction in V_p .

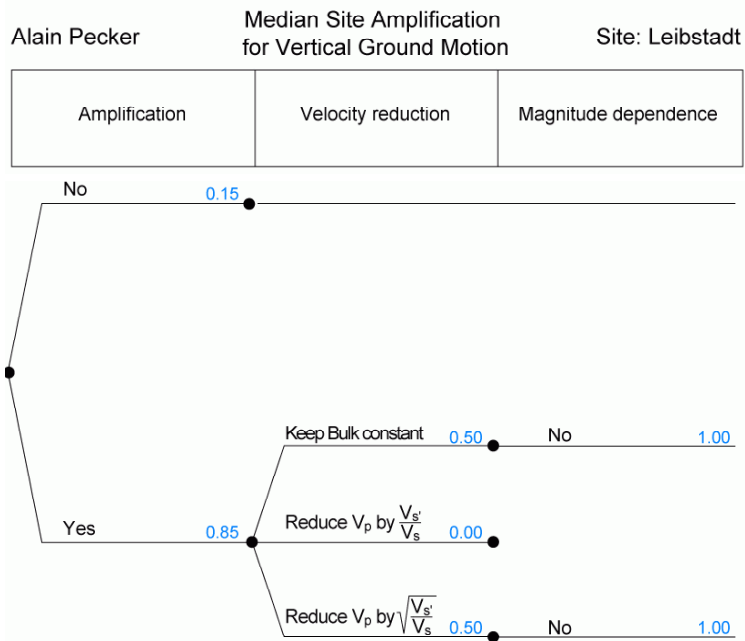


Fig. 19: Logic Tree with median site amplification for vertical ground motion – Leibstadt

3.7 Mühleberg

3.7.1 Logic Tree for Mühleberg

Figure 20 shows the Logic Tree with median site amplification for vertical ground motion for Mühleberg.

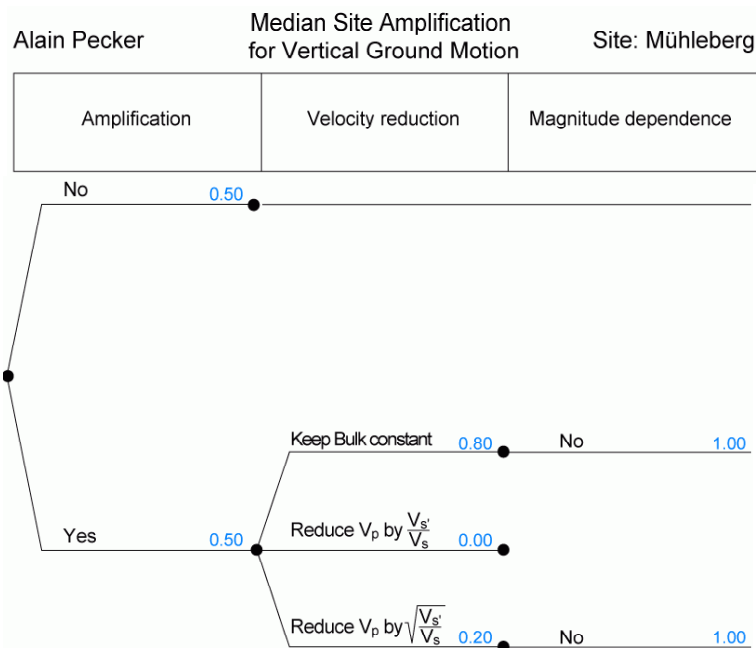


Fig. 20: Logic Tree with median site amplification for vertical ground motion – Mühleberg

3.7.2 Site-Specific Model Evaluations

The Mühleberg site is the stiffer site for which non linear soil behavior should be limited. Therefore the no amplification branch is given a significant weight. Furthermore, since the water table is shallow (3.25 m below the ground surface), more weight is given to the constant bulk modulus assumption.

4 ALEATORY VARIABILITY OF HORIZONTAL GROUND MOTION

4.1 Approach

The aleatory variability is assumed to arise from the variability in the input motions (reflected in the SHAKE and RVT runs), from the variability observed in the P-SV runs arising from different incidence angles and, from that observed, when available, in the 2D runs and linked to the position of the receivers. However, in order not to indiscriminately increase the overall variability, these different parameters are not added on top of each other but considered as alternatives to assess the variability; these different alternatives are assigned different weights in the logic tree.

4.2 Logic Tree Structure

The logic tree starts with the same branches as the logic tree for the mean horizontal motion related to the velocity profile and to the material characteristics. The next branches discriminate between the various causes of variability as explained above.

4.3 Evaluations Common to All Sites

The same weight as in the median ground motion logic tree is assigned to the different branches related to the velocity profile and material characteristics. For all sites, the same weights are used for the Approach and the RVT subset, except for Liebstadt which includes some weight for the 2D branch. The variability is taken as the standard deviation calculated in PEGASOS TP3-TN-0167 for the P-SV runs, considering only the total horizontal motion amplification. The maximum standard deviation between the two sets of calculations (first source set and second source set) is taken.

For the RVT runs the variability is taken as half the value of the standard deviation from the base case without randomization on the soil properties and half the value of the standard deviation for the calculations with randomization. It would have been more appropriate to consider only randomization on the layer thickness but, as explained previously, it was not possible to derive significant statistical estimates.

4.4 Beznau

4.4.1 Logic Tree for Beznau

The Logic Tree with aleatory variability for amplification of horizontal ground motion for Beznau is shown in Figure 21.

4.4.2 Site-Specific Model Evaluations

Since 2D calculations are not available, no variability is associated with this parameter.

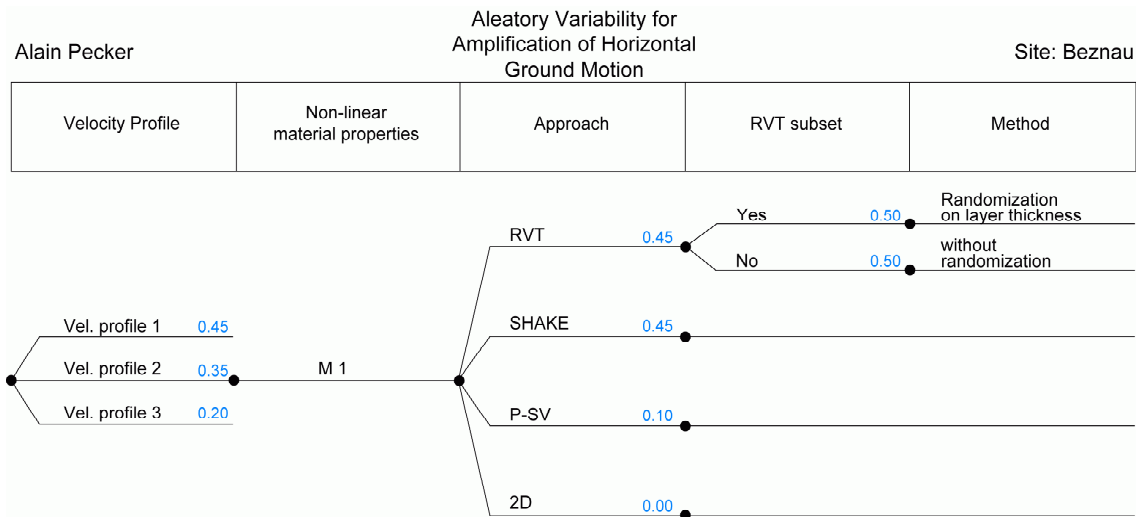


Fig. 21: Logic Tree with aleatory variability for amplification of horizontal ground motion for Beznau

4.5 Gösgen

4.5.1 Logic Tree for Gösgen

The Logic Tree with aleatory variability for amplification of horizontal ground motion for Gösgen is shown in Figure 22.

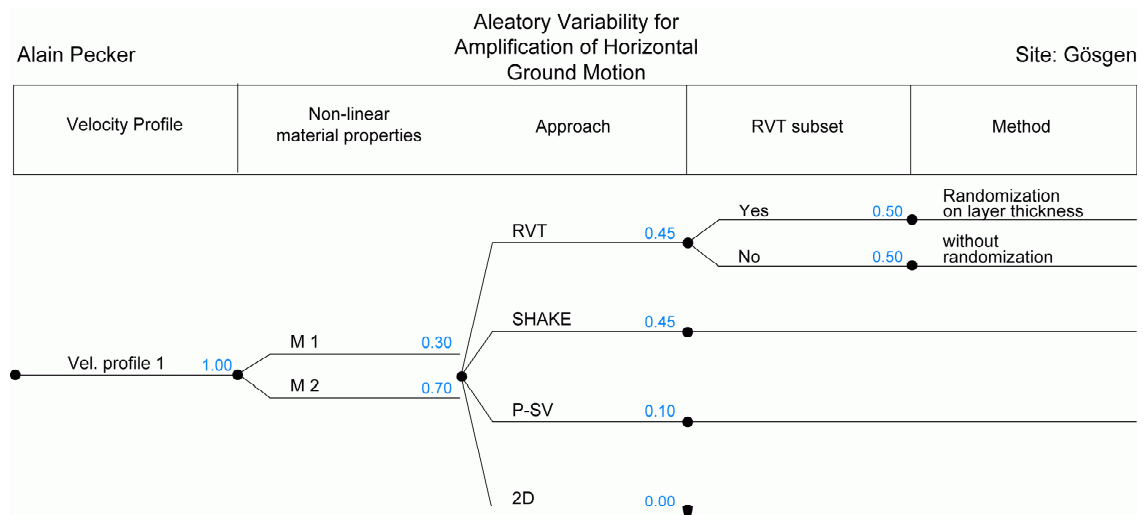


Fig. 22: Logic Tree with aleatory variability for amplification of horizontal ground motion for Gösgen

4.5.2 Site-Specific Model Evaluations

Since 2D calculations are not available, no variability is associated with this parameter.

4.6 Leibstadt

4.6.1 Logic Tree for Leibstadt

The Logic Tree with aleatory variability for amplification of horizontal ground motion for Leibstadt is shown in Figure 23.

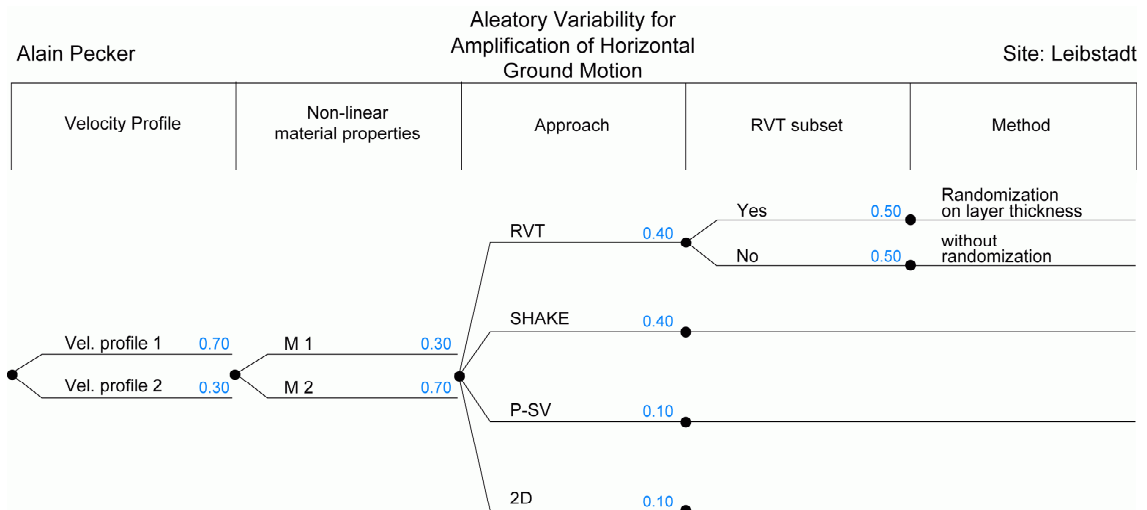


Fig. 23: Logic Tree with aleatory variability for amplification of horizontal ground motion for Leibstadt

4.6.2 Site-Specific Model Evaluations

The aleatory variability linked to 2D effect for this site is taken from PEGASOS TP3-TN-0186 considering only the high strain case and the average for the receivers 10 to 19.

4.7 Mühleberg

4.7.1 Logic Tree for Mühleberg

The Logic Tree with aleatory variability for amplification of horizontal ground motion for Mühleberg is shown in Figure 24.

4.7.2 Site-Specific Model Evaluations

Since 2D calculations are not available, no variability is associated with this parameter. In addition, for the P-SV branch since no specific calculations are available, the standard deviation is taken equal to the average standard deviation computed for the three other sites.

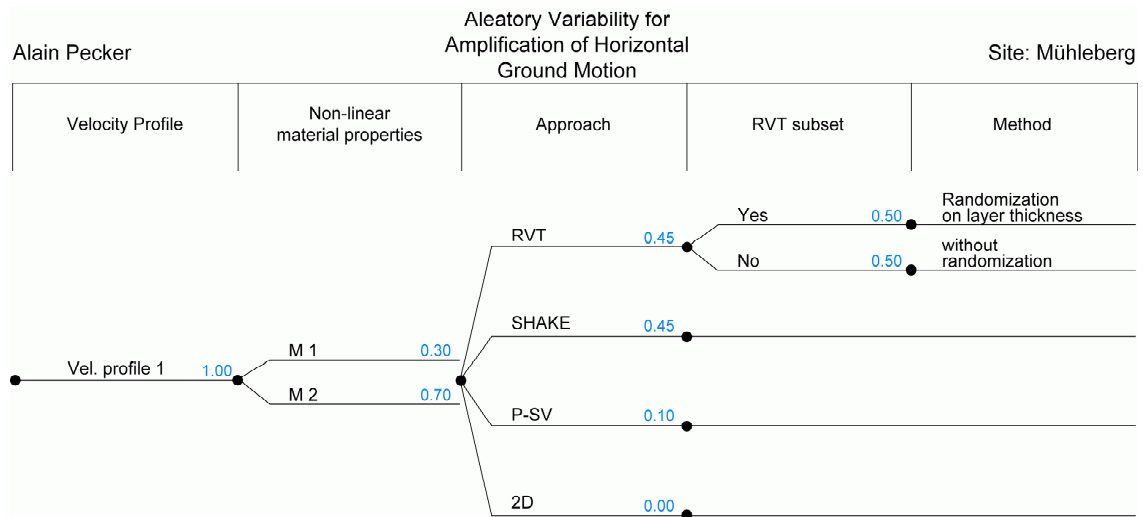


Fig. 24: Logic Tree with aleatory variability for amplification of horizontal ground motion for Mühleberg

5 ALEATORY VARIABILITY OF VERTICAL GROUND MOTION

5.1 Approach

The same approach as for the aleatory variability related to the horizontal motion is followed. The aleatory variability is assumed to arise from the variability in the input motions (reflected in the SHAKE and RVT runs), from the variability observed in the P-SV runs arising from different incidence angles. However, in order not to indiscriminately increase the overall variability, these different parameters are not added on top of each other but considered as alternatives to assess the variability; these different alternatives are assigned different weights in the logic tree.

5.2 Logic tree structure

The logic tree is identical for all the sites with only three active branches related to the calculation model. In the RVT branch the same two alternatives as for the aleatory variability of the horizontal motion is considered.

5.3 Evaluations common to all sites

The same weight as in the aleatory variability of the mean ground motion is assigned to the different branches related to the calculation model. For all sites, the same weights are used for the Approach and the RVT subset. The variability is taken as the standard deviation calculated in PEGASOS TP3-TN-0167 for the P-SV runs, considering only the vertical motion amplification. The maximum standard deviation between the two sets of calculations (first source set and second source set) is taken. For frequencies above 10 Hz, the value of the standard deviation is kept at its value at 10 Hz.

For the RVT runs the variability is taken as half the value of the standard deviation from the base case without randomization on the soil properties and half the value of the standard deviation for the calculations with randomization. It would have been more appropriate to consider only randomization on the layer thickness but, as explained previously, it was not possible to derive significant statistical estimates.

5.4 Beznau

5.4.1 Logic Tree for Beznau

Figure 25 shows the Logic Tree with aleatory variability for amplification of vertical ground motion for Beznau

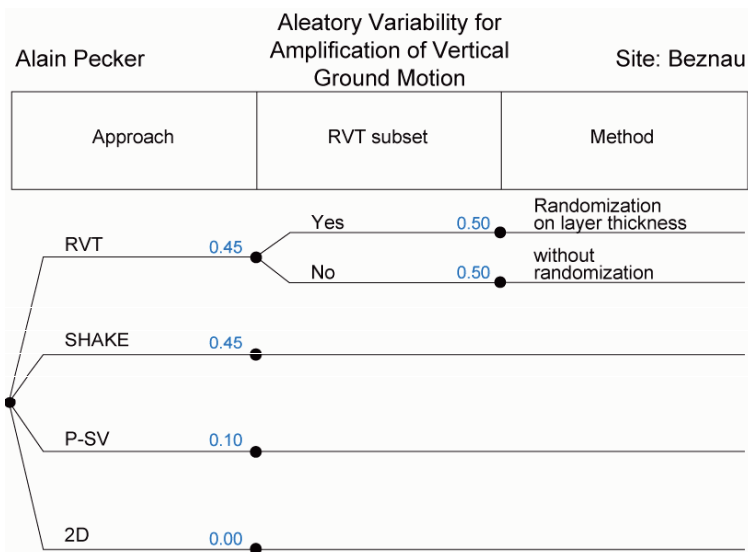


Fig. 25: Logic Tree with aleatory variability for amplification of vertical ground motion for Beznau

5.5 Gösgen

5.5.1 Logic Tree for Gösgen

Figure 26 shows the Logic Tree with aleatory variability for amplification of vertical ground motion for Gösgen.

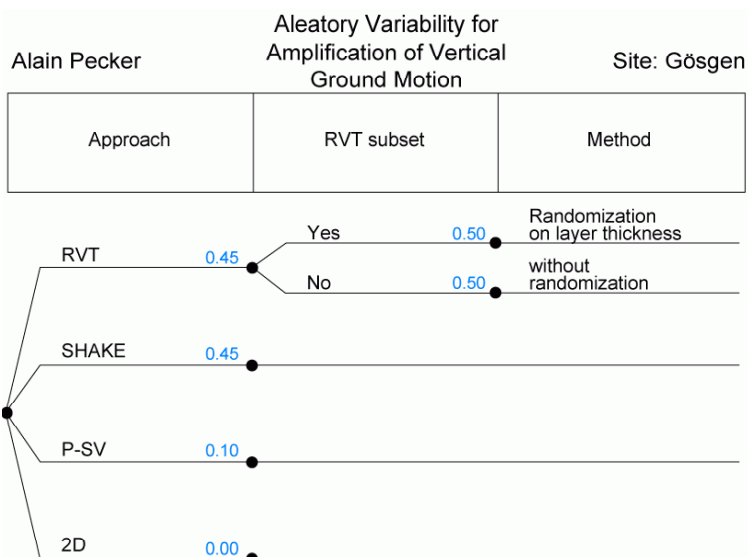


Fig. 26: Logic Tree with aleatory variability for amplification of vertical ground motion for Gösgen

5.6 Leibstadt

5.6.1 Logic Tree for Leibstadt

Figure 27 shows the Logic Tree with aleatory variability for amplification of vertical ground motion for Leibstadt.

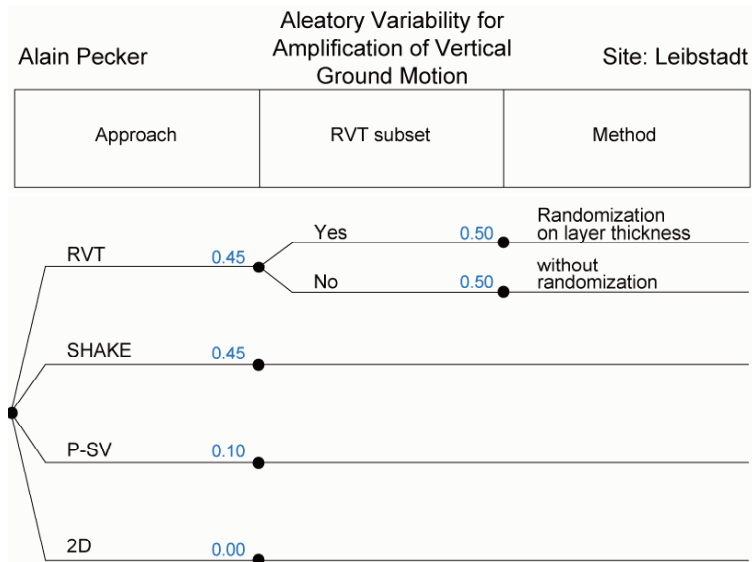


Fig. 27: Logic Tree with aleatory variability for amplification of vertical ground motion for Leibstadt

5.7 Mühleberg

5.7.1. Logic Tree for Mühleberg

Figure 28 shows the Logic Tree with aleatory variability for amplification of vertical ground motion for Mühleberg.

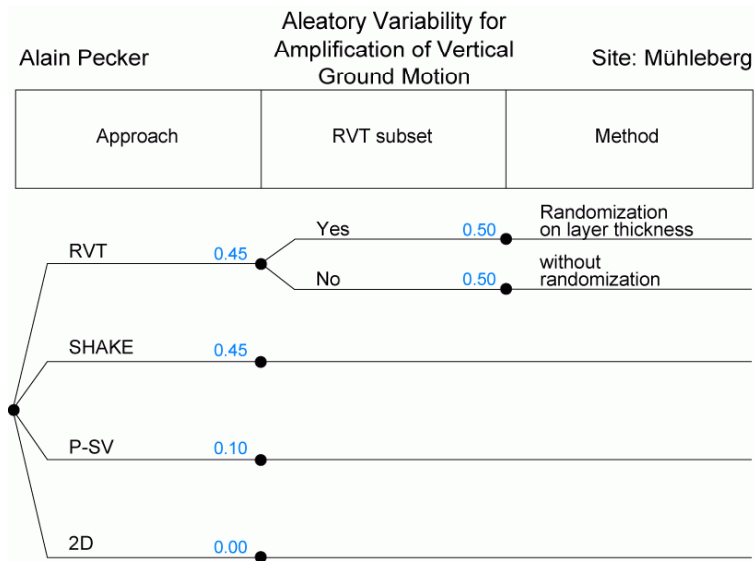


Fig. 28: Logic Tree with aleatory variability for amplification of vertical ground motion for Mühleberg

6 MAXIMUM GROUND MOTIONS

6.1 Horizontal Component

There does not exist a well established method to estimate the maximum ground motion that a soil profile can transmit to the ground surface. However, it is recognized and well admitted that the soil cannot transmit arbitrarily large motion due to its limited shear resistance capacity. This maximum motion can be estimated from numerical analyses as those carried out for the four NPP sites with increasing input motions, from theoretical models based on an assumed soil constitutive behavior and from experimental evidences gathered during actual earthquakes. All these approaches are taken into account in the foregoing evaluation.

6.1.1 Evaluation of Proponent Models

6.1.1.1 Maximum peak ground acceleration

The numerical analyses have been carried out by Geodeco with increasing values of the input motion at the bedrock level. These results are presented in PEGASOS TP3-TB-0048 and TP3-TN-0353. These values have been used in the theoretical model developed (figure 19 in TP3-TN-0354) and are summarized below for convenience:

- Leibstadt: 11.5 m/s²
- Beznau: 23.0 m/s²
- Gösgen: 13.0 m/s²

Two theoretical models are available for the evaluation of the maximum pga; they are presented in PEGASOS TP3-TN-0354: the first one (Pecker) has been developed specifically for this study and the second one (Betbeder) is published in the literature. The applications of both models to the four NPP sites are given in table 3 (Pecker's model) and in paragraph 3.2 (Betbeder's model) of the document. They are recalled in Table 1 below in m/s².

Tab. 1: Maximum peak ground accelerations of the NPP sites according to Pecker's and Betbeder's models

	Pecker's model	Betbeder's model
Leibstadt	15.7	12.9
Beznau	13.2	6.0
Gösgen	13.7	11.6
Mühleberg	15.9	10.4

The observed motion during actual earthquakes have been reviewed by D. Fäh and presented in PEGASOS TP3-TN-0359. The results presented in figure 1 of his report do not allow for a definite conclusion since some results may seem controversial regarding the relationship between geology and maximum pga. This is probably due to the fact that the data represents the maximum recorded motion on a given site but not necessarily the maximum ground motion that the site can sustain. It can, however, be noted that the results are not in contradiction with those obtained by the other approaches.

6.1.1.2 Response spectra

Linear site response analyses have been performed by P.Y. Bard and the results presented in PEGASOS TP3-TN-0358; the soil properties used for those analyses are "reduced" shear moduli and high damping ratios, which is relevant for a near failure condition. From the response spectra computed at the ground surface we have derived normalized spectral shapes for each of the four NPP sites. These spectral shapes are based on the median response spectrum at the ground surface; they are defined by a set of controlled frequencies, related to the eigenfrequencies of the soil column (computed in PEGASOS TP3-TN-0354), and by amplification factors for the pseudo-acceleration.

If f_i , ($i = 1,3$) are the first three eigenfrequencies of the soil column, the values of which are given in paragraphs 2.6 to 2.9 of PEGASOS TP3-TN-0354, the controlled frequencies are respectively:

$$f_a = 0.5 f_1, f_b = 0.8 f_1, f_c = 0.5 (f_1 + f_2), f_d = f_3, f_e = 10 f_1$$

For convenience, the values of the first three eigenfrequencies are recalled in Table 2.

Tab. 2: First three theoretical natural frequencies of the NPP sites

Frequencies	f_1 (Hz)	f_2 (Hz)	f_3 (Hz)
Beznau	0.97	2.44	3.85
Gösgen	0.56	1.41	2.27
Leibstadt	0.43	1.08	1.72
Mühleberg	0.88	2.04	3.22

The amplification factors at the controlled frequencies are respectively 0.8, 1.5, 3.0, 3.0, 1.0. It must be noted that these amplification factors are not consistent with the amplification factors from the observed data collected in PEGASOS TP3-TN-0359; however, if these amplification factors are multiplied by the maximum peak acceleration, the resulting maximum spectra are not exceeded by the maximum observed motions. In addition, the values of the amplification factors have been compared to the values obtained from the non linear site response analyses; the overall agreement is fair.

Figures 29 to 32 present the normalized spectral shapes computed according to this approach and compare them to the computed surface response spectra for the 4 NPP.

6.1.2 Logic Tree Structure

Each of the approaches listed above corresponds to a different branch of the logic tree. Depending on the degree of confidence in the approaches different weights are assigned for the branches. The logic tree applies to the determination of the peak ground surface acceleration. Once this value is determined, a normalized spectral shape is anchored to the pga.

In order to reflect the uncertainty in the determination of the soil resistance, to each of the three main branches of the logic tree, three sub-branches are added: the main sub-branch corresponds to the maximum pga given in 6.1.1.1; the two additional sub-branches correspond to maximum peak ground accelerations equal to 0.85 and 1.25 times the previous values.

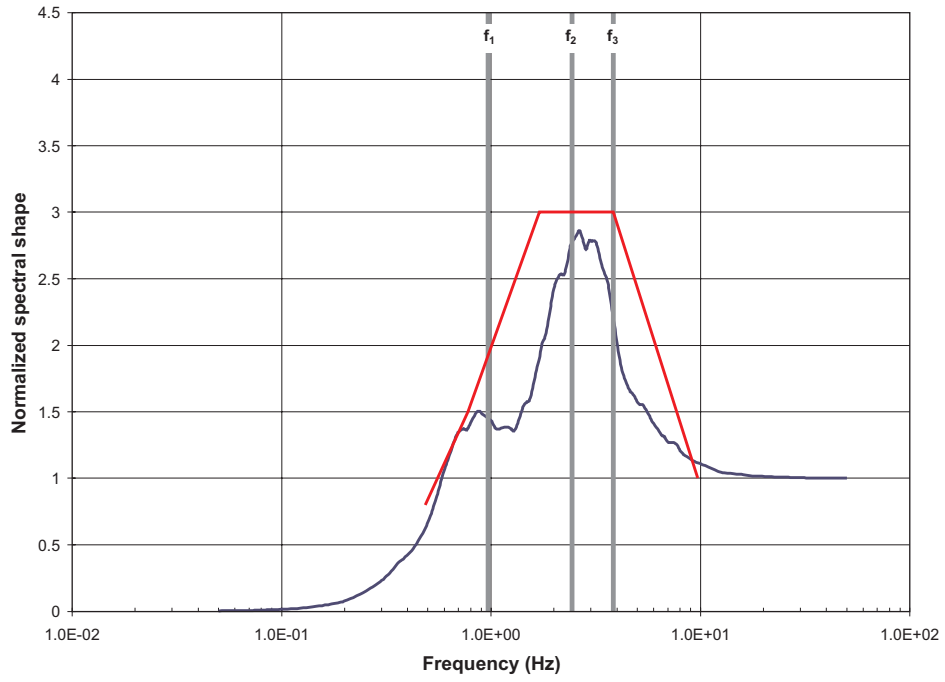


Fig. 29: Normalized spectral shape for Beznau

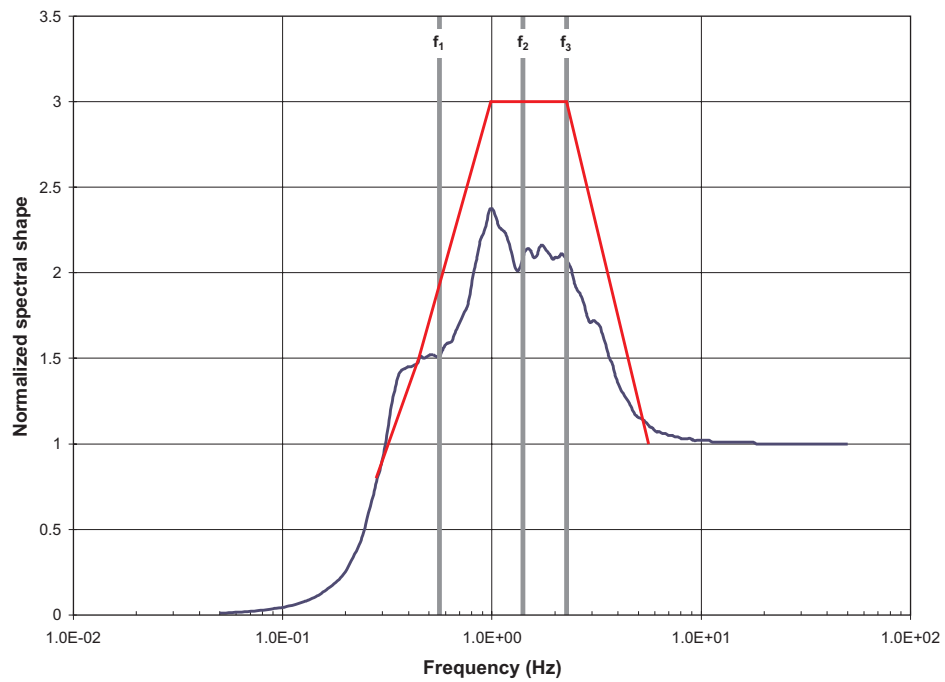


Fig. 30: Normalized spectral shape for Gösgen

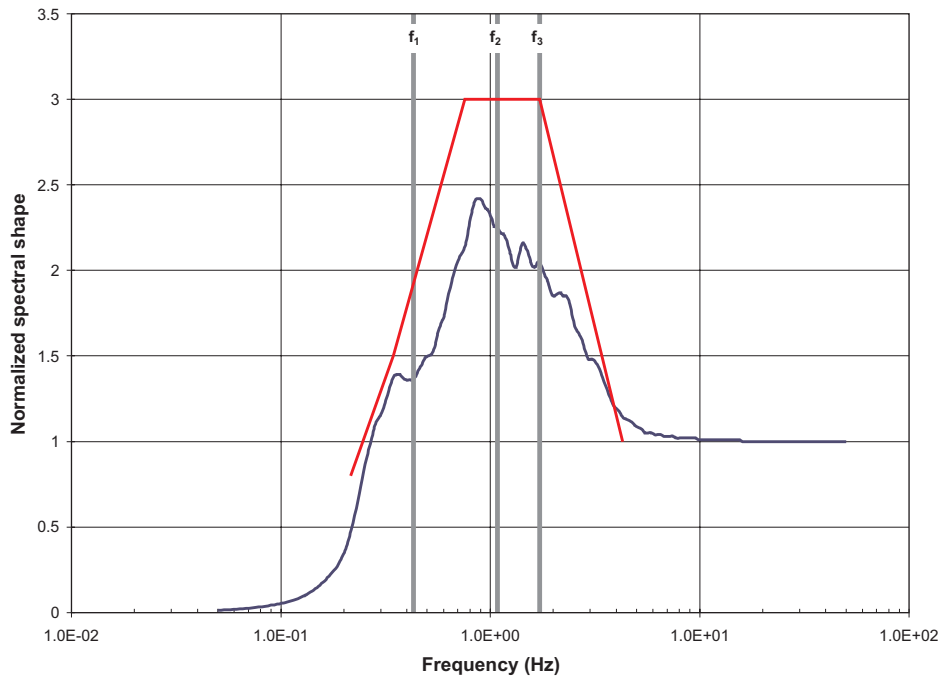


Fig. 31: Normalized spectral shape for Leibstadt

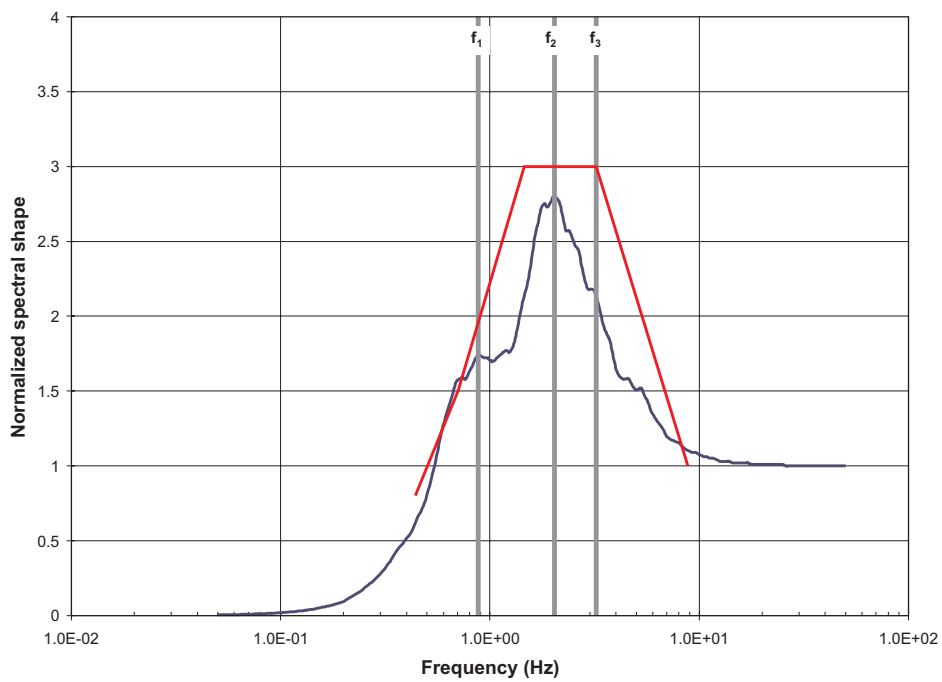


Fig. 32: Normalized spectral shape for Mühleberg

6.1.3 Weights for Maximum Ground Motions

For all sites, the same weights are assigned to the various branches of the logic tree. They are listed below:

- Non linear site response calculations (Pelli's reports): 45 %
- Theoretical model (Pecker's model): 45 %
- Theoretical model (Betbeder's model): 10 %

The rationale for the values given above is that the non linear site response analyses and Pecker's theoretical model do not contradict the observations; furthermore, they account for the soil resistance which controls the maximum ground motion. They are assigned the same weight because if, on one hand, Pecker's model is probably more accurate for the evaluation of the soil resistance because the parameters entering the model are reliable and easy to estimate, it is obviously more crude than Pelli's model with respect to the variation with depth of the soil properties. On the other hand, the parameters entering the constitutive model used by Pelli involves more uncertainty. It is believed that both phenomena more or less compensate, hence the equivalent weights.

Betbeder's model is assigned a rather low weight because it has been shown (PEGASOS TP3-TN-0354) that in some instances it underpredicts the observations; in addition the constitutive model implicitly used in the model involves parameters which are very uncertain.

For the sub-branches the weight are as follows: the main sub-branch corresponds to the maximum pga given in section 6.1.1.1 and is assigned a weight of 80 %; the two additional sub-branches are assigned weights of 10 % each and correspond to maximum peak ground accelerations equal to 0.85 and 1.25 times the previous values.

The range of values (0.85 to 1.25) is based on the finding that, given the range of eigenfrequencies recalled in Table 2, the spectral relative velocity is constant for small variations of the soil stiffness (which is proportional to the soil strength) and subsequently, the maximum peak ground acceleration is proportional to the soil strength for all four sites. For an average friction angle of 42° , the proposed range of variation corresponds to friction angles included between 37° and 48° ; this range is an upper bound of the conceivable range for the materials encountered at the four NPP, and would be associated to a median plus two sigma value.

6.2 Vertical Component

For the horizontal motion, there is a physical background for limiting the maximum surface motion. The vertical motion is associated mainly with P waves traveling through the soil deposit. Granular soils do not exhibit a failure condition, which would limit the transmitted stresses, for stress paths corresponding to uniaxial compression-tension; this is especially obvious when the soil is saturated because the P wave travels through the fluid. Therefore, there is no reason for limiting the maximum vertical ground surface motion.

7 GROUND MOTION AT DEPTH

It is requested that the ground motions be computed at two different depths at each site: the mean buildings depth and the maximum buildings depth. These depths are listed in Table 3.

Tab. 3: Mean and maximum building depths for the NPP sites

	Beznau	Gösgen	Leibstadt	Mülheberg
Mean building depth	-6 m	-5 m	-5 m	-7 m
Maximum building depth	-15 m	-9 m	-10 m	-14 m

7.1 Median amplification of horizontal ground motion

The derivation of the logic tree for the ground motions at depth follows the same line of reasoning as for the ground surface motion, therefore preserving the structure of the logic trees. Nevertheless some adaptations are required to account for the missing information. That information relates to the outcropping motions in the non linear analyses.

The branches of the logic trees remain the same with the same weights, because it has been checked that the control parameters (strains converted to peak ground accelerations and frequencies) are identical to those of the surface motion. This result could have been anticipated because, as a matter of fact, the same soil column is analyzed; only the processing of the output data is different.

For the RVT and SHAKE runs the amplification factors of the surface motions are just replaced by the amplification factors of the outcrop motions at depth; these amplification factors are readily available from the numerical simulations.

For the non linear analyses, only the amplification factors for the surface motion and the within motion at depth are available. To estimate what would be the outcrop amplification factors from the non linear runs (would this information have any meaning), two options are available:

- Either, use the ratio between the outcrop motion and the surface motion from the SHAKE (or RVT) runs, and apply the same ratio to the non linear surface motions;
- Or, use the ratio between the outcrop motion and the within motion from the SHAKE (or RVT) runs, and apply the same ratio to the non linear within motions.

Both options have been tested on a single site and for a given rock acceleration; the site chosen for the tests is Gösgen and the rock acceleration is equal to 1.5 g. This choice is guided by the fact that the non linear analyses, soil profile, and input time histories have already been used for the non linear site response analyses at Gösgen (PEGASOS TP3-TN-0205, July 2002). For the two analyzed depths, the amplification factors have been computed for the following cases:

- Outcrop / within for the SHAKE analysis
- Outcrop / surface for the SHAKE analysis
- Within / surface for the SHAKE analysis
- Within / surface for the non linear analysis

The results are presented in the next two Figures 33 and 34.

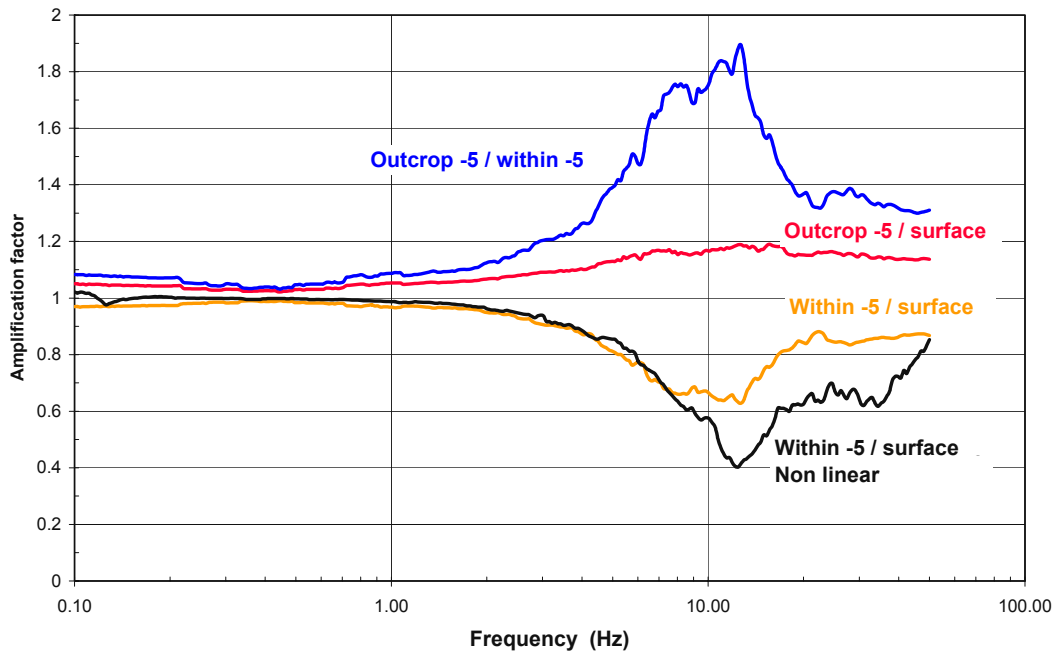


Fig. 33: Gösgen – Depth 5 m – Rock acceleration 1.5 g

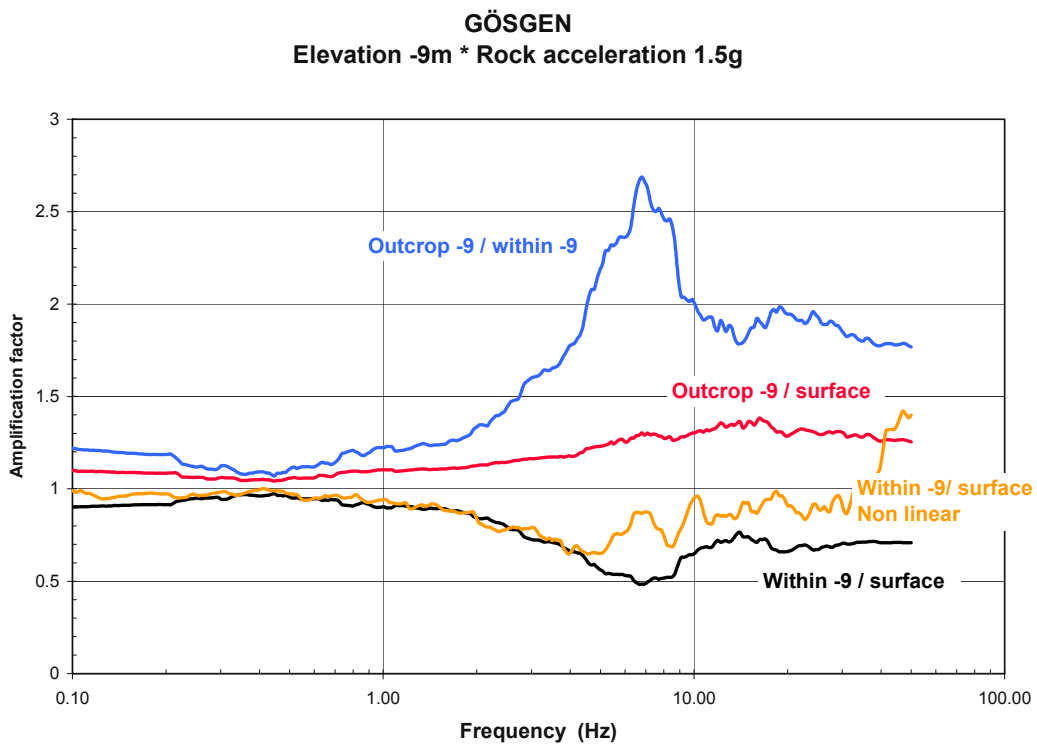


Fig. 34: Gösgen – Depth 9 m – Rock acceleration 1.5 g

Examination of the two previous figures shows that the overall behavior is not essentially different between the equivalent linear analyses and the non linear ones for the ratios within/surface, although the values themselves are different. This finding more or less justifies the use of the trends computed from the equivalent linear analyses to estimate the outcrop motion from the non linear analyses.

Also obvious from the figures is that the ratio outcrop/surface presents a smoother variation with frequency than the ratio outcrop/within. This also has been observed in all the figures prepared by Proseis for different sites and rock accelerations.

Therefore it is recommended, for the non linear analyses to use the ratios outcrop/surface derived from the SHAKE analyses and to apply them to the amplification factors computed at the ground surface in the non linear analyses.

Along the same lines as for the surface motion, the interpolation procedure for the missing runs will be the same:

Since all cases are computed for the RVT runs, no interpolation is needed for those runs to compute the ratios outcrop/surface. Since no magnitude dependence is assumed in our model, these ratios should be taken equal to the arithmetic mean of the ratios for the three magnitudes. These results are used to fit a polynomial equation through all the data points: if n is the number of data points, the degree of the polynomial equation is $(n - 1)$. This polynomial equation is obtained for each frequency as a function of the p_{ga} . For the SHAKE analyses, interpolations between calculated cases should be made on the basis of the RVT runs without randomization : the same polynomial function is used with the three SHAKE data points but is anchored at the appropriate level (equation 6). Further on, the interpolated, or extrapolated, ratios of amplification factors from the SHAKE runs will be applied to the surface amplification factors from the non linear runs to obtain the outcrop amplification factors for the non linear runs.

For the only site for which 2D effects are incorporated in the median amplification (Leibstadt), the same amplification factors as for the surface motions are used; this is based on the fact that the amplification is created by the cliff geometry that is much higher than the buildings depths.

7.2 Median amplification of vertical ground motion

The logic tree for the mean vertical motion is kept unchanged, except for the amplification factors which are the outcrop amplification factors.

7.3 Aleatory variability of horizontal ground motion

The logic trees are kept unchanged, referring now to the outcrop motions. Furthermore, the variability associated with P-SV effects and 2D effects calculated for the surface motions are used for the outcrop motions, even if the analyzed depth is in the "rock" formation.

7.4 Aleatory variability of vertical ground motion

No changes are implemented to the logic trees developed for the surface motion, except for the amplification factors which are those of the outcrop motions.

7.5 Maximum horizontal ground motion

The maximum ground motions at depths have been computed in document "Maximum ground motions-Sensitivity studies and ground motions at depth" (TP3-TN-0403). Two different approaches have been used: a theoretical model and the non linear finite element site response analyses. Both evaluations refer to within ground motions. It has been noted in the previously mentioned document that the evaluations derived from the theoretical model certainly overestimate the attenuation with depth especially for depths located close to the bedrock interface. From those evaluations it appears that the attenuation in the peak ground acceleration should range from factors of 1.0 to 2.0. The lower attenuation factor is applicable to the shallow depth, whereas the larger one is applicable to the deeper depth. Given the fact that these attenuation factors are based on within-motions, they have to be amplified to go from the within-motion to the outcrop-motion. Figures 33 and 34 show that this amplification factor could be in the range of 1.2 (for shallow depths) to 1.7 (for deeper depths). Multiplying both factors would give a net multiplication factor of 0.8 (1.7/2.0) to 1.2 (1.2/1.0) to be applied to the maximum ground surface motion. Since the depths of interest are rather close to the ground surface, a large reduction in the maximum ground surface motion does not seem appropriate; this is clearly evidenced by the SHAKE runs, at high rock acceleration, where the ratios outcrop/surface are in the range 0.8 to 1.2. Therefore it is proposed to use the maximum ground surface motion as a base case and to add, at the end of the logic tree for maximum ground motions, 3 branches with weights 80 %, 10 % and 10 %. These branches are respectively associated with multiplication factors of 1.0, 0.8 and 1.2 applied to the base case.

The response spectra for the maximum outcropping ground motions have the same normalized shapes as for the surface motions and are anchored at the appropriate pga.

7.6 Maximum vertical ground motion

No maximum bound is put on the vertical motion, like for the surface motion.

8 REFERENCES

- Assimaki, D., Pecker, A., Popescu, R. & Prévost, J.H. 2003: Effects of spatial variability of soil properties on surface ground motion. *Journal of Earthquake Engineering* 7, Special issue 1, 1-44.
- Assimaki, D., Kausel, E., & Whittle, A. 2000: Model for dynamic shear modulus and damping for granular soils. *Journal of Geotechnical and Geoenvironmental Engineering* 126, N10, 859-869.
- Bard, P.Y. 2003: A short note on the reliability of SHAKE amplification factors at low frequencies (March 2003). PEGASOS TP3-TN-0340.
- Betbeder-Matibet, J. 1993: Calcul de l'effet de site pour une couche de sol. Troisième Colloque National de Génie Parasismique, Saint-Rémy-lès-Chevreuse 1, DS1-DS10 (March 1993).
- Martin, P.P. 1975: Non linear methods for dynamic analyses of ground response. PhD thesis, University of California, Berkeley.
- Mohammadioun, B. & Pecker, A. 1984: Low frequency transfer of seismic energy by superficial soil deposits and soft rocks. *Earthquake Engineering and Structural Dynamics* 12, 537-564.
- PEGASOS TP3-ASW-0024: Hölker, A.: Matlab software package and databases for the computation of the SP3 / site amplification models.
- PEGASOS TP3-RF-0310: Bard, P.Y. 2002: Variability of 1D-response for the 4 NPP sites under plane, oblique, SH, SV and P incidence.
- PEGASOS TP3-TB-0048: Pelli, F. 2002: Nonlinear Site Response Analyses for Beznau, Gösgen, Leibstadt.
- PEGASOS TP3-TN-0167: Fäh, D. 2002: Spectral Amplification for SH-and PSV waves at sites Beznau, Gösgen and Leibstadt.
- PEGASOS TP3-TN-0186: Bard, P.Y. 2002: 2D SH computations for the Leibstadt nuclear power plant site Amplification factors in the low and high strain cases.
- PEGASOS TP3-TN-0205: Pecker, A. 2002: Gösgen Nuclear Power Plant Site, True Nonlinear Site Response Analysis.
- PEGASOS TP3-TN-0340: Bard, P.Y. 2003: A short note on the reliability of SHAKE amplification factors at low frequencies.
- PEGASOS TP3-TN-0353: Pelli, F.: Additional Nonlinear Site Response Analyses for Beznau and Gösgen at a high shaking level considering cyclic mobility effects.
- PEGASOS TP3-TN-0354: Pecker, A. 2003: Evaluation of Maximum Ground Motions.
- PEGASOS TP3-TN-0358: Bard, P.Y.: Response spectra associated with maximum peak ground acceleration for the 4 PEGASOS sites.
- PEGASOS TP3-TN-0359: Rippberger, J. & Fäh, D. 2003: Maximum Recorded Horizontal and Vertical Ground Motions.
- PEGASOS TP3-TN-0401: Hölker, A.: Summarizing the SP3 site effect models to Soil hazard Input Files (SIFs).
- PEGASOS TP3-TN-0403: Pecker, A.: Pegasos-Maximum Ground Motions-Sensitivity Studies and Motions at Depth, Rev. A.

APPENDIX 1 EG3-HID-0051 SITE AMPLIFICATION AT THE SURFACE AND EMBEDDED LAYER DEPTHS FINAL MODEL A. PECKER

A1.1 Introduction

This document describes the implementation of Alain Pecker's models of site amplification at the surface, mean and maximum building depths (Table A-1) as well as his assessment of maximum possible ground motions at the four Swiss NPP sites: Beznau, Gösgen, Leibstadt and Mühleberg. The purpose of this document is to translate the expert's evaluation of amplification factors into a Soil hazard Input File (SIF) for the hazard computation software (SOILHAZP) and to provide the expert with the necessary information to review the results of his model.

The implementation of Alain Pecker's model is based on the July 14th 2003 (surface) and November 13th (embedded layers) versions of his elicitation summary (EG3-ES-0039) and additional clarifications.

The following document and software are directly linked to this HID:

- TP3-TN-0401: A technical note describing the computational steps performed to create the soil hazard input files (SIFs)
- TP3-ASW-0024: The software used to implement the SP3 models

This HID consists of four sub-sections:

- A description of the computational steps leading to the development of amplification factor spectra and their associated aleatory variabilities for each site and combination of magnitudes, input PGAs and ground motion types.
- A description of the expert's assessment of maximum ground motion spectra.
- A summarized description of creation of SIFs for site amplification, the associated aleatory variability. A detailed description is available in the technical note TP3-TN-0401.
- The generalized logic tree for horizontal ground motion.

The implementation of Alain Pecker's model was done by the SP3 TFI Team at Proseis using Matlab R13. The complete implementation is archived as TP3-ASW-0024. It consists of a software module and a database.

Tab. A-1: Mean and maximum building depth for the four Swiss NPP sites

	Beznau	Gösgen	Leibstadt	Mühleberg
Mean building depth	6 m	5 m	5 m	7 m
Max. building depth	15 m	9 m	10 m	14 m

A1.2 Site amplification and its aleatory variability

In this section the key-elements of Alain Pecker's model are outlined, the crucial aspects are detailed, and the results are illustrated by means of a single example figure per computational step. Figures showing the results for all cases and sites are available as an electronic appendix in PDF format. The logic tree architecture is detailed in the elicitation summary. Crucial aspects of the logic tree are reviewed here and a generalized display of the tree for horizontal ground motion is given at the end of this HID. The results given in this section are an intermediate product, since they are summarized to discrete fractiles and associated with spectral accelerations before being used as an input for the soil hazard computations.

A1.2.1 Amplification of horizontal ground motion

Amplification factors for the surface and the embedded layer depths are based in Alain Pecker's model on RVT base case, SHAKE and non-linear (NL) simulations. In the case of embedded layers the RVT and SHAKE simulations of outcropping motion have been used. In order to obtain an estimate of NL amplification factors for outcropping motion at the embedded layers, the NL surface motion simulations are modified by the ratio $\text{SHAKE}_{\text{outcrop motion}} / \text{SHAKE}_{\text{surface motion}}$. The weighting of the different approaches depends on the input PGA level and the frequency considered. It is the same for the surface and embedded layer cases. Generally Alain Pecker considers amplification factors to be independent of the earthquake magnitude. Regardless of the considered magnitude, the arithmetic mean of the available simulations for magnitudes 5, 6 and 7 is used. 2D effects are only considered for Leibstadt site. They are based on Pierre-Yves Bard's models (TP3-TN-0186).

SHAKE simulations at intermediate PGA levels are estimated for each individual frequency based on the existing RVT base case. A polynomial best fit over all PGA levels is derived for the RVT base case (10 points) and then applied, minimizing the error, to the three SHAKE points. NL simulations at intermediate PGA levels are estimated using linear interpolation between the available results.

The example in Figure A-1 shows the assessment of alternative amplification factors considered for the mean building depth at NPP Beznau for the case of a magnitude 6 earthquake with PGA on rock of 1.5 g. For corresponding figures showing the results for all other cases and sites see the *Pecker.AF_AVar.<site>.HM<depth>.pdf* files in the appendix. Figure A-2 shows the weighted arithmetic mean amplification factors for mean building depth in Beznau as function of PGA on rock and frequency. For the other sites and magnitudes see the *Pecker.SiteModAF.<site>.HM<depth>.pdf*.

A1.2.2 Aleatory variability of amplification of horizontal ground motion

The aleatory variability is considered to be independent of magnitude as in the case of site amplification, but it is developed in a logic tree completely decoupled from that for site amplification.

The aleatory variability values associated with the SHAKE computations, the RVT computations, the P-SV effects, and the 2D effects (only Leibstadt) are considered to be alternative representations of the aleatory component. Therefore, they appear as different branches at the same level of the logic tree. Since the NL methods use a subset of the 15 time histories that were used for the SHAKE computations, no aleatory variability is associated with these methods. The aleatory variability of ground motions at the surface and at the embedded layers are considered to be identical. Figure A-3 shows an assessment of the aleatory variability, corresponding to the site amplification case shown in Figure A-1. For the results of all other cases and sites please see the *Pecker.AF_AVar.<site>.HM<depth>.pdf* files in the appendix. For the plots of mean aleatory variability corresponding to that in Figure A-2, see the *Pecker.SiteModAVar.<site>.HM<depth>.pdf* files.

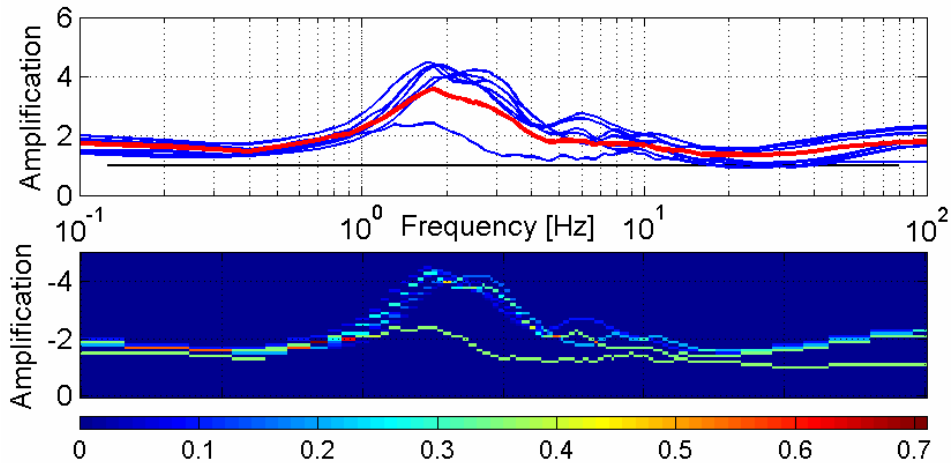


Fig. A-1: Site amplifications factors for horizontal ground motion at the mean building depth of NPP Beznau for the case of a magnitude 6 earthquake with PGA on rock of 1.5 g

The upper plot shows the alternative amplification factors (blue curves) and their weighted mean (red curve). The lower plot shows the distribution of weights in the amplification-frequency space. Corresponding plots are available for all sites and cases in the appendix: See the *Pecker.AF_AVar.<site>.HM<depth>.pdf* files.

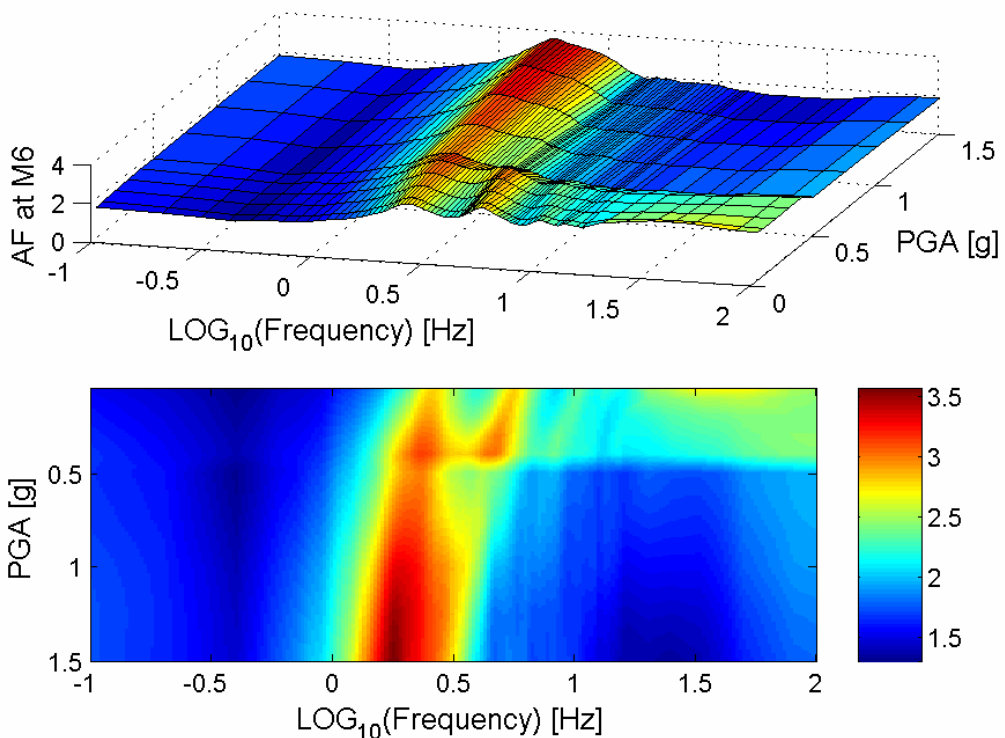


Fig. A-2: Weighted arithmetic mean amplification factors (AF as function of PGA on rock and frequency) for horizontal ground motion of a magnitude 6 scenario at mean building depth of NPP Beznau

Corresponding plots are available for all sites and cases in the appendix: See the *Pecker.SiteModAF.<site>.HM<depth>.pdf* files.

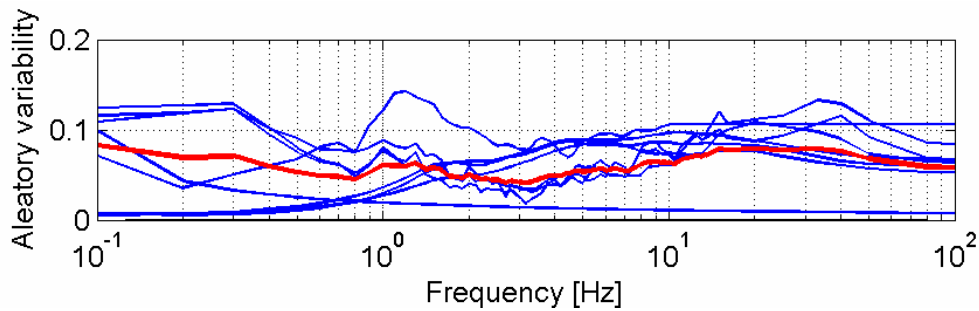


Fig. A-3: Aleatory variability of amplifications factors for horizontal ground motion at the mean building depth of NPP Beznau for the case of a magnitude 6 earthquake with PGA on rock of 1.5 g

The blue curves correspond to the alternative aleatory variabilities and the red curve is the weighted mean aleatory variability. Corresponding plots are available for all sites and cases in the appendix: See the *Pecker.AF_AVar.<site>.HM<depth>.pdf* files in the appendix.

A1.2.3 Amplification of vertical ground motion

The development of amplification factors for vertical ground motion is based on two alternatives: The first one is the assumption that there is no amplification of the rock motion, and the other alternative is the assumption that site effects exist. These two alternatives are developed in the first level of the logic tree. If site effects are considered to be relevant, their quantification is based on the P-wave SHAKE simulations for surface or outcrop motion respectively, which themselves are based on two alternative p-wave degradation methods: a constant bulk modulus and a reduction of V_p by $\sqrt{V_{s'}/V_s}$.

Figures showing the assessment of amplification factors (corresponding to Figure A-1) are available in the files *Pecker.AF_AVar.<site>.VM<depth>.pdf*. Figures showing mean site amplification factors as function of frequency and PGA on rock (corresponding to Figure A-2) are available in the *Pecker.SiteModAF.<site>.VM<depth>.pdf* files.

A1.2.4 Aleatory variability of amplification of vertical ground motion

The development of aleatory variability is based on the uncertainty in the RVT (with and without randomization), P-wave SHAKE, P-SV and 2D models. These uncertainties are considered as alternatives and are assigned specific weights.

Plots of the assessment of aleatory variability of vertical ground motion are available in *Pecker.AF_AVar.<site>.VM<depth>.pdf* and figures showing mean aleatory variability as function of frequency and PGA on rock are given in the *Pecker.SiteModAVar.<site>.VM<depth>.pdf* files.

A1.2.5 Parameter ranges

Alain Pecker's model has been computed for the following input shaking levels (PGA on rock): 0.05, 0.1, 0.2, 0.3, 0.4, 0.5, 0.75, 1.0, 1.25 and 1.5g and for magnitudes 5, 6 and 7. Due to the magnitude independence (generally the arithmetic mean of magnitude 5, 6, 7 simulations was used), the results for the magnitude 5, 6 and 7 computations of Alain Pecker's model are identical. However, for technical reasons, we need the magnitude 5, 6 and 7 results in order to run the parameterization. All SP3 expert models are computed for a set of 76 spectral frequencies. These frequencies are 0.1, 0.2, 0.3, 0.4, 0.5, 0.6, 0.7, 0.8, 0.9, 1, 1.1, 1.2, 1.3, 1.4,

1.5, 1.6, 1.7, 1.8, 1.9, 2, 2.1, 2.2, 2.3, 2.4, 2.5, 2.6, 2.7, 2.8, 2.9, 3, 3.15, 3.3, 3.45, 3.6, 3.8, 4, 4.2, 4.4, 4.5, 4.6, 4.7, 4.8, 5, 5.1, 5.25, 5.5, 5.75, 6, 6.25, 6.5, 6.75, 7, 7.25, 7.5, 7.75, 8, 8.5, 9, 9.5, 10, 10.5, 11, 12, 12.5, 13, 13.5, 15, 16, 20, 25, 33, 40, 50, 80 and 100 Hz.

A1.3 Maximum ground motion at the surface

A1.3.1 Horizontal ground motion

Alain Pecker uses three approaches to determine the maximum possible PGA: after Pelli, Pecker and Betbeder. He then anchors a site-specific synthetic spectrum at these PGA values. In contrast to the surface layer, an additional sub-branching with three uncertainty factors is introduced for the case of the embedded layer depths, in order to account for the additional uncertainty.

The resulting alternative maximum ground motion spectra are shown in the appendix in the files *Pecker.MaxGM.AllSites.HM<depth>.pdf*, where the blue curves represent the alternative maximum ground motion spectra and where the red curve corresponds to the weighted mean of the alternative spectra. Figure A-4 shows the assesment of maximum horizontal ground motion for the surface at Beznau.

A1.3.2 Vertical ground motion

For the case of P-waves Alain Pecker does not see a physical reason for limiting the maximum surface motion. Therefore no maximum ground motion limit is specified.

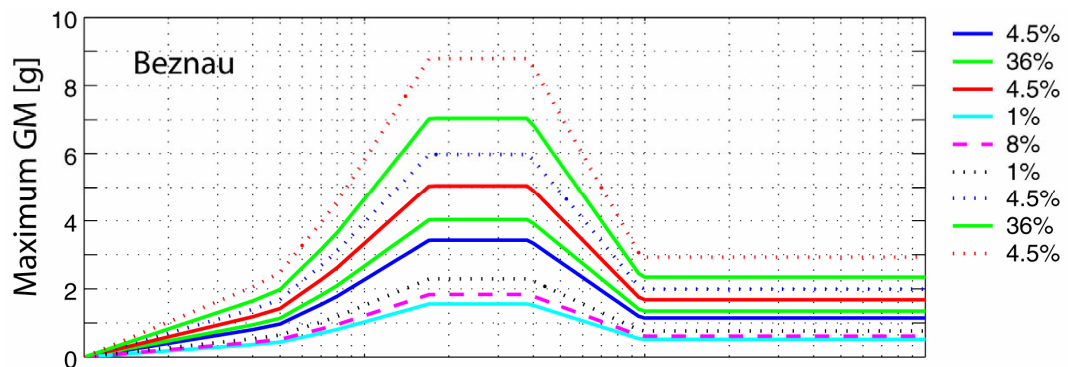


Fig. A-4: Assessment of maximum horizontal ground motion at the surface layer of NPP Beznau

Figures showing maximum ground motion spectra for the embedded layers at Beznau and the other NPP sites are available in the appendix in the files *Pecker.MaxGM.AllSites.HM<depth>.pdf*.

A1.4 Soil hazard input files (SIFs)

The compilation of SIFs of the site amplification factors and their aleatory variability requires two computational steps, whereas the results of maximum ground motion assessment are used directly. The two computational steps are firstly the association of site amplification factors and their aleatory variability with spectral accelerations of the underlying input motions, and

secondly summarizing site amplification and variability to a set of discrete fractiles. Both steps are outlined below and described in detail in the technical note TP3-TN-0401.

A1.4.1 Associating site amplification factors with input spectral accelerations

The amplification factors and their aleatory variability (Section 2) are modeled for a set of input shaking levels (PGA on rock), a set of magnitudes, and a set of frequencies. In order to apply them to the rock hazard results, which are modeled for different spectral accelerations on rock and combinations of magnitudes and distances, the amplification factors must be associated with a spectral acceleration corresponding to the particular input shaking level (PGA) and considered frequency. The spectral acceleration is derived from the spectral shape of the input motion, which underlies the simulation of the amplification factors (figures 1 and 2 in TP3-TN-0401). In this first step, every single amplification factor is assigned a spectral acceleration (on rock) to which it can be applied.

A1.4.2 Summarizing epistemic uncertainty

The epistemic uncertainty in the expert's assessments of site amplification and aleatory variability is expressed by the branch tips and weights. For the soil hazard computations these branch tips are summarized to 17 discrete fractiles of both site amplification and aleatory variability, which is necessary in order to interpolate the data for any spectral acceleration and magnitude occurring in the rock hazard results. By using discrete fractiles no assumptions are made regarding the shape of the distribution of epistemic uncertainties. The 17 fractiles used are: 0.13 %, 0.62 %, 2.28 %, 5 %, 10 %, 20 %, 30 %, 40 %, 50 %, 60 %, 70 %, 80 %, 90 %, 95 %, 97.72 % (2 sigma), 99.38 % (2.5 sigma), and 99.87 % (3 sigma).

For the soil hazard computations these fractiles are associated with a weight and are considered as alternative models in the same way, as the original results from the branch tips represent alternative models each of which associated a weight.

A1.4.3 Plots of the soil hazard input files

Figure A-5 shows an example of the SIF of site amplification for horizontal ground motion of 4 Hz at Beznau at mean building depth. Plots showing the SIFs for site amplification and aleatory variability in all cases (sites and spectral frequencies) are available as PDF files in the appendix: *Pecker.SIFaf.<site>.<motion-depth>.pdf* and *Pecker.SIFavar.<site>.<motion-depth>.pdf*

A1.5 Logic tree for horizontal ground motion

A generalized view of the logic tree for horizontal ground motion is given in Figure A-6. Differences between the sites are restricted to parameters and the weighting of individual branch tips, but the overall structure is same for all sites. The only exceptions forms the consideration of 2D effects, which is only included for the case Leibstadt.

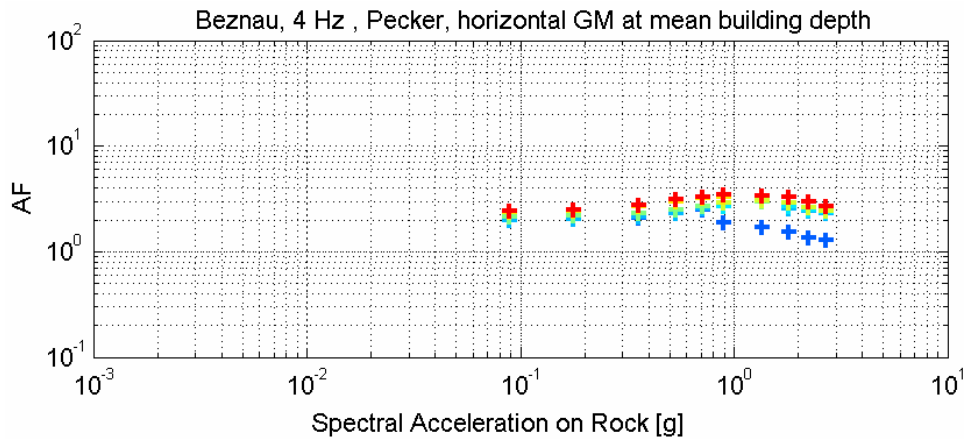


Fig. A-5: Summarized model of site amplification factors for ground motion of 4 Hz at mean building depth at NPP Beznau and earthquake magnitudes 5, 6 and 7

The crosses represent the results of the expert model after summarizing the epistemic uncertainty to 17 fractiles. The color-coding corresponds to these fractiles. In fact several fractiles are plotted on top of each other, since the model contains less epistemic uncertainty than sampled by the 17 fractiles. Linear interpolation and nearest neighbor extrapolation respectively will be performed in the hazard software to obtain amplification factors for any spectral acceleration on rock and any considered earthquake magnitude. The full set of figures is available in the appendix in the files *Pecker.SIFaf.<site>.<motion-depth>.pdf* and *Pecker.SIFavar.<site>.<motion-depth>.pdf*.

A1.6 Appendix

The appendix is available only in electronic form on CD-ROM. All figures are stored as PDF files. The files are named according to the convention: *<expert>.<content>.<site>.<motion><depth>.pdf*. Contents are *AF_AVAR* (assessment of site amplification and aleatory variability), *SiteModAF* (mean site amplification factors), *SiteModAvar* (mean aleatory variability), *SIFaf* (amplification factors as input to the soil hazard computations), *SIFavar* (parameterized aleatory variability as input to the soil hazard computations), and *MaxGM* (maximum ground motion, also input to the soil hazard computations). Motions are *HM* for horizontal ground motion and *VM* for vertical ground motion. Depth codes are *surf* for surface, *d1* for mean building depth and *d2* for the maximum building depth.

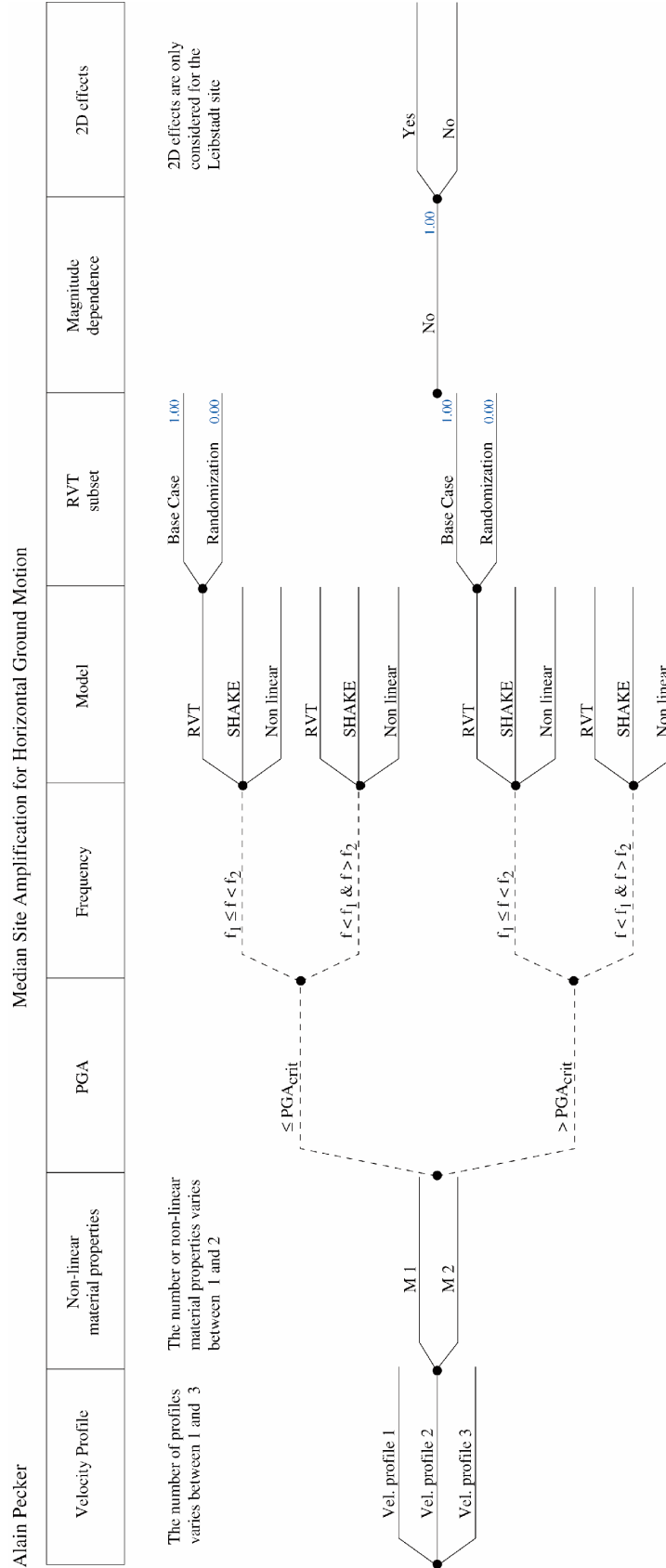


Fig. A-6: General logic tree structure for horizontal ground motion
 Dashed lines indicate conditional branches rather than alternative branches.

Part IV:

Site Response Characterisation, Elicitation Summary

Dr. Jost A. Studer

Studer Engineering,
Zürich – Switzerland

Probabilistische Erdbeben-Gefährdungs-Analyse für die KKW-Stand Orte
in der Schweiz (PEGASOS)

SP3 Site Response Characterisation

Elicitation Summary

Jost A. Studer

Studer Engineering,
Zürich – Switzerland



TABLE OF CONTENTS

TABLE OF CONTENTS	1
LIST OF TABLES	6
LIST OF FIGURES	7
1 INTRODUCTION	9
2 MEDIAN AMPLIFICATION OF HORIZONTAL GROUND MOTION	9
2.1 Approach	9
2.2 Logic Tree Structure	9
2.3 Model Evaluations Common to All Sites	11
2.3.1 Maximum Input ground motion	11
2.3.2 Velocity profiles	11
2.3.3 Non-linear material properties	11
2.3.4 Method: SHAKE vs. RVT	11
2.3.5 Method: True nonlinear calculations 2.5 g	12
2.3.6 Magnitude dependence of site amplification	13
2.3.7 Correction Factors for non-linearity	15
2.3.8 Effect of inclined waves	16
2.3.9 Correction for 2D-effects	16
2.4 Beznau	16
2.4.1 Logic Tree for Beznau	16
2.4.2 Site-Specific Model Evaluations for Beznau	18
2.4.2.1 Alternative velocity profiles	18
2.4.2.2 Alternative non-linear properties	19
2.4.2.3 SHAKE vs. RVT	19
2.4.2.4 RVT: Use of soil randomization runs	19
2.4.2.5 Magnitude dependence for RVT calculations	19
2.4.2.6 Magnitude dependence for SHAKE calculations	19
2.4.2.7 Use of results from non-linear sensitivity runs (correction factor for non-linearity) in RVT and SHAKE branches	20
2.4.2.8 Use of results from 2-D sensitivity runs	21
2.5 Gösgen	21
2.5.1 Logic Tree for Gösgen	21
2.5.2 Site-Specific Model Evaluations for Gösgen	22
2.5.2.1 Alternative velocity profiles	22
2.5.2.2 Alternative non-linear properties	23
2.5.2.3 SHAKE vs. RVT	23
2.5.2.4 RVT: Use of soil randomization runs	23
2.5.2.5 Magnitude dependence for RVT calculations	23
2.5.2.6 Magnitude dependence for SHAKE calculations	23
2.5.2.7 Use of results from non-linear sensitivity runs (correction factor for non-linearity)	24
2.5.2.8 Use of results from 2-D sensitivity runs	25
2.6 Leibstadt	25
2.6.1 Logic Tree for Leibstadt	25
2.6.2 Site-Specific Model Evaluations	27
2.6.2.1 Alternative velocity profiles	27
2.6.2.2 Alternative non-linear properties	27
2.6.2.3 SHAKE vs. RVT	27

2.6.2.4	RVT: Use of soil randomization runs	27
2.6.2.5	Magnitude dependence for RVT calculations	27
2.6.2.6	Magnitude dependence for SHAKE calculations	28
2.6.2.7	Use of results from non-linear sensitivity runs (correct. factor for non-linearity)	28
2.6.2.8	Use of results from 2-D sensitivity runs	29
2.7	Mühleberg	32
2.7.1	Logic Tree for Mühleberg	32
2.7.2	Site-Specific Model Evaluations	33
2.7.2.1	Alternative velocity profiles	33
2.7.2.2	Alternative non-linear properties	33
2.7.2.3	SHAKE vs. RVT	33
2.7.2.4	RVT: Use of soil randomization runs	33
2.7.2.5	Magnitude dependence for RVT calculations	34
2.7.2.6	Magnitude dependence for SHAKE calculations	34
2.7.2.7	Use of results from non-linear sensitivity runs (correction factor for non-linearity)	34
2.7.2.8	Use of results from 2-D sensitivity runs	34
3	MEDIAN AMPLIFICATION OF VERTICAL GROUND MOTION	35
3.1	Approach	35
3.2	Logic Tree Structure	35
3.3	Model Evaluations Common to All Sites	35
3.3.1	Maximum input motion, horizontal component	35
3.3.2	Different methods for computing the vertical site response	36
3.3.2.1	Vertical P-wave (SHAKE)	36
3.3.2.2	NRC NUREG 6728	37
3.3.2.3	V/H ratio from SP2	38
3.4	Beznau	38
3.4.1	Logic Tree for Beznau	38
3.4.2	Site-Specific Model Evaluations	39
3.4.2.1	Approaches for P-wave Degradation	39
3.4.2.2	Vertical component of Profiles 1 and 3	39
3.5	Gösgen	39
3.5.1	Logic Tree for Gösgen	39
3.5.2	Site-Specific Model Evaluations	39
3.5.2.1	Approaches for P-wave Degradation	39
3.5.2.2	Vertical component for Material 2	40
3.6	Leibstadt	40
3.6.1	Logic Tree for Leibstadt	40
3.6.2	Site-Specific Model Evaluations	40
3.6.2.1	Approaches for P-wave Degradation, Material 1	40
3.6.2.2	Vertical component for Material 2	41
3.7	Mühleberg	41
3.7.1	Logic Tree for Mühleberg	41
3.7.2	Site-Specific Model Evaluations	41
3.7.2.1	Approaches for P-wave Degradation	41
3.7.2.2	Vertical component for Material 2	41
3.8	Summary tables of models and weights for the median amplification of vertical ground motion	42
3.8.1	Results for Beznau site	42

3.8.2	Results for Gösgen site	43
3.8.3	Results for Leibstadt site	43
3.8.4	Results for Mühleberg site	44
4	ALEATORY VARIABILITY OF HORIZONTAL GROUND MOTION	45
4.1	Approach	45
4.2	Logic Tree Structure	45
4.3	Beznau	48
4.4	Gösgen	49
4.5	Leibstadt	50
4.6	Mühleberg	51
5	ALEATORY VARIABILITY OF VERTICAL GROUND MOTION	52
5.1	Approach	52
6	MAXIMUM GROUND MOTIONS	53
6.1	General Concept for Horizontal Motion	53
6.1.1	Methods and general law	53
6.1.2	Material Characterisation	53
6.1.3	Site characterisations	54
6.1.4	General Evaluation of Proponent Models	55
6.2	Logic Tree and Weights for Horizontal Motion	56
6.2.1	Soil mechanics model branch	56
6.2.1.1	Maximum pga Surface	56
6.2.1.2	Maximum pga, at mean elevation	57
6.2.1.3	Maximum pga, at minimum Elevation	57
6.2.1.4	Spectral shape for all sites and elevations	58
6.2.2	Non-linear branch	58
6.2.2.1	Beznau and Gösgen	58
6.2.2.2	Leibstadt	59
6.2.2.3	Mühleberg, Horizontal Motion	59
6.3	General Concept for Vertical Motion	59
6.3.1	Methods	59
6.3.2	Material Characterisation	60
6.4	Logic Tree and Weights for Vertical Motion	60
6.4.1	Surface, mean and minimum elevation	60
6.4.2	Beznau, Vertical Motion; Surface, mean and minimum elevation	60
6.4.3	Gösgen, Vertical Motion; Surface, mean and minimum elevation	60
6.4.4	Leibstadt, Vertical Motion	61
6.4.4.1	Characteristics of soil profile	61
6.4.4.2	Logic tree	61
6.4.4.3	Surface	62
6.4.4.4	Mean and minimum elevation	62
6.4.5	Mühleberg, Vertical Motion; Surface, mean and minimum elevation	62
7	REFERENCES	63

APPENDIX 1: MEDIAN AMPLIFICATION OF HORIZONTAL GROUND MOTION	65
A1.1 Beznau, Magnitude dependence for RVT calculations	65
A1.1.1 Profile 2, Material 1	65
A1.1.2 Profile 3	66
A1.2 Beznau, Magnitude dependence for SHAKE calculations	67
A1.2.1 Profile 1, Material 1	67
A1.3 Beznau, Use of results from non-linear sensitivity runs	68
A1.3.1 RVT runs, Profile 1	68
A1.3.2 SHAKE runs, Profile 1	69
A1.4 Gösigen, Magnitude dependence for RVT calculations	70
A1.4.1 Profile 1, Material 1	70
A1.4.2 Profile 1, Material 2	71
A1.5 Gösigen, Magnitude dependence for SHAKE calculations	72
A1.5.1 Profile 1, Material 1	72
A1.5.2 Profile 1, Material 2	72
A1.6 Gösigen, Use of results from non-linear sensitivity runs	73
A1.6.1 RVT runs, Profile 1	73
A1.6.2 SHAKE runs, Profile 1	74
A1.7 Leibstadt, Magnitude dependence for RVT calculations	75
A1.7.1 Profile 1, Material 1	75
A1.7.2 Profile 1, Material 2	76
A1.7.3 Profile 2, Material 1	77
A1.7.4 Profile 2, Material 2	78
A1.8 Leibstadt, Magnitude dependence for SHAKE calculations	79
A1.8.1 Profile 2, Material 1	79
A1.9 Leibstadt, Use of results from non-linear sensitivity runs	80
A1.9.1 RVT runs, Profile 1	80
A1.9.2 RVT runs, Profile 2	81
A1.9.3 SHAKE runs, Profile 1	82
A1.9.4 SHAKE runs, Profile 2	83
A1.10 Mühleberg, Magnitude dependence for RVT calculations	84
A1.10.1 Profile 1, Material 1	84
A1.10.2 Profile 1, Material 2	85
A1.11 Mühleberg, Magnitude dependence for SHAKE calculations	86
A1.11.1 Profile 1, Material 1	86
APPENDIX 2: MEDIAN AMPLIFICATION OF VERTICAL GROUND MOTION	87
A2.1 Beznau	87
A2.1.1 Evaluation of approaches for computing the vertical site response (SHAKE runs)	87
A2.1.2 Interpolation / Extrapolation to a case not considered in the available vertical computations	88
A2.2 Gösigen	89
A2.2.1 Evaluation of approaches for computing the vertical site response (SHAKE runs)	89
A2.2.2 Interpolation / Extrapolation to a case not considered in the available vertical computations	90

A2.3	Leibstadt	91
A2.3.1	Evaluation of approaches for computing the vertical site response (SHAKE runs), Profile 1	91
A2.3.2	Evaluation of approaches for computing the vertical site response (SHAKE runs), Profile 2	92
A2.3.3	Interpolation / Extrapolation to a case not considered in the available vertical computations, Profile 1	93
A2.3.4	Interpolation / Extrapolation to a case not considered in the available vertical computations, Profile 2	94
A2.4	Mühleberg	95
A2.4.1	Evaluation of approaches for computing the vertical site response (SHAKE runs)	95
A2.4.2	Interpolation / Extrapolation to a case not considered in the available vertical computations	96
APPENDIX 3: TABLES FOR INTERPOLATION / EXTRAPOLATION		97
APPENDIX 4: EG3-HID-0053 SITE AMPLIFICATION AT THE SURFACE AND EMBEDDED LAYER DEPTHS FINAL MODEL J. STUDER		115
A4.1	Introduction	115
A4.2	Site amplification and its aleatory variability	116
A4.2.1	Amplification of horizontal ground motion	116
A4.2.1.1	Site amplification for input PGAs from 0.05 to 1.5 g	116
A4.2.1.2	Site amplification for input PGAs ≥ 2.5 g	118
A4.2.2	Aleatory variability of amplification of horizontal ground motion	119
A4.2.3	Amplification of vertical ground motion	119
A4.2.3.1	Site amplification for input PGAs within the range from 0.05 to 1.5 g	120
A4.2.4	Aleatory variability of amplification of vertical ground motion	121
A4.2.5	Parameter ranges	121
A4.3	Maximum ground motion at the surface	121
A4.3.1	Horizontal ground motion	121
A4.3.2	Vertical ground motion	122
A4.4	Soil hazard input files (SIFs)	123
A4.4.1	Associating site amplification factors with input spectral accelerations	124
A4.4.2	Summarizing epistemic uncertainty	124
A4.4.3	Plots of the soil hazard input files	124
A4.5	Generalized logic tree	124
A4.6	Appendix	124

LIST OF TABLES

Tab. 2-1:	Weights of model logic tree for median horizontal site amplification for Beznau site	18
Tab. 2-2:	Weights of model logic tree for median horizontal site amplification for Gösgen site	21
Tab. 2-3:	Weights of model logic tree for median horizontal site amplification for Leibstadt	25
Tab. 2-4:	Weights of model logic tree for median horizontal site amplification for Mühleberg site	33
Tab. 3-1:	Weights of model logic tree for median vertical site amplification for Beznau site	42
Tab. 3-2:	Weights of model logic tree for median vertical site amplification for Gösgen site	43
Tab. 3-3:	Weights of model logic tree for median vertical site amplification for Leibstadt site	43
Tab. A4-1:	Mean and maximum building depth for the four NPP sites	115

LIST OF FIGURES

Fig. 2-1:	Structure of model logic tree for median horizontal site amplification	10
Fig. 2-2:	Magnitude dependence: Ratio of amplification functions (RVT Beznau, Profile1, Material 1)	14
Fig. 2-3:	Model logic tree for Beznau site	17
Fig. 2-4:	Model logic tree for Gösgen site	22
Fig. 2-5:	Model logic tree for Leibstadt site	26
Fig. 2-6:	Ratio 2D / 1D for low strain (0.1 g)	30
Fig. 2-7:	Ratio 2D / 1D for high strain (0.4 g)	30
Fig. 2-8:	Envelope of ratios 2D / 1D for low strain (0.1g), incl. mean	31
Fig. 2-9:	Envelope of ratios 2D / 1D for high strain (0.4g), incl. mean	31
Fig. 2-10:	Model logic tree for Mühleberg site	32
Fig. 3-1:	Structure of model logic tree for median vertical site amplification	35
Fig. 3-2:	NRC V/H for WUS rock conditions	38
Fig. 4-1:	Structure of model logic tree for aleatory variability	46
Fig. 4-2:	Structure of model logic tree for aleatory variability Beznau, multiplication factors for sigma and corresponding weights	48
Fig. 4-3:	Structure of model logic tree for aleatory variability Gösgen, multiplication factors for sigma and corresponding weights	49
Fig. 4-4:	Structure of model logic tree for aleatory variability Leibstadt, multiplication factors for sigma and corresponding weights	50
Fig. 4-5:	Structure of model logic tree for aleatory variability Mühleberg, multiplication factors for sigma and corresponding weights	51
Fig. 6-1:	Logic tree for horizontal motion	56
Fig. 6-2:	Logic tree for maximum vertical motion, Leibstadt	61
Fig. 6-3:	Increase of pga over time	62
Fig. A4-1:	Site amplifications factors for horizontal ground motion at the mean building depth of NPP Beznau for the case of a magnitude 6 earthquake with PGA on rock of 1.5 g	117
Fig. A4-2:	Weighted arithmetic mean amplification factors (AF as function of PGA on rock and frequency) for horizontal ground motion of a magnitude 6 scenario at mean building depth of NPP Beznau	118
Fig. A4-3:	Aleatory variability of amplifications factors for horizontal ground motion at the mean building depth of NPP Beznau for the case of a magnitude 6 earthquake with PGA on rock of 1.5 g	120
Fig. A4-4:	Assessment of maximum horizontal ground motion for NPP Beznau at mean building depth	123

Fig.A4-5: Summarized model of site amplification factors for ground motion of 4 Hz at mean building depth at NPP Beznau and earthquake magnitudes 5, 6 and 7	125
Fig. A4-6: General logic tree for horizontal ground motion	126

1 INTRODUCTION

This document is the final version of the elicitation summary and is based on all documents and comments from Workshops 1 to 4 of SP3. It contains horizontal and vertical motion for surface as well as mean and minimum elevation at each site. It is consistent with the document EG3-HID-0048. Due to procedure requirements of the PSHA motions at all elevations (surface, mean, minimum) have to be outcrop motions.

2 MEDIAN AMPLIFICATION OF HORIZONTAL GROUND MOTION

2.1 Approach

The logic tree structure was constructed according to the following criteria:

- Take into account all results of performed calculations if physically appropriate.
- Assume a smooth transition from small to high input acceleration levels so that interpolation is always possible. Extrapolation will be discussed in the individual chapters.
- Assume there are no bifurcations in the physical behaviour.
- As a principle, always chose the simplest law for interpolation (linear or nearly linear interpolation). This principle should contribute to the simplicity and clarity of the model.
- All steps have been visualised to check if the intermediate results behave as expected.
- All velocity profiles and all magnitudes have been used. If some data were missing, data from similar calculation were used (see individual chapters) if available and physically reasonable. Otherwise, only the existing results were incorporated in the logic tree and the aleatory variability was increased.

2.2 Logic Tree Structure

In principle, for all elevations the logic tree has the same structure. Derivations are indicated in the corresponding chapters. The general structure of the model logic tree for the median horizontal site amplification is shown in Figure 2-1. The weights for the branches and correction laws depend on individual site characteristics. There are actually three different logic trees. Depending on the input rock motion level, the appropriate logic tree is selected.

Rationale: Depending on the shaking level, different calculation procedures have to be taken into account according to their validity ranges. E.g., in the lower shaking level, methods are based on (modified) linear equivalent calculations, whereas in the higher shaking level only true nonlinear calculations are taken into account. In the intermediate range, an interpolation procedure will be applied.

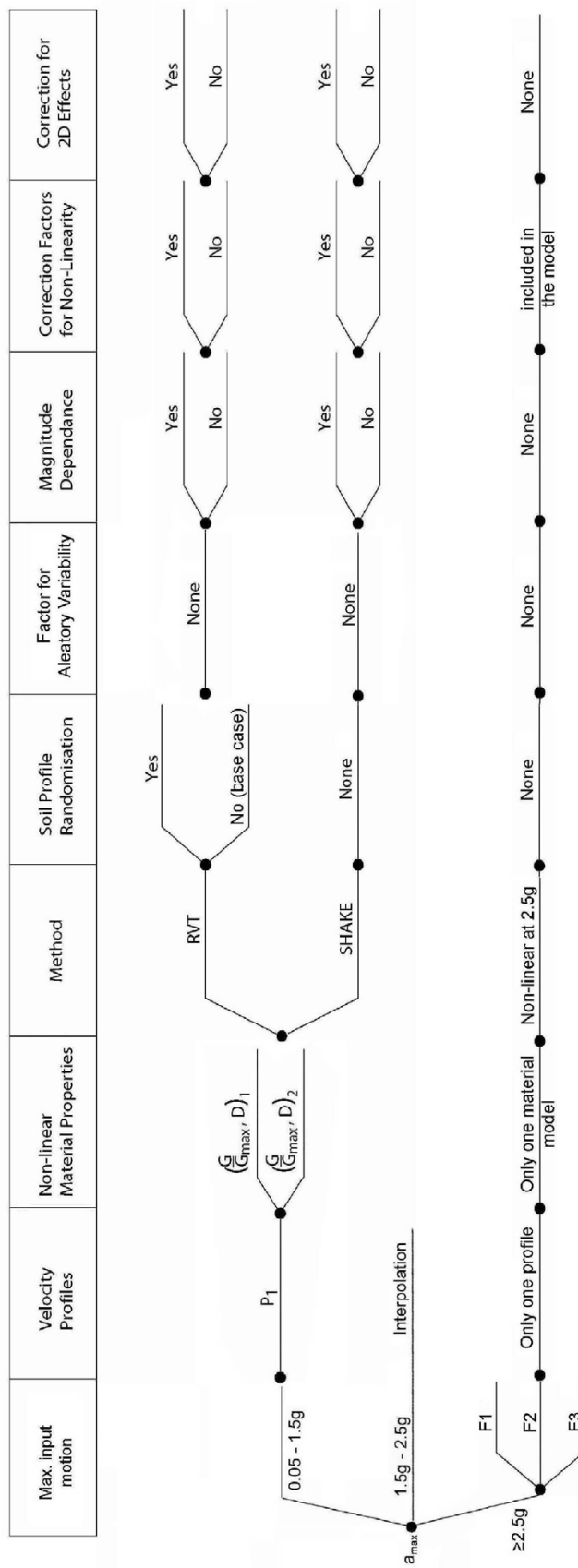


Fig. 2-1: Structure of model logic tree for median horizontal site amplification

2.3 Model Evaluations Common to All Sites

The description follows the elements in the logic tree.

2.3.1 Maximum Input ground motion

This chapter is valid for all elevations.

Originally, the logic tree was constructed for peak ground acceleration (pga) between 0.05 g and 1.5 g. Later, the range was expanded up to 2.5 g.

For site Beznau and Gösigen, non-linear calculations (Pelli, TP3-TN-0353) were performed using material properties (strength) given by Studer and reviewed by Pecker. At this high input level, all sites will behave strongly non-linear. Therefore, these results are directly used to calculate the results for 2.5 g acceleration level. The same results have to be taken for all velocity profiles and the other branches. No magnitude dependence is assumed for high acceleration levels. It is assumed that in this high acceleration range with its high resulting shear strains, the material properties and the constitutive model handling these properties dominate the behaviour of the soil. The other tree elements have minor influence. This assumption cannot be proved physically due to lack of research results, but it is a reasonable assumption, supported by the broad experience from practice (normal foundation and earth structure design).

Between 1.5 g and 2.5 g input motion, the corresponding results are linearly interpolated (this was done in the HID parameterisation directly). For higher levels, the results for 2.5 g are taken as valid. It is clear if the input level exceeds 2.5 g, the range of validity will be lost and the results become more and more unreliable. Up to around 3 g, the results for 2.5 g level can be used.

For the Leibstadt and Mühleberg sites, no such results exist. So for input motions greater than 1.5 g, the same results as for 1.5 g are taken. The same comments as above apply.

Rationale: Linear interpolation procedure between 1.5 g and 2.5 g is the simplest procedure. There are no physical reasons to use a more complex interpolation law. Linear or nearly linear interpolation laws are also used in other branches and have shown reasonable results.

To take into consideration uncertainties in the calculation, beside the original results for 2.5g, two other branches with modification factors have been added in the logic tree:

- Factor F1 = 0.8, with weight 30 %
- Factor F2 = 1.0, with weight 40 %
- Factor F3 = 1.2, with weight 30 %

2.3.2 Velocity profiles

See individual chapter for each site.

2.3.3 Non-linear material properties

See individual chapter for each site.

2.3.4 Method: SHAKE vs. RVT

This chapter is valid for all elevations. For RVT and SHAKE, the calculated motions are in all elevations outcropping motions and can be used directly.

Common to both methods:

- 1-D vertical shear wave propagations
- Linear equivalent soil properties model

Advantages: Easy to understand and to use. Extensive experience available

Disadvantages: Only one wave type (S-wave and only vertically travelling). In reality, all wave types and all incident angles exist.
Linear equivalent soil model is only valid in the small and medium shear strain range. Results of both methods in the larger strain range are questionable.

Differences:

SHAKE: Individual time histories and appropriate selection of soil profile

Advantages: Specific soil conditions and time histories can be modelled

Disadvantages: Compared to RVT, only a limited number of time histories can be used. A soil profile randomisation is not possible.

RVT:

- Randomization of time histories and soil profiles for a large number of cases is practical
- For all acceleration levels, amplification results are available

Advantages: For all acceleration levels amplification results are available. Statistical values easy to be obtained.

Disadvantages: Also unrealistic, unnatural soil profiles and time histories will be considered if not strict boundary conditions are introduced. Therefore, eigenfrequencies of the profile have to fulfil certain given ranges. This restriction was introduced in the RVT calculations.

General weights:

- RVT runs: 65 %
- SHAKE runs: 35 %

Rationale: SHAKE and RVT have a similar theoretical background. But there are only limited time histories with SHAKE runs. With RVT, soil profiles also can be randomized, giving information about the aleatory randomness. The PEGASOS study aims at statistical data to estimate uncertainties. Therefore, RVT is given a higher weight.

There was a discussion, if the SHAKE runs produce reliable results in the low frequency range. Pierre-Yves Bard (in TP3-TN-0340) showed that we can rely on the results.

2.3.5 Method: True nonlinear calculations 2.5 g

Surface motion: The results of the true nonlinear calculations are outcropping motions, and can be used directly.

Mean and minimum elevations: For those elevations only within motions have been calculated. To process further they have to be transferred to outcropping motions.

Two methods are used, based on results from the SHAKE calculations, both with a weight of 50 %:

$$1. \quad NL_{outcropping, at depth} = NL_{within, at depth} \cdot \frac{SHAKE_{outcropping, at depth}}{SHAKE_{within, at depth}}$$

The SHAKE ratio is taken for the input ground motion level of 0.75 g and a Magnitude of 6. In case of different profiles or materials, the average over all materials and profiles is taken (Beznau: average over all profiles, Leibstadt: average over 2 profiles and 2 materials, Gösigen and Mühleberg: average over 2 materials).

$$2. \quad NL_{outcropping, at depth} = NL_{outcropping, at surface} \cdot \frac{SHAKE_{outcropping, at depth}}{SHAKE_{outcropping, at surface}}$$

The SHAKE ratio is taken for the input ground motion level of 0.75g and a Magnitude of 6. In case of different profiles or materials, the average over all materials and profiles is taken (Beznau: average over all profiles, Leibstadt: average over 2 profiles and 2 materials, Gösigen and Mühleberg: average over two materials).

Rationale: For the true non-linear calculations, results only for within motions exist. In a wave field with different frequencies, outcrop motions can not be derived directly from the within motions. The results from SHAKE calculations are taken to modify the true non-linear within motions to outcrop motions. Two ratios are taken, both with the same weight. There are no physical reasons to give different weights to the two ratios.

2.3.6 Magnitude dependence of site amplification

This chapter is valid for all elevations.

SHAKE and RVT: The magnitude dependence of soil amplification depends on the input level, and is different for every profile. Results for magnitudes 5, 6 and 7 are available. From these results, a magnitude influence law (in function of frequency and of the input level) can be derived by interpolation.

The main arguments are explained with the aid of Figure 2-2 below, using the RVT results for Beznau site, Profile 1, Material M1. The different diagrams show the ratio of the amplification functions (median values) between the magnitudes 6/5 and 7/5. Therefore magnitude 5 is taken as reference with a constant ratio 1.0.

Estimation of SHAKE and RVT amplification factors (AF) at intermediate magnitudes (M 4.5 to M 7.5) and shaking levels (0.05 g to 1.5 g): The estimation of SHAKE and RVT AFs for magnitudes and input shaking levels for which no computations exist (TP3-TN-0294) is based on the consideration of AF as function of frequency (F), magnitude (M), and input shaking levels (A):

$$AF = f(F, M, A).$$

The following inter- and extrapolation schemes are used:

1. Step: AF is estimated for the requested shaking level (A) at magnitudes 5, 6 and 7 and all frequencies.

RVT: No extrapolation is required, since RVT models are generally available at 10 shaking levels between 0.05 g and 1.5 g. In case of intermediate shaking levels linear interpolation at each frequency will be used.

SHAKE: SHAKE models are available only for A = 0.1 g, 0.4 g and 0.75 g. Hence interpolation and extrapolation is required. Differing schemes are used for inter- and extrapolation:

Interpolation, if $A \leq 0.75$ g: A linear interpolation is used to estimate the AF for the requested A. This procedure is performed independently for each frequency of the spectrum.

Rationale: Linear interpolation is the simplest tool. Second order polynom interpolation gave in some cases interpolation values higher than the two neighbouring values, which was considered to be not realistic.

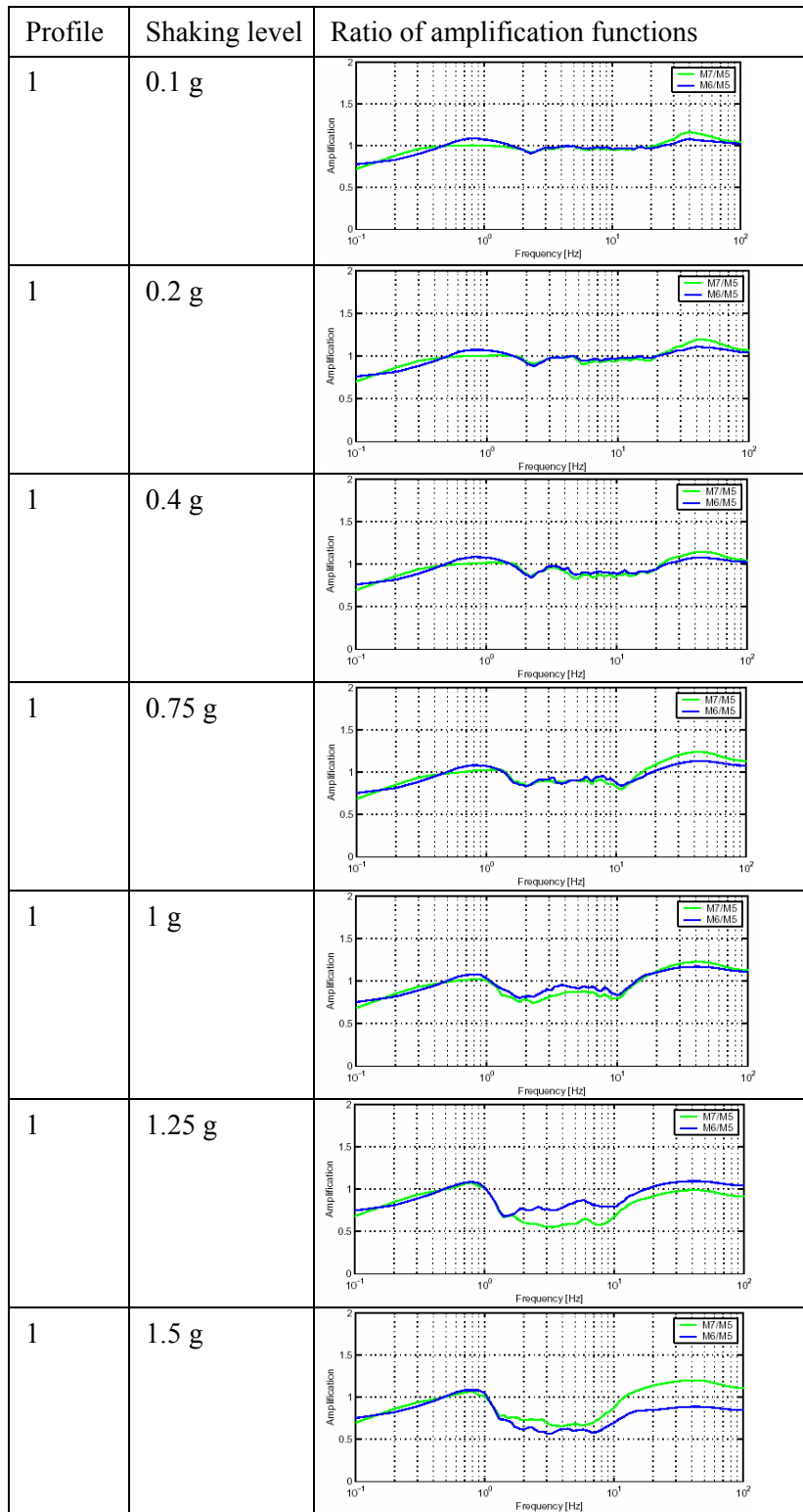


Fig. 2-2: Magnitude dependence: Ratio of amplification functions (RVT Beznau, Profile1, Material 1)

The detailed procedure is as follows: We determine five characteristic AFs in each of the spectra for 0.1 g, 0.4 g, 0.75 g input motion. These characteristic AFs are AF_1 at 0.1 Hz, minimum AF_2 below the fundamental frequency f_0 , maximum AF_3 around f_0 , minimum AF_4 above f_0 and AF_5 at 100 Hz. They correspond to the frequencies F_1 to F_5 , where F_1 and F_5 are constants (0.1 Hz and 100 Hz). The frequencies are extrapolated in PGA space using linear regression in term of least squares, e.g. F_2 (1.5 g) is based on a linear regression through F_2 (0.1 g), F_2 (0.4 g) and F_3 (0.75 g).

Once the frequencies of the five characteristic AFs are extrapolated, the AFs themselves are extrapolated the same way. By default, we extrapolate them on the basis of a linear regression. Exceptions, in which a polynomial regression (2nd order) or the nearest neighbour are used, are defined in Appendix 3, Tab. A3-2.

Finally, a generalized spectrum is built from the five extrapolated AFs, by:

$F_1 < F < F_2$: Linear interpolation between AF([F_1 F_2])

$F_2 < F < F_3$: Cubic spline based on AF([F_1 F_2 F_3])

$F_3 < F < F_4$: Cubic spline based on AF([F_3 F_4 F_5])

$F_4 < F < F_5$: Linear interpolation between AF([F_4 F_5])

Extrapolation, if $A > 0.75$ g (Mühleberg): In case of Mühleberg (all elevations) and SHAKE models of the horizontal component the above extrapolation procedure is not applied, but the same procedure as for interpolation is used for extrapolation. Moreover, in the SHAKE results, the extrapolated amplifications factors have been smoothed by a running mean filter length of 3 samples, according to the set of 76 frequencies (only for embedded layers).

2. *Step*: Interpolation for intermediate magnitudes:

AF at intermediate magnitudes (and extrapolation down to M 4.5 respectively up to M 7.5) are estimated using linear interpolation between AF at M5 and M6 or M6 and M7, respectively. Interpolation is performed for a given shaking level and independently for each frequency of the spectrum. The same procedure is used for RVT and SHAKE.

The values of the characteristic frequencies F_2 , F_3 and F_4 are defined in Appendix 3, Tab.A3-1.

Rationale: Simplest interpolation / extrapolation laws. Visual checks showed reasonable results.

True nonlinear calculations 2.5 g: No magnitude dependence taken into account.

2.3.7 Correction Factors for non-linearity

This chapter is valid for all elevations.

SHAKE and RVT: For the PEGASOS studies, specific material tests to define the soil models and their scatter have not been conducted. Therefore, the soil model used depends on the correlation from static soil tests in the 70's. We have less experience with non-linear calculations than with SHAKE-type analyses. Also, they are time consuming and costly. Therefore, non-linear calculations are used to modify known deficits of SHAKE and RVT runs.

The different sites have individual groundwater depths. The soils are predominantly dense sandy gravels. Under normal conditions, such deposits show insignificant increase of pore water pressures due to shaking. An increase of pore water pressure decreases the contact forces between the grains, leading to a softer behaviour of the matrix. Due to the high range of input motion encountered in this project, this effect has to be taken into account.

Decisions: Based on the calculation in TP3-TB-0048, correction curves will be used to modify RVT and SHAKE results. The weights will depend on the strain levels in the RVT and SHAKE calculations. The true non-linear results have to be taken from Geodeco (TP3-TB-0048 / TP3-SUP-0022).

Rationale: Theoretically, non-linear soil models represent the real conditions in a better way, particularly in the high shear strain range.

Comment: Magnitude dependence of non-linear corrections in the 'No Magnitude dependence' branch: The general logic tree in Figure 2-1 shows the distinct corrections for 'Magnitude dependence' and 'Correction factors for non-linearity'. These corrections are in fact connected, since the correction factors for non-linearity depend themselves on the magnitude. For the 'No magnitude dependence' branch however, the non-linear corrections are not dependant on the magnitude. Therefore, in this branch, for all magnitudes, the given non-linear correction for Magnitude $M = 6$ should be taken.

True nonlinear calculations 2.5 g: Already included in the model.

2.3.8 Effect of inclined waves

This chapter is valid for all elevations. Inclined waves are not taken into account and will be taken into account in the aleatory variability.

2.3.9 Correction for 2D-effects

This correction is discussed in the individual site chapters.

2.4 Beznau

2.4.1 Logic Tree for Beznau

The logic tree in Figure 2-3 below is valid for all elevations. The weights are given in Table 2-1.

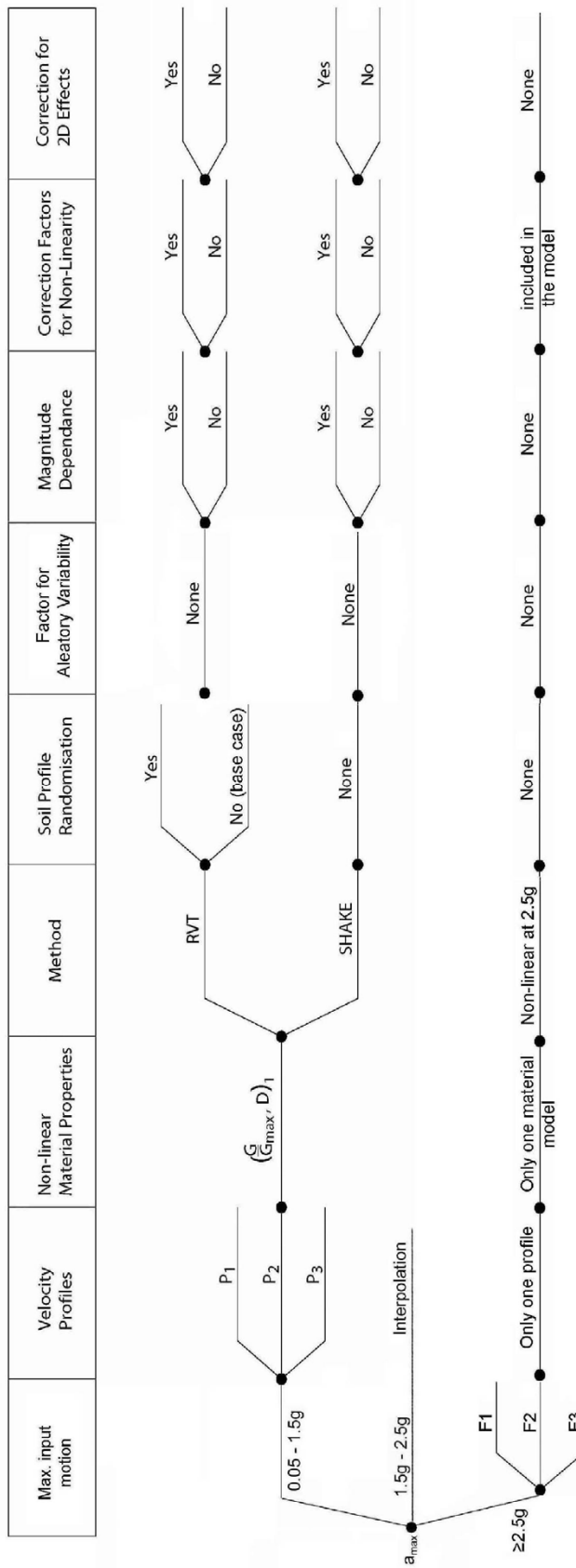


Fig. 2-3: Model logic tree for Beznau site

Tab. 2-1: Weights of model logic tree for median horizontal site amplification for Beznau site

Maximum input motion	Velocity profiles	Non-linear material properties	Method	Soil profile randomization	Factor for Aleatory Variability	Magnitude dependence	Correction factors for non-linearity	Correction for 2D - effects
0.05–1.5g	Model 1: 50 % Model 2: 30 % Model 3: 20 %	IGB Beznau: 100 %	RVT 65 % SHAKE 35 %	Yes: 70 % No: 30 %	Not considered here.	Yes: 70 % No: 30 % Yes: 70 % No: 30 %	Yes: 70 % No: 30 % Yes: 0 % No: 0 %	Yes: 0 % No: 100 % Yes: 0 % No: 100 %
1.5–2.5 g	Linear interpolation between individual results for 1.5 g and 2.5 g							
> 2.5 g	"Extrapolation" up to 3 g as suggested in the text: Results from 2.5 g input motion calculations.							
Factor F1 (0.8): 30%	Method 1: 50 %, Method 2: 50 %.							
Factor F2 (1.0): 40%								
Factor F3 (1.2): 30%								

2.4.2 Site-Specific Model Evaluations for Beznau

This chapter is valid for all elevations.

2.4.2.1 Alternative velocity profiles

The following weights are given:

- Model 1: 50 %
- Model 2: 30 %
- Model 3: 20 %

Rationale Model 1: Model 1 is based on cross-hole measurements and resonant column tests in the alluvium and in the upper part of the Opalinuston. The deeper layers are from a close Nagra deep hole log. Some adjustments have been made to the velocities in profile 1 in order to match the fundamental frequency for the profile with the fundamental frequency estimated from ambient vibration measurements. In the upper 60 meters, model 1 is considered to best represent the medium soil conditions, whereas for depths below 60 meters, the different models have no priority. Therefore, to Model 1 is given the highest weight of 50 %. Model 2 and 3 together will have a weight of 50 %.

Rationale Model 2: Model 2 was obtained from a single station inversion of ambient vibration measurements. In the upper 60 meters it is very similar to model 1. Therefore, Model 2 is given a higher weight than Model 3.

Rationale Model 3: Model 3 is based on the inversion of array measurements. A weight of 20 % is given (comments see above).

2.4.2.2 Alternative non-linear properties

Weights: Beznau IGB 1980: 100 %

Rationale: Beznau IGB 1980 soil model is considered to best represent the conditions in the alluvium. This curve is based on six cyclic triaxial tests and resonant column tests. It has been compared with Ishibashi-Zhang and Hardin-Drnevich. The curve has a steeper modulus reduction curve and in general a higher damping.

2.4.2.3 SHAKE vs. RVT

General weights: RVT runs: 65 %, SHAKE runs: 35 %

Rationale: see Chapter 2.3.4.

2.4.2.4 RVT: Use of soil randomization runs

Weights: Yes, velocity correlation model (with restrictions): 70 %; No (base case): 30 %

Rationale: Soil randomization leads to a larger dataset on potential results. Note: Randomization is done with boundary conditions (fixed eigenfrequencies band of soil column) to exclude unrealistic soil profiles. Therefore, the base case will have a significantly smaller weight compared to the soil randomization case (taken as around half the weight).

2.4.2.5 Magnitude dependence for RVT calculations

Weights: Magnitude dependence yes: 70 %; Magnitude dependence no: 30 %

Rationale: Magnitude dependence is different in all three profiles. Below 0.75 g, in general, it is less significant than above 0.75 g. The magnitude dependent model is given a higher weight primarily due to its importance in the higher pga range. But the 'no magnitude dependence' branch is still considered, to take into account the uncertainty in the higher pga range.

- Profile 1: For Profile 1, the magnitude dependence was already shown in chapter 2.3.6.
- Profile 2, Material 1: Ratios of amplification functions are shown in Appendix A1.1.1.
- Profile 3: Ratios of amplification functions are shown in Appendix A1.1.2.

The law for interpolation and extrapolation depending on the shaking level and the frequency range is proposed in the general part chapter 2.3.6.

2.4.2.6 Magnitude dependence for SHAKE calculations

Weights: Magnitude dependence yes: 70 %; Magnitude dependence no: 30 %

Rationale: Magnitude dependence is large below 2 Hz, particularly between magnitude 5 and 6, and less pronounced between magnitudes 6 and 7. The magnitude dependent model law is given a higher weight primarily due to its importance in the low frequency range below 2 Hz. But the 'no magnitude dependence' branch is still considered, to take into account the uncertainty in the low frequency range.

- Profile 1, Material 1: Ratios of amplification functions are shown in Appendix A1.2.1.
- Profiles 2 and 3: Only Magnitude 6 available, so no comparison could be made. Therefore, the same interpolation / extrapolation law as Profile 1 Material 1 will be used.

Rationale: It is physically reasonable to assume the same interpolation / extrapolation law for the same site.

The law for interpolation and extrapolation depending on the shaking level and the frequency range is proposed in the general part chapter 2.3.6.

2.4.2.7 Use of results from non-linear sensitivity runs (correction factor for non-linearity) in RVT and SHAKE branches

Weights for RVT and SHAKE runs: Non-linear corr. yes: 70 %; Non-linear corr. no: 30 %

Rationale: Theoretically, non-linear soil models represent in a better way the real conditions. The figures in Appendix A1.3.1 show a significant correction. Therefore, it is given a higher weight to the use of non-linear correction.

Ratios of amplification functions (non-linear / linear) of RVT values for Beznau Profile 1 are shown in Appendix A1.3.1.

RVT:

The correction law defines first all pga levels within magnitude 6, and adjust them for magnitudes 5 and 7:

Correction factors of RVT values for non-linearity, magnitude 6:

1. For 0.05 g assume constant ratio of non-linear / RVT = 1.0
2. Amplification ratio for 0.4 g: Figure shown in Appendix A1.3.1
3. For range between 0.05 g and 0.4 g: Linear interpolation for all frequencies
4. Amplification ratio for 0.75 g: Figure shown in Appendix A1.3.1
5. For range between 0.4 g and 0.75 g: Linear interpolation for all frequencies
6. Amplification ratio for 1.5 g: Figure shown in Appendix A1.3.1
7. For range between 0.75 g and 1.5 g: Linear interpolation for all frequencies
8. Above procedure applies for all vel. profiles (with the given figures for velocity profile 1)

Correction factors of RVT values for non-linearity, magnitudes 5 and 7:

1. To get the correction factor for pga at magnitudes 5 and 7, use the same magnitude dependent model given in chapter 2.4.2.5 for the corresponding profile (it is assumed that the magnitude dependency of the correction factor for non-linear effects is the same as the magnitude dependency of the amplification ratios).
2. For other magnitudes: Linear interpolation/extrapolation

SHAKE:

Ratios of amplification functions (non-linear / linear) of SHAKE values for Beznau Profile 1 are shown in Appendix A1.3.2. The correction law defines first all PGA levels within magnitude 6, and adjust them for magnitudes 5 and 7:

Procedure to get the correction factors of SHAKE values for non-linearity, magnitude 6:

1. For 0.05 g assume constant ratio of non-linear / SHAKE = 1.0
2. Amplification ratio for 0.4 g: Figure shown in Appendix A1.3.2
3. For range between 0.05 g and 0.4 g: Linear interpolation for all frequencies
4. Amplification ratio for 0.75 g: Figure shown in Appendix A1.3.2
5. For range between 0.4 g and 0.75 g: Linear interpolation for all frequencies
6. Compute amplification ratio non-linear/SHAKE at 1.5 g, with the given non-linear computations and the SHAKE result from chapter 2.4.2.6.

7. For range between 0.75 g and 1.5 g: Linear interpolation of the amplification ratio for all frequencies
8. The above procedure applies for all velocity profiles (with the given figures for velocity profile 1)

Correction factors of SHAKE values for non-linearity, magnitudes 5 and 7:

1. To get the correction factor for pga at magnitudes 5 and 7, use the same magnitude dependent model given in chapter 2.4.2.6 for the corresponding profile (it is assumed that the magnitude dependency of the correction factor for non-linear effects is the same as the magnitude dependency of the amplification ratios).
2. For other magnitudes: Linear interpolation/extrapolation

There is no double counting of the magnitude dependence.

2.4.2.8 Use of results from 2-D sensitivity runs

No correction for 2D effects.

Weights: 2D correction yes: 0 %; 2D correction no: 100 %

Rationale: Topographic situation suggests only small 2D effects on the median amplification. Therefore, it is neglected and only the aleatory variability will be increased for 2-D effects.

2.5 Gösgen

2.5.1 Logic Tree for Gösgen

The logic tree in Figure 2-4 is valid for all elevations. The weights are given in Table 2-2.

Tab. 2-2: Weights of model logic tree for median horizontal site amplification for Gösgen site

Maximum input motion	Velocity profiles	Non-linear material properties	Method	Soil profile randomization	Factor for Aleatory Variability	Magnitude dependence	Correction factors for non-linearity	Correction for 2D - effects
0.05–1.5g	Model 1 100 %	Ishibashi-Zhang: 30 %	RVT: 65 %	Yes: 70 % No: 30 %	Not considered here.	Yes: 70 % No: 30 %	Yes: 70 % No: 30 %	Yes: 0 % No: 100 %
		Hardin-Drnevich: 70 %	SHAKE 35 %			Yes: 70 % No: 30 %	Yes: 70 % No: 30 %	Yes: 0 % No: 100 %
1.5–2.5 g	Linear interpolation between individual results for 1.5 g and 2.5 g							
> 2.5 g Factor F1 (0.8): 30% Factor F2 (1.0): 40% Factor F3 (1.2): 30%	'Extrapolation' up to 3 g as suggested in the text: Results from 2.5 g input motion calculations. Method 1: 50 %, Method 2: 50 %.							

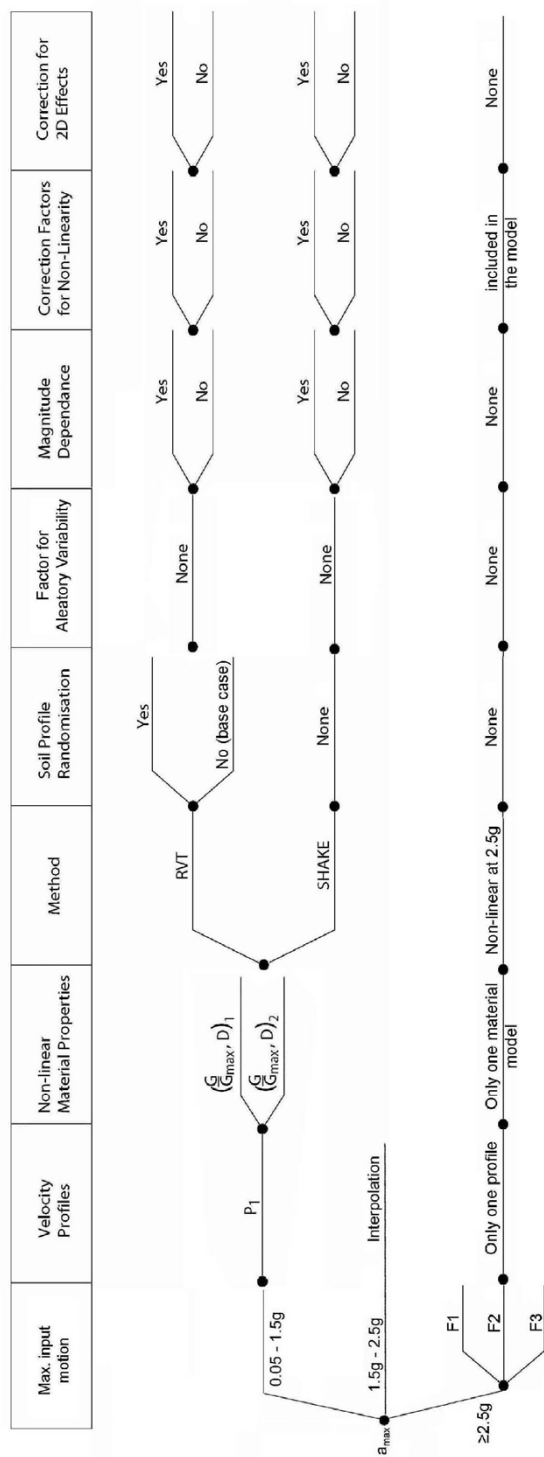


Fig. 2-4: Model logic tree for Gösgen site

2.5.2 Site-Specific Model Evaluations for Gösgen

This chapter is valid for all elevations.

2.5.2.1 Alternative velocity profiles

Only one model: weight 100 %.

2.5.2.2 Alternative non-linear properties

Weights: Ishibashi-Zhang: 30 %, Hardin-Drnevich: 70 %

Rationale: Comparison of the two models shows that the Hardin/Drnevich model has a broader validity range than Ishibashi/Zhang (based on $\gamma_r = \tau_{max} / G_{max}$, and a friction angle of about $\varphi = 45^\circ$). Beznau material has been investigated in the laboratory. Its curve shows similarity with the Hardin/Drnevich curve (see TP3-TN-0166). It is reasonable to assume that the gravels in Gösigen have similar properties. Therefore, Hardin/Drnevich is given a higher weight.

2.5.2.3 SHAKE vs. RVT

General weights: RVT runs: 65 %, SHAKE runs: 35 %

See Chapter 2.3.4.

2.5.2.4 RVT: Use of soil randomization runs

Weights: Yes, velocity correlation model (with restrictions): 70 %, No (base case): 30 %

Rationale: Soil randomization leads to a larger dataset on potential results. Note: Randomization is done with boundary conditions (fixed eigenfrequencies band of soil column) to exclude unrealistic soil profiles. Therefore, the base case will have a significantly smaller weight compared to the soil randomization (taken as around half the weight).

2.5.2.5 Magnitude dependence for RVT calculations

Profile 1, Material 1: Ratios of amplification functions are shown in Appendix A1.4.1.

Weights: Magnitude dependence yes: 70 %, Magnitude dependence no: 30 %

Rationale: Magnitude dependence is not very significant below 0.75 g, but at higher magnitudes, the correction factor is significant. The magnitude dependent model is given a higher weight primarily due to its importance in the higher pga range. But the "no magnitude dependence" branch is still considered, to take into account the uncertainty in the higher pga range.

Profile 1, Material 2: Ratios of amplification functions are shown in Appendix A1.4.2. The law for interpolation and extrapolation depending on the shaking level and the frequency range is proposed in the general part chapter 2.3.6.

2.5.2.6 Magnitude dependence for SHAKE calculations

Weights: Magnitude dependence yes: 70 %, Magnitude dependence no: 30 %

Rationale: Magnitude dependence is large below 3 Hz, particularly between magnitude 5 and 6, and less pronounced between magnitudes 6 and 7. The magnitude dependent model is given a higher weight primarily due to its importance in the low frequency range below 3 Hz. But the "no magnitude dependence" branch is still considered, to take into account the uncertainty in the low frequency range.

Profile 1, Material 1: Ratios of amplification functions are shown in Appendix A1.5.1.

Material M2: Only Magnitudes 5 and 6 were available, so no comparison between Magnitude 5 and 7 could be made.

Ratios of amplification functions are shown in Appendix A1.5.2.

The law for interpolation and extrapolation depending on the shaking level and the frequency range is proposed in the general part chapter 2.3.6.

2.5.2.7 Use of results from non-linear sensitivity runs (correction factor for non-linearity)

Weights for RVT and SHAKE runs: Non-linear correction yes: 70 %, Non-linear correction no: 30 %

Rationale: Theoretically, non-linear soil models represent the real conditions in a better way. The figures below show a significant correction law. Therefore, higher weight is given the use of non-linear correction.

Ratios of amplification functions (nonlinear / linear) of RVT values for Gösgen Profile 1 are shown in Appendix A1.6.1.

RVT:

The correction law defines first all pga levels within magnitude 6, and adjust them for magnitudes 5 and 7:

Correction factors of RVT values for non-linearity, magnitude 6:

1. For 0.05 g assume constant ratio of non-linear / RVT = 1.0
2. Amplification ratio for 0.4 g: Figure shown in Appendix A1.6.1
3. For range between 0.05 g and 0.4 g: Linear interpolation for all frequencies
4. Amplification ratio for 0.75g : Figure shown in Appendix A1.6.1
5. For range between 0.4 g and 0.75 g: Linear interpolation for all frequencies
6. Amplification ratio for 1.5 g: Figure shown in Appendix A1.6.1
7. For range between 0.75 g and 1.5 g: Linear interpolation for all frequencies
8. The above procedure applies for all velocity profiles (with the given figures for velocity profile 1)

Correction factors of RVT values for non-linearity, magnitudes 5 and 7:

1. To get the correction factor for pga at magnitudes 5 and 7, use the same magnitude dependence law in chapter 2.5.2.5, for the corresponding profile (it is assumed that the magnitude dependence of the correction factor for non-linear effects is the same as the magnitude dependence of the amplification ratios).
2. For other magnitudes: Linear interpolation / extrapolation

SHAKE:

Ratios of amplification functions (non-linear / linear) of SHAKE values for Gösgen Profile 1 are shown in Appendix A1.6.2. The correction law defines first all pga levels within magnitude 6, and adjust them for magnitudes 5 and 7:

Procedure to get the correction factors of SHAKE values for non-linearity, magnitude 6:

1. For 0.05 g assume constant ratio of non-linear / SHAKE = 1.0
2. Amplification ratio for 0.4 g: Figure shown in Appendix A1.6.2
3. For range between 0.05 g and 0.4 g: Linear interpolation for all frequencies
4. Amplification ratio for 0.75 g: Figure shown in Appendix A1.6.2
5. For range between 0.4 g and 0.75 g: Linear interpolation for all frequencies

6. Compute amplification ratio non-linear / SHAKE at 1.5 g, with the given non-linear computations and the SHAKE result from chapter 2.5.2.6.
7. For range between 0.75 g and 1.5 g: Linear interpolation of the amplification ratio for all frequencies
8. The above procedure applies for all velocity profiles (with the given figures for velocity profile 1)

Correction factors of SHAKE values for non-linearity, magnitudes 5 and 7:

1. To get the correction factor for pga at magnitudes 5 and 7, use the same magnitude dependent model given in chapter 2.5.2.6 for the corresponding profile (it is assumed that the magnitude dependency of the correction factor for non-linear effects is the same as the magnitude dependency of the amplification ratios).
2. For other magnitudes: Linear interpolation / extrapolation

2.5.2.8 Use of results from 2-D sensitivity runs

No correction for 2D effects.

Weights: 2D correction yes: 0 %, 2D correction no: 100 %

Rationale: Topographic situation suggests only small 2D effects on the median amplification. Therefore, it is neglected and only the aleatory variability will be increased.

2.6 Leibstadt

2.6.1 Logic Tree for Leibstadt

The logic tree in Figure 2-5 below is valid for all elevations. The weights are given in Table 2-3.

Tab. 2-3: Weights of model logic tree for median horizontal site amplification for Leibstadt

Maximum input motion	Velocity profiles	Non-linear material properties	Method	Soil profile randomization	Factor for Aleatory Variability	Magnitude dependence	Correction factors for non-linearity	Correction for 2D - effects
0.05–1.5g	Model 1 70 %	Ishibashi-Zhang: 30 %	RVT: 65 %	Yes: 70 % No: 30 %	Not considered here.	Yes: 70 % No: 30 %	Yes: 70 % No: 30 %	Yes: 70 % No: 30 %
	Model 2 30 %	Hardin-Drnevich: 70 %	SHAKE 35 %			Yes: 70 % No: 30 %	Yes: 70 % No: 30 %	Yes: 70 % No: 30 %
1.5–2.5 g	Same amplification functions as for 1.5 g							
> 2.5 g Factor F1 (0.8):30% Factor F2 (1.0):40% Factor F3 (1.2):30%	'Extrapolation' up to 3 g: Same amplification functions as for 1.5 g. Method 1: 50 %, Method 2: 50 %.							

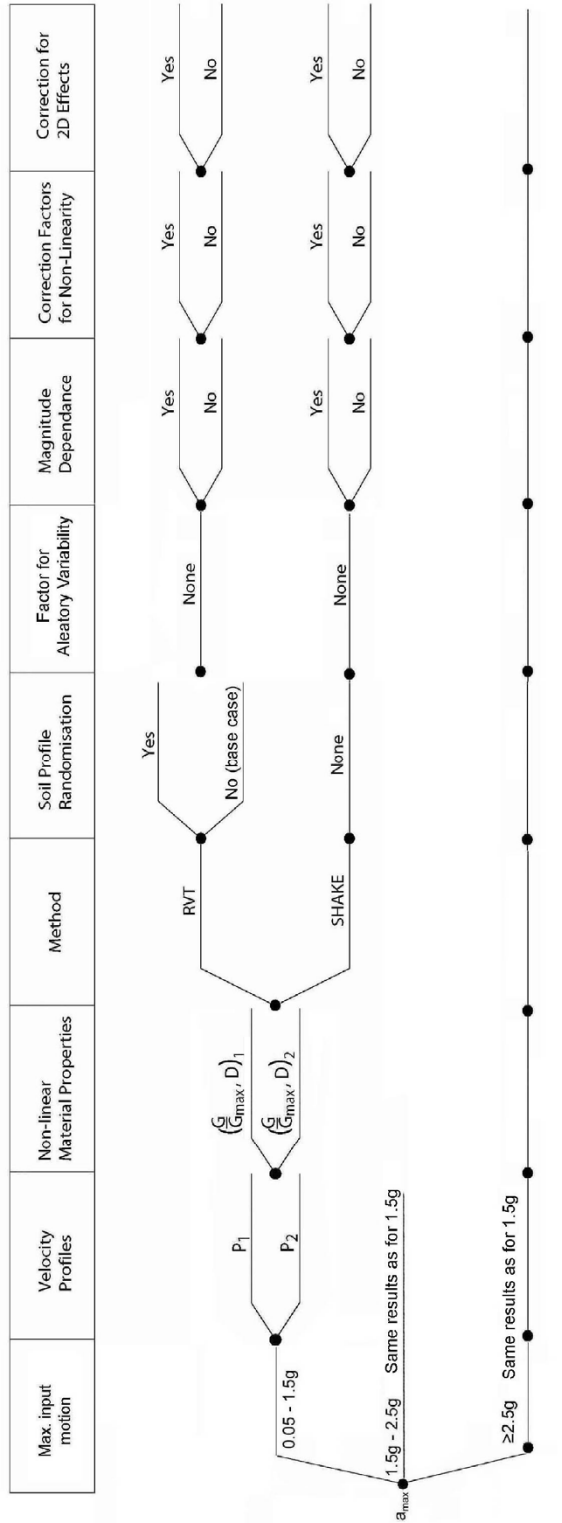


Fig. 2-5: Model logic tree for Leibstadt site

2.6.2 Site-Specific Model Evaluations

This chapter is valid for all elevations.

2.6.2.1 Alternative velocity profiles

The following weights are given: Model 1: 70 %, Model 2 (with cemented layers): 30 %

Rationale: The 2 models differ in the depth range of 30 – 50 m meters by incorporating cemented layers or not. It is more or less certain that these "cemented layers" consist of cemented lenses of different size and thickness, in different depths. Therefore, these layers consist of cemented and non-cemented elements, with resulting general properties closer to the non-cemented case than to the cemented case. Therefore, for model 1 is given a higher weight.

2.6.2.2 Alternative non-linear properties

Weights: Ishibashi-Zhang: 30 %, Hardin-Drnevich: 70 %

Rationale: A comparison of the two models shows that the Hardin/Drnevich model has a broader validity range than Ishibashi/Zhang (based on $\gamma_r = \tau_{max} / G_{max}$, and a friction angle of about $\varphi = 45^\circ$). Beznau material has been investigated in the laboratory. Its curve shows similarity with the Hardin/Drnevich curve (see TP3-TN-0166). It is reasonable to assume that the gravels in Leibstadt have similar properties. Therefore, Hardin/Drnevich is given a higher weight.

2.6.2.3 SHAKE vs. RVT

General weights: RVT runs: 65 %, SHAKE runs: 35 %

Rationale: See Chapter 2.3.4.

2.6.2.4 RVT: Use of soil randomization runs

Weights: Yes, velocity correlation model (with restrictions): 70 %, No (base case): 30 %

Rationale. Soil randomization leads to a larger dataset on potential results. Note: Randomization is done with boundary conditions (fixed eigenfrequencies band of soil column) to exclude unrealistic soil profiles. Therefore, the base case will have a significantly smaller weight compared to the soil randomization (taken as around half the weight).

2.6.2.5 Magnitude dependence for RVT calculations

Weights: Magnitude dependence yes: 70 %, Magnitude dependence no: 30 %

Rationale: Magnitude dependence is very significant. Therefore, including the magnitude dependence is given the dominant weight. But the "no magnitude dependence" branch is still considered, to take into account the uncertainty.

Profile 1, Material 1

Ratios of amplification functions are shown in Appendix A1.7.1.

Profile 1, Material 2

Ratios of amplification functions are shown in Appendix A1.7.2.

Profile 2, Material 1

Ratios of amplification functions are shown in Appendix A1.7.3.

Profile 2, Material 2

Ratios of amplification functions are shown in Appendix A1.7.4.

The law for interpolation and extrapolation depending on the shaking level and the frequency range is proposed in the general part chapter 2.3.6.

2.6.2.6 Magnitude dependence for SHAKE calculations

Weights: Magnitude dependence yes: 70 %, Magnitude dependence no: 30 %

Rationale: Magnitude dependence is very significant. Therefore magnitude dependence is given the dominant weight. But the "no magnitude dependence" branch is still considered, to take into account the uncertainty.

Profile 1, Materials 1 and 2:

Only Magnitude 6 available, so no comparison could be made.

Profile 2, Material 1:

Ratios of amplification functions are shown in Appendix A1.8.1.

Profile 2, Material 2:

Only Magnitude 6 available, so no comparison could be made. The same interpolation / extrapolation law as for Profile 2 Material 1 will be used.

The law for interpolation and extrapolation depending on the shaking level and the frequency range is proposed in the general part chapter 2.3.6.

2.6.2.7 Use of results from non-linear sensitivity runs (correct. factor for non-linearity)

Weights for RVT and SHAKE runs: Non-linear correction yes: 70 %, Non-linear correction no: 30 %

Rationale: Theoretically, non-linear soil models represent the real conditions in a better way. The figures below show a significant correction law. Therefore, higher weight is given to the use of non-linear correction.

Ratios of amplification functions (non-linear / linear) of RVT values for Leibstadt Profile 1 are shown in Appendix A1.9.1. Ratios of amplification functions (non-linear / linear) of RVT values for Leibstadt Profile 2 are shown in Appendix A1.9.2. Ratios of amplification functions (non-linear / linear) of SHAKE values for Leibstadt Profile 1 are shown in Appendix A1.9.3. Ratios of amplification functions (non-linear / linear) of SHAKE values for Leibstadt Profile 2 are shown in Appendix A1.9.4.

RVT:

Correction factors of RVT values for non-linearity, magnitude 6, for corresponding profile:

1. For 0.05 g assume constant ratio of non-linear / RVT = 1.0
2. Amplification ratio for 0.4 g: Figures shown in Appendix A1.9.1 and A1.9.2
3. For range between 0.05 g and 0.4 g: Linear interpolation for all frequencies
4. Amplification ratio for 0.75 g: Figures shown in Appendix A1.9.1 and A1.9.2
5. For range between 0.4 g and 0.75 g: Linear interpolation for all frequencies
6. Amplification ratio for 1.5 g: Figures shown in Appendix A1.9.1 and A1.9.2

7. For range between 0.75 g and 1.5 g: Linear interpolation for all frequencies
8. The above procedure applies for all velocity profiles (with the given figures for velocity profile 1)

Correction factors of RVT values for no linearity, magnitudes 5 and 7:

1. To get the correction factor for pga at magnitudes 5 and 7, use the same magnitude dependent model given in chapter 2.6.2.5 for the corresponding profile (it is assumed that the magnitude dependence of the correction factor for non-linear effects is the same as the magnitude dependence of the amplification ratios).
2. For other magnitudes: Linear interpolation/extrapolation

SHAKE:

Procedure to get the correction factors of SHAKE values for non-linearity, magnitude 6:

1. For 0.05 g assume constant ratio of non-linear / SHAKE = 1.0
2. Amplification ratio for 0.4 g: Figures shown in Appendix A1.9.3. and A1.9.4.
3. For range between 0.05 g and 0.4 g: Linear interpolation for all frequencies
4. Amplification ratio for 0.75 g: Figures shown in Appendix A1.9.3. and A1.9.4.
5. For range between 0.4 g and 0.75 g: Linear interpolation for all frequencies
6. Compute amplification ratio non-linear / SHAKE at 1.5 g, with the given non-linear computations and the SHAKE result from chapter 2.6.2.6.
7. For range between 0.75 g and 1.5 g: Linear interpolation of the amplification ratio for all frequencies
8. The above procedure applies for all velocity profiles (with the given figures for velocity profile 1)

Correction factors of SHAKE values for non-linearity, magnitudes 5 and 7:

1. To get the correction factor for pga at magnitudes 5 and 7, use the same magnitude dependent model given in chapter 2.6.2.6, for the corresponding profile (it is assumed that the magnitude dependence of the correction factor for non-linear effects is the same as the magnitude dependence of the amplification ratios).
2. For other magnitudes: Linear interpolation / extrapolation

There is no double counting of the magnitude dependence.

2.6.2.8 Use of results from 2-D sensitivity runs

Weights: 2D correction yes: 70 %, 2D correction no: 30 %

Rationale: Topographic situation suggests significant 2D effects at this site (Leibstadt NPP is located on a terrace).

The correction curves are derived from TP3-TN-0186. These curves describe the ratio between results from 2D and 1D calculations. Only measurements at the locations 10 to 19 are considered, since the relevant structures are situated within these locations.

Original curves from TP3-TN-0186 (Low strain: 0.1 g, high strain curve: 0.4 g.) are represented in Figures 2-6 and 2-7. The upper and lower envelopes including geometric and arithmetic mean values of these curves are shown in Figures 2-8 and 2-9.

2D correction law:

- $p_{ga} = 0.1$ g: Take corresponding geometric mean from figure above for low strain
- $p_{ga} = 0.4$ g: Take corresponding geometric mean from figure above for high strain
- between 0.1 and 0.4 g: linear interpolation of the values.
- above 0.4 g: take same values as for 0.4 g.

Rationale: The amplification effects of the 2D calculations from Prof. Bard show, that instead of one peak there are two peaks corresponding to the two fundamental periods located around 2.5 – 3.5 Hz and 6 – 8 Hz for the low strain range and 1 and 3 – 4 Hz for the high strain range. The 2D amplification is about 20 – 50 % higher in the frequency range from 2.5 – 8 Hz and in average 20 – 25 %. The geometric mean is selected to avoid too high weightings of extreme values. Calculations from D. Faeh (TP3-TN-0240) are very similar. For my model, I rely on the 2D amplification factors from Prof. Bard.

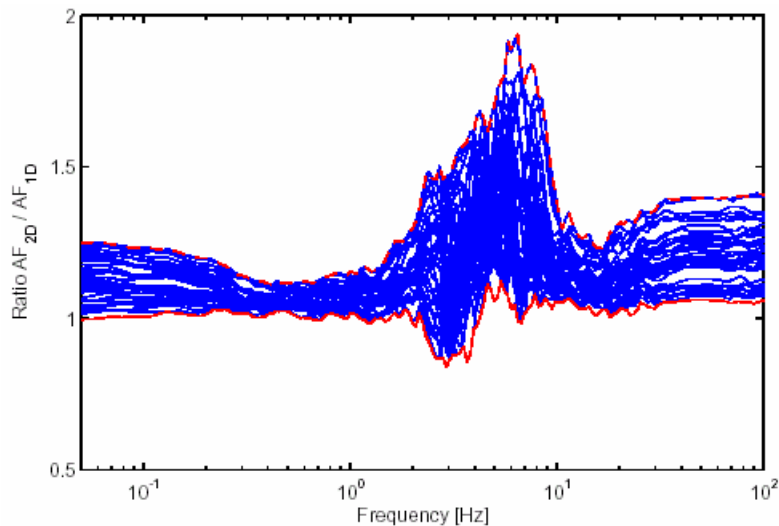


Fig. 2-6: Ratio 2D / 1D for low strain (0.1 g)

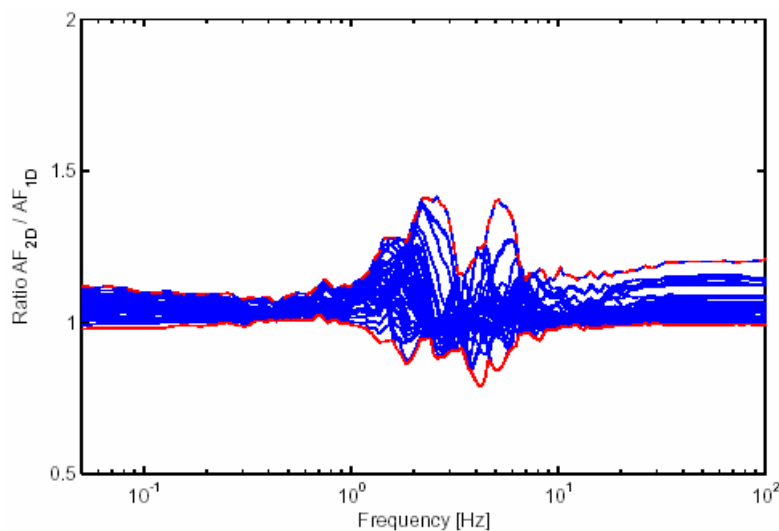


Fig. 2-7: Ratio 2D / 1D for high strain (0.4 g)

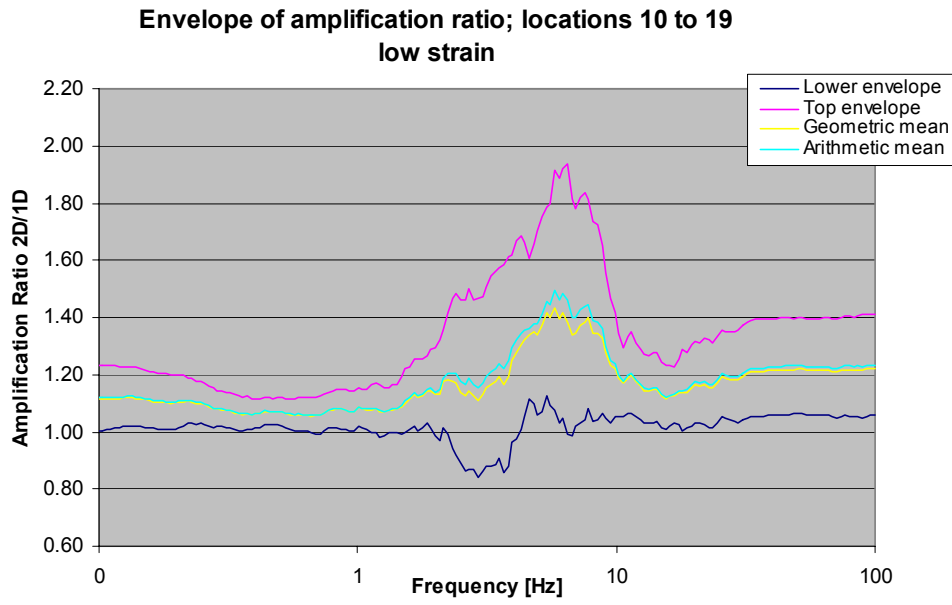


Fig. 2-8: Envelope of ratios 2D / 1D for low strain (0.1g), incl. mean

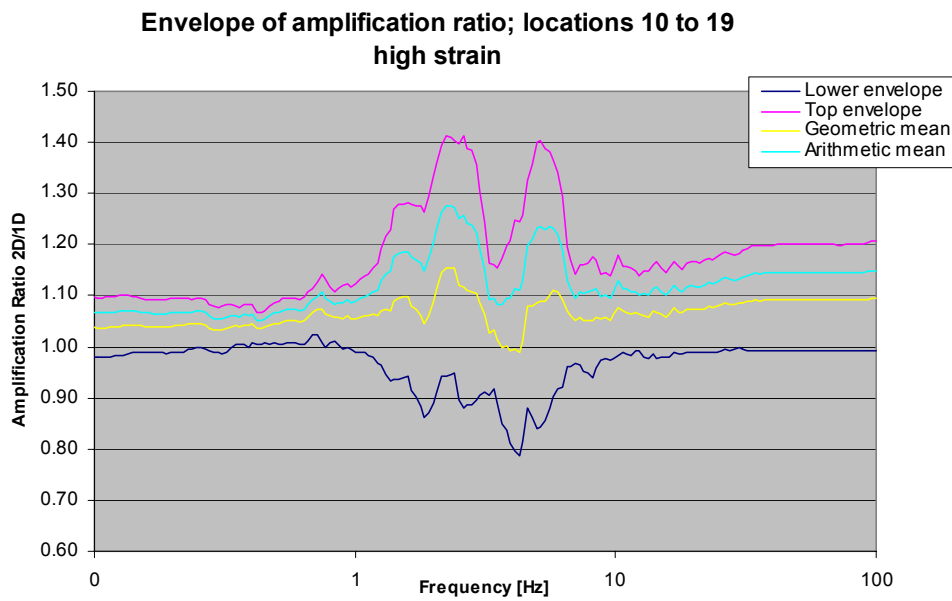


Fig. 2-9: Envelope of ratios 2D / 1D for high strain (0.4g), incl. mean

2.7 Mühleberg

2.7.1 Logic Tree for Mühleberg

The logic tree in Figure 2-10 is valid for all elevations. The weights are given in Table 2-4.

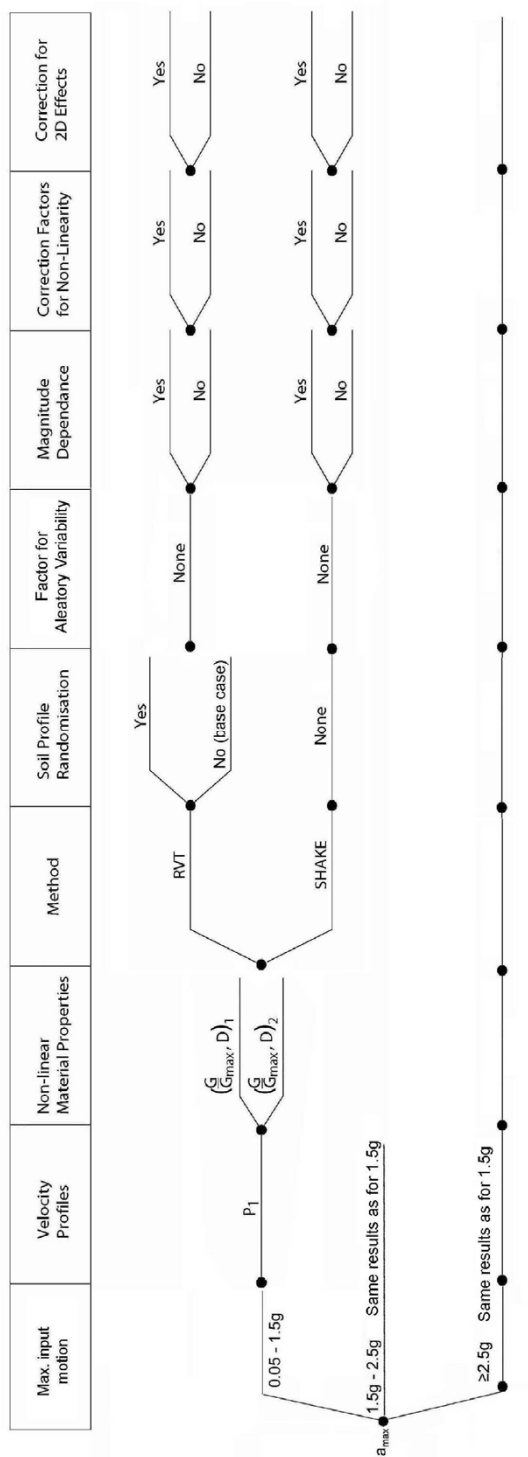


Fig. 2-10: Model logic tree for Mühleberg site

Tab. 2-4: Weights of model logic tree for median horizontal site amplification for Mühleberg site

Maximum input motion	Velocity profiles	Non-linear material properties	Method	Soil profile randomization	Factor for Aleatory Variability	Magnitude dependence	Correction factors for non-linearity	Correction for 2D - effects
0.05–1.5g	Model 1 100 %	Ishibashi-Zhang: 30 %	RVT: 65 %	Yes: 70 % No: 30 %	Not considered here.	Yes: 70 % No: 30 %	Yes: 0 % No: 100 %	Yes: 0 % No: 100 %
		Hardin-Drnevich: 70 %	SHAKE 35 %			Yes: 70 % No: 30 %	Yes: 0 % No: 100 %	Yes: 0 % No: 100 %
1.5–2.5 g	Same amplification functions as for 1.5 g							
> 2.5 g	'Extrapolation' up to 3 g: Same amplification functions as for 1.5 g.							
Factor F1 (0.8): 30%	Method 1: 50 %, Method 2: 50 %.							
Factor F2 (1.0): 40%								
Factor F3 (1.2): 30%								

2.7.2 Site-Specific Model Evaluations

This chapter is valid for all elevations.

2.7.2.1 Alternative velocity profiles

Only one model: weight 100 %.

2.7.2.2 Alternative non-linear properties

Weights: Ishibashi-Zhang: 30 %, Hardin-Drnevich: 70 %

Rationale: A comparison of the two models shows that the Hardin/Drnevich model has a broader validity range than Ishibashi/Zhang (based on $\gamma_r = \tau_{max} / G_{max}$, and a friction angle of about $\varphi = 43^\circ$). Beznau material has been investigated in the laboratory. Its curve shows similarity with the Hardin/Drnevich curve (see TP3-TN-0166). It is reasonable to assume that the gravels in Gösigen have similar properties. Therefore, Hardin/Drnevich is given a higher weight.

2.7.2.3 SHAKE vs. RVT

General weights: RVT runs: 65 %, SHAKE runs: 35 %

Rationale: See Chapter 2.3.4.

2.7.2.4 RVT: Use of soil randomization runs

Weights: Yes, velocity correlation model (with restrictions): 70 %, No (base case): 30 %

Rationale: Soil randomization leads to a larger dataset on potential results. Note: Randomization is done with boundary conditions (fixed eigenfrequencies band of soil column) to exclude unrealistic soil profiles. Therefore, the base case will have a significantly smaller weight compared to the soil randomization (taken as about half the weight).

2.7.2.5 Magnitude dependence for RVT calculations

Weights: Magnitude dependence yes: 70 %, Magnitude dependence no: 30 %

Rationale: Magnitude dependence is not very significant. But still, for consistency reasons with the other calculations at the other sites, the weights are selected according to the weights at the other sites.

Profile 1, Material 1:

Ratios of amplification functions are shown in Appendix A1.10.1.

Profile 1, Material 2:

Ratios of amplification functions are shown in Appendix A1.10.2.

The law for interpolation and extrapolation depending on the shaking level and the frequency range is proposed in the general part chapter 2.3.6.

2.7.2.6 Magnitude dependence for SHAKE calculations

Weights: Magnitude dependence yes: 70 %, Magnitude dependence no: 30 %

Rationale: Magnitude dependence is not very significant. But still, for consistency reasons with the other calculations at the other sites, the weights are selected according to the weights at the other sites.

Profile 1, Material 1:

Ratios of amplification functions are shown in Appendix A1.11.1.

Profile 1, Material 2:

Only magnitude 6 available, so no comparison could be made.

The law for interpolation and extrapolation depending on the shaking level and the frequency range is proposed in the general part chapter 2.3.6.

2.7.2.7 Use of results from non-linear sensitivity runs (correction factor for non-linearity)

Weights for RVT and SHAKE runs: Non-linear correction yes: 0 %, Non-linear correction no: 100 %

Rationale: Non-linear effects probably small (very small alluvium layer). No non-linear calculations available.

2.7.2.8 Use of results from 2-D sensitivity runs

No correction for 2D effects.

Weights: 2D correction yes: 0 %, 2D correction no: 100 %

Rationale: Topographic situation suggests only small 2D effects on the median amplification. Therefore, it is neglected and only the aleatory variability will be increased.

3 MEDIAN AMPLIFICATION OF VERTICAL GROUND MOTION

3.1 Approach

The logic tree for median amplification of vertical ground motion is constructed with the same general criteria used for median amplification of horizontal ground motion, see chapter 2.1. There is a significant different due to the fact that the ground water has a stronger influence on the P-wave than on the S-wave.

3.2 Logic Tree Structure

The general structure of the model logic tree for the median vertical site amplification is shown in Figure 3-1. The weights and correction laws depend on individual site characteristics. In principle, for all elevations the logic tree has the same structure. Derivations are indicated in the corresponding chapters. The branch starts with the input motion. Depending on its level, there are different continuations.

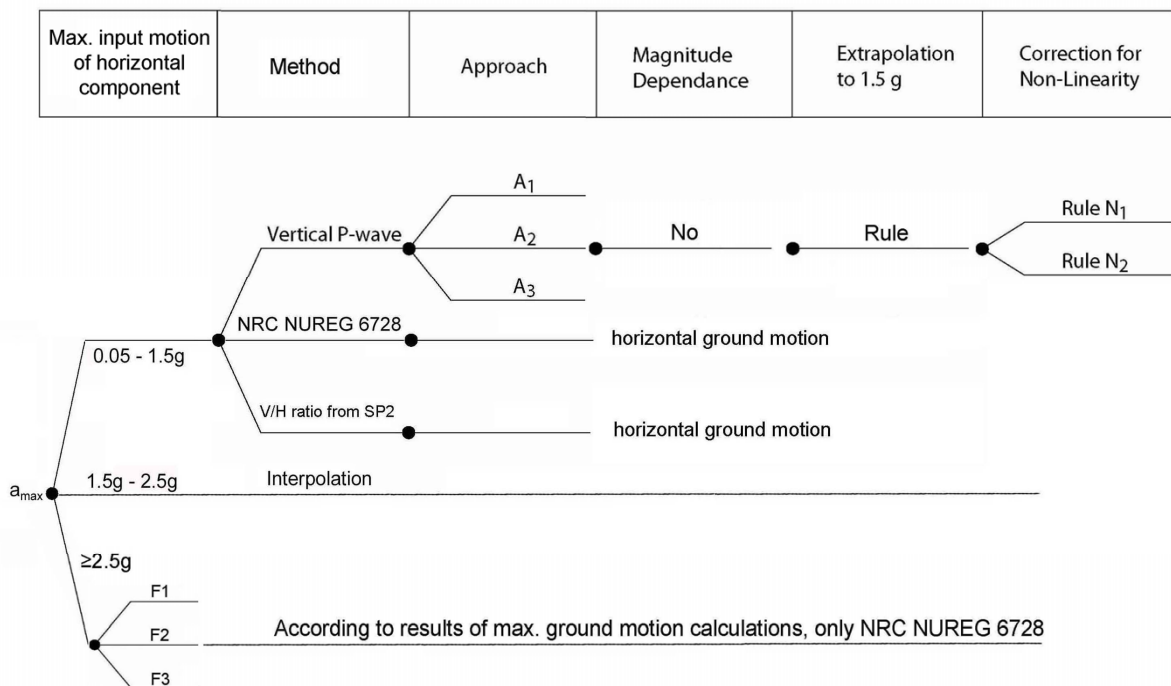


Fig. 3-1: Structure of model logic tree for median vertical site amplification

3.3 Model Evaluations Common to All Sites

3.3.1 Maximum input motion, horizontal component

Analogous to the horizontal ground motion calculations, three branches exist. The same laws are valid as for the horizontal motion.

3.3.2 Different methods for computing the vertical site response

This chapter is valid for all elevations. Exceptions are described in the individual sites. The following alternative methods will be used to define median vertical site amplification.

Methods and weights: Vertical P-wave (SHAKE): 40 %, NRC NUREG 6728: 40 %, V/H ratio from SP2: 20 %

Rationale: Important for the vertical ground motion is the location of the ground water table. At Beznau, Gösgen, and Mühleberg, the ground water table is only few meters below the surface. At Leibstadt, it lies on a depth of about 30 m. In the alluvium layers below the ground water table, we will have P-wave velocities that are partly governed by the P-wave velocity of the water (1450 m/s). Therefore, only in the non-saturated part exist some degradation of the P-wave due to the strain level. NRC NUREG 6728 and the SHAKE calculations are given the same weight for the following reasons:

- *The SHAKE runs are done on actual shear wave profiles and represent actual soil conditions best, but a limited number of calculations are available.*
- *NRC NUREG 6728 is based on extensive studies, but not for Swiss conditions.*
- *V/H ratio from SP2: Reflects the actual site condition only in a limited way (input level) so it is given a lower weight.*

3.3.2.1 Vertical P-wave (SHAKE)

This chapter is valid for all elevations.

Approaches for P-wave Degradation

- Approach 1 (no reduction, initial pre-degraded bulk modulus held constant, degraded shear wave profile is used to calculate degraded P-wave velocity profile; smallest reduction in p-wave velocity)
- Approach 2 (ratio of small strain p-wave velocity to small strain shear wave velocity constant, degraded shear wave profile is multiplied by this ratio to calculate the shear p-wave velocity profile; largest reduction in p-wave velocity)
- Approach 3 (square root of the ratio of degraded shear wave to initial shear wave is multiplied by the degraded shear wave velocity profile to degrade the p-wave velocity profile)

Rationale: The weights will be defined individually at each site, depending on the depth of the water table.

Magnitude dependence

Calculation results only for magnitude 6 exist. I assume no magnitude dependence.

Rationale: Due to the fact that in all sites large part of the profile is below the ground water table, for the area below the ground water table, the degradation of the vertical propagating P-waves will be smaller compared to the vertical propagating S-waves. Therefore, it can be expected that the magnitude dependence for the P-wave case will be smaller compared to the SH case. So I hesitate to apply directly the magnitude dependence law from the horizontal ground motion to the vertical ground motion, and assume no magnitude dependence.

Interpolation / Extrapolation to 1.5 g to a case not considered in the available vertical computations

This procedure is valid for all elevations. In principle, the same procedure applies as for horizontal motion, defined in chapter 2.3.6.

Exceptions are:

- Mühleberg, surface, degradation 1: Extrapolation by a best fit polynomial (2nd degree per frequency).
- Mühleberg, surface, degradations 2 and 3, extrapolation by by a best fit polynomial (2nd degree per frequency). Amplification taken as the larger value of the calculated amplification and the amplification for 0.75g.
- Leibstadt, Profile 2, all elevations, degradations 2 and 3, results calculated with an additional smoothing by a running mean filter (length 8 samples).

Rationale: Visual check of the extrapolation showed the best results in respect of the criteria given in chapter 2.1.

Correction for non-linearity:

Rule 1: No Correction.

Rule 2: Take the same correction function as for the corresponding horizontal case.

Weights:

For Beznau, Gösgen and Mühleberg: Rule 1: 70 %, Rule 2: 30 %

For Leibstadt: Rule 1: 30 %, Rule 2: 70 %

Rationale: At Beznau, Gösgen and Mühleberg the ground water table is at very low depths. Therefore, Rule 1 (no correction) is given a higher weight. In contrast, in Leibstadt the water table is very deep below surface. Rule 2 is given a higher weight.

2D effects:

For the vertical component no 2D effects are assumed. They will be taken into account in the aleatory variability.

Rationale: Due to the topographic situation at all sites (except Leibstadt), no significant 2D effects for horizontal motion are expected. The same is true for vertical motion. In the case of Leibstadt, it is reasonable to assume that the 2D effects for the vertical ground motion will be smaller compared to the horizontal motion. Therefore, no 2D effects are taken into account for Leibstadt site. The aleatory variability will be increased by the factors explained in Chapter 4.

3.3.2.2 NRC NUREG 6728

This chapter is valid for all elevations.

Basic law:

The NUREG report shows that the shapes for soil and rock amplification are very similar (Figure 3-2).

The following laws are applied (take values of tab. 4.4 in original documentation):

1. For pga between 0.05 and 0.2 g take above curve for < 0.2 g.
2. For pga between greater 0.2 and equal 0.5 g take above curve for $0.2 \text{ g} < \text{pga} < 0.5 \text{ g}$.
3. For pga > 0.5 g take above curve for > 0.5 g.

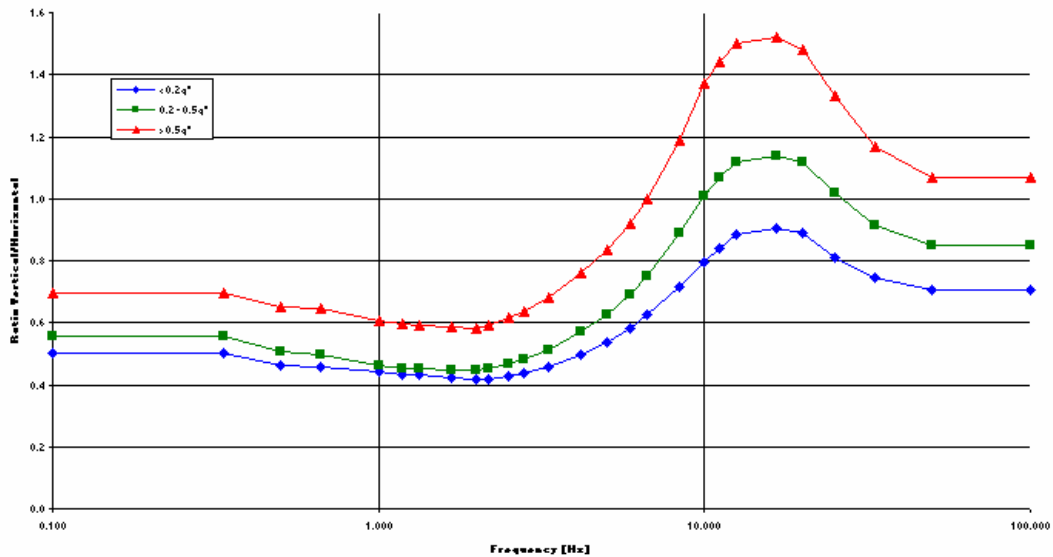


Fig. 3-2: NRC V/H for WUS rock conditions

For values see tab. 4.4 in original documentation.

Magnitude dependence:

No magnitude dependence of the V/H ratio is taken into account.

Rationale: The above curves already include magnitude dependence since the magnitude dependence is included in the horizontal calculations. The V/H ratio is independent of magnitude, but the vertical amplification factor will be dependent on magnitude since the horizontal amplification factor is magnitude dependent. This is different from the SHAKE branch. It has to be taken into account that the NUREG sites are not known in detail and cannot be compared to the PEGASOS sites.

Correction for non-linearity:

No correction for non-linearity is taken into account.

Rationale: The correction is included in the horizontal case (see above).

3.3.2.3 V/H ratio from SP2

The V/H ratio calculated from SP2 is applied directly to the corresponding amplified horizontal ground motion of chapter 2, to get the amplification for vertical ground motion. The horizontal and vertical ground motions from SP2 are a function of frequency, magnitude and distance. The needed frequencies and magnitudes can be adopted as given by the results of SP2, with the corresponding interpolation (defined in SP2) where necessary. The spectrum is taken as the average of all SP2 V/H ratios from all experts models for distances ≤ 15 km.

3.4 Beznau

3.4.1 Logic Tree for Beznau

The logic tree corresponds to the general tree in Figure 3-1.

3.4.2 Site-Specific Model Evaluations

3.4.2.1 Approaches for P-wave Degradation

For Beznau profile 2, the amplification curves for magnitude 6 are shown in Appendix A2.1.1 (blue curve: P-wave degradation 1; green curve: P-wave degradation 2; red curve: P-wave degradation 3). As approaches 2 and 3 produce similar results, the green and red line often coincide. The weights of approaches 1 to 3 reflect the thickness of the water saturated soil column in respect to the individual elevation. That means, for example, that approach 1 for the surface elevation in general has a lower weight than for larger depths (the proportion of the saturated soil column part to the entire soil column is smaller than for larger elevations).

Weights for surface elevation (0 m, GW Table 3.0 m): Approach 1: 50 %, Approach 2: 20 %, Approach 3: 30 %

Rationale: Very high water table (6 m), governing stiffness of large part of the profile. 50 % of the alluvium profile is saturated. Approach 1 with no degradation has 50 % weight due to the fact that at least three meters are unsaturated. The other two approaches have a similar weight. Approach 2 (largest degradation) is given a smaller weight compared to approach 3 because the profile is saturated in most cases.

Weights for mean elevation (6 m, GW Table 3.0 m): Approach 1: 80 %, Approach 2: 5 %, Approach 3: 15 %

Weights for minimum elevation (15 m, GW Table 3.0 m): Approach 1: 80 %, Approach 2: 5 %, Approach 3: 15 %

Rationale: Water table is above mean and minimum elevation, strong influence on P-wave. The weighting takes this fact into account. Approach 1 (no reduction) is given clearly the largest weight. Approach 2 (largest reduction) has only a small weighting of 5 %.

3.4.2.2 Vertical component of Profiles 1 and 3

Law: Calculate the V/H ratio for profile 2 material 1 and apply the same ratio to calculate the vertical components of profiles 1 and 3 (with corresponding H values in chapter 2). The V/H ratio has to be built with the already corrected runs.

Rationale: It is reasonable to use the same law.

3.5 Gösgen

3.5.1 Logic Tree for Gösgen

The logic tree corresponds to the general tree in Figure 3-1.

3.5.2 Site-Specific Model Evaluations

3.5.2.1 Approaches for P-wave Degradation

For Gösgen Profile 1 Material 1, the amplification curves for magnitude 6 are shown in Appendix A2.2.1 (blue curve: P-wave degradation 1; green curve: P-wave degradation 2; red curve: P-wave degradation 3). As approaches 2 and 3 produce similar results, the green and red line often coincide.

Weights for surface elevation (0 m, GW table 5 m): Approach 1: 65 %, Approach 2: 10 %, Approach 3: 25 %

Rationale: Very high water table (5m), governing stiffness of large part of the profile. About 2/3 of the profile is saturated. Compared to the Beznau site, a larger proportion of the alluvium part of the soil profile is saturated. Therefore, Approach 1 with no degradation has 65 % weight. The other two approaches have a similar weight. Approach 2 (largest degradation) is given a smaller weight compared to approach 3 because the profile is saturated in most cases.

Weights for mean elevation (5 m, GW table 5 m): Approach 1: 75 %, Approach 2: 5 %, Approach 3: 20 %

Weights for minimum elevation (9 m, GW table 5 m): Approach 1: 80 %, Approach 2: 5 %, Approach 3: 15 %

Rationale: Ground water lies at mean elevation. The weights depend on the amount of unsaturated layer thickness below the individual elevation. For mean elevation, some fluctuating of the ground water table is reflected. Approach 1 (no reduction) is given clearly the largest weight. Approach 2 (largest reduction) has only a small weighting of 5 %.

3.5.2.2 Vertical component for Material 2

Law: Calculate the V/H ratio for the profile 1 material 1 and apply the same ratio to calculate the vertical components for material 2 (with H values corresponding to chapter 2). The V/H ratio has to be built with the already corrected runs.

Rationale: It is reasonable to use the same law.

3.6 Leibstadt

3.6.1 Logic Tree for Leibstadt

The logic tree corresponds to the general tree in Figure 3-1.

3.6.2 Site-Specific Model Evaluations

3.6.2.1 Approaches for P-wave Degradation, Material 1

For Leibstadt profile 1, the amplification curves for magnitude 6 are shown in Appendix A2.3.1 (blue curve: P-wave degradation 1; green curve: P-wave degradation 2; red curve: P-wave degradation 3). As approaches 2 and 3 produce similar results, the green and red line often coincide.

Weights for surface elevation (0 m, GW table 25.5 m): Approach 1: 25 %, Approach 2: 30 %, Approach 3: 45 %

Weights for mean elevation (6 m, GW table 25.5 m): Approach 1: 25 %, Approach 2: 30 %, Approach 3: 45 %

Weights for minimum elevation (10 m, GW table 25.5 m): Approach 1: 25 %, Approach 2: 30 %, Approach 3: 45 %

Rationale: The water table is around 30m below ground surface. About 1/3 of the alluvium deposit is water saturated. All elevations are clearly above the ground water table, therefore, a higher weight is given to the P-wave degradations (Approaches 2 and 3) than for the saturated

cases at the other sites. The degradation of the P-wave curve is unknown. It is reasonable to assume that the P-wave degradation is smaller than the S-wave degradation. Therefore a somewhat higher weight is given to Approach 3 than to Approach 2.

For Leibstadt profile 2, the amplification curves for magnitude 6 are shown in Appendix A2.3.2. The same procedures apply.

3.6.2.2 Vertical component for Material 2

Law: Calculate the V/H ratio for the corresponding profile of material 1 and apply the same ratio to calculate the vertical components for material 2 (with H values corresponding to chapter 2). The V/H ratio has to be built with the already corrected runs.

Rationale: It is reasonable to use the same law.

3.7 Mühleberg

3.7.1 Logic Tree for Mühleberg

The logic tree corresponds to the general tree in Figure 3-1.

3.7.2 Site-Specific Model Evaluations

3.7.2.1 Approaches for P-wave Degradation

For Mühleberg profile 1, the amplification curves for magnitude 6 are shown in Appendix A2.4.1 (blue curve: P-wave degradation 1; green curve: P-wave degradation 2; red curve: P-wave degradation 3). As approaches 2 and 3 produce similar results, the green and red line often coincide.

Weights for surface elevation (0 m, GW table 4 m): Approach 1: 50 %, Approach 2: 20 %, Approach 3: 30 %

Rationale: Very high water table (4m), governing stiffness of large part of the profile. 50 % of the alluvium profile is saturated. We have a similar situation than for Beznau. The weights are therefore the same.

Weights for mean elevation (7 m, GW table 4 m): Approach 1: 80 %, Approach 2: 5 %, Approach 3: 15 %

Weights for minimum elevation (14 m, GW table 4 m): Approach 1: 80 %, Approach 2: 5 %, Approach 3: 15 %

Rationale: Ground water lies at mean elevation. The weights depend on the amount of unsaturated layer thickness below the individual elevation. For mean elevation, some fluctuating of the ground water table is reflected. We have a similar situation than for Beznau. The weights are therefore the same.

3.7.2.2 Vertical component for Material 2

Law: Calculate the V/H ratio for the profile 1 material 1 and apply the same ratio to calculate the vertical components for material 2 (with H values corresponding to chapter 2). The V/H ratio has to be built with the already corrected runs.

Rationale: It is reasonable to use the same law.

3.8 Summary tables of models and weights for the median amplification of vertical ground motion

3.8.1 Results for Beznau site

Tab. 3-1: Weights of model logic tree for median vertical site amplification for Beznau site

Maximum input motion	Method	Approach	Magnitude dependence	Extrapolation to 1.5 g	Correction for non-linearity
0.05 – 1.5 g	Vertical P-wave (SHAKE): 40 % NRC NUREG 6728: 40 % V/H ratio from SP2: 20	<u>Surface:</u> Approach 1: 50 % Approach 2: 20 % Approach 3: 30 % <u>Mean elevation:</u> Approach 1: 80 % Approach 2: 5 % Approach 3: 15 % <u>Minimum Elevation:</u> Approach 1: 80 % Approach 2: 5 % Approach 3: 15 %	No: 100 %	Interpolation and extrapolation rule in corresponding chapter.	Rule 1: 70 % Rule 2: 30 %
1.5 – 2.5 g	Linear interpolation between individual results for 1.5 g and 2.5 g				
> 2.5 g Factor F1 (0.8): 30 % Factor F2 (1.0): 40 % Factor F3 (1.2): 30 %	Results based on 2.5 g input motion calculations and NRC NUREG 6728				

3.8.2 Results for Gösgen site

Tab. 3-2: Weights of model logic tree for median vertical site amplification for Gösgen site

Maximum input motion	Method	Approach	Magnitude dependence	Extrapolation to 1.5 g	Correction for non-linearity
0.05 – 1.5 g	Vertical P-wave (SHAKE): 40 % NRC NUREG 6728: 40 % V/H ratio from SP2: 20	<u>Surface:</u> Approach 1: 65 % Approach 2: 10 % Approach 3: 25 % <u>Mean elevation:</u> Approach 1: 75 % Approach 2: 5 % Approach 3: 20 % <u>Minimum Elevation:</u> Approach 1: 80 % Approach 2: 5 % Approach 3: 15 %	No: 100 %	Interpolation and extrapolation rule in corresponding chapter.	Rule 1: 70 % Rule 2: 30 %
1.5 – 2.5 g	Linear interpolation between individual results for 1.5 g and 2.5 g				
> 2.5 g Factor F1 (0.8): 30 % Factor F2 (1.0): 40 % Factor F3 (1.2): 30 %	Results based on 2.5 g input motion calculations and NRC NUREG 6728				

3.8.3 Results for Leibstadt site

Tab. 3-3: Weights of model logic tree for median vertical site amplification for Leibstadt site

Maximum input motion	Method	Approach	Magnitude dependence	Extrapolation to 1.5 g	Correction for non-linearity
0.05 – 1.5 g	Vertical P-wave (SHAKE): 40 % NRC NUREG 6728: 40 % V/H ratio from SP2: 20	<u>Surface:</u> Approach 1: 30 % Approach 2: 30 % Approach 3: 40 % <u>Mean elevation:</u> Approach 1: 25 % Approach 2: 30 % Approach 3: 45 % <u>Minimum Elevation:</u> Approach 1: 25 % Approach 2: 30 % Approach 3: 45 %	No: 100 %	Interpolation and extrapolation rule in corresponding chapter.	Rule 1: 30 % Rule 2: 70 %
1.5 – 2.5 g	Same amplification functions as for 1.5 g				
> 2.5 g	Same amplification functions as for 1.5 g				

3.8.4 Results for Mühleberg site

Tab. 3-4: Weights of model logic tree for median vertical site amplification for Mühleberg site

Maximum input motion	Method	Approach	Magnitude dependence	Extrapolation to 1.5 g	Correction for non-linearity
0.05 – 1.5 g	Vertical P-wave (SHAKE): 40 % NRC NUREG 6728: 40 % V/H ratio from SP2: 20	<u>Surface:</u> Approach 1: 50 % Approach 2: 20 % Approach 3: 30 % <u>Mean elevation:</u> Approach 1: 80 % Approach 2: 5 % Approach 3: 15 % <u>Minimum Elevation:</u> Approach 1: 80 % Approach 2: 5 % Approach 3: 15 %	No: 100 %	Interpolation and extrapolation rule in corresponding chapter.	Rule 1: 70 % Rule 2: 30 %
1.5 – 2.5 g	Same amplification functions as for 1.5 g				
> 2.5 g	Same amplification functions as for 1.5 g				

4 ALEATORY VARIABILITY OF HORIZONTAL GROUND MOTION

The procedure below is valid for all elevations.

4.1 Approach

The following approach is followed for the aleatory variability:

- For input motions up to 1.5 g, the aleatory variability is developed in a logic tree parallel to that of the amplification factor. The tree weights are the same as the corresponding weights in the logic tree for the amplification factor. The corresponding standard deviation (σ) is multiplied by the factors given in the logic trees for aleatory variability. Where no factor is given, the original σ is applied (factor 1.0).
- For input motions equal or above 2.5 g, the aleatory variability equals that of the corresponding non-linear model.
- For input motions between 1.5 g and 2.5 g, the aleatory variability is linearly interpolated.

Both models, SHAKE and RVT have the following model deficits compared to nature:

- Only one wave type is used instead of a full wave field
- Only vertical waves is used instead of different incident angles
- The linear equivalent soil model is used instead of a true non-linear soil model

These deficiencies will lead to smaller aleatory variability compared to a model that includes the above missing elements.

To avoid double counting of aleatory variability, σ for the rock input is kept as estimated empirically. Only the median amplification factor is applied for rock.

The same rule applies for the aleatory variability for true non-linear model. Variability of very high levels of shaking is taken into account in the non-linear part by using multiple time histories.

4.2 Logic Tree Structure

General structure of model logic tree for the aleatory variability of the horizontal site amplification:

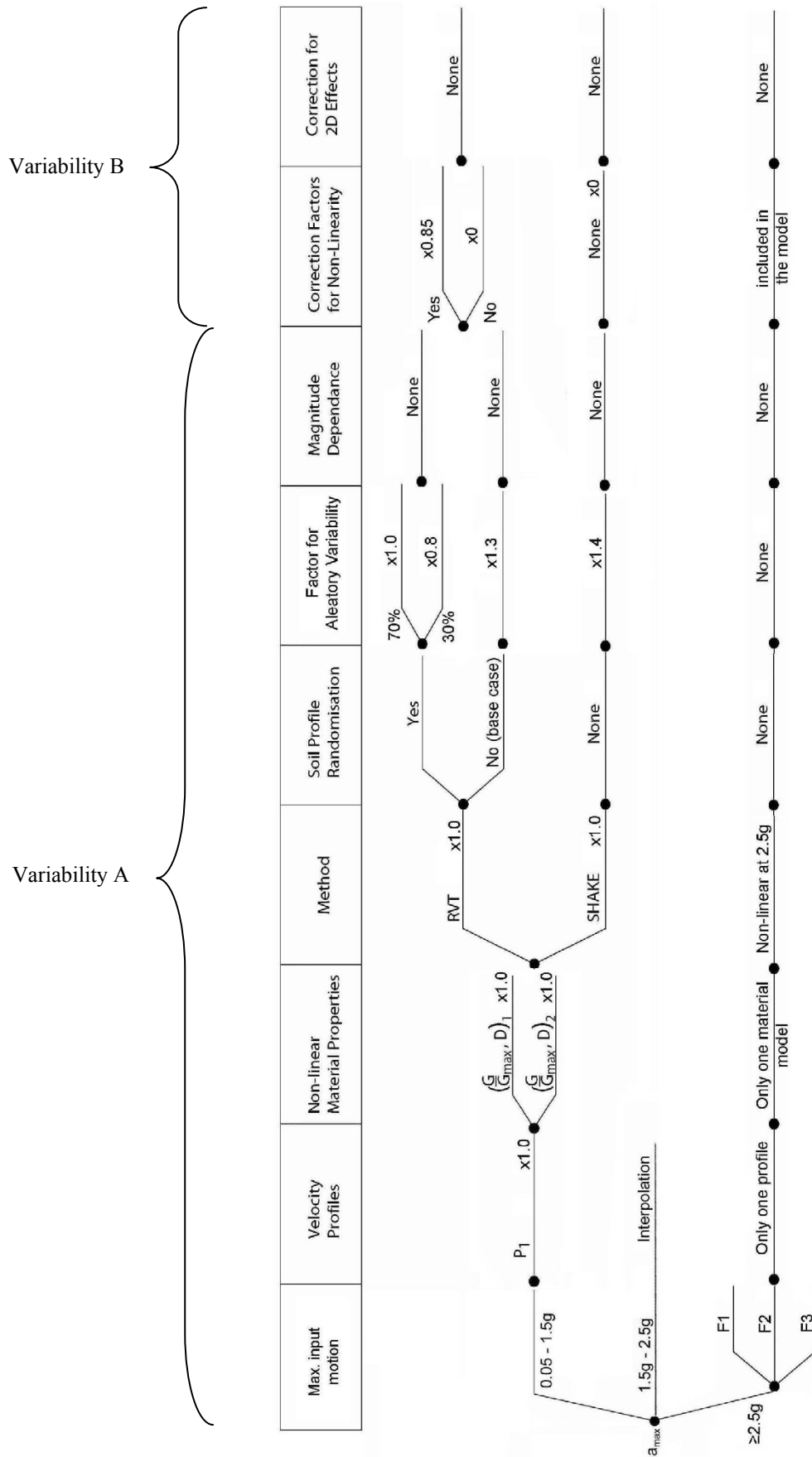


Fig. 4-1: Structure of model logic tree for aleatory variability

The final value of aleatory variability is given by: $\sqrt{(\text{Variability } A)^2 + (\text{Variability } B)^2}$

Remarks:

- The variability A uses the sigma values from either the RVT and SHAKE runs depending on the branch and then scales that sigma value by the factors in the "Factors for Aleatory Variability" branch. The variability B uses the sigma values from the multiple time histories used in the non-linear runs and then scales that sigma value by the factors in the "Correction Factors for Non-Linearity" and the "Correction for 2-D Effects" branches.
- No non-linear correction for SHAKE runs (0 % Yes), to avoid double counting (time histories for non-linear calculations are subsets of original SHAKE time histories).
- Factor 1.4 for SHAKE runs: to take into account 2D/3D effects and inclined waves.
- Factor 1.3 for RVT runs: to take into account 2D/3D effects and inclined waves.

Rationale: Soil randomization within RVT can be viewed to represent the aleatory variability representing wave propagation effects (2D, 3D effects and inclined waves). Therefore, to the branch with RVT soil randomisation has been given a smaller variability (factors 1.0 and 0.8 in Figure 4-1) than to the branch without RVT soil randomisation (factor 1.3). The SHAKE model will have a higher aleatory variability compared to the RVT models. A factor of 1.4 is taken to take also 2D/3D effects and a smaller amount of time histories into account.

4.3 Beznau

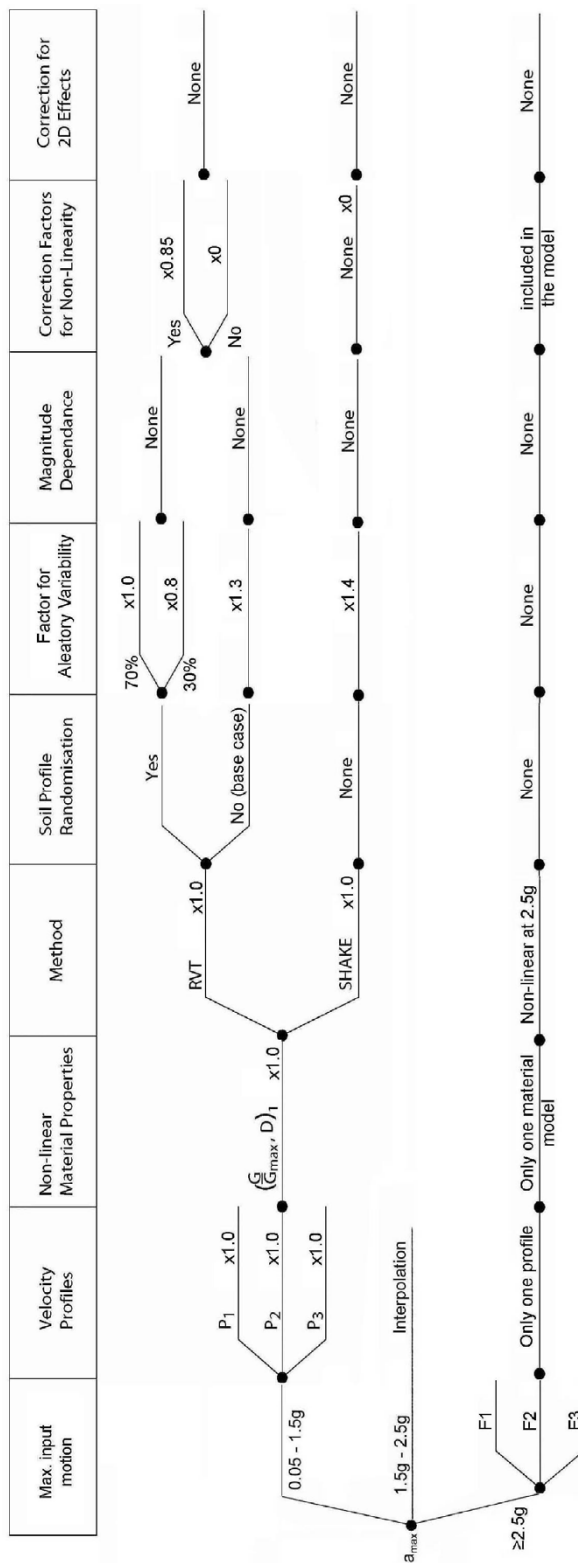


Fig. 4-2: Structure of model logic tree for aleatory variability Beznau, multiplication factors for sigma and corresponding weights

4.5 Leibstadt

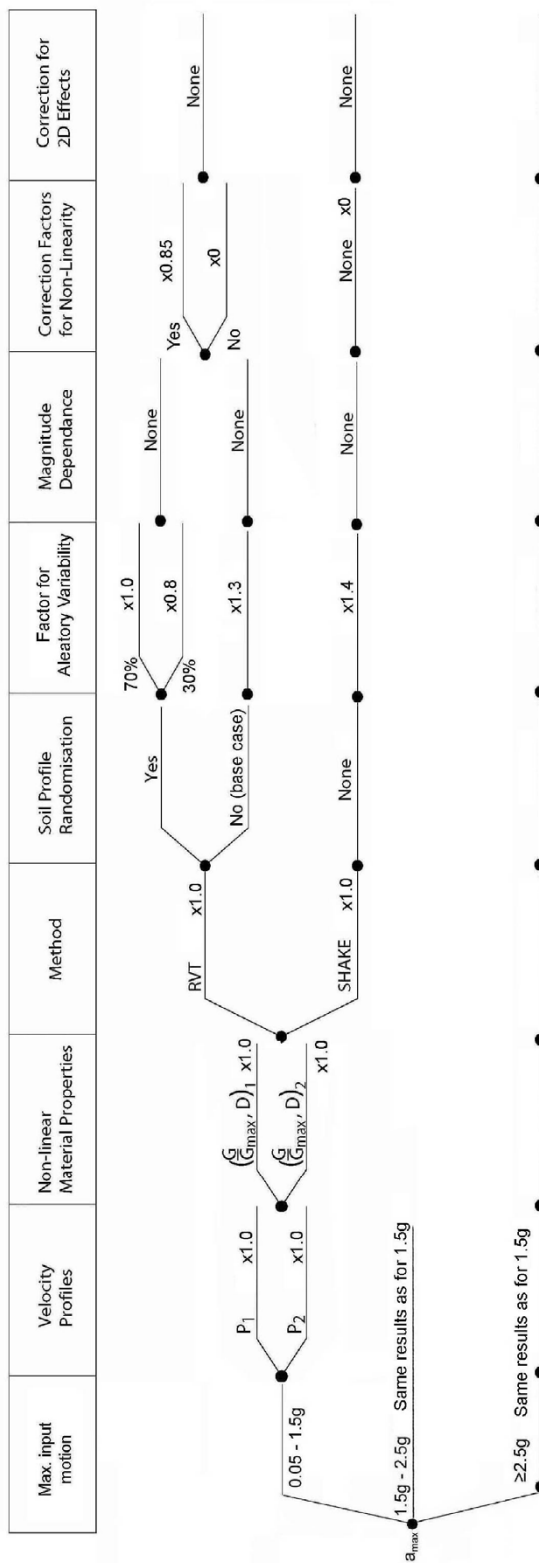


Fig. 4-4: Structure of model logic tree for aleatory variability Leibstadt, multiplication factors for sigma and corresponding weights

5 ALEATORY VARIABILITY OF VERTICAL GROUND MOTION

The procedure below is valid for all elevations.

5.1 Approach

SHAKE model has the following deficits compared to nature:

- Only one wave type is used instead of a full wave field
- Only vertical incidence is used instead of different incident angles
- The linear equivalent soil model is used instead of a true non-linear soil model

This will lead to smaller aleatory variability compared to a model that includes the above missing elements.

Decision: For the vertical ground motion, the aleatory variability is the same as for the horizontal case for the corresponding site.

Rationale: The median amplification for vertical ground motion is based on the same model as the horizontal. The final result is the V/H ratio applied to horizontal ground motion. The V/H ratio leads to no additional aleatory variability to first order.

6 MAXIMUM GROUND MOTIONS

The description of the model follows the individual branches.

6.1 General Concept for Horizontal Motion

6.1.1 Methods and general law

The maximum ground motion that can be transmitted depends on the soil strength.

In principle, the same methodology is used for all elevations. Only weights and initial values reflect the individual elevations.

Two branches are used to calculate the maximum ground motion. They are based on:

- soil mechanics model
- non-linear calculations

For the assessment, the following data are available:

- Soil mechanic model: [TP3-TN-0354, Evaluation of Max. ground Motions, A. Pecker]
- Non-linear Calculations:
 - [TP3-TN-0353, Additional Nonlinear Sites Response Analyses for Beznau and Gösgen Sites, F. Pelli]
 - [TP3-TB-0048, Nonlinear Site Response Analyses for Beznau, Gösgen, Leibstadt, F. Pelli]
 - [TP3-TN-0354, Evaluation of Max. ground Motions, A. Pecker]
- Betbeder Method: [TP3-TN-0354, Evaluation of Max. ground Motions, A. Pecker]
- Observed data: [TP3-TN-0359, Maximum Recorded Horizontal and Vertical Ground Motions, J. Ripperger, D. Fäh]

6.1.2 Material Characterisation

The same characteristics as for the Horizontal Median ground motion are used.

Additionally, characteristic values for the shear strength, φ , have been taken.

To account for uncertainties of the material properties in the failure range, a ratio of $\pm 20\%$ is taken. This ratio will account for the uncertainties of the shear strength (internal friction); this leads to a range of φ for the individual soil layers of about 37° to 48° . This uncertainty is considered as a 2σ value. Therefore, the weights are taken in general 80% for the representative value and 10% for the upper and lower ranges.

6.1.3 Site characterisations

Beznau

Characteristics of soil profile:

- 9 m Gravel / Sand
- 4 m weathered Opalinus clay
- ⇒ total 13 m top layer
- Ground water table -3.0 m from surface.

Depth of elevations: Mean elevation 6 m, minimum elevation 15 m.

Gösgen

Characteristics of soil profile:

- 26 m Gravel / Sand
- 4 m weathered Bedrock
- ⇒ total 30 m top layer
- Ground water table -5.0 m from surface.

Depth of elevations: Mean elevation 5 m, minimum elevation 9 m.

Leibstadt

Characteristics of soil profile:

- 50 m Gravel / Sand
- 4 m weathered Bedrock
- ⇒ total 54 m top layer
- Ground water table -25.5 m from surface.

Depth of elevations: Mean elevation 6 m, minimum elevation 10 m.

Mühleberg

Characteristics of soil profile:

- 11 m Gravel / Sand
- 4 m wheatered Bedrock
- ⇒ total 15 m top layer
- Ground water table -4 m from surface.

Depth of elevations: Mean elevation 7 m, minimum elevation 14 m.

6.1.4 General Evaluation of Proponent Models

Soil mechanic model: The model developed by Pecker is based on wave equation and shear strength of granular soil. It has the following assumptions:

- The increase of shear wave velocity originally is a power function of depth
- Material properties: Elasto-perfectly plastic
- Unit weight: constant
- Mode shape: First three modes

The calculations have been performed for each site individually, and with the best fit for the actual shear wave velocities and strength profiles. In the frequency range of earthquakes, the soil properties depend primarily on the shear strain and only to a smaller extent on the loading velocities. In the failure strain range, use of static material properties is a good approach. This model works with classical soil mechanics assumptions; its validity is therefore proven in daily design practice, where we have extensive experience for the behaviour of soils in the failure range. The material parameters of the individual sites are taken into account, which means the model is site specific. Therefore, Pecker's model is taken as the most relevant model with a weight (in general) of 70 %.

Non-linear Calculations: These calculations use different up-to-date computer programs. The calculations are site specific. From experience in daily design work, a non-linear site response analysis depends on a large number of parameters, which are difficult to evaluate. I have less confidence to those results than to the classical soil mechanics, particularly in the failure range,. The influence of the individual parameters is often not very clear, and results from different non-linear programs can differ. Therefore, the results of this model are taken into account, but with a smaller weight than the soil mechanics model: in general, with a weight of 30 %.

Method Betbeder: It is based on the following assumptions:

- Only the fundamental mode is taken into consideration
- The shear modulus is constant with depth
- The constitutive law for the soil is represented by the hyperbolic model
- The average soil column acceleration is limited by the available shear strength at the base of the profile divided by the mass of the soil column
- The solution consists in relating the maximum surface acceleration to the average soil column acceleration

This method is very simple and gives low values, which are considered not to be representative. In stiff soils, the higher frequencies have a significant influence. Therefore, Betbeder's model is not taken into account: weight 0 %.

Observed data: This data provides lower bound values. The site characteristic of the observed data are not known in detail, therefore those data are not site specific. For the horizontal motion, those results are not taken into account. The results for pga are in the order of the values derived from the soil mechanics model and have been used to adjust the soil mechanics model. Therefore, this data is not taken further into account.

6.2 Logic Tree and Weights for Horizontal Motion

The following logic tree in Figure 6-1 is valid for all elevations.

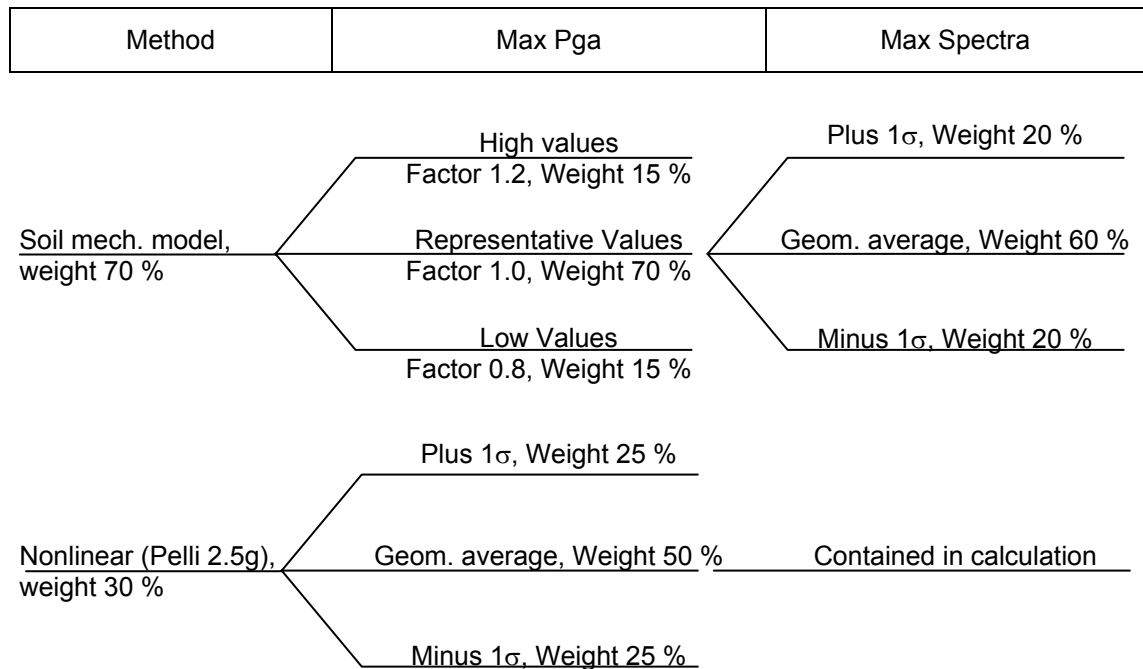


Fig. 6-1: Logic tree for horizontal motion

Exceptions:

- Beznau, minimum elevation: Non-linear branch has weight 100 %
- Mühleberg, surface and mean elevation: Soil mechanics model branch has weight 100 %
- Mühleberg, minimum elevation: Elevation is located in rock, therefore no cut-off values for the alluvium are applicable.

6.2.1 Soil mechanics model branch

6.2.1.1 Maximum pga Surface

Based on the individual results of the calculations performed in [TP3-TN-0354], taking into account the results from the soil mechanics model and the field observation, the following maximum peak ground accelerations (outcrop motions) are proposed for the individual sites at surface:

- Beznau: $\ddot{u}_{max} = 20 \text{ m/s}^2$
- Gösgen: $\ddot{u}_{max} = 15 \text{ m/s}^2$
- Leibstadt: $\ddot{u}_{max} = 15 \text{ m/s}^2$
- Mühleberg: $\ddot{u}_{max} = 16 \text{ m/s}^2$

6.2.1.2 Maximum pga, at mean elevation

The following values for maximum peak ground accelerations (within motions!) are proposed for the individual sites at mean elevation:

- Beznau (6 m): $\ddot{u}_{\max} = 5.7 - 7.9 \text{ m/s}^2$
- Gösgen (5 m): $\ddot{u}_{\max} = 6.7 - 7.7 \text{ m/s}^2$
- Leibstadt (6 m): $\ddot{u}_{\max} = 7.2 - 7.6 \text{ m/s}^2$
- Mühleberg (7 m): $\ddot{u}_{\max} = 3.5 - 5.2 \text{ m/s}^2$

Take the mean value with a weight of 70 %, the higher and lower value with a weight of each 15 %.

The above pga_max values are within motions, they have to be transferred by the following laws to outcropping motions (each law with a weight of 50 %):

$$pga_max_{outcropping, at depth} = pga_max_{within, at depth} \cdot \frac{SHAKE_{outcropping, at depth}}{SHAKE_{within, at depth}}$$

$$pga_max_{outcropping, at depth} = pga_max_{outcropping, at surface} \cdot \frac{SHAKE_{outcropping, at depth}}{SHAKE_{outcropping, at surface}}$$

whereby for the corresponding SHAKE values, the average between 30 Hz and 100 Hz is taken. The SHAKE ratio is taken for the input ground motion level of 0.75 g and a Magnitude of 6. In case of different profiles or materials, the average over all materials and profiles is taken.

6.2.1.3 Maximum pga, at minimum Elevation

Beznau

The minimum elevation is located in rock. It can be assumed that the "rock layer" has a higher strength than the alluvium. Therefore, the soil mechanics branch is not taken into account, weight of 0 %. Non-linear branch (see chapter 6.2.2.1) is taken with weight 100 %.

Gösgen and Leibstadt

The following values for maximum peak ground accelerations are proposed for the individual sites at minimum elevation:

- Gösgen (9 m): $\ddot{u}_{\max} = 6.2 - 8.1 \text{ m/s}^2$
- Leibstadt (10 m): $\ddot{u}_{\max} = 7.4 - 8.9 \text{ m/s}^2$

Take the mean value with a weight of 70 %, the higher and lower value with a weight of each 15 %.

The above pga_max values are within motions, they have to be transferred by the following law to outcropping motions (each law with a weight of 50 %):

$$pga_max_{outcropping, at depth} = pga_max_{within, at depth} \cdot \frac{SHAKE_{outcropping, at depth}}{SHAKE_{within, at depth}}$$

$$pga_max_{outcropping, at depth} = pga_max_{outcropping, at surface} \cdot \frac{SHAKE_{outcropping, at depth}}{SHAKE_{outcropping, at surface}}$$

whereby for the corresponding SHAKE values, the average between 30 Hz and 100 Hz is taken. The SHAKE ratio is taken for the input ground motion level of 0.75 g and a Magnitude of 6. In case of different profiles or materials, the average over all materials and profiles is taken.

Mühleberg

The minimum elevation is located in rock. It can be assumed that the "rock layer" has a higher strength than the alluvium.

No cut off value based on the soil mechanics model is taken into consideration at minimum elevation. There are also no non-linear calculations available. Therefore, no cut-off values for minimum elevation at Mühleberg are applicable.

6.2.1.4 Spectral shape for all sites and elevations

The normalized spectra shape is taken as calculated by Bard (TP3-TN-0358).

Surface: Take the above spectra directly.

Mean and minimum elevation: Modify the above spectra with a correction factor based on Factor A by Faeh [e-mail "Value of the factor A for H/V at depth" of October 22, 2003] at all frequencies:

$$normalized\ spectra_{at\ depth} = normalized\ spectra_{Bard, at\ surface} \cdot \frac{Factor\ A_{Faeh, at\ depth}}{Factor\ A_{Faeh, at\ surface}}$$

6.2.2 Non-linear branch

6.2.2.1 Beznau and Gösigen

This chapter is valid for all elevations, with the corresponding values at the elevation considered. Exception: For Beznau, minimum elevation, the non-linear branch takes 100 % weight. As representative values for the non-linear branch in the logic tree, the results from report [TP3-TN-0353, Additional Nonlinear Sites Response Analyses for Beznau and Gösigen Sites, F. Pelli] are taken. This because of the following reasons:

- True non-linear calculations
- Cyclic mobility effects are taken into account.

Surface motion can be taken directly from the above report.

Mean and minimum elevations are within motions and need to be transferred to outcropping motions with the formulas (each law with a weight of 50 %):

$$\text{spectral amplification}_{\text{outcropping, at depth}} = \text{spectral amplification}_{\text{within, at depth}} \cdot \frac{\text{SHAKE}_{\text{outcropping, at depth}}}{\text{SHAKE}_{\text{within, at depth}}}$$

$$\text{spectral amplification}_{\text{outcropping, at depth}} = \text{spectral amplification}_{\text{outcropping, at surface}} \cdot \frac{\text{SHAKE}_{\text{outcropping, at depth}}}{\text{SHAKE}_{\text{outcropping, at surface}}}$$

for the corresponding frequency. The SHAKE ratio is taken for the input ground motion level of 0.75 g and a Magnitude of 6. In case of different profiles or materials, the average over all materials and profiles is taken.

6.2.2.2 Leibstadt

This chapter is valid for all elevations, with the corresponding values at the elevation considered. As representative values for the nonlinear branch in the logic tree, the available results from report [TP3-TB-0048, Nonlinear Site Response Analyses for Bezna, Gösigen, Leibstadt, F. Pelli] are taken. Cyclic mobility is less significant here, due to the fact that ground water table is very low.

Surface motion can be taken directly from the above report.

Mean and minimum elevations are within motions and need to be transferred to outcropping motions with the formulas (each law with a weight of 50 %):

$$\text{spectral amplification}_{\text{outcropping, at depth}} = \text{spectral amplification}_{\text{within, at depth}} \cdot \frac{\text{SHAKE}_{\text{outcropping, at depth}}}{\text{SHAKE}_{\text{within, at depth}}}$$

$$\text{spectral amplification}_{\text{outcropping, at depth}} = \text{spectral amplification}_{\text{outcropping, at surface}} \cdot \frac{\text{SHAKE}_{\text{outcropping, at depth}}}{\text{SHAKE}_{\text{outcropping, at surface}}}$$

for the corresponding frequency. The SHAKE ratio is taken for the input ground motion level of 0.75 g and a Magnitude of 6. In case of different profiles or materials, the average over all materials and profiles is taken.

6.2.2.3 Mühleberg, Horizontal Motion

No nonlinear branch is considered for Mühleberg. The weight of the soil mechanics model is therefore 100 %.

Exception: For Mühleberg, minimum elevation, no cut-off value is considered.

6.3 General Concept for Vertical Motion

6.3.1 Methods

In principle, the same methodology is used for all elevations. Only weights and initial values reflect the individual elevations.

Below the minimum ground water table, we can assume 100 % saturation and the characteristics are dominated by the stiffness of the water. The vertical motion is dominated by vertical propagating P-waves. Under one-dimensional P-waves conditions, the soil strength will depend mainly on crushing of the grains. Based on experience in soil mechanics for such soils, the materials at these sites will show no failure under P-waves in the pressure range of interest for

this problem. The individual sites have generally high water tables. Therefore, for motions in sites with high water table in respect to the entire height of the soil deposit, no maximum ground motion is taken into account as cut-off value. In case a significant part of the soil column is unsaturated, a limitation caused by shear strength is taken into account. In general, first the p_{ga} is calculated, and then a normalized spectrum is used to obtain the entire response spectra. The maximum ground motion that can be transmitted depends on the soil strength.

The proposed model is based on the following data:

- Depth of the ground water table
- Observed data [TP3-TN-0359, Maximum Recorded Horizontal and Vertical Ground Motions, J. Ripperger, D. Fäh]

6.3.2 Material Characterisation

No specific material characterisation is taken into account.

6.4 Logic Tree and Weights for Vertical Motion

6.4.1 Surface, mean and minimum elevation

The logic tree is discussed in the individual chapters, where relevant.

6.4.2 Beznau, Vertical Motion; Surface, mean and minimum elevation

Characteristics of soil profile:

- 9 m Gravel / Sand
- 4 m weathered Opalinus clay
- \Rightarrow total 13 m top layer
- Ground water table -3.0 m from surface.

Depth of elevations: Mean elevation 6 m, minimum elevation 15 m

Decision: No maximum ground motion is taken into account as cut-off value.

Reasoning: See 6.1.

6.4.3 Gösgen, Vertical Motion; Surface, mean and minimum elevation

Characteristics of soil profile:

- 26 m Gravel / Sand
- 4 m weathered Bedrock
- \Rightarrow total 30 m top layer
- Ground water table -5.0 m from surface.

Depth of elevations: Mean elevation 5 m, minimum elevation 9 m.

Decision: No maximum ground motion is taken into account as cut-off value.

Reasoning: See 6.1.

6.4.4 Leibstadt, Vertical Motion

6.4.4.1 Characteristics of soil profile

- 50 m Gravel/Sand
- 4 m weathered Bedrock
- ⇒ total 54 m top layer
- Ground water table -25.5 m from surface.

The unsaturated part of the soil profile is around 26 m.

Depth of elevations: Mean elevation 6m, minimum elevation 10m.

6.4.4.2 Logic tree

The corresponding logic tree, valid for all elevations is represented in Fig. 6-2.

The following weights apply:

- Take the unbounded values: weight 50 %
- Take the observed vertical data from Faeh (figure 3, solid black line; local geology is stiff, soft soil or alluvium, smoothly enveloped) with factor 1.4: 25 %
- Take the observed vertical data from Faeh (figure 3, solid black line; local geology is stiff, soft soil or alluvium, smoothly enveloped) with factor 1.0: 25 %

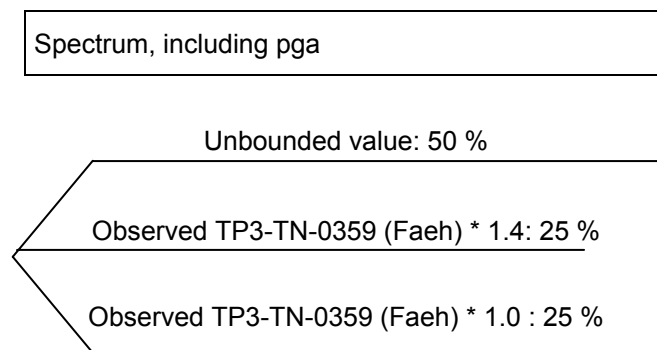


Fig. 6-2: Logic tree for maximum vertical motion, Leibstadt

Rationale: Leibstadt site has a significant depth of unsaturated soil. Therefore, a certain limitation due to the strength of the soil has to be taken into account. All calculations for the vertical ground motion are primarily based on vertical wave propagation. Inclined waves will also have shear components. Therefore, a limitation due to shear strength has to be taken into account. The observed data by Faeh is taken as representative, including also these effects. This data provides lower bound values. The site characteristic of the observed data are not known in detail, therefore those data are not site specific. The spectra for the vertical max. ground motion are based on observed data [TP3-TN-0359, "Max. recorded horizontal and vertical ground motions". It is certain, that observed motion will provide a lower bound for the maximum vertical motion. Therefore, an estimate of the potential true maximum ground motion is needed.

Figure 6-3 by [Abrahamson] shows a continuous increase of maximum spectral values since 1950. It has to be assumed that in future, again higher values will be recorded with the increased number of sites instrumented. Therefore, the upper bound of the spectral values will be estimated by multiplying the existing database by a factor 1.4.

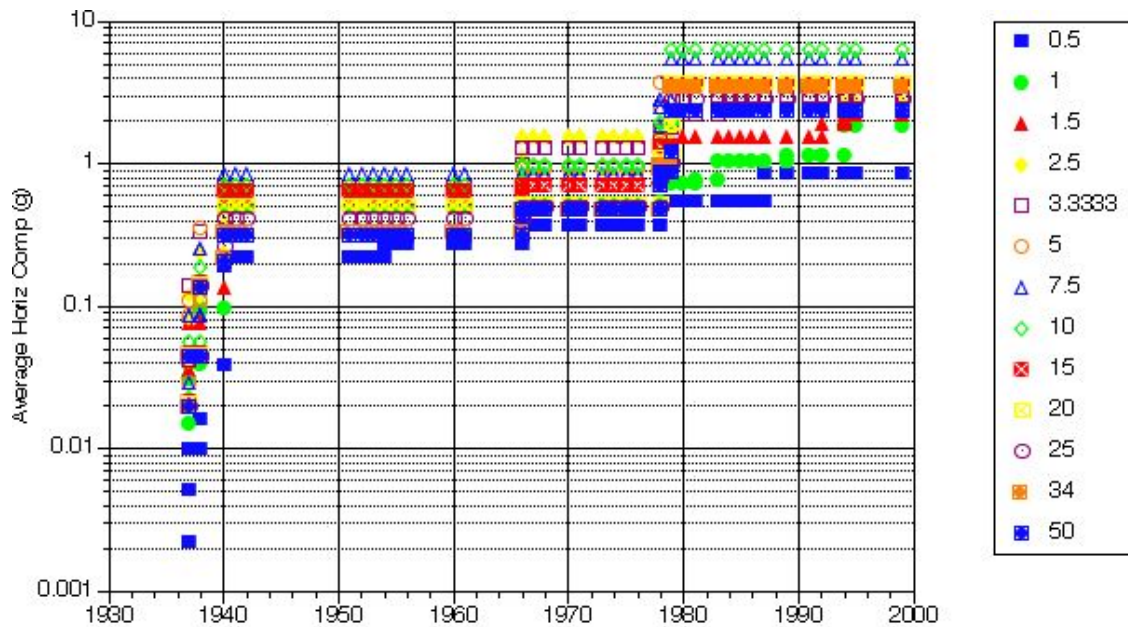


Fig. 6-3: Increase of pga over time

6.4.4.3 Surface

The enveloped spectrum is used directly.

6.4.4.4 Mean and minimum elevation

Modify the enveloped spectrum with a correction factor based on Factor A by Faeh [e-mail "Value of the factor A for H/V at depth" of October 22, 2003] at all frequencies:

$$enveloped\ spectra_{at\ depth} = enveloped\ spectra_{Bard,\ at\ surface} \cdot \frac{Factor\ A_{Faeh,\ at\ depth}}{Factor\ A_{Faeh,\ at\ surface}}$$

6.4.5 Mühleberg, Vertical Motion; Surface, mean and minimum elevation

No maximum ground motion is taken into account as cut-off value.

Reasoning: See 6.1.

7 REFERENCES

- NRC NUREG 6728: Technical Basis for Revision of Regulatory Guidance on Design Ground Motions: Hazard- and Risk-consistent Ground Motion Spectra Guidelines. U.S. Nuclear Regulatory Commission, NUREG/CR-6728 (McGuire et al. 2002).
- PEGASOS TP3-ASW-0024: Hölker, A.: Matlab software package and databases for the computation of the SP3 / site amplification models.
- PEGASOS TP3-SUP-0022: Pelli, F.: Non-linear Site Response Analyses for Beznau, Gösgen and Leibstadt.
- PEGASOS TP3-SUP-0062: Pelli, F.: Additional Nonlinear Site Response Analyses for Beznau and Gösgen at a high shaking level considering cyclic mobility effects.
- PEGASOS TP3-TB-0048: Pelli, F. 2002: Nonlinear Site Response Analyses for Beznau, Gösgen, Leibstadt (6.8.2002).
- PEGASOS TP3-TN-0166: Koller, M. 2002: PEGASOS Soil Profiles for Supporting Computations (22.5.2002).
- PEGASOS TP3-TN-0186: Bard, P.-Y. 2002: 2D SH computations for the Leibstadt nuclear power plant site Amplification factors in the low and high strain cases (4.8.2002).
- PEGASOS TP3-TN-0240: Fäh, D. 2002: Two Dimensional Modelling of SH-wave Amplification (5.9.2002).
- PEGASOS TP3-TN-0294: Tinic, S.: Overview of supporting computations.
- PEGASOS TP3-TN-0340: Bard, P.-Y. 2003: A short note on the reliability of SHAKE amplification factors at low frequencies (20.3.2003).
- PEGASOS TP3-TN-0353: Pelli, F. 2003: Nonlinear Site Response Analyses for Beznau and Gösgen at a high shaking levels considering cyclic mobility effects (6.5.2003).
- PEGASOS TP3-TN-0354: Pecker, A. 2003: Evaluation of maximum ground motions (14.4.2003).
- PEGASOS TP3-TN-0358: Bard, P.-Y. 2003: Response spectra associated with maximum peak ground acceleration for the 4 PEGASOS sites (6.5.2003).
- PEGASOS TP3-TN-0359: Rippberger, J. & Fäh, D. 2003: Maximum Recorded Horizontal and Vertical Ground Motions (13.5.2003).
- PEGASOS TP3-TN-0401: Hölker, A.: Summarizing the SP3 site effect models to Soil hazard Input Files (SIFs).

APPENDIX 1: MEDIAN AMPLIFICATION OF HORIZONTAL GROUND MOTION

A1.1 Beznau, Magnitude dependence for RVT calculations

A1.1.1 Profile 2, Material 1

Profile	Shaking level	Ratio of amplification functions
2	0.1 g	
2	0.2 g	
2	0.4 g	
2	0.75 g	
2	1 g	
2	1.25 g	
2	1.5 g	

A1.1.2 Profile 3

Profile	Shaking level	Ratio of amplification functions
3	0.1 g	
3	0.2 g	
3	0.4 g	
3	0.75 g	
3	1 g	
3	1.25 g	
3	1.5 g	

A1.2 Beznau, Magnitude dependence for SHAKE calculations

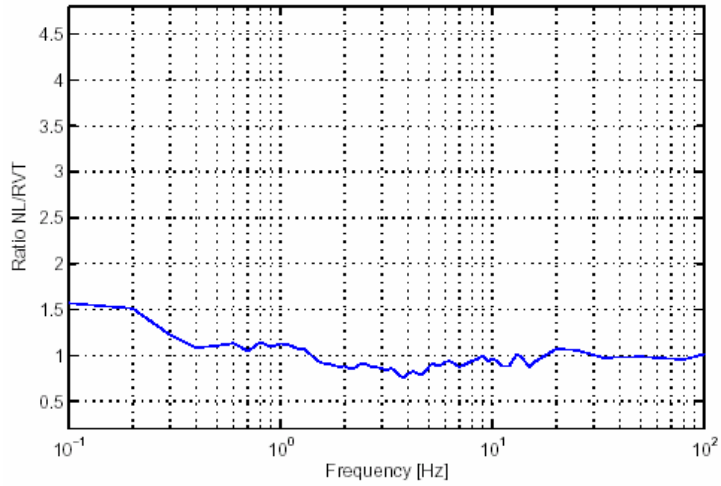
A1.2.1 Profile 1, Material 1

Profile	Shaking level	Ratio of amplification functions
1	0.1 g	
1	0.4 g	
1	0.75 g	

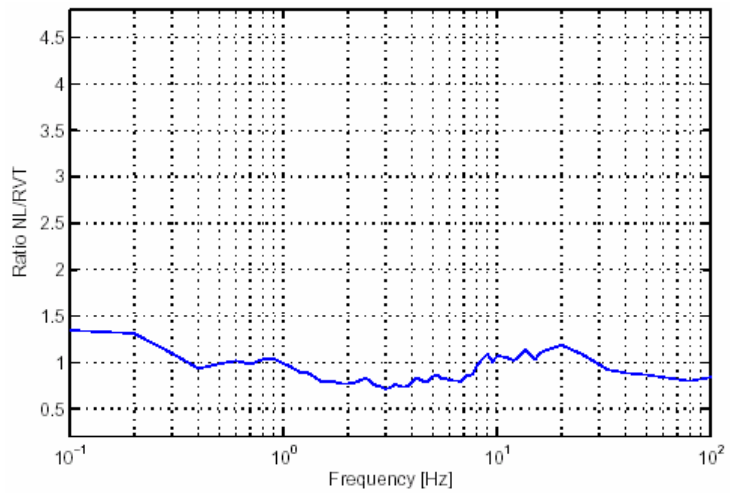
A1.3 Beznau, Use of results from non-linear sensitivity runs

A1.3.1 RVT runs, Profile 1

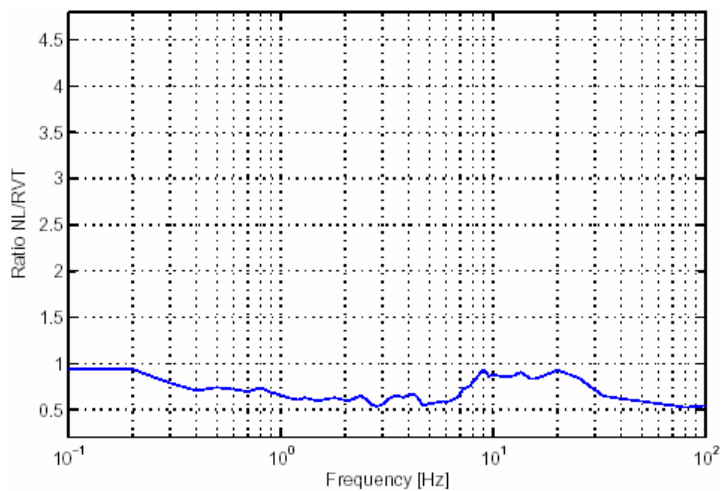
For 0.4 g:



For 0.75 g:

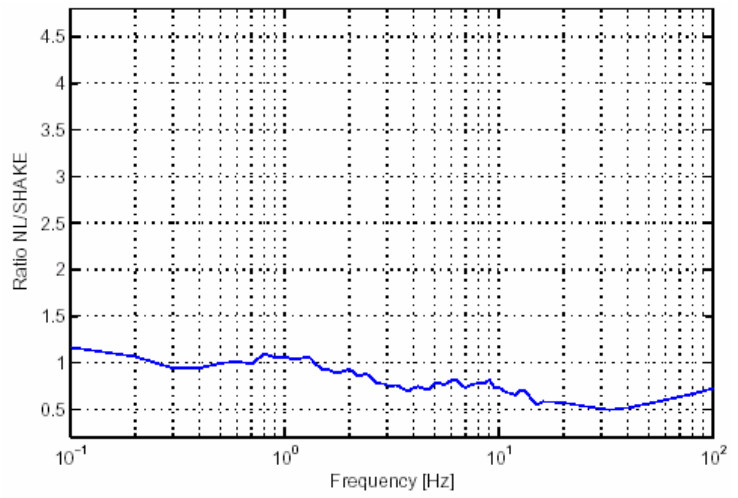


For 1.5 g:

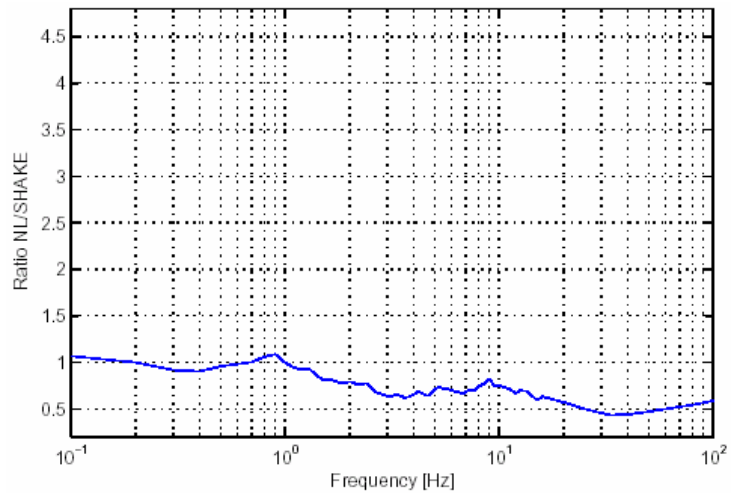


A1.3.2 SHAKE runs, Profile 1

For 0.4 g:



For 0.75 g:

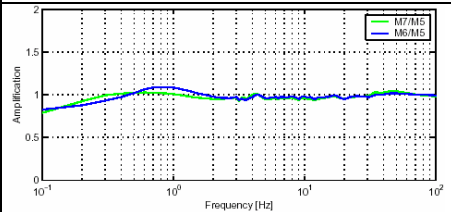
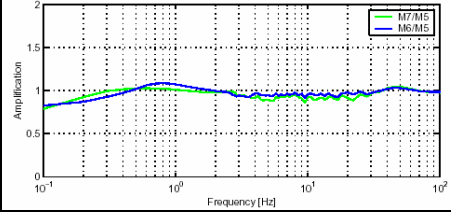
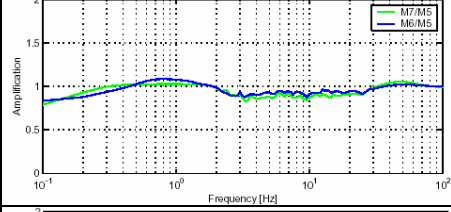
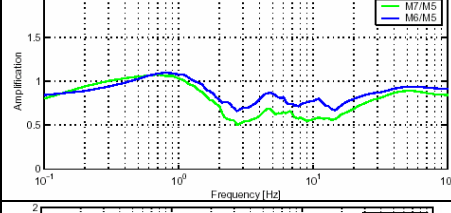
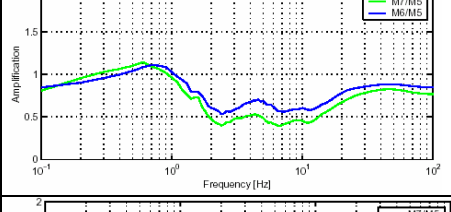
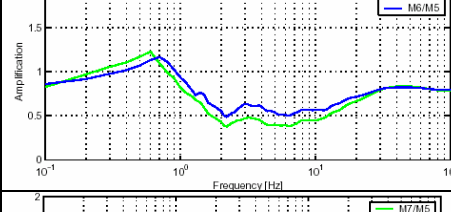
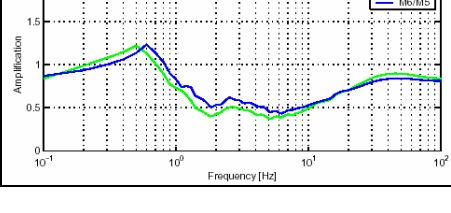


A1.4 Gösgen, Magnitude dependence for RVT calculations

A1.4.1 Profile 1, Material 1

Profile	Shaking level	Ratio of amplification functions
1	0.1 g	
1	0.2 g	
1	0.4 g	
1	0.75 g	
1	1 g	
1	1.25 g	
1	1.5 g	

A1.4.2 Profile 1, Material 2

Profile	Shaking level	Ratio of amplification functions
1	0.1 g	
1	0.2 g	
1	0.4 g	
1	0.75 g	
1	1 g	
1	1.25 g	
1	1.5 g	

A1.5 Gösgen, Magnitude dependence for SHAKE calculations

A1.5.1 Profile 1, Material 1

Profile	Shaking level	Ratio of amplification functions
1	0.1 g	
1	0.4 g	
1	0.75 g	

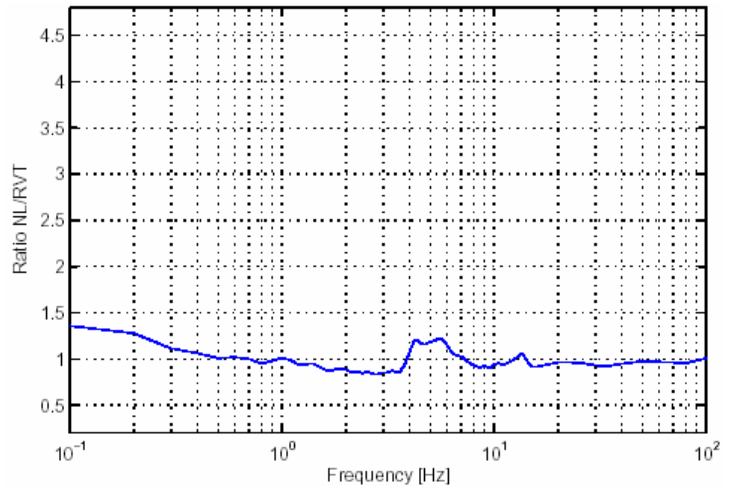
A1.5.2 Profile 1, Material 2

Profile	Shaking level	Ratio of amplification functions
1	0.1 g	
1	0.4 g	
1	0.75 g	

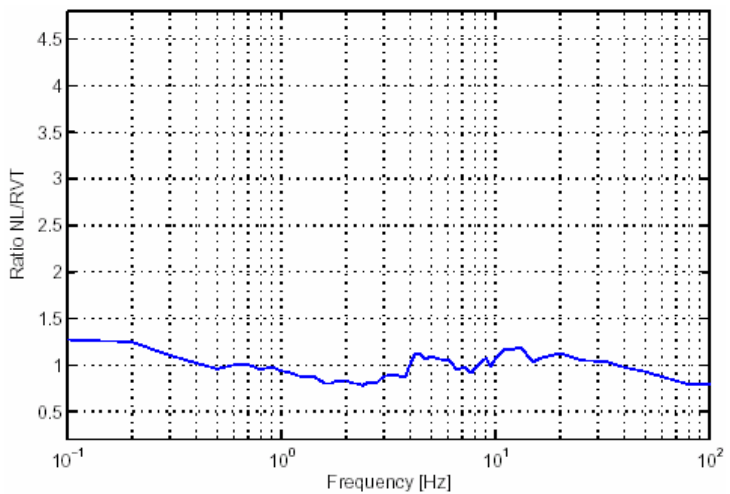
A1.6 Gösgen, Use of results from non-linear sensitivity runs

A1.6.1 RVT runs, Profile 1

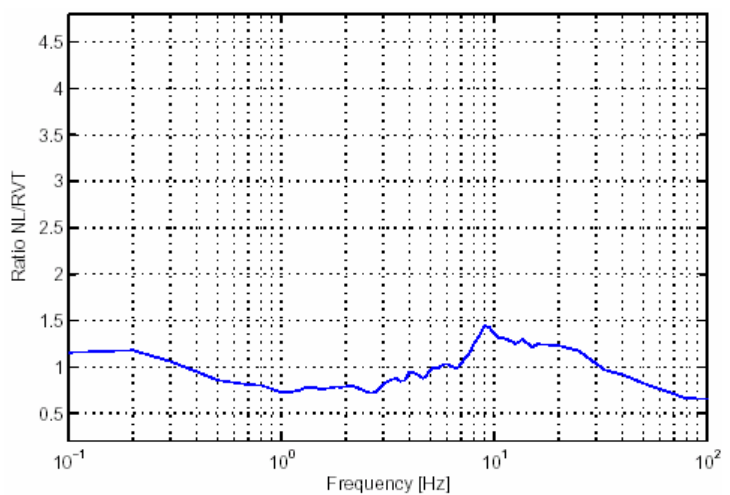
For 0.4 g:



For 0.75 g:

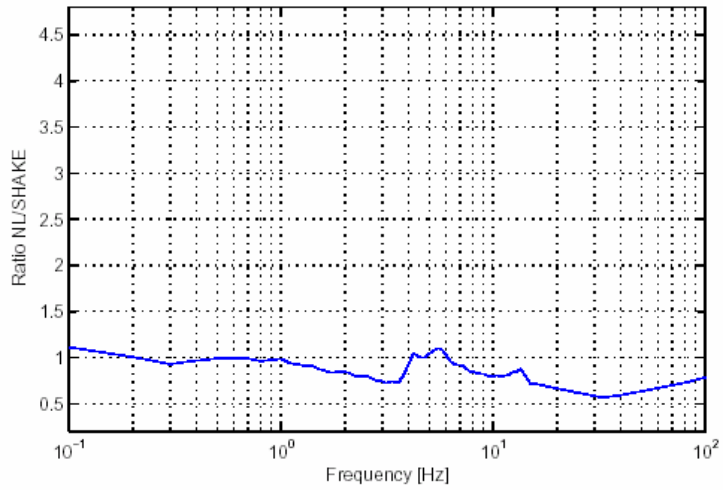


For 1.5 g:

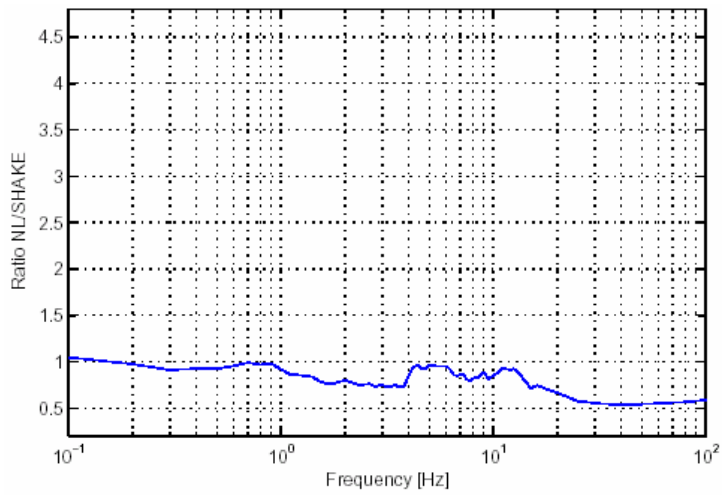


A1.6.2 SHAKE runs, Profile 1

For 0.4 g:

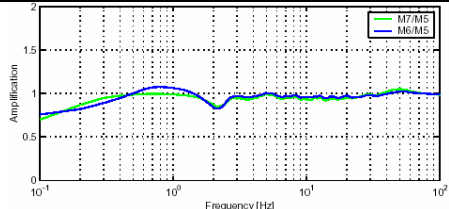
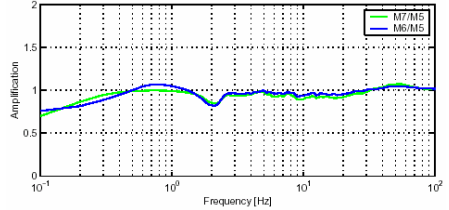
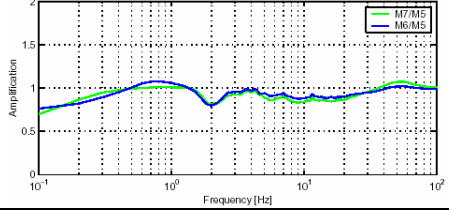
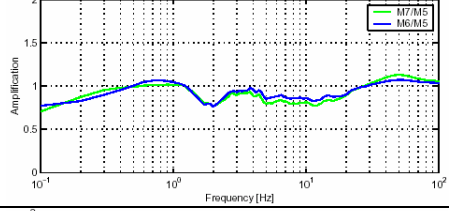
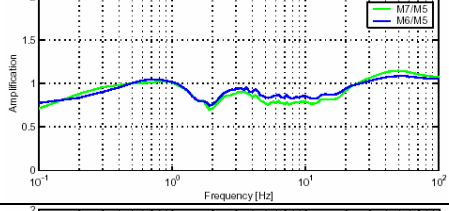
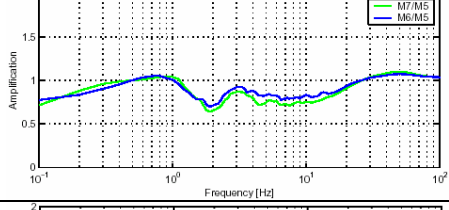
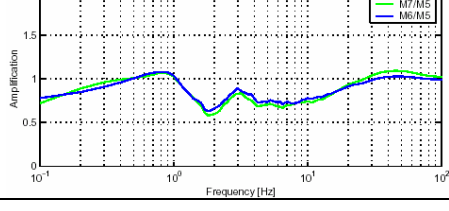


For 0.75 g:



A1.7 Leibstadt, Magnitude dependence for RVT calculations

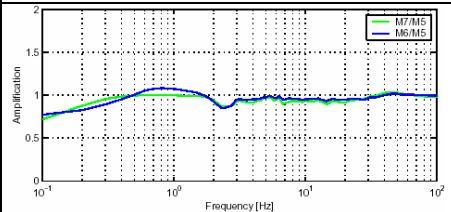
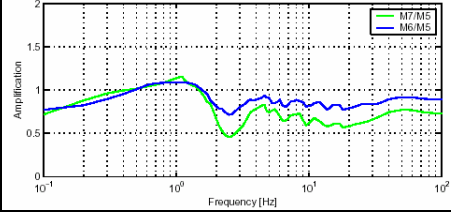
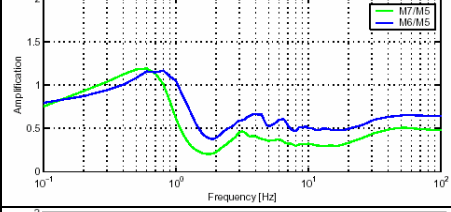
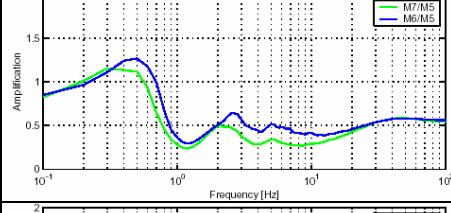
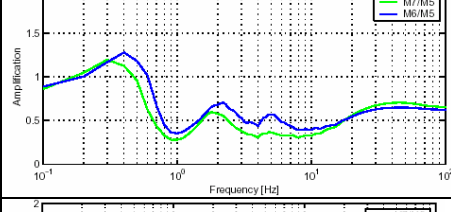
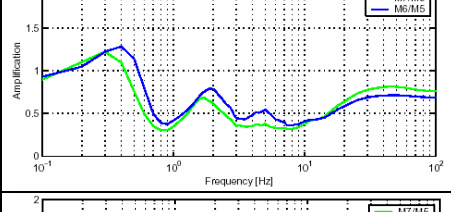
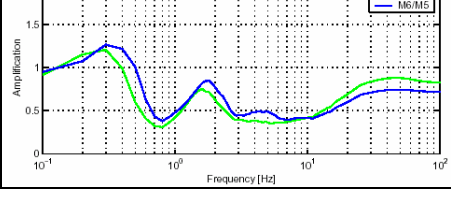
A1.7.1 Profile 1, Material 1

Profile	Shaking level	Ratio of amplification functions
1	0.1 g	
1	0.2 g	
1	0.4 g	
1	0.75 g	
1	1 g	
1	1.25 g	
1	1.5 g	

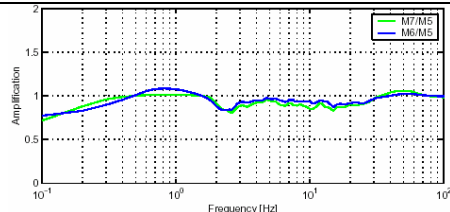
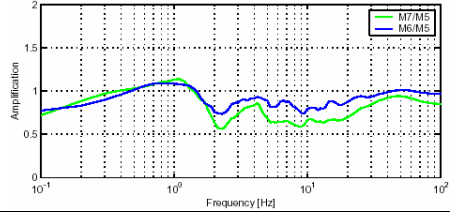
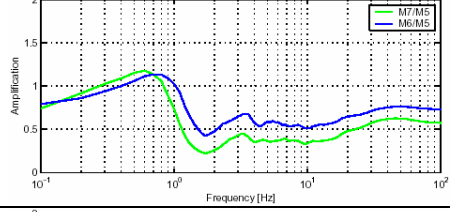
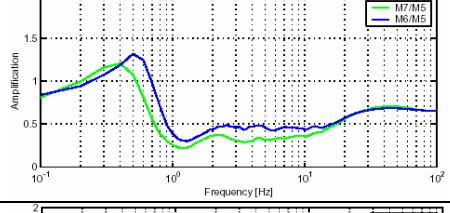
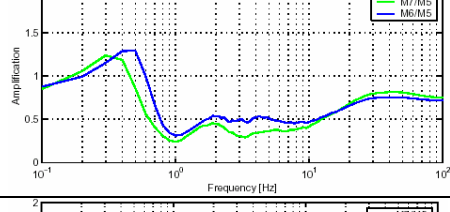
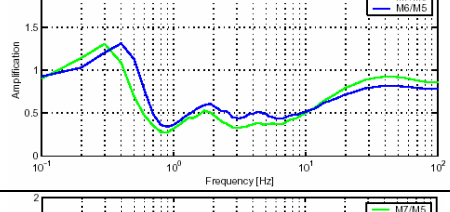
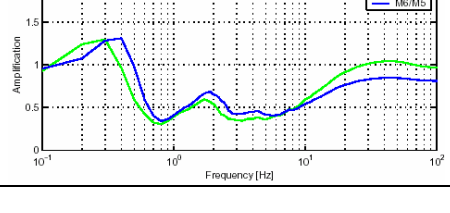
A1.7.2 Profile 1, Material 2

Profile	Shaking level	Ratio of amplification functions
1	0.1 g	
1	0.2 g	
1	0.4 g	
1	0.75 g	
1	1 g	
1	1.25 g	
1	1.5 g	

A1.7.3 Profile 2, Material 1

Profile	Shaking level	Ratio of amplification functions
2	0.1 g	
2	0.2 g	
2	0.4 g	
2	0.75 g	
2	1 g	
2	1.25 g	
2	1.5 g	

A1.7.4 Profile 2, Material 2

Profile	Shaking level	Ratio of amplification functions
2	0.1 g	
2	0.2 g	
2	0.4 g	
2	0.75 g	
2	1 g	
2	1.25 g	
2	1.5 g	

A1.8 Leibstadt, Magnitude dependence for SHAKE calculations

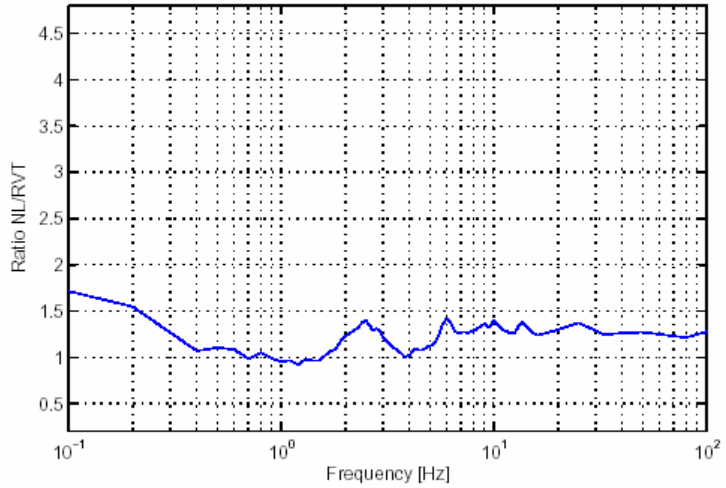
A1.8.1 Profile 2, Material 1

Profile	Shaking level	Ratio of amplification functions
2	0.1 g	
2	0.4 g	
2	0.75 g	

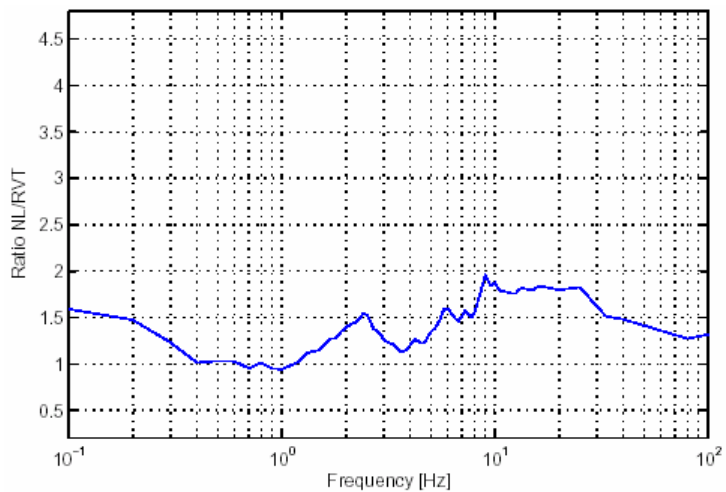
A1.9 Leibstadt, Use of results from non-linear sensitivity runs

A1.9.1 RVT runs, Profile 1

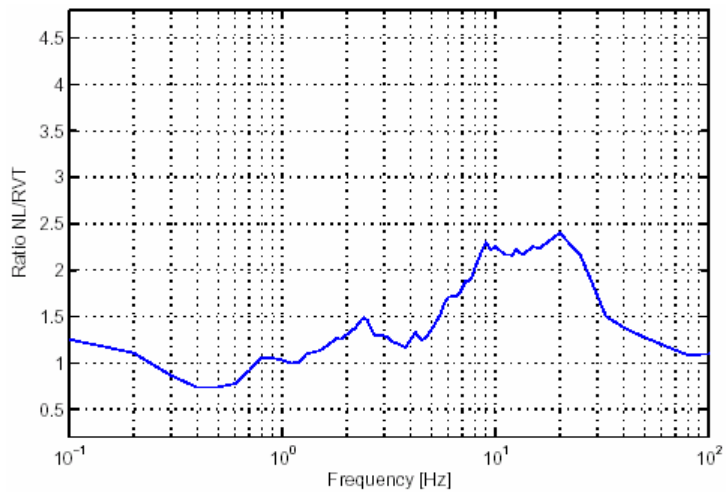
For 0.4 g:



For 0.75 g:

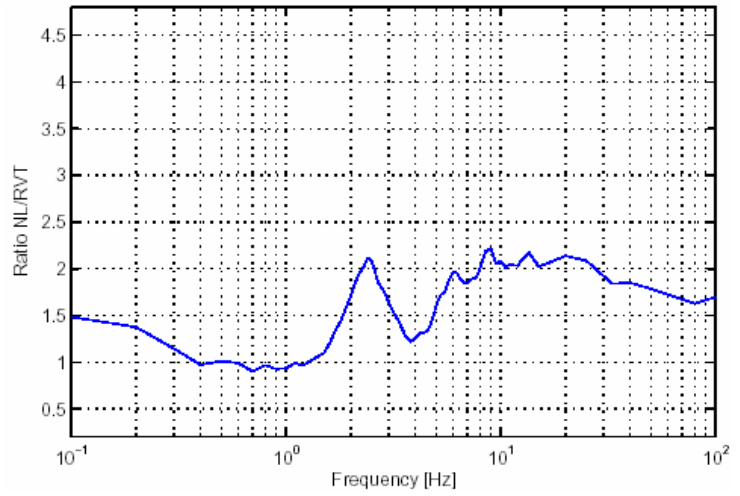


For 1.5 g:

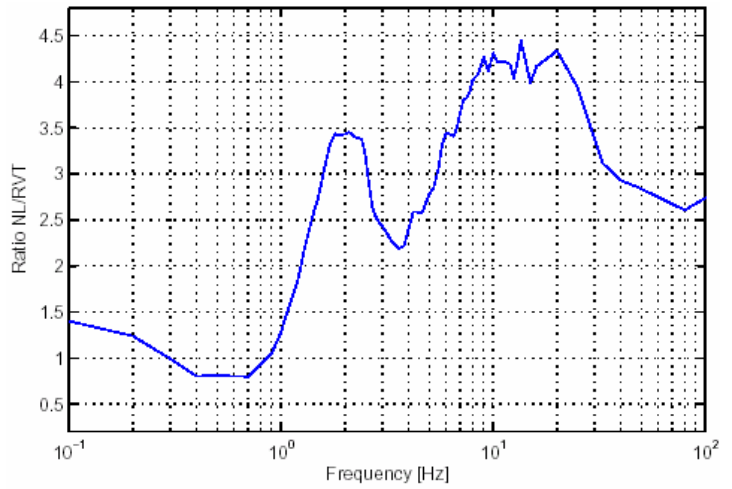


A1.9.2 RVT runs, Profile 2

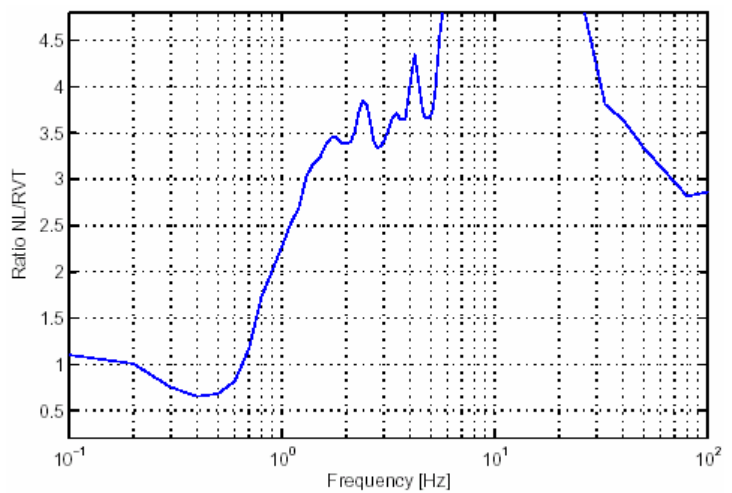
For 0.4 g:



For 0.75 g:

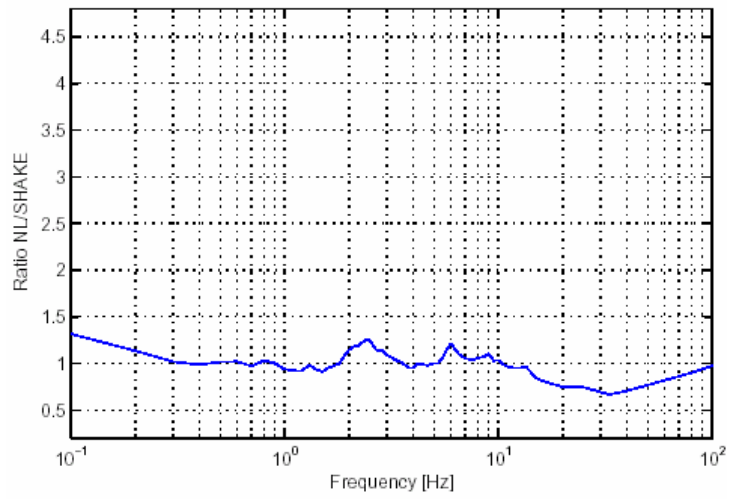


For 1.5 g:

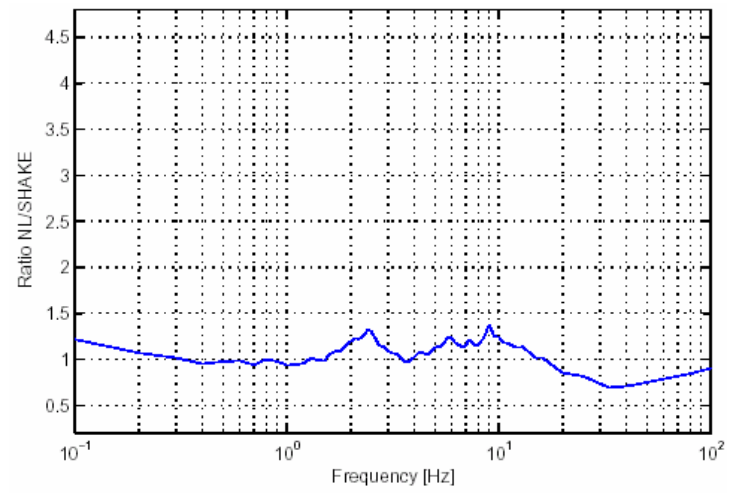


A1.9.3 SHAKE runs, Profile 1

For 0.4 g:

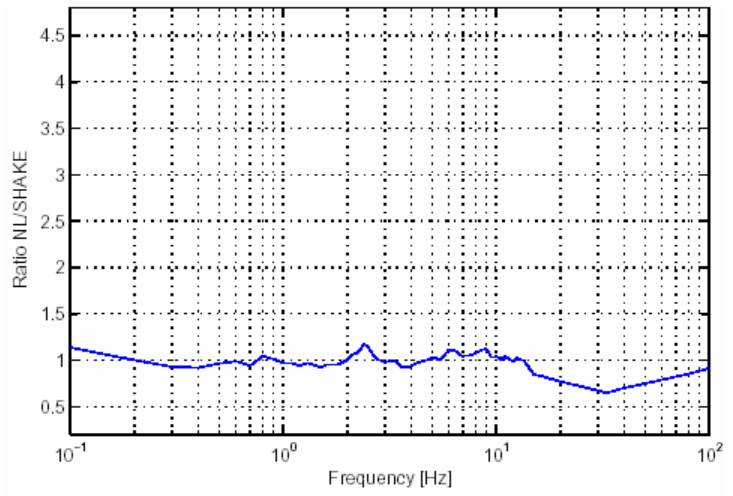


For 0.75 g:

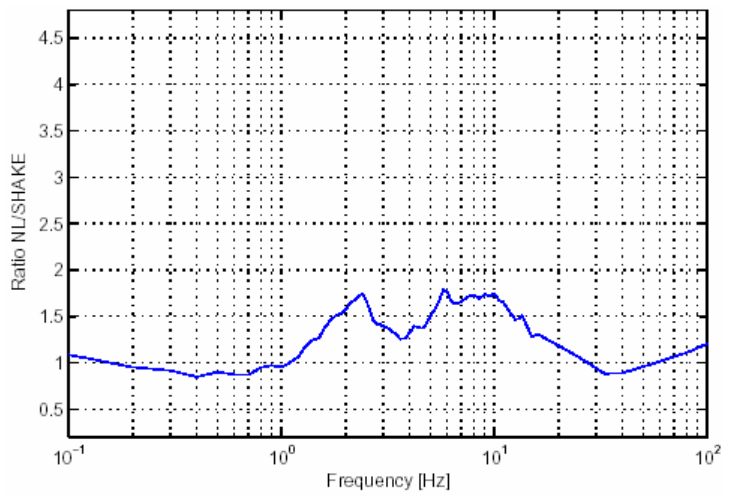


A1.9.4 SHAKE runs, Profile 2

For 0.4 g:

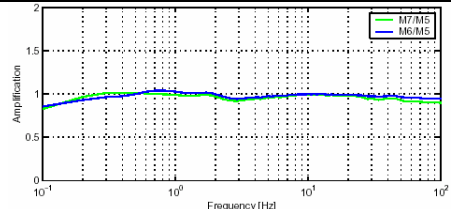
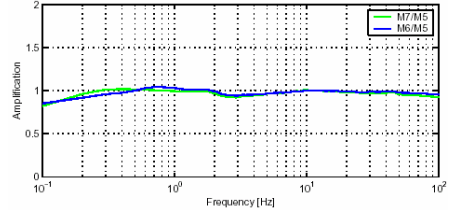
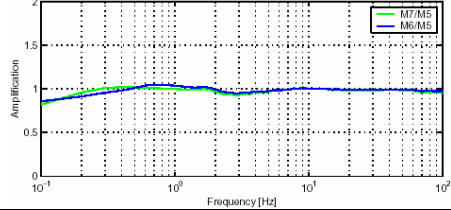
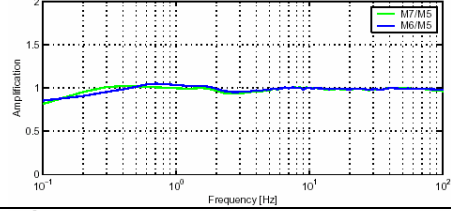
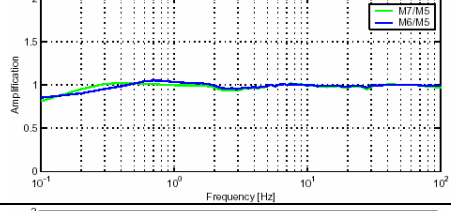
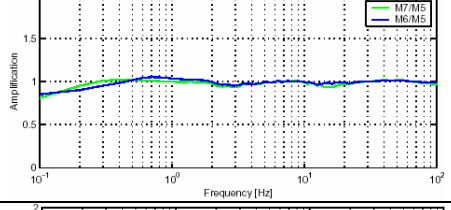
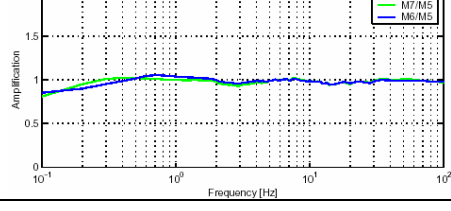


For 0.75 g:



A1.10 Mühleberg, Magnitude dependence for RVT calculations

A1.10.1 Profile 1, Material 1

Profile	Shaking level	Ratio of amplification functions
1	0.1 g	
1	0.2 g	
1	0.4 g	
1	0.75 g	
1	1 g	
1	1.25 g	
1	1.5 g	

A1.10.2 Profile 1, Material 2

Profile	Shaking level	Ratio of amplification functions
1	0.1 g	
1	0.2 g	
1	0.4 g	
1	0.75 g	
1	1 g	
1	1.25 g	
1	1.5 g	

A1.11 Mühleberg, Magnitude dependence for SHAKE calculations

A1.11.1 Profile 1, Material 1

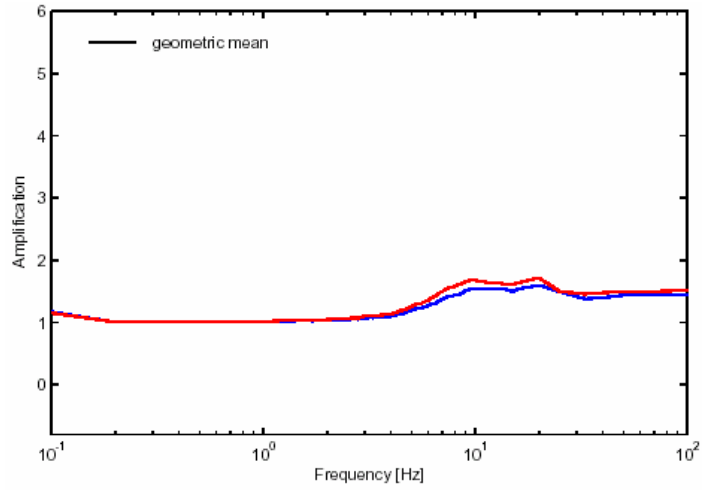
Profile	Shaking level	Ratio of amplification functions
1	0.1g	
1	0.4g	
1	0.75g	

APPENDIX 2: MEDIAN AMPLIFICATION OF VERTICAL GROUND MOTION

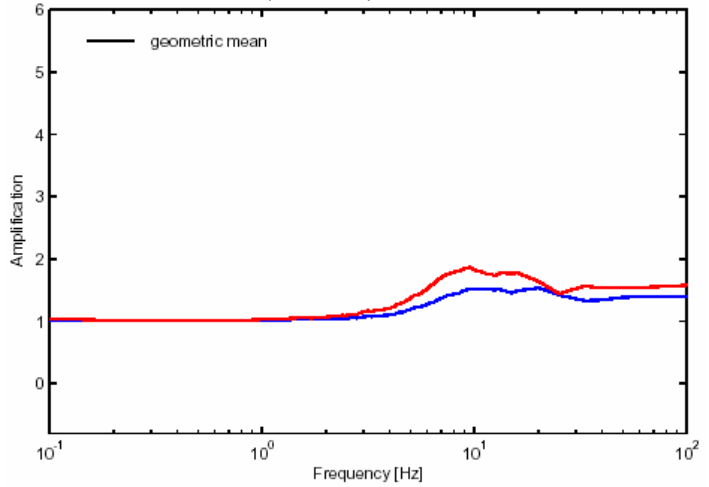
A2.1 Beznau

A2.1.1 Evaluation of approaches for computing the vertical site response (SHAKE runs)

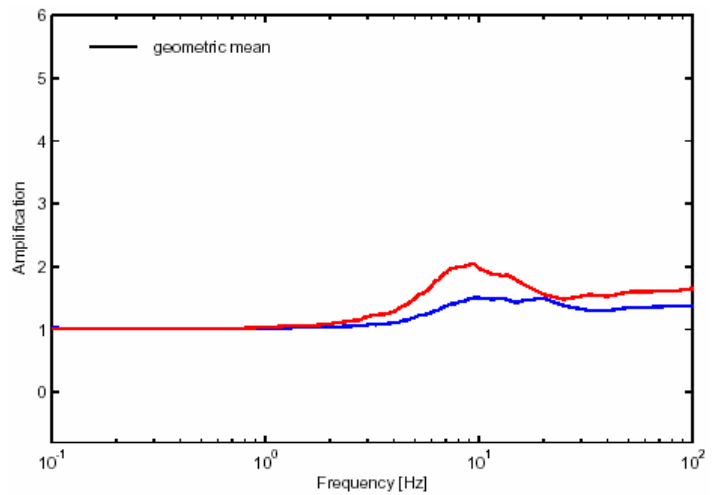
For 0.1 g:



For 0.4 g:

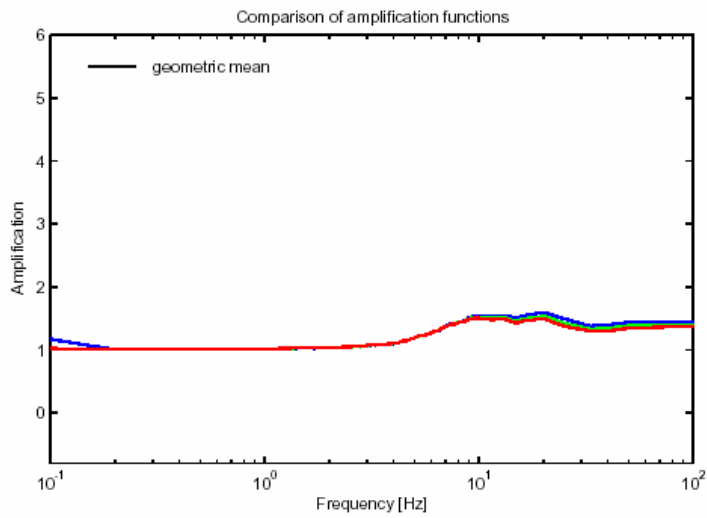


For 0.75 g:

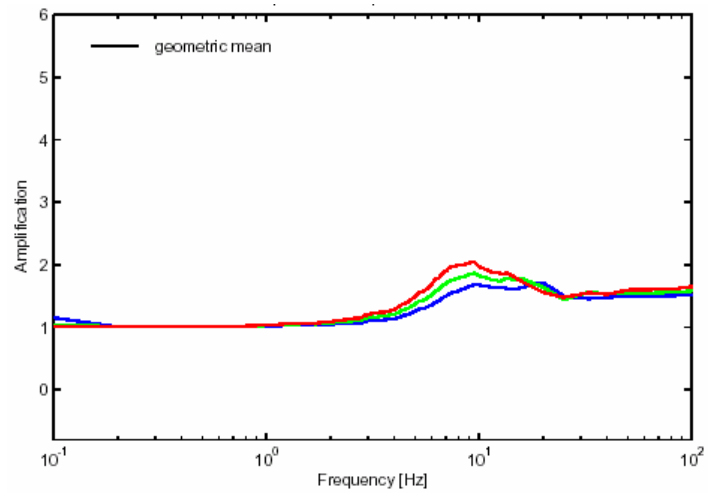


A2.1.2 Interpolation / Extrapolation to a case not considered in the available vertical computations

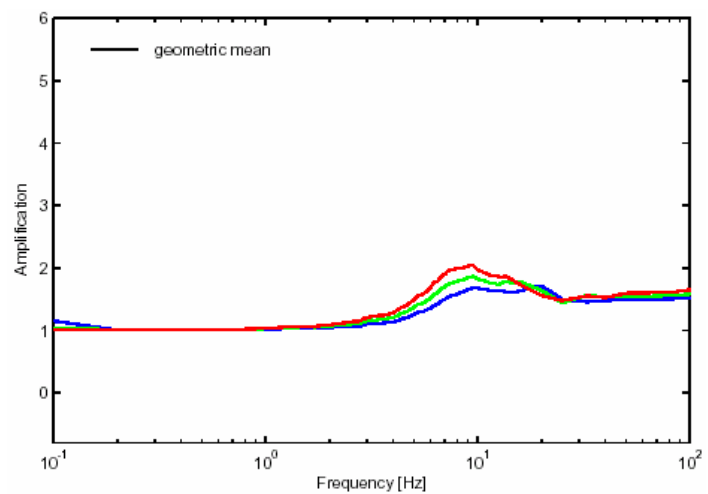
For P-wave degradation 1:



For P-wave degradation 2:



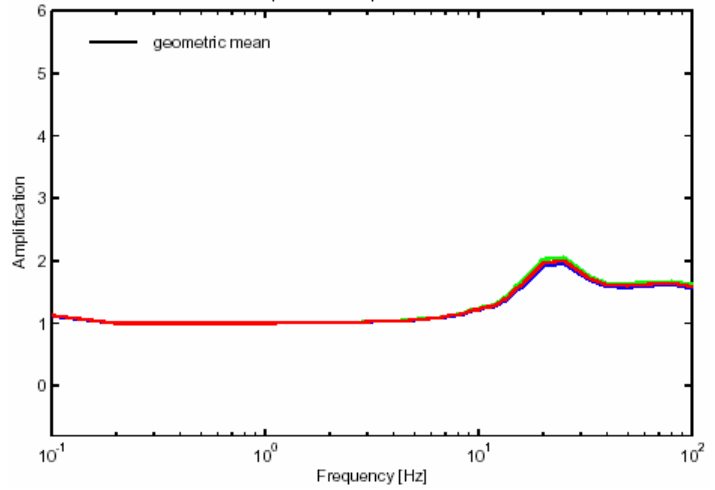
For P-wave degradation 3:



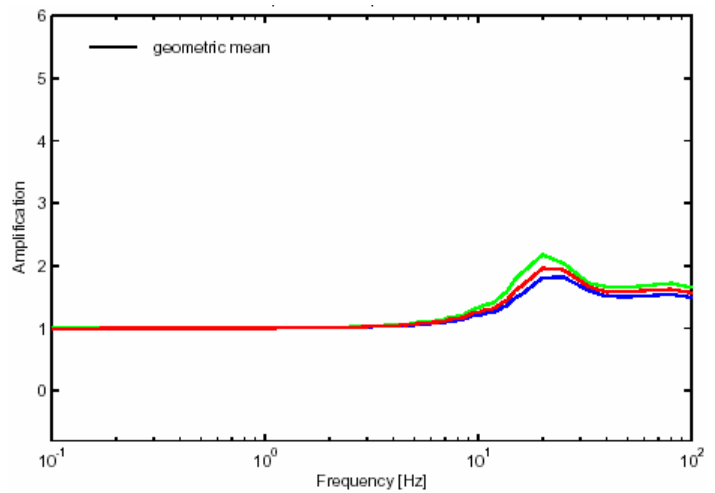
A2.2 Gösgen

A2.2.1 Evaluation of approaches for computing the vertical site response (SHAKE runs)

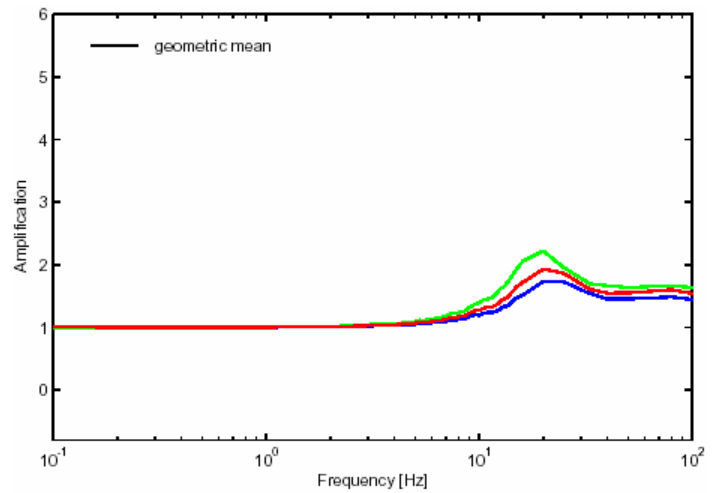
For 0.1 g:



For 0.4 g:

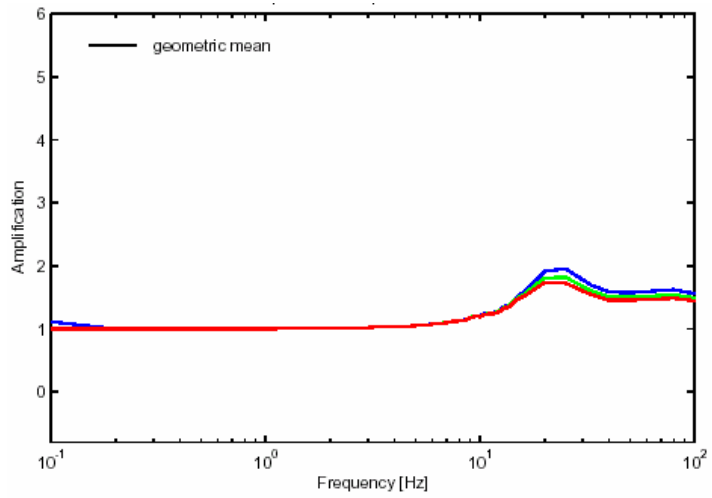


For 0.75 g:

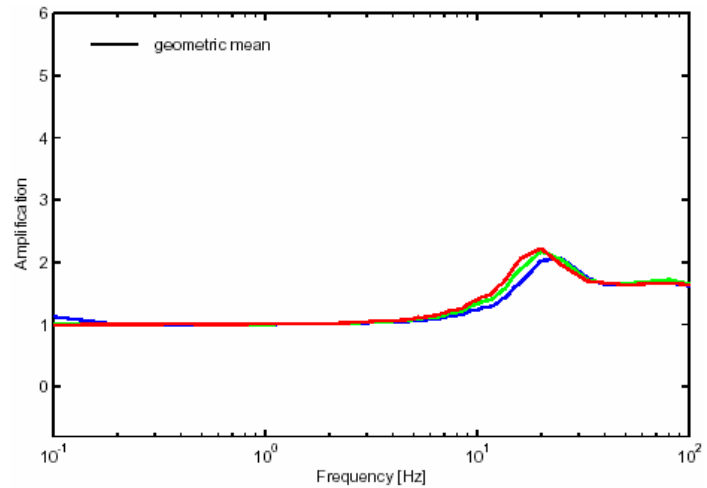


A2.2.2 Interpolation / Extrapolation to a case not considered in the available vertical computations

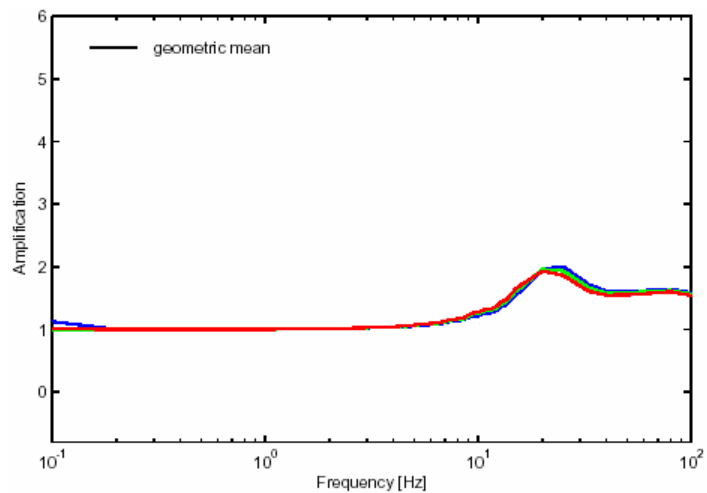
For P-wave degradation 1:



For P-wave degradation 2:



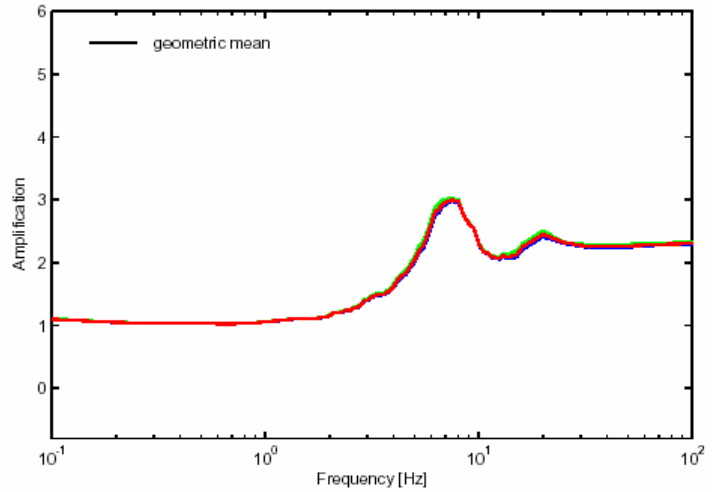
For P-wave degradation 3:



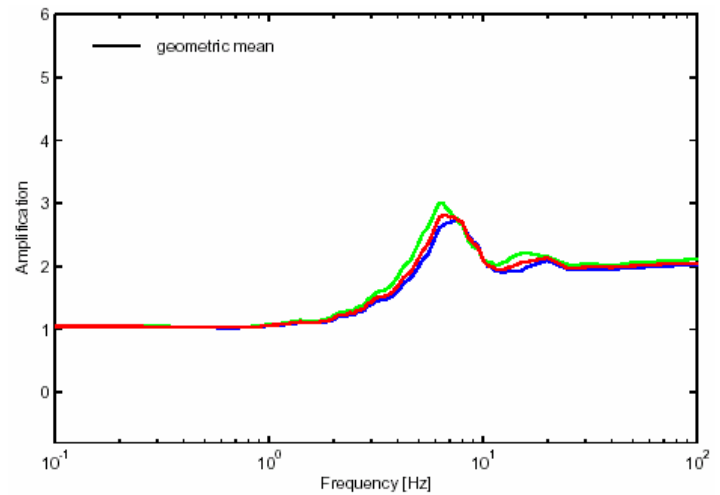
A2.3 Leibstadt

A2.3.1 Evaluation of approaches for computing the vertical site response (SHAKE runs), Profile 1

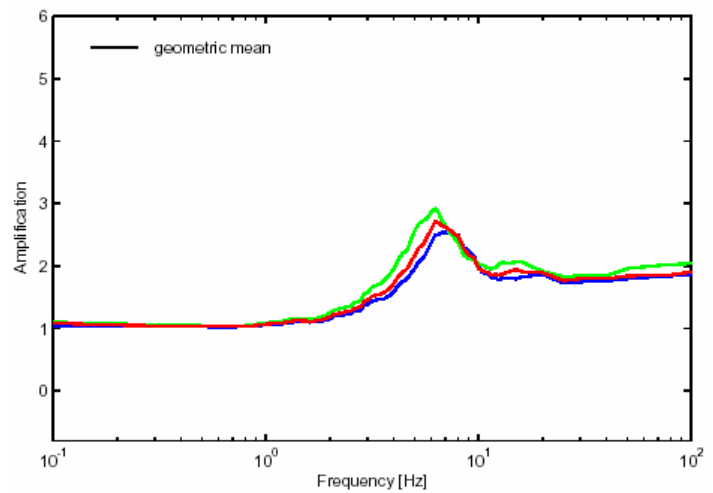
For 0.1 g:



For 0.4 g:

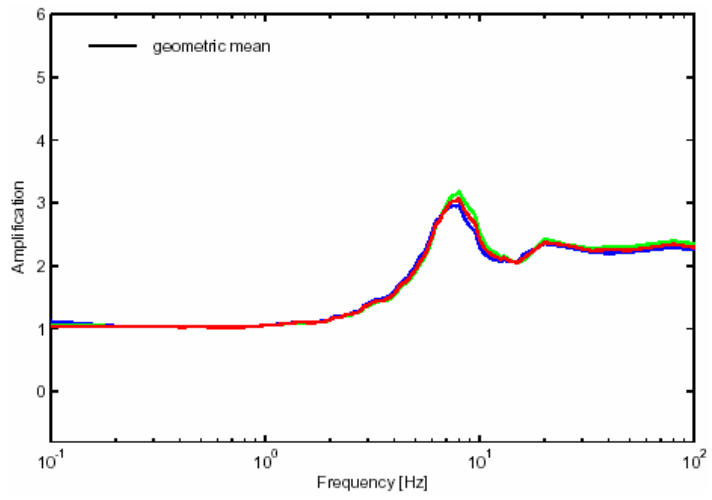


For 0.75 g:

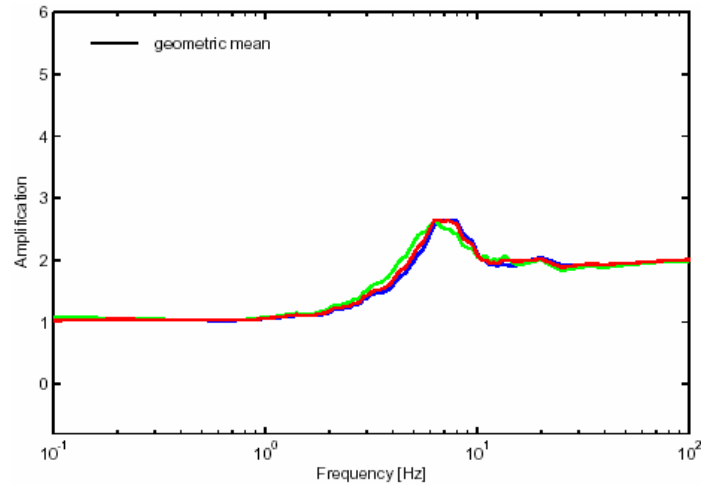


A2.3.2 Evaluation of approaches for computing the vertical site response (SHAKE runs), Profile 2

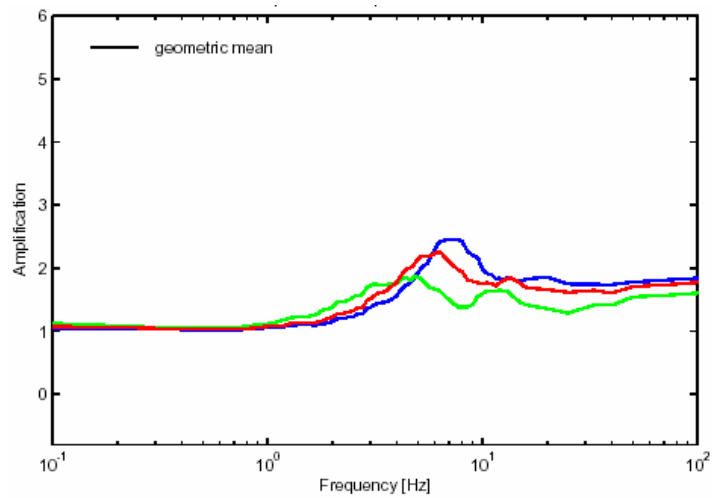
For 0.1 g:



For 0.4 g:

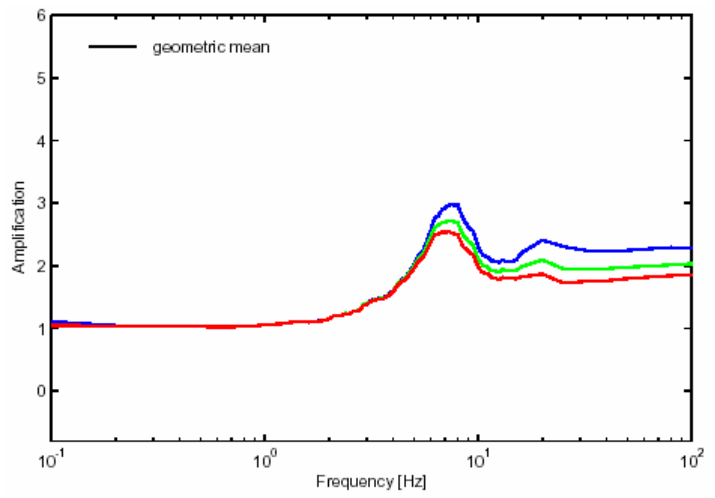


For 0.75 g:

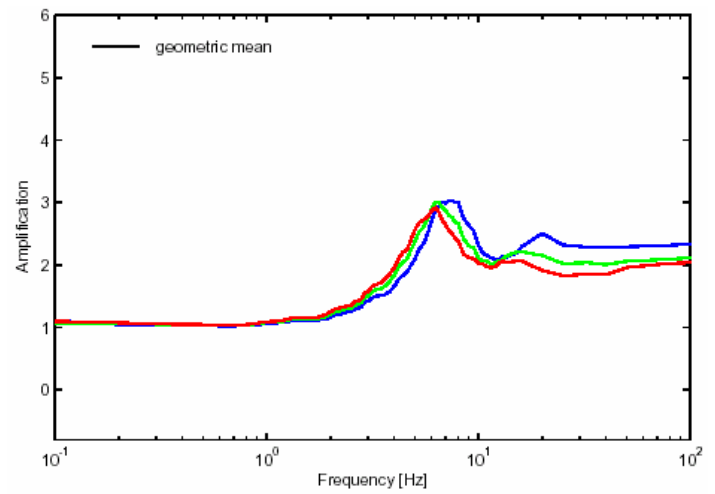


A2.3.3 Interpolation / Extrapolation to a case not considered in the available vertical computations, Profile 1

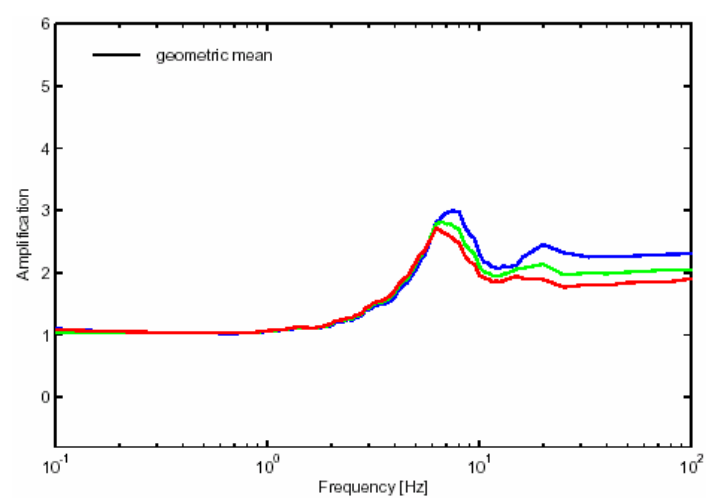
For P-wave degradation 1:



For P-wave degradation 2:

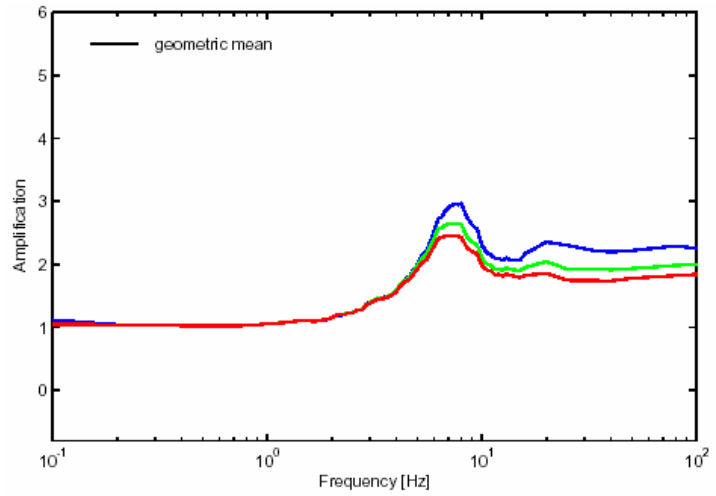


For P-wave degradation 3:

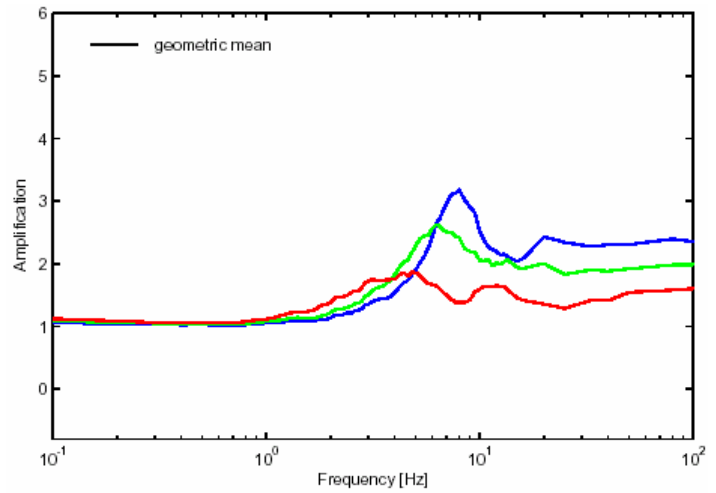


A2.3.4 Interpolation / Extrapolation to a case not considered in the available vertical computations, Profile 2

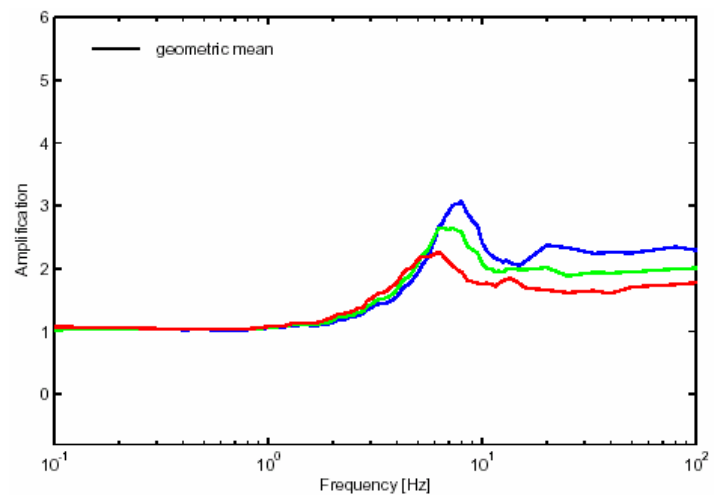
For P-wave degradation 1:



For P-wave degradation 2:



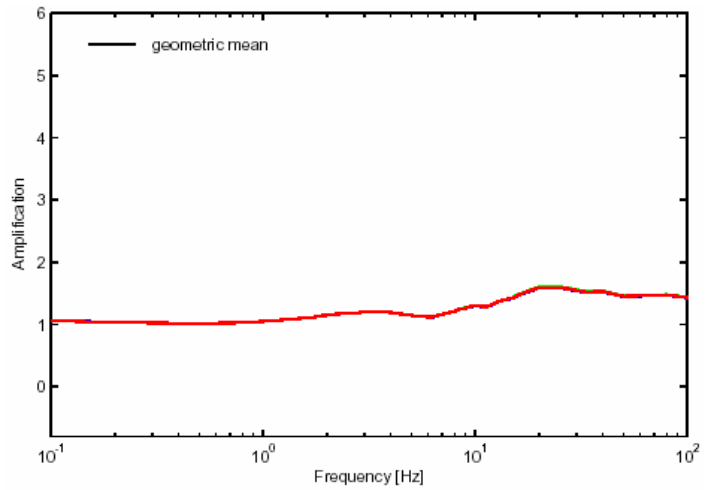
For P-wave degradation 3:



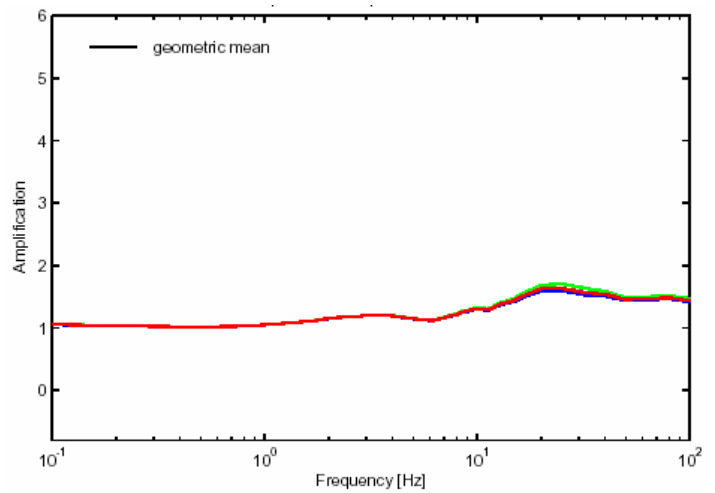
A2.4 Mühleberg

A2.4.1 Evaluation of approaches for computing the vertical site response (SHAKE runs)

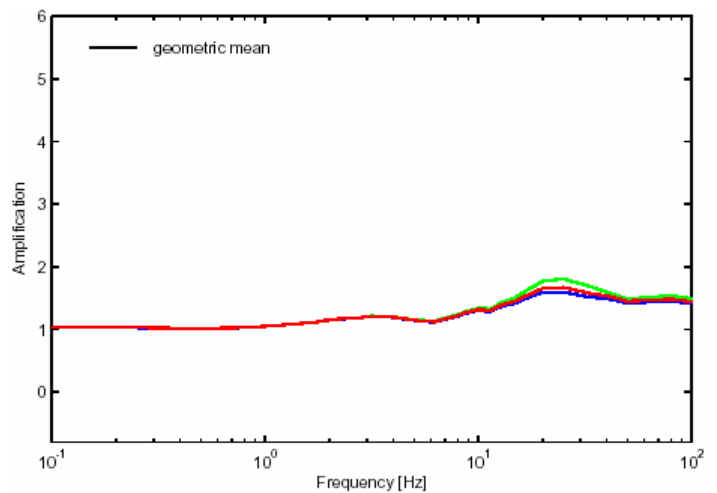
For 0.1 g:



For 0.4 g:

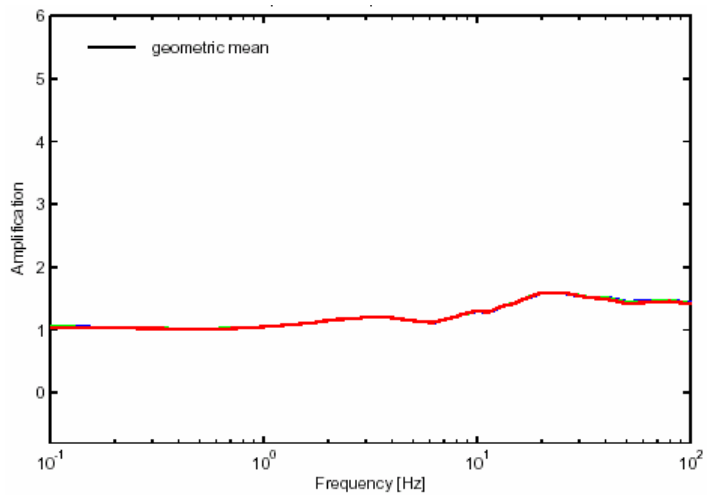


For 0.75 g:

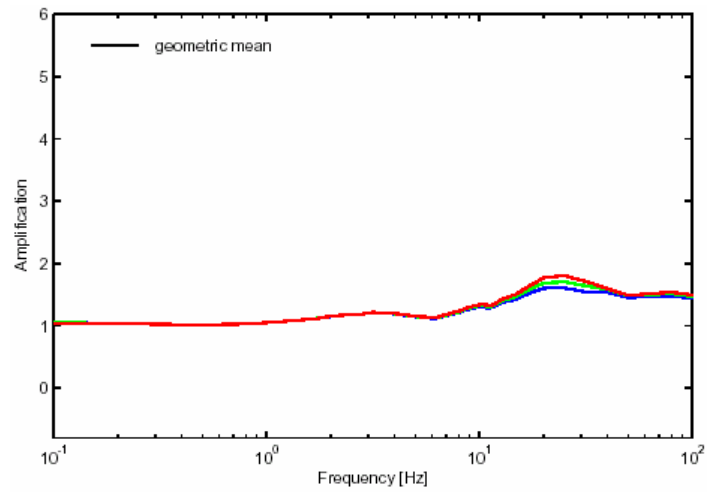


A2.4.2 Interpolation / Extrapolation to a case not considered in the available vertical computations

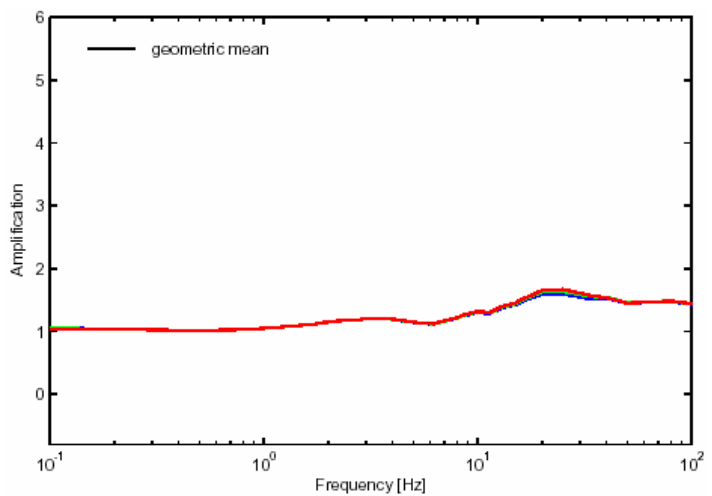
For P-wave degradation 1:



For P-wave degradation 2:



For P-wave degradation 3:



APPENDIX 3: TABLES FOR INTERPOLATION / EXTRAPOLATION

Legend for "Extreme value":

- 1 Amplification Factor minimum at $f < f_0$ (low frequency, F2)
- 2 Amplification Factor maximum at f_0 (fundamental frequency, F3)
- 3 Amplification Factor minimum at $f > f_0$ (high frequency, F4)

a) Horizontal Motion:

Site	Material	Magnitude	PGA shaking level	Depth	Motion	Extreme value	Frequency (log10)	Amplification factor
Beznau P1	M1	5	0.1	surface	surface	2	0.415	3
Beznau P1	M1	6	0.1	surface	surface	2	0.447	2.97
Beznau P2	M1	5	0.75	surface	surface	3	1.22	1.57
Beznau P2	M1	6	0.1	surface	surface	3	1.097	1.75
Beznau P3	M1	5	0.75	surface	surface	1	-0.45	1.87
Beznau P3	M1	5	0.75	surface	surface	3	1.21	1.68
Beznau P3	M1	6	0.75	surface	surface	2	0.52	2.62
Beznau P3	M1	7	0.1	surface	surface	2	0.65	2.27
Beznau P3	M1	7	0.4	surface	surface	2	0.52	2.39
Beznau P3	M1	7	0.75	surface	surface	2	0.37	2.64
Gösigen P1	M1	5	0.1	surface	surface	3	1.205	2.23
Gösigen P1	M1	6	0.1	surface	surface	3	1.205	2.25
Gösigen P1	M1	7	0.1	surface	surface	3	1.205	2.03
Gösigen P1	M2	6	0.1	surface	surface	3	1.2	1.97
Gösigen P1	M2	7	0.1	surface	surface	3	1.4	1.78
Leibstadt P1	M1	5	0.1	surface	surface	3	1.2	2.32
Leibstadt P1	M1	6	0.75	surface	surface	3	1.21	1.49
Leibstadt P1	M1	7	0.75	surface	surface	2	0.28	1.51
Leibstadt P1	M1	7	0.4	surface	surface	2	0.26	1.43
Leibstadt P1	M2	6	0.75	surface	surface	2	0.14	2.15
Leibstadt P1	M2	6	0.1	surface	surface	3	1.097	1.855
Leibstadt P1	M2	7	0.4	surface	surface	2	0.08	1.83
Leibstadt P1	M2	7	0.75	surface	surface	2	-0.04	1.57
Leibstadt P1	M2	7	0.75	surface	surface	1	-0.55	1.3

Site	Material	Magnitude	PGA shaking level	Depth	Motion	Extreme value	Frequency (log10)	Amplification factor
Leibstadt P2	M1	5	0.1	surface	surface	3	1.1	2.48
Leibstadt P2	M1	6	0.75	surface	surface	2	0.04	1.66
Leibstadt P2	M1	6	0.1	surface	surface	3	1.1	2.26
Mühleberg P1	M1	5	0.1	surface	surface	3	1.3	1.99
Mühleberg P1	M1	5	0.1	surface	surface	2	1.04	2.37
Mühleberg P1	M1	6	0.1	surface	surface	3	1.4	2.04
Mühleberg P1	M1	6	0.4	surface	surface	3	1.4	2.05
Mühleberg P1	M2	5	0.1	surface	surface	3	1.3	1.95
Mühleberg P1	M2	5	0.75	surface	surface	2	0.93	2.67
Mühleberg P1	M2	6	0.1	surface	surface	3	1.4	2.02
Mühleberg P1	M2	6	0.4	surface	surface	3	1.3	2.08
Mühleberg P1	M2	7	0.1	surface	surface	1	-0.4	1.07
Beznau P1	1	6	0.1	mean	outcrop	2	0.43	2.94
Beznau P2	1	6	0.1	mean	outcrop	3	1.095	1.82
Beznau P2	1	5	0.75	mean	outcrop	3	1.2	2.15
Beznau P3	1	5	0.75	mean	outcrop	3	1.2	2.55
Beznau P3	1	7	0.1	mean	outcrop	2	0.325	2.33
Beznau P3	1	7	0.4	mean	outcrop	2	0.3	2.87
Beznau P3	1	7	0.75	mean	outcrop	3	1.042	2.042
Gösigen P1	1	6	0.1	mean	outcrop	3	1.205	2
Gösigen P1	1	6	0.1	mean	outcrop	2	0.6405	3.5
Gösigen P1	2	6	0.1	mean	outcrop	3	1.21	1.92
Gösigen P1	1	5	0.1	mean	outcrop	3	1.204	2.15
Gösigen P1	1	5	0.1	mean	outcrop	2	0.643	3.75
Gösigen P1	2	5	0.1	mean	outcrop	2	0.625	3
Gösigen P1	1	7	0.1	mean	outcrop	3	1.205	1.96
Gösigen P1	1	7	0.1	mean	outcrop	2	0.623	3.5
Gösigen P1	2	7	0.4	mean	outcrop	3	1.08	1.45
Gösigen P1	2	7	0.75	mean	outcrop	3	1.04	1.16
Leibstadt P1	2	6	0.75	mean	outcrop	2	0.147	2.21
Leibstadt P1	2	5	0.1	mean	outcrop	3	1.205	1.7
Leibstadt P1	1	7	0.4	mean	outcrop	2	0.255	1.44
Leibstadt P1	1	7	0.75	mean	outcrop	2	0.28	1.56
Leibstadt P1	1	7	0.75	mean	outcrop	1	-0.5	1.32

Site	Material	Magnitude	PGA shaking level	Depth	Motion	Extreme value	Frequency (log10)	Amplification factor
Leibstadt P1	2	7	0.4	mean	outcrop	2	0.08	1.85
Leibstadt P1	2	7	0.75	mean	outcrop	2	-0.04	1.6
Leibstadt P1	1	7	0.1	mean	outcrop	2	0	1.8
Leibstadt P1	2	7	0.1	mean	outcrop	2	0	1.8
Beznau P3	1	5	0.1	max	outcrop	1	-0.53	1.65
Beznau P3	1	5	0.4	max	outcrop	1	-0.53	1.72
Beznau P3	1	5	0.75	max	outcrop	1	-0.53	1.695
Beznau P3	1	5	0.4	max	outcrop	2	0.3	2.1
Beznau P3	1	5	0.75	max	outcrop	2	0.3	2.092
Beznau P3	1	5	0.4	max	outcrop	3	0.88	1.43
Beznau P3	1	5	0.75	max	outcrop	3	0.82	1.52
Beznau P2	1	7	0.1	max	outcrop	3	0.84	1.65
Beznau P2	1	7	0.4	max	outcrop	3	0.82	1.54
Beznau P3	1	7	0.1	max	outcrop	3	0.74	1.38
Beznau P3	1	7	0.75	max	outcrop	1	-0.53	0.94
Gösgen P1	2	6	0.1	max	outcrop	3	1.2	1.87
Gösgen P1	1	5	0.1	max	outcrop	3	1.205	2.07
Gösgen P1	2	5	0.1	max	outcrop	2	0.625	3.2
Leibstadt P1	1	7	0.1	max	outcrop	2	0	1.8
Leibstadt P1	2	7	0.1	max	outcrop	2	0.1	2
Leibstadt P2	1	7	0.1	max	outcrop	2	0.1	1.7
Leibstadt P2	2	7	0.1	max	outcrop	2	0.1	1.7
Mühleberg P1	1	6	0.1	max	outcrop	3	1.3	1.383
Mühleberg P1	1	6	0.4	max	outcrop	3	1.3	1.385
Mühleberg P1	1	6	0.75	max	outcrop	3	1.3	1.385
Mühleberg P1	1	6	0.1	max	outcrop	2	0.5	1.55
Mühleberg P1	1	6	0.4	max	outcrop	2	0.5	1.55
Mühleberg P1	1	6	0.75	max	outcrop	2	0.5	1.55
Mühleberg P1	2	6	0.1	max	outcrop	3	1.04	1.38
Mühleberg P1	2	6	0.4	max	outcrop	3	1.04	1.398
Mühleberg P1	2	6	0.75	max	outcrop	3	1.04	1.402
Mühleberg P1	2	5	0.1	max	outcrop	2	0.5	1.544
Mühleberg P1	2	5	0.4	max	outcrop	2	0.5	1.555
Mühleberg P1	2	5	0.75	max	outcrop	2	0.5	1.564

b) Vertical Motion:

Site	Material	Magnitude	PGA shaking level	Depth	Motion	P-Wave degradation method	Extreme value	Frequency (log10)	Amplification factor
Beznav P2	1	6	0.75	surface	surface	1	1	0	1.03
Beznav P2	1	6	0.75	surface	surface	1	2	1.3	1.5
Beznav P2	1	6	0.75	surface	surface	1	3	1.52	1.3
Beznav P2	1	6	0.4	surface	surface	1	1	0	1.03
Beznav P2	1	6	0.4	surface	surface	1	2	1.3	1.53
Beznav P2	1	6	0.4	surface	surface	1	3	1.52	1.335
Beznav P2	1	6	0.1	surface	surface	1	1	0	1.03
Beznav P2	1	6	0.1	surface	surface	1	2	1.3	1.6
Beznav P2	1	6	0.1	surface	surface	1	3	1.52	1.38
Beznav P2	1	6	0.1	surface	surface	2	1	0.2	1.04
Beznav P2	1	6	0.4	surface	surface	2	1	0.2	1.05
Beznav P2	1	6	0.75	surface	surface	2	1	0.2	1.065
Beznav P2	1	6	0.1	surface	surface	2	2	0.98	1.68
Beznav P2	1	6	0.1	surface	surface	2	3	1.4	1.46
Beznav P2	1	6	0.1	surface	surface	3	1	0.2	1.04
Beznav P2	1	6	0.4	surface	surface	3	1	0.2	1.05
Beznav P2	1	6	0.75	surface	surface	3	1	0.2	1.065
Beznav P2	1	6	0.1	surface	surface	3	2	0.98	1.68
Beznav P2	1	6	0.1	surface	surface	3	3	1.4	1.46
Gösge P1	1	6	0.1	surface	surface	1	1	0.6	1.03
Gösge P1	1	6	0.4	surface	surface	1	1	0.6	1.03
Gösge P1	1	6	0.75	surface	surface	1	1	0.6	1.03
Gösge P1	1	6	0.1	surface	surface	1	2	1.3	1.93
Gösge P1	1	6	0.4	surface	surface	1	2	1.3	1.82
Gösge P1	1	6	0.75	surface	surface	1	2	1.3	1.73
Gösge P1	1	6	0.1	surface	surface	1	3	1.65	1.58
Gösge P1	1	6	0.4	surface	surface	1	3	1.65	1.515
Gösge P1	1	6	0.75	surface	surface	1	3	1.65	1.45
Gösge P1	1	6	0.1	surface	surface	2	1	0.6	1.04
Gösge P1	1	6	0.4	surface	surface	2	1	0.6	1.05
Gösge P1	1	6	0.75	surface	surface	2	1	0.6	1.06
Gösge P1	1	6	0.1	surface	surface	2	2	1.2	2.04
Gösge P1	1	6	0.4	surface	surface	2	2	1.2	2.157

Site	Material	Magnitude	PGA shaking level	Depth	Motion	P-Wave degradation method	Extreme value	Frequency (log10)	Amplification factor
Gösigen P1	1	6	0.75	surface	surface	2	2	1.2	2.21
Gösigen P1	1	6	0.1	surface	surface	2	3	1.6	1.64
Gösigen P1	1	6	0.4	surface	surface	2	3	1.6	1.655
Gösigen P1	1	6	0.75	surface	surface	2	3	1.6	1.65
Gösigen P1	1	6	0.1	surface	surface	3	1	0.6	1.03
Gösigen P1	1	6	0.4	surface	surface	3	1	0.6	1.04
Gösigen P1	1	6	0.75	surface	surface	3	1	0.6	1.05
Gösigen P1	1	6	0.1	surface	surface	3	2	1.3	1.98
Gösigen P1	1	6	0.4	surface	surface	3	2	1.3	1.96
Gösigen P1	1	6	0.75	surface	surface	3	2	1.3	1.91
Gösigen P1	1	6	0.1	surface	surface	3	3	1.6	1.61
Gösigen P1	1	6	0.4	surface	surface	3	3	1.6	1.58
Gösigen P1	1	6	0.75	surface	surface	3	3	1.6	1.55
Leibstadt P1	1	6	0.1	surface	surface	1	1	0.2	1.1
Leibstadt P1	1	6	0.4	surface	surface	1	1	0.2	1.1
Leibstadt P1	1	6	0.75	surface	surface	1	1	0.2	1.1
Leibstadt P1	1	6	0.1	surface	surface	1	2		
Leibstadt P1	1	6	0.4	surface	surface	1	2		
Leibstadt P1	1	6	0.75	surface	surface	1	2		
Leibstadt P1	1	6	0.1	surface	surface	1	3	1.1	2.06
Leibstadt P1	1	6	0.4	surface	surface	1	3	1.1	1.9
Leibstadt P1	1	6	0.75	surface	surface	1	3	1.1	1.8
Leibstadt P1	1	6	0.1	surface	surface	2	1	0.2	1.1
Leibstadt P1	1	6	0.4	surface	surface	2	1	0.2	1.13
Leibstadt P1	1	6	0.75	surface	surface	2	1	0.2	1.15
Leibstadt P1	1	6	0.1	surface	surface	2	2	0.8	3.04
Leibstadt P1	1	6	0.1	surface	surface	2	3	1.1	2.1
Leibstadt P1	1	6	0.4	surface	surface	2	3	1.09	2.05
Leibstadt P1	1	6	0.75	surface	surface	2	3	1.07	1.98
Leibstadt P1	1	6	0.1	surface	surface	3	1	0.2	1.1
Leibstadt P1	1	6	0.4	surface	surface	3	1	0.2	1.105
Leibstadt P1	1	6	0.75	surface	surface	3	1	0.2	1.11
Leibstadt P1	1	6	0.1	surface	surface	3	3	1.1	2.08
Leibstadt P1	1	6	0.4	surface	surface	3	3	1.1	1.95

Site	Material	Magnitude	PGA shaking level	Depth	Motion	P-Wave degradation method	Extreme value	Frequency (log10)	Amplification factor
Leibstadt P1	1	6	0.75	surface	surface	3	3	1.1	1.86
Leibstadt P2	1	6	0.1	surface	surface	1	1	0.2	1.1
Leibstadt P2	1	6	0.4	surface	surface	1	1	0.2	1.1
Leibstadt P2	1	6	0.75	surface	surface	1	1	0.2	1.1
Leibstadt P2	1	6	0.1	surface	surface	1	3	1.1	2.07
Leibstadt P2	1	6	0.4	surface	surface	1	3	1.1	1.9
Leibstadt P2	1	6	0.75	surface	surface	1	3	1.1	1.8
Leibstadt P2	1	6	0.1	surface	surface	2	1	-0.1	1.025
Leibstadt P2	1	6	0.4	surface	surface	2	1	-0.1	1.04
Leibstadt P2	1	6	0.75	surface	surface	2	1	-0.1	1.06
Leibstadt P2	1	6	0.75	surface	surface	2	2	0.7	1.75
Leibstadt P2	1	6	0.4	surface	surface	2	3	1.1	1.9
Leibstadt P2	1	6	0.75	surface	surface	2	3	1.1	1.5
Leibstadt P2	1	6	0.1	surface	surface	3	1	-0.2	1.04
Leibstadt P2	1	6	0.4	surface	surface	3	1	-0.2	1.04
Leibstadt P2	1	6	0.75	surface	surface	3	1	-0.2	1.04
Beznau P1	1	6	0.75	mean	outcrop	1	1	0.23	1.012
Beznau P1	1	6	0.75	mean	outcrop	1	2	1	1.52
Beznau P1	1	6	0.75	mean	outcrop	1	3	1.5	1.255
Beznau P2	1	6	0.75	mean	outcrop	1	1	0.23	1.012
Beznau P2	1	6	0.75	mean	outcrop	1	2	1	1.52
Beznau P2	1	6	0.75	mean	outcrop	1	3	1.5	1.255
Beznau P3	1	6	0.75	mean	outcrop	1	1	0.23	1.012
Beznau P3	1	6	0.75	mean	outcrop	1	2	1	1.52
Beznau P3	1	6	0.75	mean	outcrop	1	3	1.5	1.255
Beznau P1	1	6	0.1	mean	outcrop	1	1	0.23	1.004
Beznau P1	1	6	0.4	mean	outcrop	1	1	0.23	1.01
Beznau P2	1	6	0.1	mean	outcrop	1	1	0.23	1.004
Beznau P2	1	6	0.4	mean	outcrop	1	1	0.23	1.01
Beznau P3	1	6	0.1	mean	outcrop	1	1	0.23	1.004
Beznau P3	1	6	0.4	mean	outcrop	1	1	0.23	1.01

c) Exceptions for horizontal extrapolation

Legend for "Method":

- 1 Linear, nearest neighbour
- 2 Linear, best fit
- 3 2nd degree polynomial interpolation (default)

Site	Material	Magnitude	Depth	Motion	Extreme Value	Method
Beznau P1	M1	5	surface	surface	1	0
Beznau P2	M1	5	surface	surface	3	0
Beznau P2	M1	6	surface	surface	3	0
Beznau P2	M1	7	surface	surface	3	0
Beznau P2	M1	5	surface	surface	1	0
Beznau P3	M1	5	surface	surface	3	1
Beznau P3	M1	5	surface	surface	5	1
Beznau P3	M1	5	surface	surface	4	1
Beznau P3	M1	5	surface	surface	1	0
Beznau P3	M1	6	surface	surface	4	1
Beznau P3	M1	6	surface	surface	5	1
Beznau P3	M1	7	surface	surface	3	1
Beznau P3	M1	7	surface	surface	5	1
Beznau P3	M1	7	surface	surface	4	1
Gösgen P1	M1	5	surface	surface	3	0
Gösgen P1	M1	6	surface	surface	3	0
Gösgen P1	M1	7	surface	surface	3	0
Gösgen P1	M2	5	surface	surface	3	0
Gösgen P1	M2	5	surface	surface	1	0
Gösgen P1	M2	6	surface	surface	3	0
Gösgen P1	M2	6	surface	surface	2	1
Gösgen P1	M2	5	surface	surface	5	1
Gösgen P1	M2	7	surface	surface	3	0
Mühleberg P1	M2	7	surface	surface	3	0
Mühleberg P1	M2	7	surface	surface	4	1
Mühleberg P1	M2	6	surface	surface	4	1
Leibstadt P1	M1	5	surface	surface	3	1
Leibstadt P1	M1	5	surface	surface	2	1

Site	Material	Magnitude	Depth	Motion	Extreme Value	Method
Leibstadt P1	M1	6	surface	surface	3	1
Leibstadt P1	M1	6	surface	surface	2	1
Leibstadt P1	M1	7	surface	surface	1	0
Leibstadt P1	M1	7	surface	surface	2	0
Leibstadt P1	M1	7	surface	surface	3	0
Leibstadt P1	M1	7	surface	surface	4	0
Leibstadt P1	M1	7	surface	surface	5	0
Leibstadt P1	M2	5	surface	surface	1	1
Leibstadt P1	M2	5	surface	surface	2	1
Leibstadt P1	M2	5	surface	surface	3	1
Leibstadt P1	M2	5	surface	surface	4	0
Leibstadt P1	M2	5	surface	surface	5	0
Leibstadt P1	M2	6	surface	surface	1	1
Leibstadt P1	M2	6	surface	surface	2	1
Leibstadt P1	M2	6	surface	surface	3	0
Leibstadt P1	M2	6	surface	surface	4	0
Leibstadt P1	M2	6	surface	surface	5	0
Leibstadt P1	M2	7	surface	surface	1	0
Leibstadt P1	M2	7	surface	surface	2	0
Leibstadt P1	M2	7	surface	surface	3	0
Leibstadt P1	M2	7	surface	surface	4	0
Leibstadt P1	M2	7	surface	surface	5	0
Leibstadt P2	M1	5	surface	surface	1	1
Leibstadt P2	M1	5	surface	surface	2	1
Leibstadt P2	M1	5	surface	surface	3	0
Leibstadt P2	M1	5	surface	surface	4	0
Leibstadt P2	M1	5	surface	surface	5	0
Leibstadt P2	M1	6	surface	surface	1	1
Leibstadt P2	M1	6	surface	surface	2	1
Leibstadt P2	M1	6	surface	surface	3	0
Leibstadt P2	M1	6	surface	surface	4	0
Leibstadt P2	M1	6	surface	surface	5	0
Leibstadt P2	M1	7	surface	surface	1	0
Leibstadt P2	M1	7	surface	surface	2	0
Leibstadt P2	M1	7	surface	surface	3	0
Leibstadt P2	M1	7	surface	surface	4	0

Site	Material	Magnitude	Depth	Motion	Extreme Value	Method
Leibstadt P2	M1	7	surface	surface	5	0
Leibstadt P2	M2	5	surface	surface	1	1
Leibstadt P2	M2	5	surface	surface	2	1
Leibstadt P2	M2	5	surface	surface	3	0
Leibstadt P2	M2	5	surface	surface	4	0
Leibstadt P2	M2	5	surface	surface	5	0
Leibstadt P2	M2	6	surface	surface	1	1
Leibstadt P2	M2	6	surface	surface	2	1
Leibstadt P2	M2	6	surface	surface	3	0
Leibstadt P2	M2	6	surface	surface	4	0
Leibstadt P2	M2	6	surface	surface	5	0
Leibstadt P2	M2	7	surface	surface	1	0
Leibstadt P2	M2	7	surface	surface	2	0
Leibstadt P2	M2	7	surface	surface	3	0
Leibstadt P2	M2	7	surface	surface	4	0
Leibstadt P2	M2	7	surface	surface	5	0
Beznau P1	M1	5	mean	outcrop	1	1
Beznau P1	M1	5	mean	outcrop	2	1
Beznau P1	M1	5	mean	outcrop	3	1
Beznau P1	M1	5	mean	outcrop	4	1
Beznau P1	M1	5	mean	outcrop	5	1
Beznau P2	M1	5	mean	outcrop	1	0
Beznau P2	M1	5	mean	outcrop	2	1
Beznau P2	M1	5	mean	outcrop	3	1
Beznau P2	M1	5	mean	outcrop	4	1
Beznau P2	M1	5	mean	outcrop	5	1
Beznau P3	M1	5	mean	outcrop	1	1
Beznau P3	M1	5	mean	outcrop	2	1
Beznau P3	M1	5	mean	outcrop	3	1
Beznau P3	M1	5	mean	outcrop	4	0
Beznau P3	M1	5	mean	outcrop	5	0
Beznau P1	M1	6	mean	outcrop	3	1
Beznau P1	M1	6	mean	outcrop	4	1
Beznau P1	M1	6	mean	outcrop	5	1
Beznau P2	M1	6	mean	outcrop	3	1

Site	Material	Magnitude	Depth	Motion	Extreme Value	Method
Beznau P2	M1	6	mean	outcrop	4	1
Beznau P2	M1	6	mean	outcrop	5	1
Beznau P3	M1	6	mean	outcrop	3	1
Beznau P3	M1	6	mean	outcrop	4	0
Beznau P3	M1	6	mean	outcrop	5	0
Beznau P1	M1	7	mean	outcrop	3	1
Beznau P1	M1	7	mean	outcrop	4	1
Beznau P1	M1	7	mean	outcrop	5	1
Beznau P2	M1	7	mean	outcrop	3	1
Beznau P2	M1	7	mean	outcrop	4	1
Beznau P2	M1	7	mean	outcrop	5	1
Beznau P3	M1	7	mean	outcrop	3	1
Beznau P3	M1	7	mean	outcrop	4	1
Beznau P3	M1	7	mean	outcrop	5	0
Gösgen P1	M1	6	mean	outcrop	2	1
Gösgen P1	M1	6	mean	outcrop	3	1
Gösgen P1	M1	6	mean	outcrop	4	1
Gösgen P1	M1	6	mean	outcrop	5	1
Gösgen P1	M2	6	mean	outcrop	2	1
Gösgen P1	M2	6	mean	outcrop	3	0
Gösgen P1	M2	6	mean	outcrop	4	1
Gösgen P1	M1	5	mean	outcrop	1	1
Gösgen P1	M1	5	mean	outcrop	3	1
Gösgen P1	M1	5	mean	outcrop	4	1
Gösgen P1	M1	5	mean	outcrop	5	1
Gösgen P1	M2	5	mean	outcrop	1	1
Gösgen P1	M2	5	mean	outcrop	3	1
Gösgen P1	M2	5	mean	outcrop	5	1
Gösgen P1	M1	7	mean	outcrop	3	1
Gösgen P1	M1	7	mean	outcrop	4	1
Gösgen P1	M1	7	mean	outcrop	5	1
Leibstadt P1	M1	6	mean	outcrop	2	1
Leibstadt P1	M1	6	mean	outcrop	3	1
Leibstadt P1	M1	6	mean	outcrop	4	1
Leibstadt P1	M1	6	mean	outcrop	5	1

Site	Material	Magnitude	Depth	Motion	Extreme Value	Method
Leibstadt P1	M2	6	mean	outcrop	1	1
Leibstadt P1	M2	6	mean	outcrop	2	1
Leibstadt P1	M2	6	mean	outcrop	3	0
Leibstadt P1	M2	6	mean	outcrop	4	0
Leibstadt P1	M2	6	mean	outcrop	5	0
Leibstadt P2	M1	6	mean	outcrop	1	1
Leibstadt P2	M1	6	mean	outcrop	2	1
Leibstadt P2	M1	6	mean	outcrop	3	0
Leibstadt P2	M1	6	mean	outcrop	4	0
Leibstadt P2	M1	6	mean	outcrop	5	0
Leibstadt P2	M2	6	mean	outcrop	1	0
Leibstadt P2	M2	6	mean	outcrop	2	0
Leibstadt P2	M2	6	mean	outcrop	3	0
Leibstadt P2	M2	6	mean	outcrop	4	0
Leibstadt P2	M2	6	mean	outcrop	5	0
Leibstadt P1	M1	5	mean	outcrop	1	1
Leibstadt P1	M1	5	mean	outcrop	2	1
Leibstadt P1	M1	5	mean	outcrop	3	1
Leibstadt P1	M1	5	mean	outcrop	4	1
Leibstadt P1	M1	5	mean	outcrop	5	1
Leibstadt P1	M2	5	mean	outcrop	1	1
Leibstadt P1	M2	5	mean	outcrop	2	1
Leibstadt P1	M2	5	mean	outcrop	3	1
Leibstadt P1	M2	5	mean	outcrop	4	1
Leibstadt P1	M2	5	mean	outcrop	5	1
Leibstadt P2	M1	5	mean	outcrop	1	1
Leibstadt P2	M1	5	mean	outcrop	2	1
Leibstadt P2	M1	5	mean	outcrop	3	0
Leibstadt P2	M1	5	mean	outcrop	4	0
Leibstadt P2	M1	5	mean	outcrop	5	0
Leibstadt P2	M2	5	mean	outcrop	1	0
Leibstadt P2	M2	5	mean	outcrop	2	0
Leibstadt P2	M2	5	mean	outcrop	3	0
Leibstadt P2	M2	5	mean	outcrop	4	0
Leibstadt P2	M2	5	mean	outcrop	5	0
Leibstadt P1	M1	7	mean	outcrop	1	0

Site	Material	Magnitude	Depth	Motion	Extreme Value	Method
Leibstadt P1	M1	7	mean	outcrop	2	0
Leibstadt P1	M1	7	mean	outcrop	3	0
Leibstadt P1	M1	7	mean	outcrop	4	0
Leibstadt P1	M1	7	mean	outcrop	5	0
Leibstadt P1	M2	7	mean	outcrop	1	1
Leibstadt P1	M2	7	mean	outcrop	2	1
Leibstadt P1	M2	7	mean	outcrop	3	0
Leibstadt P1	M2	7	mean	outcrop	4	0
Leibstadt P1	M2	7	mean	outcrop	5	0
Leibstadt P2	M1	7	mean	outcrop	1	0
Leibstadt P2	M1	7	mean	outcrop	2	0
Leibstadt P2	M1	7	mean	outcrop	3	1
Leibstadt P2	M1	7	mean	outcrop	4	0
Leibstadt P2	M1	7	mean	outcrop	5	0
Leibstadt P2	M2	7	mean	outcrop	1	0
Leibstadt P2	M2	7	mean	outcrop	2	0
Leibstadt P2	M2	7	mean	outcrop	3	1
Leibstadt P2	M2	7	mean	outcrop	4	0
Leibstadt P2	M2	7	mean	outcrop	5	0
Mühleberg P1	M1	6	mean	outcrop	3	1
Mühleberg P1	M1	6	mean	outcrop	4	1
Mühleberg P1	M1	6	mean	outcrop	5	1
Mühleberg P1	M2	6	mean	outcrop	3	1
Mühleberg P1	M2	6	mean	outcrop	4	1
Mühleberg P1	M2	6	mean	outcrop	5	1
Mühleberg P1	M1	5	mean	outcrop	3	1
Mühleberg P1	M1	5	mean	outcrop	4	1
Mühleberg P1	M1	5	mean	outcrop	5	1
Mühleberg P1	M2	5	mean	outcrop	3	1
Mühleberg P1	M2	5	mean	outcrop	4	1
Mühleberg P1	M2	5	mean	outcrop	5	1
Mühleberg P1	M1	7	mean	outcrop	3	1
Mühleberg P1	M1	7	mean	outcrop	4	1
Mühleberg P1	M1	7	mean	outcrop	5	1
Mühleberg P1	M2	7	mean	outcrop	3	1

Site	Material	Magnitude	Depth	Motion	Extreme Value	Method
Mühleberg P1	M2	7	mean	outcrop	4	1
Mühleberg P1	M2	7	mean	outcrop	5	1
Beznau P1	M1	5	max	outcrop	1	1
Beznau P1	M1	5	max	outcrop	2	1
Beznau P1	M1	5	max	outcrop	3	1
Beznau P1	M1	5	max	outcrop	4	1
Beznau P1	M1	5	max	outcrop	5	1
Beznau P2	M1	5	max	outcrop	1	0
Beznau P2	M1	5	max	outcrop	2	0
Beznau P2	M1	5	max	outcrop	3	1
Beznau P2	M1	5	max	outcrop	4	1
Beznau P2	M1	5	max	outcrop	5	1
Beznau P3	M1	5	max	outcrop	1	0
Beznau P3	M1	5	max	outcrop	2	0
Beznau P3	M1	5	max	outcrop	3	0
Beznau P3	M1	5	max	outcrop	4	1
Beznau P3	M1	5	max	outcrop	5	1
Beznau P1	M1	6	max	outcrop	2	1
Beznau P1	M1	6	max	outcrop	3	1
Beznau P1	M1	6	max	outcrop	4	1
Beznau P1	M1	6	max	outcrop	5	1
Beznau P2	M1	6	max	outcrop	1	1
Beznau P2	M1	6	max	outcrop	2	1
Beznau P2	M1	6	max	outcrop	3	1
Beznau P2	M1	6	max	outcrop	4	1
Beznau P2	M1	6	max	outcrop	5	1
Beznau P3	M1	6	max	outcrop	1	1
Beznau P3	M1	6	max	outcrop	2	1
Beznau P3	M1	6	max	outcrop	3	1
Beznau P3	M1	6	max	outcrop	4	1
Beznau P3	M1	6	max	outcrop	5	1
Beznau P1	M1	7	max	outcrop	3	1
Beznau P1	M1	7	max	outcrop	4	1
Beznau P1	M1	7	max	outcrop	5	1
Beznau P2	M1	7	max	outcrop	1	1
Beznau P2	M1	7	max	outcrop	3	1
Beznau P2	M1	7	max	outcrop	4	1
Beznau P2	M1	7	max	outcrop	5	1

Site	Material	Magnitude	Depth	Motion	Extreme Value	Method
Beznau P3	M1	7	max	outcrop	1	1
Beznau P3	M1	7	max	outcrop	2	1
Beznau P3	M1	7	max	outcrop	3	1
Beznau P3	M1	7	max	outcrop	4	1
Beznau P3	M1	7	max	outcrop	5	0
Gösgen P1	M1	6	max	outcrop	1	1
Gösgen P1	M1	6	max	outcrop	2	1
Gösgen P1	M1	6	max	outcrop	3	1
Gösgen P1	M1	6	max	outcrop	4	1
Gösgen P1	M1	6	max	outcrop	5	1
Gösgen P1	M2	6	max	outcrop	2	1
Gösgen P1	M2	6	max	outcrop	3	0
Gösgen P1	M2	6	max	outcrop	4	1
Gösgen P1	M1	6	max	outcrop	5	1
Gösgen P1	M1	5	max	outcrop	1	1
Gösgen P1	M1	5	max	outcrop	3	1
Gösgen P1	M1	5	max	outcrop	4	1
Gösgen P1	M1	5	max	outcrop	5	1
Gösgen P1	M2	5	max	outcrop	1	1
Gösgen P1	M2	5	max	outcrop	2	1
Gösgen P1	M2	5	max	outcrop	3	1
Gösgen P1	M2	5	max	outcrop	4	1
Gösgen P1	M2	5	max	outcrop	5	1
Gösgen P1	M1	7	max	outcrop	3	1
Gösgen P1	M1	7	max	outcrop	4	1
Gösgen P1	M1	7	max	outcrop	5	0
Gösgen P1	M2	7	max	outcrop	3	1
Gösgen P1	M2	7	max	outcrop	4	1
Gösgen P1	M2	7	max	outcrop	5	1
Gösgen P1	M2	7	mean	outcrop	3	1
Gösgen P1	M2	7	mean	outcrop	4	1
Gösgen P1	M2	7	mean	outcrop	5	1
Leibstadt P1	M1	6	max	outcrop	2	1
Leibstadt P1	M1	6	max	outcrop	3	1
Leibstadt P1	M1	6	max	outcrop	4	1
Leibstadt P1	M1	6	max	outcrop	5	1
Leibstadt P1	M2	6	max	outcrop	1	1
Leibstadt P1	M2	6	max	outcrop	2	1

Site	Material	Magnitude	Depth	Motion	Extreme Value	Method
Leibstadt P1	M2	6	max	outcrop	3	0
Leibstadt P1	M2	6	max	outcrop	4	0
Leibstadt P1	M2	6	max	outcrop	5	0
Leibstadt P2	M1	6	max	outcrop	1	1
Leibstadt P2	M1	6	max	outcrop	2	1
Leibstadt P2	M1	6	max	outcrop	3	0
Leibstadt P2	M1	6	max	outcrop	4	0
Leibstadt P2	M1	6	max	outcrop	5	0
Leibstadt P2	M2	6	max	outcrop	1	0
Leibstadt P2	M2	6	max	outcrop	2	0
Leibstadt P2	M2	6	max	outcrop	3	0
Leibstadt P2	M2	6	max	outcrop	4	0
Leibstadt P2	M2	6	max	outcrop	5	0
Leibstadt P1	M1	5	max	outcrop	1	1
Leibstadt P1	M1	5	max	outcrop	2	1
Leibstadt P1	M1	5	max	outcrop	3	1
Leibstadt P1	M1	5	max	outcrop	4	1
Leibstadt P1	M1	5	max	outcrop	5	1
Leibstadt P1	M2	5	max	outcrop	1	1
Leibstadt P1	M2	5	max	outcrop	2	1
Leibstadt P1	M2	5	max	outcrop	3	1
Leibstadt P1	M2	5	max	outcrop	4	1
Leibstadt P1	M2	5	max	outcrop	5	1
Leibstadt P2	M1	5	max	outcrop	1	1
Leibstadt P2	M1	5	max	outcrop	2	1
Leibstadt P2	M1	5	max	outcrop	3	0
Leibstadt P2	M1	5	max	outcrop	4	0
Leibstadt P2	M1	5	max	outcrop	5	0
Leibstadt P2	M2	5	max	outcrop	1	0
Leibstadt P2	M2	5	max	outcrop	2	0
Leibstadt P2	M2	5	max	outcrop	3	0
Leibstadt P2	M2	5	max	outcrop	4	0
Leibstadt P2	M2	5	max	outcrop	5	0
Leibstadt P1	M1	7	max	outcrop	1	0
Leibstadt P1	M1	7	max	outcrop	2	0
Leibstadt P1	M1	7	max	outcrop	3	0
Leibstadt P1	M1	7	max	outcrop	4	0
Leibstadt P1	M1	7	max	outcrop	5	0
Leibstadt P1	M2	7	max	outcrop	1	0

Site	Material	Magnitude	Depth	Motion	Extreme Value	Method
Leibstadt P1	M2	7	max	outcrop	2	0
Leibstadt P1	M2	7	max	outcrop	3	0
Leibstadt P1	M2	7	max	outcrop	4	0
Leibstadt P1	M2	7	max	outcrop	5	0
Leibstadt P2	M1	7	max	outcrop	1	0
Leibstadt P2	M1	7	max	outcrop	2	0
Leibstadt P2	M1	7	max	outcrop	3	0
Leibstadt P2	M1	7	max	outcrop	4	0
Leibstadt P2	M1	7	max	outcrop	5	0
Leibstadt P2	M2	7	max	outcrop	1	0
Leibstadt P2	M2	7	max	outcrop	2	0
Leibstadt P2	M2	7	max	outcrop	3	1
Leibstadt P2	M2	7	max	outcrop	4	0
Leibstadt P2	M2	7	max	outcrop	5	0
Mühleberg P1	M1	6	max	outcrop	3	1
Mühleberg P1	M1	6	max	outcrop	4	1
Mühleberg P1	M1	6	max	outcrop	5	1
Mühleberg P1	M2	6	max	outcrop	3	1
Mühleberg P1	M2	6	max	outcrop	4	1
Mühleberg P1	M2	6	max	outcrop	5	1
Mühleberg P1	M1	5	max	outcrop	1	0
Mühleberg P1	M1	5	max	outcrop	3	1
Mühleberg P1	M1	5	max	outcrop	4	1
Mühleberg P1	M1	5	max	outcrop	5	1
Mühleberg P1	M2	5	max	outcrop	3	1
Mühleberg P1	M2	5	max	outcrop	4	1
Mühleberg P1	M2	5	max	outcrop	5	1
Mühleberg P1	M1	7	max	outcrop	3	1
Mühleberg P1	M1	7	max	outcrop	4	1
Mühleberg P1	M1	7	max	outcrop	5	1
Mühleberg P1	M2	7	max	outcrop	3	1
Mühleberg P1	M2	7	max	outcrop	4	1
Mühleberg P1	M2	7	max	outcrop	5	1

d) Exceptions for vertical extrapolation

Site	Material	Magnitude	Depth	Motion	P-Wave degradation method	Extreme Value	Method
Beznau P2	M1	6	mean	outcrop	1	1	1
Beznau P2	M1	6	mean	outcrop	1	2	1
Beznau P2	M1	6	mean	outcrop	1	3	1
Beznau P2	M1	6	mean	outcrop	1	4	1
Beznau P2	M1	6	mean	outcrop	1	5	1
Beznau P2	M1	6	surface	surface	2	4	1
Beznau P2	M1	6	surface	surface	2	1	0
Beznau P2	M1	6	surface	surface	3	1	0
Beznau P2	M1	6	surface	surface	3	4	1
Leibstadt P1	M1	6	surface	surface	1	3	1
Leibstadt P1	M1	6	surface	surface	1	4	1
Leibstadt P1	M1	6	surface	surface	1	5	1
Leibstadt P1	M1	6	surface	surface	2	5	1
Leibstadt P1	M1	6	surface	surface	3	3	1
Leibstadt P1	M1	6	surface	surface	3	4	1
Leibstadt P1	M1	6	surface	surface	3	5	1
Leibstadt P2	M1	6	surface	surface	1	3	1
Leibstadt P2	M1	6	surface	surface	1	4	1
Leibstadt P2	M1	6	surface	surface	1	5	1
Leibstadt P2	M1	6	surface	surface	2	3	0
Leibstadt P2	M1	6	surface	surface	2	4	0
Leibstadt P2	M1	6	surface	surface	2	5	0
Leibstadt P2	M1	6	surface	surface	3	3	1
Leibstadt P2	M1	6	surface	surface	3	4	1
Leibstadt P2	M1	6	surface	surface	3	5	1
Beznau P2	M1	6	surface	surface	1	1	1
Beznau P2	M1	6	surface	surface	1	2	1
Beznau P2	M1	6	surface	surface	1	3	1
Beznau P2	M1	6	surface	surface	1	4	1
Beznau P2	M1	6	surface	surface	1	5	1
Gösigen P1	M1	6	surface	surface	1	1	1
Gösigen P1	M1	6	surface	surface	1	2	2
Gösigen P1	M1	6	surface	surface	1	3	1
Gösigen P1	M1	6	surface	surface	1	4	2
Gösigen P1	M1	6	surface	surface	1	5	1
Gösigen P1	M1	6	surface	surface	2	1	1

Site	Material	Magnitude	Depth	Motion	P-Wave degradation method	Extreme Value	Method
Gösgen P1	M1	6	surface	surface	2	2	2
Gösgen P1	M1	6	surface	surface	2	3	1
Gösgen P1	M1	6	surface	surface	2	4	1
Gösgen P1	M1	6	surface	surface	2	5	1
Gösgen P1	M1	6	surface	surface	3	1	1
Gösgen P1	M1	6	surface	surface	3	2	2
Gösgen P1	M1	6	surface	surface	3	3	1
Gösgen P1	M1	6	surface	surface	3	4	2
Gösgen P1	M1	6	surface	surface	3	5	2

APPENDIX 4: EG3-HID-0053 SITE AMPLIFICATION AT THE SURFACE AND EMBEDDED LAYER DEPTHS FINAL MODEL J. STUDER

A4.1 Introduction

This document describes the implementation of Jost Studer's models of site amplification at the surface, mean and maximum building depths (Table A4-1) as well as his assessment of maximum possible ground motions at the four Swiss NPP sites: Beznau, Gösgen, Leibstadt and Mühleberg. The purpose of this document is to translate the expert's evaluation of amplification factors into a Soil hazard Input File (SIF) for the hazard computation software (SOILHAZP) and to provide the expert with the necessary information to review the results of his model.

The implementation of Jost Studer's model is based on the July 11th 2003 (surface) and November 27th (embedded layers) versions of his elicitation summary (EG3-EXM-0028) and additional clarifications. This HID also includes post WS5 revisions of the maximum ground motion assessment for horizontal motion, described in an email by Jost Studer dated March 11th, 2004. It must be emphasized, that due to additional oral clarifications, the implementation of the model may contain elements not described in the above versions of the elicitation summary.

The following document and software are directly linked to this HID:

- TP3-TN-0401: A technical note describing the computational steps performed to create the soil hazard input files (SIFs)
- TP3-ASW-0024: The software used to implement the SP3 models

This HID consists of four sub-sections:

- Section 1: A description of the computational steps leading to the development of amplification factor spectra and their associated aleatory variabilities for each site and combination of magnitudes, input PGAs and ground motion types.
- Section 2: A description of the expert's assessment of maximum ground motion spectra.
- Section 3: A summarized description of creation of SIFs for site amplification, the associated aleatory variability and maximum ground motion. A detailed description is available in the technical note TP3-TN-0401.
- Section 4: The generalized logic tree for horizontal ground motion at the surface.

The implementation of Jost Studer's model was done by the SP3 TFI Team at Proseis using Matlab R13. The complete implementation is archived as TP3-ASW-0024. It consists of a software module and a database.

Tab. A4-1: Mean and maximum building depth for the four NPP sites

	Beznau	Gösgen	Leibstadt	Mühleberg
Mean building depth	6 m	5 m	5 m	7 m
Max. building depth	15 m	9 m	10 m	14 m

A4.2 Site amplification and its aleatory variability

The key-elements of Jost Studer's model are outlined and the crucial aspects, such as the inter- and extrapolation of amplification factors for various input PGA levels are detailed. Moreover, the results of Jost Studer's models are illustrated by means of one example per computational step. Figures showing the results for all cases and sites are available as an electronic Appendix in PDF format.

The logic tree architecture is not reviewed here detail, but a generalized logic tree for horizontal ground motion is given at the end of this HID. Finally it shall be noticed, that the results given in this section are an intermediate product, since they are summarized to discrete fractiles and associated with spectral accelerations before being used as an input for the soil hazard computations.

A4.2.1 Amplification of horizontal ground motion

Jost Studer developed two models for site amplification of horizontal ground motion: The first is applicable for input motion (PGA on rock) within the interval from 0.05 to 1.5 g. The second is applicable for input motion larger than or equal to 2.5 g. This second model is available only for the sites Beznau and Gösigen. For the case of 2.5 g input PGA being requested for Leibstadt or Mühleberg, simply the results of the first model for 1.5 g are used as a substitute. Given the bounds of these two models Jost Studer's model cannot be computed for input PGAs, between 1.5 g and 2.5 g. However, this is no drawback as interpolation is performed in the hazard software.

The example in Figure A4-1 shows the assessment of alternative amplification factors considered for the mean building depth at NPP Beznau for the case of a magnitude 6 earthquake with PGA on rock of 1.5 g, which are results of the first model. Figure A4-2 shows the weighted arithmetic mean amplification factors for mean building depth in Beznau as function of PGA on rock and frequency, which includes results of both models. Both models are described individually below. Corresponding plots showing the results for the other sites and scenarios are available in the appendix as *Studer.AF AVar.<site>.HM<depth>.pdf* and *Studer.SiteModAF.<site>.HM<depth>.pdf* files.

A4.2.1.1 Site amplification for input PGAs from 0.05 to 1.5 g

Site amplification for input PGAs below or equal to 1.5 g are based on either RVT (base case and randomizations) or SHAKE simulations. For the embedded layers the RVT or SHAKE simulations of outcropping motion are used.

Generally all velocity profiles and material models, which are available for a site, are considered. The possibility of magnitude independence is accounted for by developing the model for the requested magnitude and for magnitude 6 on two parallel branches.

Non-linear behavior of amplification factors with increasing shaking level is considered by applying a correction factor to the linear-equivalent (LE) simulation. Correction for non-linear behavior is considered as an alternative branch, hence a parallel branch on which the LE simulation remains unchanged always exists. The correction factor for non-linearity is computed for each frequency as the ratio of the magnitude and PGA corresponding truly non-linear (NL) simulation (generally for surface motion) and the LE simulation underlying the particular branch. Non-linear behavior is not considered for the Mühleberg site. The possibility of 2D effects is accounted for by alternatively using a 2D correction factor and leaving the amplification factor unchanged. The 2D correction factor is based on Bard's models (TP3-TN-0186) by using ratios of corresponding 1D and 2D simulations. 2D effects are only considered for the Leibstadt site.

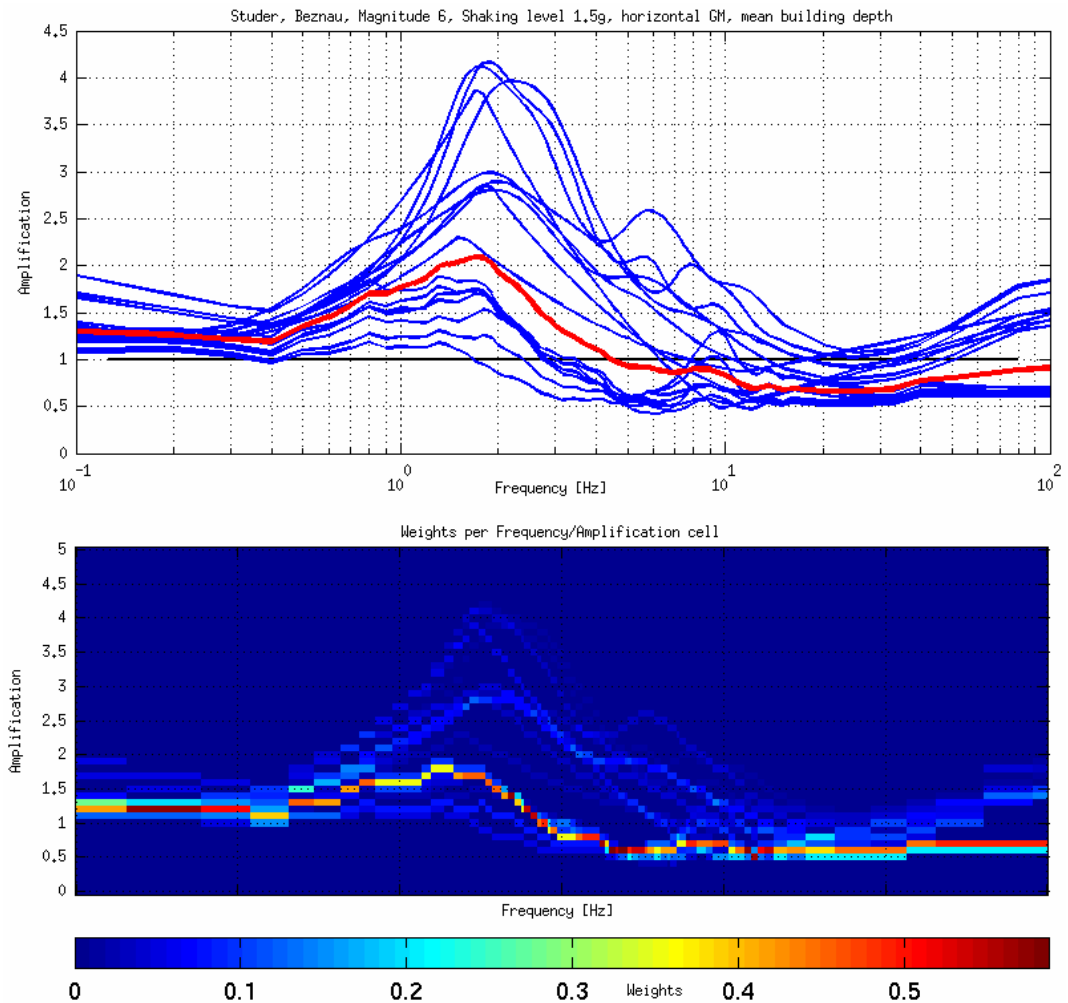


Fig. A4-1: Site amplification factors for horizontal ground motion at the mean building depth of NPP Beznau for the case of a magnitude 6 earthquake with PGA on rock of 1.5 g

The upper plot shows the alternative amplification factors (blue curves) and their weighted mean (red curve). The lower plot shows the distribution of weights in the amplification-frequency space. Corresponding plots are available for all sites and cases in the appendix: See the *Studer.AF_AVar.<site>.HM<depth>.pdf* files.

Since RVT and SHAKE amplification factors are not available for every magnitude and/or input PGA being requested, an inter- and extrapolation scheme was developed by the expert.

Magnitude interpolation is not implemented at this stage, since the soil hazard software utilizes linear interpolation between the magnitudes 5, 6 and 7 results. For the case of RVT, linear interpolation between the simulations at the available PGA levels was implemented. Extrapolation is not required, since RVT simulations are available for all material models and velocity profiles at 10 PGA levels in the interval from 0.05 to 1.5 g. For the case of SHAKE simulations linear interpolation is performed for input PGAs within the interval 0.1 to 0.75 g. Difficulties occur due to the fact, that SHAKE simulations are not available for all velocity profiles and material models. If, for instance, the SHAKE model for profile 2 and magnitude 5 (SHAKE_{P2,M5}) is missing, we apply the ratio SHAKE_{P1,M5} / SHAKE_{P1,M6} to the SHAKE_{P2,M6} simulation, in order to get an estimate for the missing model. For the case of extrapolation to lower input PGA (< 0.05 g), the 0.1g results are adopted. For the case of extrapolation to higher

input PGA ($0.75 \text{ g} < \text{PGA} \leq 1.5 \text{ g}$) at Beznau, Gösigen and Leibstadt sites the "five point extrapolation" detailed in the elicitation summary is used. For extrapolation of AF to higher input PGA at Mühleberg site, linear extrapolation of the AF spectra at 0.1, 0.5 and 0.75 g is used with a smoothing of the extrapolated spectrum by a running mean filter. In all cases of extrapolations, the minimum amplification factor is limited to 0.3. This intervention is required to prevent the "correction factors for non-linearity" (ratio $\text{AF}_{\text{non-lin}} / \text{AF}_{\text{SHAKE}}$) to develop asymptotic features at frequencies, where SHAKE amplification factors would otherwise go to zero.

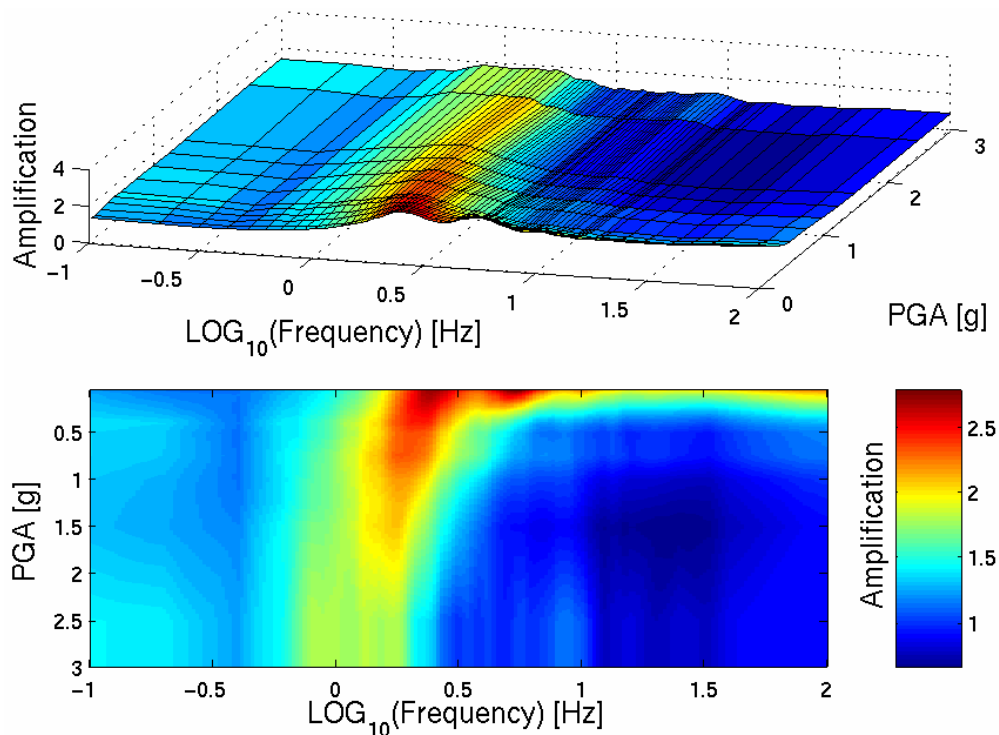


Fig. A4-2: Weighted arithmetic mean amplification factors (AF as function of PGA on rock and frequency) for horizontal ground motion of a magnitude 6 scenario at mean building depth of NPP Beznau

Corresponding plots are available for all sites and cases in the appendix: See the *Studer.SiteModAF.<site>.HM<depth>.pdf* files.

A4.2.1.2 Site amplification for input PGAs $\geq 2.5 \text{ g}$

Site amplification models for Beznau and Gösigen at input PGAs equal to or higher than 2.5 g are based on Pelli's 2.5 g NL models to which three uncertainty factors (0.8, 1.0 and 1.2) are applied. For the sites Leibstadt and Mühleberg, the above results for 1.5 g are adopted. For the consideration of the embedded layer depths, the 2.5 g NL (within motion) models are modified by two kind of factors in order to estimated NL outcrop motion at depth. The first kind of factor is $\text{SHAKE}_{\text{outcrop, at depth}} / \text{SHAKE}_{\text{within, at depth}}$, which is applied to $\text{NL}_{\text{at depth}}$ models. The other kind of factor is $\text{SHAKE}_{\text{outcrop, at depth}} / \text{SHAKE}_{\text{surface}}$, which is applied to the $\text{NL}_{\text{surface}}$ models. These SHAKE/SHAKE ratios are generally based on magnitude 6 and input PGA 0.75 g simulations.

A4.2.2 Aleatory variability of amplification of horizontal ground motion

The aleatory variability of the amplification of the horizontal component is fully correlated to the development of the amplification factors themselves. There is no difference in aleatory variability for the surface and the embedded layer depths. Aleatory variability assessments are generally based on site effect models for the surface layer.

As in the case of amplification factors for the Beznaun and Gösigen sites, two models exist: One for input PGA levels up to 1.5 g and another one for PGA levels larger than 2.5 g. Both models are interpolated for intermediate accelerations in the hazard software.

The following are the characteristic elements of the development of the aleatory variability for input PGAs up to 1.5 g:

- The aleatory variability consists of two components: (i) the uncertainty in the LE simulation underlying the particular branch tip and (ii) the uncertainty of the correction factor for non-linear behavior of amplification factors at higher PGAs.
- In the case of RVT simulations underlying a branch tip, the uncertainty is varied by applying two different factors.
- In the case of SHAKE simulations underlying a branch tip, the uncertainty in the correction for non-linearity is not accounted for, since the NL simulations are based on a subset of the input motions already used for the SHAKE simulations.
- Uncertainty in the correction factor for 2D effects is not considered.

For the sites Beznaun and Gösigen and for input shaking levels of 2.5 g or higher, aleatory variability corresponds to the uncertainty of the NL simulation, modified by the same uncertainty factors (0.8, 1.0, 1.2), which are applied to the corresponding amplification factors.

Figure A4-3 shows an assessment of the aleatory variability, corresponding to the site amplification case shown in Figure A4-1. For the results of all other cases and sites please see the files *Studer.AF AVar.<site>.HM<depth>.pdf* in the appendix. For the plots of mean aleatory variability corresponding to that in Figure A4-2, see files *Studer. SiteModAVar.<site>.HM<depth>.pdf*

A4.2.3 Amplification of vertical ground motion

Two models are implemented, as in the case of horizontal ground motion: The first model is valid for site amplifications for input PGAs from 0.05 to 1.5 g and the second model applies to site effects at 2.5 g or higher input PGA. Both models are described in detail below. Site effects for input PGAs between 1.5 and 2.5 g cannot be directly computed. They are interpolated within the hazard software.

Figures showing the assessment of amplification factors (corresponding to Figure A4-1) are available in the files *Studer.AF AVar.<site>.VM<depth>.pdf*. Figures showing mean site amplification factors as function of frequency and PGA on rock (corresponding to Figure A4-2) are available in the *Studer.SiteModAF.<site>.VM<depth>.pdf* files.

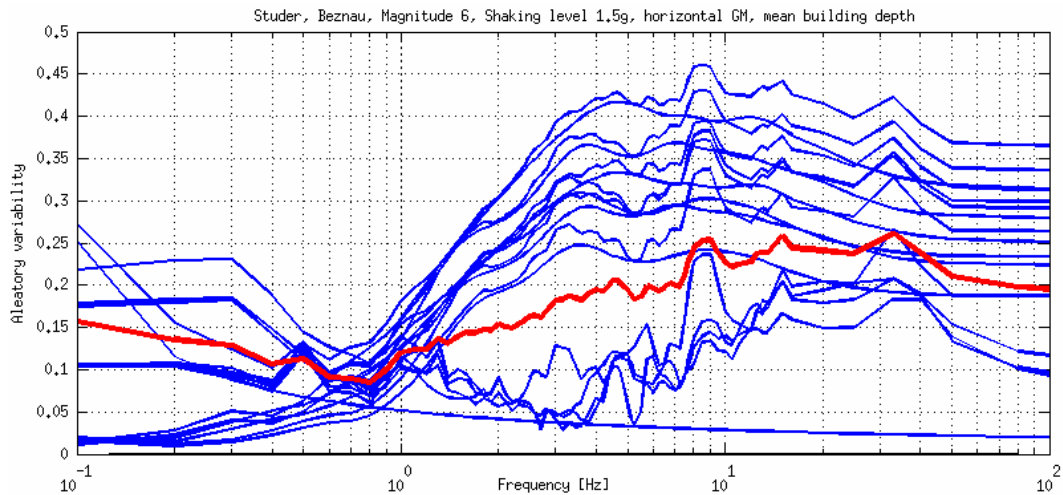


Fig. A4-3: Aleatory variability of amplification factors for horizontal ground motion at the mean building depth of NPP Beznau for the case of a magnitude 6 earthquake with PGA on rock of 1.5 g

The blue curves correspond to the alternative aleatory variabilities and the red curve is the weighted mean aleatory variability. Corresponding plots are available for all sites and cases in the appendix:

See *Studer.AF_AVar.<site>.HM<depth>.pdf* files in the appendix.

A4.2.3.1 Site amplification for input PGAs within the range from 0.05 to 1.5 g

Site amplification assessment of vertical ground motion at input PGAs ≤ 1.5 g is based on three main alternatives:

- A logic tree model based on SHAKE simulations of p-wave propagation
- V/H ratios from the NRC NUREG 6728 report, which are applied to the results of site amplification assessment of horizontal ground motion at corresponding PGA and magnitude.
- V/H ratios derived from SP2 results, which are also applied to the results of site amplification assessment of horizontal ground motion.

(a) P-wave SHAKE models

The branch considering SHAKE models of p-waves, involves a logic tree model detailing alternative p-wave degradation methods and considering non-linear effects. The key elements are:

- Three different p-wave degradation methods are considered as alternatives. The weighting of these alternatives is different for the assessment of site effects at the surface and embedded layer depths.
- Magnitude dependence is not considered.
- Amplification factors for input PGAs within the range from 0.1 to 0.75 g are interpolated by means of linear interpolation in PGA direction at each frequency of the spectrum. Amplification factors for input PGAs above 0.75 g are extrapolated as described below.

- Amplification factors for the embedded layer depths were modeled as "outcropping motion".
- For the Beznau, Gösgen and Leibstadt sites either both corrections for non-linear behavior, or no such correction are considered as alternatives. In the case where corrections are applied, the same factors as for the horizontal component are used.

Extrapolation of SHAKE amplification factors for input PGAs above 0.75 g is based on a linear best-fit of amplification factors at each frequency to the three available input PGAs (0.1, 0.4 and 0.75 g). For the case of Leibstadt profile 2 the extrapolated spectra was smoothed by an 8 point running mean filter. For all cases of extrapolation the minimum amplification is limited to 0.3.

(b) NUREG V/H ratios

The NUREG V/H ratios were provided by Jost Studer. They are applied to all final branches of the site effects assessment for horizontal ground motion.

(c) V/H ratios from Pegasos SP2

V/H ratios from SP2 are applied to all final branches of the site effects assessment for horizontal ground motion. They are derived directly from the SP2 results (state of 28-Nov-2003). In order to obtain a single spectrum of SP2 V/H ratios all alternatives by the five experts and for the different faults styles, magnitudes, distance definitions, and distances smaller than or equal to 15 km are averaged.

A4.2.4 Aleatory variability of amplification of vertical ground motion

The aleatory variability of amplification of the vertical component is considered to be equal to that of the horizontal component. Plots showing the assessment of aleatory variability of vertical ground motion are available in the files *Studer.AF AVar.<site>.VM<depth>.pdf* and figures showing mean aleatory variability as function of frequency and PGA on rock are given in the *Studer.SiteModAVar.<site>.VM <depth>.pdf* files.

A4.2.5 Parameter ranges

Jost Studer's model has been computed for the following input shaking levels (PGA on rock): 0.05, 0.1, 0.2, 0.3, 0.4, 0.5, 0.75, 1.0, 1.25, 1.5, 2.5 and 3.0 g and for magnitudes 5, 6 & 7. All SP3 expert model are computed for a set of 76 spectral frequencies as follows: 0.1, 0.2, 0.3, 0.4, 0.5, 0.6, 0.7, 0.8, 0.9, 1, 1.1, 1.2, 1.3, 1.4, 1.5, 1.6, 1.7, 1.8, 1.9, 2, 2.1, 2.2, 2.3, 2.4, 2.5, 2.6, 2.7, 2.8, 2.9, 3, 3.15, 3.3, 3.45, 3.6, 3.8, 4, 4.2, 4.4, 4.5, 4.6, 4.7, 4.8, 5, 5.1, 5.25, 5.5, 5.75, 6, 6.25, 6.5, 6.75, 7, 7.25, 7.5, 7.75, 8, 8.5, 9, 9.5, 10, 10.5, 11, 12, 12.5, 13, 13.5, 15, 16, 20, 25, 33, 40, 50, 80 and 100 Hz.

A4.3 Maximum ground motion at the surface

A4.3.1 Horizontal ground motion

The assessment of maximum horizontal ground motions is based on two alternative approaches: (a) Maximum ground motion spectra are derived from maximum PGA values, which were modeled by Pecker based on a mechanical soil model (TP3-TN-0354), and synthetic spectra modeled by Bard (TP3-TN-0358). (b) Maximum ground motion spectra are directly adopted from NL response spectra modeled by Pelli (TP3-SUP-0022 and TP3-SUP-0062).

When considering approach (a) and surface motion the maximum PGA value is selected depending on the site. This PGA value is multiplied by three alternative uncertainty factors (1.2, 1.0 and 0.8 with weights 15 %, 70 % and 15 %), resulting in three PGA values, which are then used to scale the synthetic spectra modeled by Bard. The spectra being used are the mean and the mean \pm one standard deviation.

In the case of approach (a) and motion at the embedded layer depths, both the maximum PGA at the surface and the considered depth are used in Jost Studer's assessment. The maximum PGA value for the surface is multiplied by the average ratio of $AF_{SHAKE, outcrop, depth}(0.75g, 30-100 \text{ Hz})$ over $AF_{SHAKE, outcrop, surface}(0.75 \text{ g}, 30 - 100 \text{ Hz})$. The maximum PGA value for the considered depth is multiplied by the average ratio of $AF_{SHAKE, outcrop, depth}(0.75 \text{ g}, 30 - 100 \text{ Hz})$ over $AF_{SHAKE, within, depth}(0.75 \text{ g}, 30 - 100 \text{ Hz})$. Both maximum PGA values are then multiplied by the three uncertainty factors as described above, resulting in six alternative maximum PGA values. As for the surface case the six maximum PGA values are used to scale the synthetic spectra (mean and mean \pm one standard deviation) modeled by Bard. However, these spectra are multiplied first by the ratio of V/H_{depth} over $V/H_{surface}$ described in an email by Donat Fäh, dated Oct. 22, 2003.

When considering approach (b) and surface motion, the NL response spectra plus minus one standard deviation are used as three alternative maximum ground motion spectra. For the sites Beznau and Gösigen the 2.5g models are used and for Leibstadt the average of the 1.5g models for profiles 1 and 2 is used. In the case of embedded layer depths, the above spectra for surface motion are modified by the average ratio of $AF_{SHAKE, outcrop, depth}(0.75 \text{ g}, 30 - 100 \text{ Hz})$ over $AF_{SHAKE, outcrop, surface}(0.75 \text{ g}, 30 - 100 \text{ Hz})$ and as an alternative the NL response spectra (mean \pm one standard deviation) for the considered embedded layer are used and modified by the average ratio of $AF_{SHAKE, outcrop, depth}(0.75 \text{ g}, 30 - 100 \text{ Hz})$ over $AF_{SHAKE, within, depth}(0.75 \text{ g}, 30 - 100 \text{ Hz})$.

In the case of Beznau and maximum building depth, only alternative (b) is considered. In the case of Mühleberg and the surface layer or mean building depth only the alternative (a) is used. Finally, for the case of Mühleberg and maximum building depth no limits are defined for maximum ground motion.

Figures showing the maximum horizontal ground motions for all sites and depths are available in the appendix in the files *Studer.MaxHM<depth>.AllSites.pdf*. Figure A4-4 shows the alternative maximum horizontal ground motions at the mean building depth at NPP Beznau as an example.

A4.3.2 Vertical ground motion

For the sites Beznau, Gösigen and Mühleberg, Jost Studer suggests that there is no limit to ground motion due to P-waves.

For Leibstadt site three alternatives are considered. The first alternative is, as for the other sites, no limit in maximum ground motion. The other two alternatives are based on the upper envelope of the empirical spectrum of maximum vertical ground motion in Ripperger and Fäh (TP3-TN-0359). Either the envelope of the spectrum is taken as is or it is multiplied by a factor of 1.4. For the case of the embedded layer depths Jost Studer multiplies the above spectra by the ratio of a "Factor A" at the surface over this "Factor A" at depth, where these "Factors A" are V/H ratios, distributed by Donat Fäh in an email dated 22-Oct-2003.

Plots showing Jost Studer's assessment of maximum vertical ground motion for Leibstadt are available in the *Studer.MaxVM<depth>.AllSites.pdf* files in the appendix.

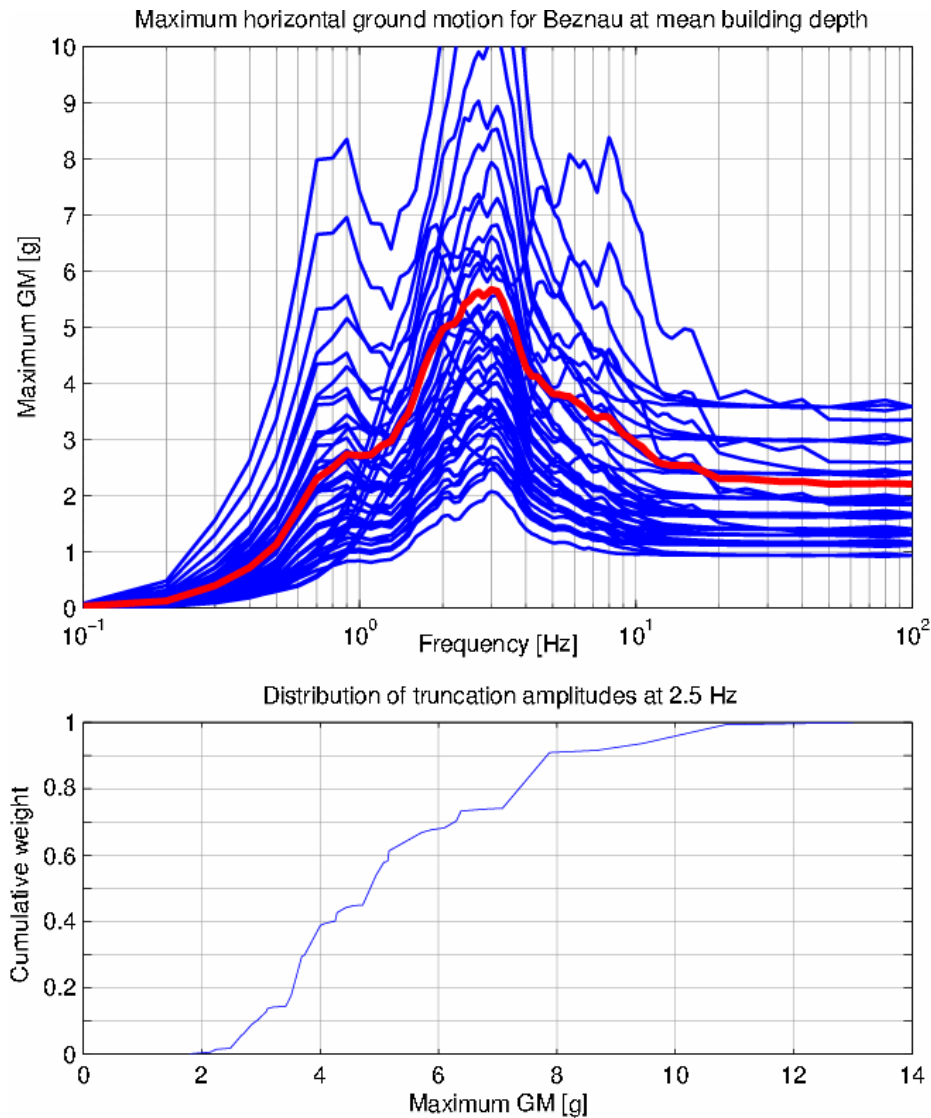


Fig. A4-4: Assessment of maximum horizontal ground motion for NPP Beznau at mean building depth

The blue lines in the upper plot show the alternative maximum ground motion spectra and the red line represents the weighted mean. The lower plot shows the cumulative distribution of maximum ground motion amplitudes at 2.5 Hz. Corresponding plots showing the assessments for the other sites and vertical ground motion are available in the *Studer.Max<motion><depth>.AllSites.pdf* files in the appendix.

A4.4 Soil hazard input files (SIFs)

The compilation of SIFs of the site amplification factors and their aleatory variability requires two computational steps, whereas the results of maximum ground motion assessment are used directly as shown in Figure A4-4.

The two computational steps are firstly the association of site amplification factors and their aleatory variability with spectral accelerations of the underlying input motions, and secondly summarizing site amplification and variability to a set of discrete fractiles. Both steps are outlined below and described in detail in a technical note TP3-TN-0401.

A4.4.1 Associating site amplification factors with input spectral accelerations

The amplification factors and their aleatory variability (Section 2) are modeled for a set of input shaking levels (PGA on rock), a set of magnitudes, and a set of frequencies. In order to apply them to the rock hazard results, which are modeled for different spectral accelerations on rock and combinations of magnitudes and distances, the amplification factors must be associated with a spectral acceleration corresponding to the particular input shaking level (PGA) and considered frequency. The spectral acceleration is derived from the spectral shape of the input motion, which underlies the simulation of the amplification factors (figures 1 and 2 in TP3-TN-0401). In this first step, every single amplification factor is assigned a spectral acceleration (on rock) to which it can be applied.

A4.4.2 Summarizing epistemic uncertainty

The epistemic uncertainty in the expert's assessments of site amplification and aleatory variability is expressed by the branch tips and weights. For the soil hazard computations these branch tips are summarized to 17 discrete fractiles of both site amplification and aleatory variability. In contrast to using all individual amplification factors and aleatory uncertainty values in the hazard computations, the usage of discrete fractiles increases the computational efficiency without making any assumptions regarding the shape of the distribution of epistemic uncertainties. The 17 fractiles used are: 0.13 %, 0.62 %, 2.28 %, 5 %, 10 %, 20 %, 30 %, 40 %, 50 %, 60 %, 70 %, 80 %, 90 %, 95 %, 97.72 % (2 sigma), 99.38 % (2.5 sigma), and 99.87 % (3 sigma).

For the soil hazard computations these fractiles are associated with a weight and are considered as alternative models in the same way, as the original results from the branch tips represent alternative models each of which associated a weight.

A4.4.3 Plots of the soil hazard input files

Figure A4-5 shows an example of the SIF of site amplification for horizontal ground motion of 4 Hz at Beznau at mean building depth. The crosses represent the results of the expert model after summarizing the epistemic uncertainty to 17 fractiles. The color-coding corresponds to these fractiles. Please note that some of the fractiles are identical and are hence plotted on top of each other, since the model contains less epistemic uncertainty than sampled by the 17 fractiles.

Plots showing the SIFs for site amplification and aleatory variability in all cases (sites and spectral frequencies) are available as PDF files in the appendix: *Studer.SIFaf.<site>.<motion-depth>.pdf* and *Studer.SIFavar.<site>.<motion-depth>.pdf*

A4.5 Generalized logic tree

The generalized logic tree of Jost Studer for the assessment of horizontal ground motion amplification factors is shown in Figure A4-6.

A4.6 Appendix

The appendix is available only in electronic form on CD-ROM. All figures are stored as PDF files. The files are named according to the convention: *<expert>.<content>.<site>.<motion><depth>.pdf*. Contents are *AF_AVAR* (assessment of site amplification and aleatory variability), *SiteModAF* (mean site amplification factors), *SiteModAvar* (mean aleatory variability), *SIFaf* (amplification factors as input to the soil hazard computations), *SIFavar*

(parameterized aleatory variability as input to the soil hazard computations), and MaxGM (maximum ground motion, also input to the soil hazard computations). Motions are *HM* for horizontal ground motion and *VM* for vertical ground motion. Depth codes are *surf* for surface, *d1* for mean building depth and *d2* for the maximum building depth.

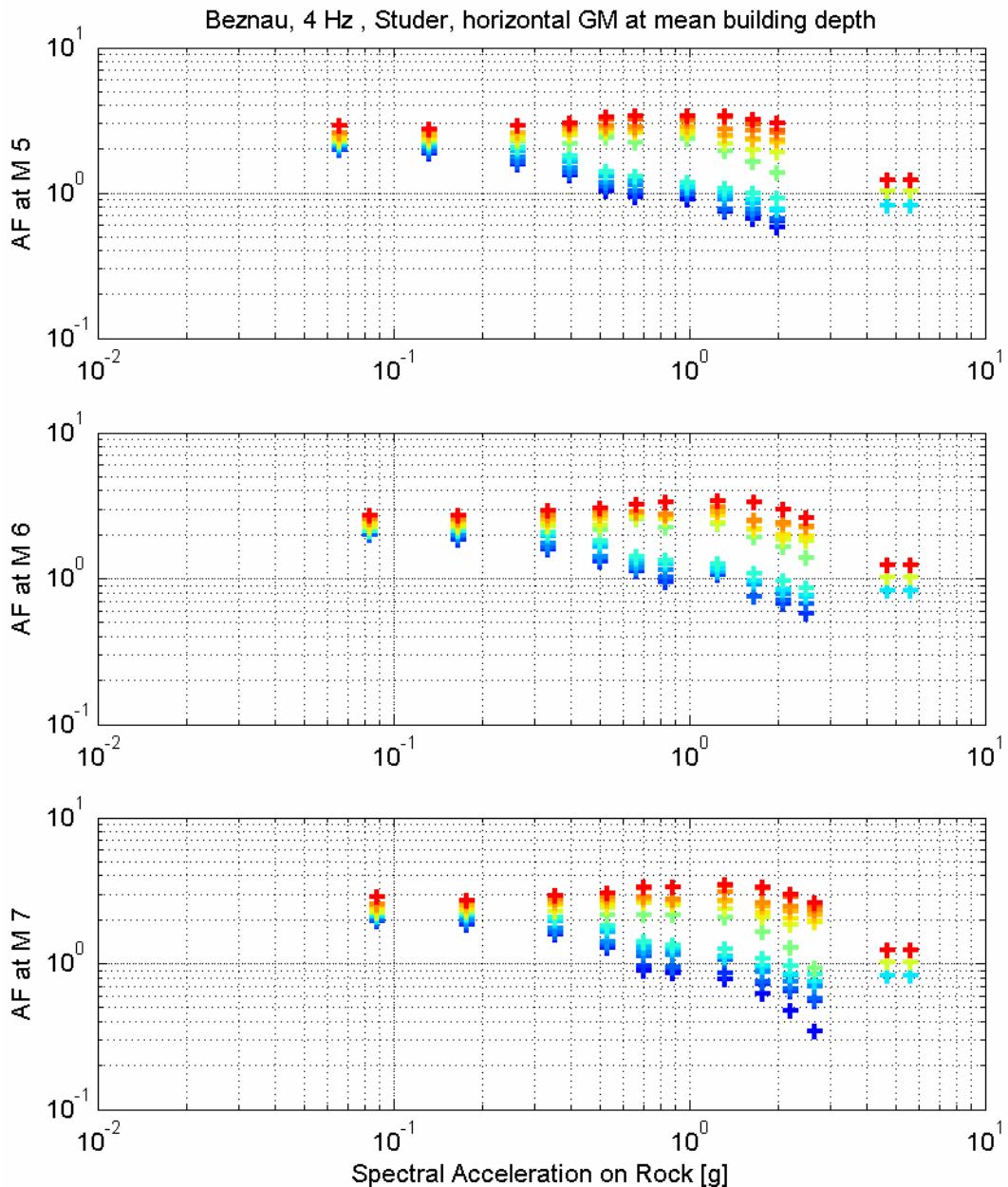


Fig.A4-5: Summarized model of site amplification factors for ground motion of 4 Hz at mean building depth at NPP Beznau and earthquake magnitudes 5, 6 and 7

The color coding corresponds to the fractiles of summarized epistemic uncertainty. Linear interpolation and nearest neighbor extrapolation respectively will be performed in the hazard software to obtain amplification factors for any spectral acceleration on rock and any considered earthquake magnitude. The full set of figures is available in the appendix in the files *Studer.SIFaf.<site>.<motion-depth>.pdf* and *Studer.SIFavar.<site>.<motion-depth>.pdf*.

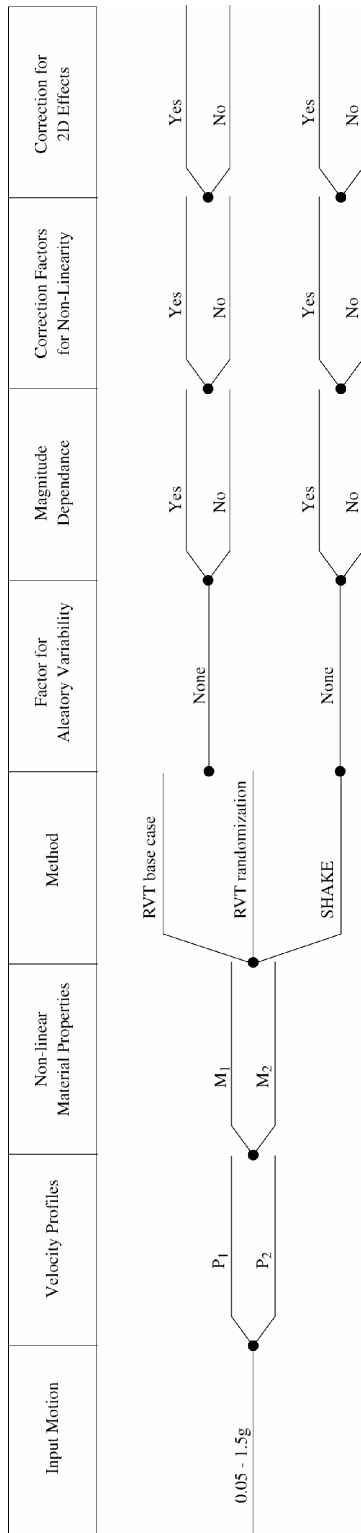


Fig. A4-6: General logic tree for horizontal ground motion

Site-specific differences are the number of branches for the shear-wave velocity profiles and non-linear material properties as well as the weights of the individual alternatives. The logic tree model shown applies to ground motions of max. 1.5 g. For higher ground motions Jost Studer uses 2.5 g NL models with three uncertainty factors applied.

